VIRGINIA MAZZINI

SPECIFIC-ION EFFECTS IN NON-AQUEOUS SOLUTIONS

Australian
National
University

VIRGINIA MAZZINI

SPECIFIC-ION EFFECTS IN NON-AQUEOUS SOLUTIONS

December 2017

A thesis submitted for the degree of Doctor of Philosophy
of The Australian National University

Virginia Mazzini: *Specific-ion effects in non-aqueous solutions*, A thesis submitted for the degree of Doctor of Philosophy of The Australian National University © December 2017.

E-MAIL: virginia.mazzini@anu.edu.au

This document was typeset using LaTeX and Lorenzo Pantieri's ArsClassica package, a reworking of the ClassicThesis style designed by André Miede, inspired to the masterpiece *The Elements of Typographic Style* by Robert Bringhurst.
Graphics were typeset using the `tikz` package, to achieve continuity of the typographic style in text and graphics. Calculations were performed, and plots made, in `R` (R Core Team, 2017), using mainly the packages `plyr` and `ggplot2`; the package `tikzDevice` was employed to translate the `R` graphics into LaTeX `tikz-pgf` commands.

The front cover displays the Coat of Arms of The Australian National University, stating the University motto '*Naturam Primum Cognoscere Rerum*'—'First to learn the nature of things' (Lucretius, *De Rerum Natura*, l. VI).

This thesis is an account of my own original research work, undertaken between May 2013 and December 2017 at the Department of Applied Mathematics in the Research School of Physics and Engineering at the Australian National University (Canberra, Australia).
Parts of the contents presented have been produced in collaboration with colleagues, and published or submitted for publication in peer-reviewed journals. These are listed in the section 'List of Publications' and are clearly marked in the body of the document.
None of this material has been submitted in whole or part to any other institution for the award of a degree or diploma. To the best of my knowledge, this thesis contains no work previously published by another person, except where due reference is made in the text.
This research is supported by an Australian Government Research Training Program (RTP) Scholarship.
This manuscript contains approximately 40000 words.

I acknowledge and celebrate the First Australians on whose traditional lands I have been living during the production of this thesis, and I pay my respect to the elders of the Ngunnawal people past and present.

Canberra, December 2017

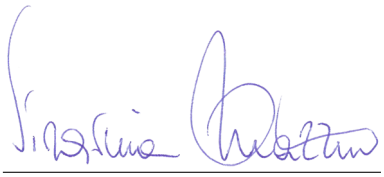

Virginia Mazzini

ACKNOWLEDGEMENTS

I am grateful to all that have supported me, professionally and/or personally, during this demanding journey.

I thank my supervisor Prof. Vince Craig for providing positive incentives, creative and honest scientific discussions, genuine advice, and for striving to adapt his supervision methods to the different needs of his students. I am particularly grateful for the opportunities of development and networking Prof. Craig has enabled me to attend, and for his commitment to promoting an inclusive and diverse research environment.

My advisor Prof. Pierandrea Lo Nostro has introduced me to the topic of specific-ion effects, and has been a participating mentor since my Masters' studies. I am thankful for the scientific guidance, the lifting conversations in moments of discouragement, and for the light-hearted humour.

Dr. Drew Parsons, also in the role of advisor, has willingly given assistance in some more abstract aspects of my research. In addition, I am appreciative of the fruitful discussions that I have shared with Dr. Andrea Salis during his time as a visiting fellow in the Department of Applied Mathematics; and of the caring advisory support and frank opinions provided by Prof. Barry Ninham.

I also have received invaluable technical support for the completion of my work. I am indebted to Mr. Tim Sawkins and Mr. Ron Cruikshank at the Department of Applied Mathematics for general technical support; to Mr. David Anderson, Mr. Dennis Gibson and Mr. Luke Materne of the Research School of Physics and Engineering Electronics Unit at the ANU — especially for assembling the 'button-bot'; to Ms. Bozena Belzowski, Mrs. Avis Paterson and Mr. Vance Lawrence at the ANU Research School of Chemistry for providing Blue Dextran; to Dr. Fouad Karouta from the Department of Electronics Materials Engineering for granting access to experimental equipment.

On a personal note, I am blessed with the friendship and affection of many. I thank my parents Katia and Gino, for being devoted to us daughters, and for educating us in the values of laicism, freedom, progress and solidarity. My sister Elisa, endless love and priceless wit. I look forward to reading your thesis. Manuela and Massimo, for welcoming me as your own daughter and hosting me and chauffeuring me around Florence and Prato when I visited.

Among my friends far and near, Daria, Jane, Viv, Anna, Lorena — offering banter, shenanigans and sisterhood. Namsoon, Martin, Muidh, Rohini, Alison, E-Jen, Rick, Matt, Ben and all the other fellow students and researchers in the Applied Mathematics Department.

Finally, Andrea, you had the wild idea of coming all the way down here to Australia, and, in hindsight, you *might have been* right. Thanks for choosing to stand beside me every day. May all our dreams come true.

ABSTRACT

Electrolyte solutions play a central role in life and technological processes because of their complexity. This complexity is yet to be described by a predictive theory of the specific effects that different ions induce in solution. The vast majority of investigations of specific-ion effects have been conducted in aqueous solutions. These studies have revealed that amongst the complexity, the effectiveness of the ions often follow trends that are apparent across a number of very different experiments, revealing an underlying order, (e.g. the Hofmeister series). It is often assumed that water itself is intricately involved in these trends.

Here I investigate specific-ion effects in non-aqueous solvents rather than water. By extending the investigation to a number of non-aqueous solvents, the role of the solvent in specific-ion effect trends can be elucidated and a better understanding of the general phenomenon gained.

Firstly, a more definite terminology is developed for describing the specific-ion effects trends in order to address the current confusion in the literature and provide a basis for the following investigations. An extensive investigation of the scarce literature demonstrates that water is by no means a special solvent with regards to ion-specificity, and that within the complexity there is universality. An investigation of electrostriction under the conditions of infinite dilution shows that the same fundamental specific ion trends are observed across all solvents, demonstrating that ion-specificity arises from the ions themselves. In this regard the influence of solvents, surfaces and real concentrations of electrolytes can be seen as perturbations to this fundamental series. Further work shows that for systems that are perturbed, the trends in non-aqueous protic solvents can be expected to follow the same trend in water; and in aprotic solvents the cations are more likely to adhere to the trend in water than the anions.

My experimental work focuses on specific-anion effects of seven Hofmeister sodium salts in the solvents: water, methanol, formamide, dimethyl sulfoxide and propylene carbonate. Two very different experiments were performed; the elution of electrolytes from a size-exclusion chromatography column and an investigation of the electrolyte moderated swelling of a cationic brush (PMETAC) using a Quartz Crystal Microbalance (QCM). The trends observed are consistent across these experiments. A forward or reverse Hofmeister series is observed in practically all salt-solvent combinations, and the reversal is attributed to the polarisability of the solvent.

Finally, a qualitative model of ion specific trends is formulated, where the specific-ion effects are fundamentally a property of the ion, and the associated trends correspond to the Hofmeister series for anions and the lyotropic series for cations. When the concentration is increased, or surfaces introduced, the effects of ion-ion interactions and ion-surface interactions can perturb the fundamental series. The perturbation of the series is related to the proticity of the solvent for ion-ion interactions, whereas the polarisability of the solvent and ion are important when a surface is present. This work for the first time individuates the principal properties of the solvent that affect their ordering: proticity and polarisability.

If you think education is expensive, try ignorance.

— Robert Orben

CONTENTS

LIST OF FIGURES

LIST OF TABLES

ACRONYMS & ABBREVIATIONS

1PentOH	1-pentanol (pentan-1-ol). 198
2BuOH	2-butanol (butan-2-ol). 192
2PrOH	2-propanol (propan-2-ol). 16, 173, 177, 199
ACE	acetone (propan-2-one). 16, 25, 30–32, 38, 42–47, 50–52, 150, 153, 155, 157, 173, 191
ACS	American Chemical Society. 88, 90
BuOH	butanol (butan-1-ol). 70, 191, 192
DLVO	Derjaguin, Landau, Verwey, Overbeek. 4
DMA	*N*,*N*-dimethylacetamide. 16, 173, 192
DMC	dimethyl carbonate. 173
DME	dimethoxyethane (1,2-dimethoxyethane). 173
DMF	*N*,*N*-dimethylformamide. 16, 23, 24, 26, 30–32, 38, 43, 44, 46, 47, 51, 52, 95, 150, 151, 153, 155, 157, 173, 192, 193
DMSO	dimethyl sulfoxide. 7, 16, 24–26, 29–32, 38, 43, 44, 46, 47, 51, 52, 83, 90, 91, 93–95, 97, 99, 100, 103, 106, 109, 110, 112, 113, 116, 119–121, 127, 128, 132, 134, 139–142, 144, 149, 150, 153, 155, 157, 162, 163, 168, 173, 174, 177, 193, 205, 207
EC	ethylene carbonate (1,3-dioxolan-2-one). 16, 25–28, 30–32, 38, 42–44, 46, 47, 51, 52, 66, 68, 83, 149, 153, 155, 157, 162, 168, 174, 177, 193
EG	ethylene glycol (ethane-1,2-diol). 16, 25, 28, 30, 31, 38, 42–44, 46, 47, 51, 52, 70, 148, 149, 152, 154, 156, 193
EtOH	ethanol. 7, 16, 25–27, 29–31, 38, 43–47, 51, 52, 148, 152, 154, 156, 174, 177, 193, 194
FA	formamide. 7, 16, 21, 22, 24, 28, 30–32, 38, 43–47, 51, 52, 70, 90, 93, 94, 97, 99, 100, 103, 106, 109, 110, 112, 113, 116–119, 121, 122, 127, 128, 132, 134, 139–142, 144, 148, 152, 154, 156, 194, 212

FEP fluorinated ethylene propylene. 98, 105

FT-IR Fourier-transform infrared spectroscopy. 28, 102

i-BuOH *iso*-butanol (2-methylpropan-1-ol). 192

i-PentOH *iso*-pentanol (3-methylbutan-1-ol). 198

KF Karl Fischer. 90, 91, 94–97, 205

LMC limiting molar ionic conductivity. 15, 18, 19, 21–27, 30–32, 48, 53, 118, 122

LMWA law of matching water affinities. 8, 29, 37, 57, 60–64, 66–68, 81, 82, 84, 89, 101, 118, 124, 143, 172

MD molecular dynamics simulations. 4, 64

MeCN acetonitrile. 7, 16, 25, 29–31, 38, 43, 44, 46, 47, 51, 52, 85, 95, 141, 150, 153, 155, 157, 174, 194, 195

$MeNO_2$ nitromethane. 25, 30–32, 141, 195

MeOH methanol. 7, 16, 19–21, 29–32, 38, 43–47, 51, 52, 67, 70, 82, 83, 85, 90, 93–97, 99, 100, 103, 105–107, 109–113, 115–117, 119–122, 127, 130–134, 139–141, 144, 147, 148, 152, 154, 156, 162, 168, 174, 175, 177, 195–197, 205, 206, 208, 209, 211, 212

MHC constant pressure standard partial molar heat capacity of the ion. 18–21, 23–27, 31, 32, 48

MRT NMR molecular reorientation time. 18–25, 31

MSA^- methanesulfonate. 28

NMA *N*-methylacetamide. 83, 141, 162, 163, 168, 175–177, 197

NMF *N*-methylformamide. 16, 22–26, 30–32, 38, 43–47, 51, 52, 83, 84, 150, 152, 154, 156, 162, 168, 176, 197

NMR nuclear magnetic resonance. 17, 20, 29, 61, 102, 111, 125, 145, 212

PC propylene carbonate (4-methyl-1,3-dioxolan-2-one). 7, 16, 25–28, 30, 31, 38, 43, 44, 46, 47, 51, 52, 66, 68, 72, 82, 83, 90, 93–95, 97, 99, 100, 103, 109–113, 120, 121, 127, 129, 131, 132, 134, 139–141, 144, 149, 153, 155, 157, 162, 168, 176, 197, 198, 205–207, 212

PEEK polyether ether ketone. 105

PMETAC poly(2-methacryloyloxyethyl-trimethyl-ammonium chloride. 123, 124, 127, 129–134, 140

PrOH 1-propanol (propan-1-ol). 16, 25, 30, 31, 72, 198, 199

PTFE polytetrafluoroethylene. 98, 105, 106, 108, 128

QCM quartz crystal microbalance. 8, 91, 95, 97, 98, 122, 124, 126–129, 131, 132, 134, 139, 140, 205, 208

QCM-D quartz crystal microbalance with dissipation monitoring. 125–127

RDD relative limiting static dielectric decrement. 18, 19, 21–23, 31, 32

SEC size-exclusion chromatography. 8, 95, 98, 99, 101, 102, 114, 115, 120–122, 134, 138–140, 144, 203, 205, 206

SIE specific-ion effects. 1–12, 14, 15, 17, 19–28, 30–33, 35, 37, 43–47, 51–55, 57, 62, 64, 84, 85, 87, 89, 90, 93–95, 99, 113, 122, 131, 132, 134–145, 205

SULF sulfolane (tetrahydrothiophene 1,1-dioxide). 163, 176, 177

t-BuOH *tert*-butanol (2-methylpropan-2-ol). 141, 192

VBC viscosity B-coefficients (*see* B_η). 15, 18, 19, 21–27, 30–32, 48, 53, 83

LIST OF SYMBOLS

α	static polarisability. 16, 141
α_P	isobaric expansivity. 211
AN	Gutmann-Mayer acceptor number. 16, 17, 19, 70
B_η	*B*-coefficients from the empirical Jones-Dole viscosity equation. 37, 48, 53, 61, 65–67, 83, 85
c_i	amount-of-substance concentration of solute i, units $\mathrm{mol\,dm^{-3}}$. 90, 210–212
CN	coordination number. 65
D_n	QCM dissipation factor of the overtone n $2\Gamma_n/f_n$. 125, 126
ΔD_n	shift of —. 126, 128, 129, 132, 134
DN	Gutmann donor number. 15, 16, 19, 70
η	viscosity. 16
ϵ_0	electric constant or vacuum permittivity, $8.854 \times 10^{-12}\,\mathrm{F\,m^{-1}}$. 171
ϵ_R	relative permittivity. 16, 38, 60, 171
e	elementary charge, $1.602\,176\,634 \times 10^{-19}$ C. 60, 171
f_n	QCM resonance frequency of the overtone n. 125, 126
Δf_n	shift of the —. 126, 128–131, 133, 134, 208
ΔF_n	normalised ——. 129–134, 208
γ	activity coefficient. 82, 83, 163, 168, 171–176, 181, 183, 185
Γ_n	QCM half-height half-bandwidth of the overtone n. 125
$\Delta_{\text{abs. hydr.}} G^{\ominus}$	absolute standard molar Gibbs free energy of hydration (solvation in water). 65
$\Delta_{\text{abs. soln.}} G$	molar Gibbs free energy of solvation. 58
$\Delta_{\text{abs. soln.}} G^{\ominus}$	absolute standard —. 58, 70, 71, 78, 165
$\Delta_f G^{\ominus}$	standard molar Gibbs free energy of formation. 58

$\Delta_{hydr.}G^{\ominus}$ standard molar Gibbs free energy of dissolution in water. 65

$\Delta_{soln.}G^{\ominus}$ standard molar Gibbs free energy of dissolution. 58, 69, 71, 75, 78, 80, 165, 167

$\Delta_{abs.\ hydr.}H^{\ominus}$ absolute standard molar enthalpy of hydration (solvation in water). 65

$\Delta_{abs.\ soln.}H$ molar enthalpy of solvation. 58

$\Delta_{abs.\ soln.}H^{\ominus}$ absolute standard —. 58, 59, 70, 77, 160, 164

$\Delta_f H^{\ominus}$ standard molar enthalpy of formation. 58, 59, 69

$\Delta_{hydr.}H$ molar enthalpy of dissolution in water. 60

$\Delta_{hydr.}H^{\ominus}$ standard molar —. 65, 69

$\Delta_{soln.}H^{\ominus}$ standard molar enthalpy of dissolution. 58, 59, 69, 74, 77, 79, 160, 164, 166

k Boltzmann constant, $1.381 \times 10^{-23}\,J\,K^{-1}$. 171

K_a association constant. 65

K_{AV} size exclusion chromatography available retention factor. 102, 111, 115

K_d dissociation constant. 65

K_{SEC} size exclusion chromatography retention factor. 101, 102, 111, 113, 120, 121

κ_T isothermal compressibility. 16, 38

μ dipole moment. 16

M_i molar mass of species i in $g\,mol^{-1}$. 3, 16, 40, 100, 111, 115, 209–211

m_i molality of solute i, units $mol\,kg^{-1}$. 90, 171–185, 210

ν_i stoichiometric coefficient of species i. 3

N_A Avogadro constant $6.022 \times 10^{23}\,mol^{-1}$. 171

N% electrostrictive volume normalised by the intrinsic volume. 49–53, 147–151, 156, 157

n_i number of moles of species i in mol. 36, 94, 209, 210

π 3.1415926536. 100, 125, 171

ϕ osmotic coefficient. 65, 66, 162, 163, 168, 171, 172, 180, 182, 184

P pressure. 36, 209

ρ_i^* density of a pure substance i. 171, 210, 211

ρ_i density of species i in $g\,cm^{-3}$. 16, 40, 191–200, 209–212

r_i radius of species i. 60, 65, 74, 75, 79, 80, 83, 100, 159, 162, 163, 166–170

S solubility. 65, 82, 92, 169, 170, 191–200

$\Delta_{abs.\ soln.}S$ molar entropy of solvation. 58

$\Delta_f S^{\ominus}$ standard molar entropy of formation. 58

T absolute temperature in K. 36, 58, 171, 174–179, 209

t temperature in °C. 16, 88, 92, 191–200

V volume. 36, 100, 209

$\overline{V}_{cryst}$ partial molar volume of a species in its crystalline form. 40

$\overline{V}_i$ partial molar volume of the species i in solution. 36, 209

$\overline{V}_i^{\ominus}$ standard —. 36, 38, 39, 41–44, 49, 53, 147–153, 209–211

$^{\Phi}\overline{V}_i$ apparent —. 209–212

$\overline{V}_{i\ intr}$ intrinsic molar volume of the species i. 36, 38, 40, 41, 49, 147–151

$\overline{V}_{i\ el}$ electrostrictive partial molar volume caused by the species i. 36

$\overline{V}_{i\ el}^{\ominus}$ standard —. 36, 38, 46–49, 147–151, 154, 155

V_i internal pore volume of a stationary phase. 101, 102, 110–114, 116, 117, 119, 120

V_R elution volume of an analyte. 101, 102

V_t total geometric volume of a stationary phase. 102, 110, 111, 114, 116, 117, 119, 120

V_o void volume of a chromatography column. 101, 102, 110–114, 116, 117, 119, 120

Wt.% percentage by weight. 92, 94, 97, 111, 191–200, 205

z charge number. 60, 65, 171

LIST OF PUBLICATIONS

Part of the work presented in this thesis has been published in the following papers:

Mazzini, V. and V. S. J. Craig

2016 'Specific-ion effects in non-aqueous systems', *Curr. Opin. Colloid Interface Sci.* 23, pp. 82–93, DOI: 10.1016/j.cocis.2016.06.009.

2017 'What is the fundamental ion-specific series for anions and cations? Ion specificity in standard partial molar volumes of electrolytes and electrostriction in water and non-aqueous solvents', *Chem. Sci.* 8 (10 2017), pp. 7052–7065, DOI: 10.1039/C7SC02691A.

2018 'Volcano plots emerge from a sea of non-aqueous solvents: The law of matching water affinities extends to all solvents', Submitted.

Mazzini, V., G. Liu and V. S. J. Craig

2018 'Probing the Hofmeister series beyond water: Specific-ion effects in non-aqueous solvents', *J. Chem. Phys.* 148, 22, p. 222805, DOI: 10.1063/1.5017278.

1 INTRODUCTION

The phrase 'specific-ion effects (SIE)' encompasses all those cases where a property of an electrolyte solution, or the behaviour of a substance dissolved therein, depends on the particular cations and anions present *beyond* their electrostatic charge.

1.1 THE IMPORTANCE OF SPECIFIC-ION EFFECTS

Between the years 2000 and 2017, *Web of Science*™ indexes more than 1700 publications investigating SIE, that span across (bio)chemistry, (bio)physics, materials science, biotechnology, pharmacology, engineering, medicine, water resources and plant science. This interdisciplinary interest in SIE stems from the fact that electrolyte solutions are omnipresent: pure, neat water containing no dissolved salts is extremely rare in nature.

Salts are what enables the specificity and complexity of interactions in life processes. Everyone is aware of the essential role water has for life, but it is often overlooked that this water must be salty to be of any use: drinking demineralised water for long periods of time has deleterious effects on health due to osmotic shock and disruption of the body homeostasis mechanisms (Kozisek, 2005). The details of 'life' is one of the most pressing research topics. Untangling its mechanisms and one day explaining its mystery is a major ambition of scientific progress. This cannot be achieved without acknowledging the importance of salts for life: ions interact with proteins and affect their solvated structure (Baldwin, 1996; Y. Zhang and Cremer, 2006); the activity of enzymes is salt-dependent (Bilaničová et al., 2008). Striking examples are provided by the fields of medicine and biology (Lo Nostro and Ninham, 2012). The fine-tuned equilibrium that allows the human body to function largely relies on the specificity allowed by electrolytes. For instance, intravenous injections of NaCl and KCl solutions, that differ only by the cations they contain, both of charge $+1$, have dramatically distinct effects on a subject. The first one is known as saline solution, and can be injected to treat dehydration. The latter instead alters the resting potential of the cardiac muscle and can quickly induce death by cardiac arrest (Weidmann, 1956). Strict protocols are constantly discussed to avoid accidental administration of the latter to a patient (Reeve et al., 2005). An extensive account of

SIE in biology can be found in: Kunz (2010), Lo Nostro and Ninham (2012) and Ninham and Lo Nostro (2010).

Ions have a fundamental role in climate and natural equilibria as well. Seawater is quite rich in a variety of ions, and as a consequence foams more than freshwater. One of the causes of the foaming of sea water (pollution and algae aside) is the presence of salts that inhibit bubble coalescence (Craig, Ninham et al., 1993a). Salts also reduce the solubility of gases in water (Millero, Huang et al., 2002a,b) and therefore affect aquatic life.

Important SIE are also observed in a vast variety of other settings, such as the processing of colloids, where the stability (Lyklema, 2009) and rheological behaviour of the system can be controlled (Franks, 2002; Franks et al., 1999). Also, the supramolecular self-assembly of surfactants is salt-dependent (Lo Nostro, Ninham, Ambrosi et al., 2003; Lo Nostro, Ninham, Milani et al., 2006). The above have consequences in applications such as mineral processing and wastewater treatment, and also in drug delivery and in food processing (cheesemaking for instance). In addition, polymer conformations show rich ion-specificity (Y. Zhang and Cremer, 2006), with consequences for instance in the development of responsive surface coatings (Azzaroni et al., 2005; G. Liu and G. Zhang, 2013; Willott et al., 2015; Y. Zhang, Furyk et al., 2005). Finally, SIE are also relevant in corrosion kinetics (Trompette, 2015).

1.2 A BRIEF HISTORICAL ACCOUNT OF SIE

The realisation that the electrostatic charge of an ion is not sufficient to describe the properties of its solutions occurred early on, but the theoretical connection of solution behaviour to the fundamental properties of the electrolytes remains a work in progress.

Although Poiseuille already had worked on the electrolyte-dependent viscosity of salt solutions (Kunz, 2009), the work of Franz Hofmeister and collaborators at the end of the 19th century (Hofmeister, 1888a,b) is considered the starting point of the topic of SIE in contemporary scientific literature. An English translation of this landmark work is available (Kunz, Henle et al., 2004).

Hofmeister and co-workers observed that different salts had a different power to precipitate egg white proteins (globulins and albumins, the first precipitate at lower salt concentration) out of solution. The ordering that emerges is reported in Table 1. The precipitating power of the salts in the table diminishes in going from left to right and top to bottom. This regularity was highlighted by Hofmeister who noted that the ability of the salt to precipitate proteins depends *both* on the anion and cation (Kunz, Henle

Table 1: Values from Hofmeister's original study on the precipitation of egg globulin (Hofmeister, 1888a; Kunz, Henle et al., 2004). Each cell shows the lowest concentration of the salt composed by the corresponding ions that is able to precipitate the protein. The concentration is expressed in $Eq\,l^{-1}$, where the equivalent molar mass of each ion corresponds to its molar mass ($M_I/g\,mol^{-1}$) divided by its stoichiometric coefficient (ν): $Eq = m_{salt}/(M_{cation}/\nu_{cation} + M_{anion}/\nu_{anion})$, where m_{salt}/g is the salt mass per litre. The cell background shading highlights the groups individuated by Hofmeister based on the salt effectiveness in precipitating proteins. The darker the shade, the lower the salt precipitating power. The cells with the darkest shade and no value indicate salts for which no protein precipitation could be achieved within their solubility interval. The grey cell indicates a salt with very poor solubility. Where the cell background is white, the salt has not been tested.

	Li^+	Na^+	K^+	NH_4^+	Mg^{2+}
SO_4^{2-}	1.57	1.60		2.03	2.65
HPO_4^{2-}		1.65	1.61	2.51	
CH_3COO^-		1.69	1.67		
$citrate^{3-}$		1.68	1.67	2.71	
$tartrate^{2-}$		1.56	1.51	2.72	
HCO_3^-			2.53		
CrO_4^{2-}		2.62	2.64		
Cl^-		3.63	3.52		
NO_3^-		5.42			
ClO_3^-		5.53			

et al., 2004). The explanation that he provided for this phenomenon was that salts withdraw water from the solubilised protein, causing it to precipitate. Different salts have different potency in 'absorbing' water. Hofmeister went on to test the generality of his hypothesis by salt-precipitating a range of very chemically distinct colloids: isinglass (collagen derived from the swim bladders of fish), colloidal ferric oxide and sodium oleate. Very similar responses to the blood serum and egg globulin were found, consolidating the hypothesis and calling for further studies.

Research into SIE has had surges in the following 150 years, and exhaustive reviews of the literature and the evolution of scientific thought on SIE are available (Cacace et al., 1997; Collins and Washabaugh, 1985; Jungwirth and Cremer, 2014; Kunz, Lo Nostro et al., 2004; Kunz and Neueder, 2009; Lo Nostro and Ninham, 2012; Ninham and Lo Nostro, 2010).

1.3 THEORIES OF ION-SPECIFICITY

A definition of SIE that effectively conveys the weight of history on our understanding of the matter is that of Lo Nostro and Ninham (2012): 'by specific ion effects we mean effects not accommodated by classical theories of electrolytes'.

In fact, the classical theories that have been developed and employed during the 19th and 20th century, such as the Debye-Hückel theory of the activity of strong electrolytes and the Derjaguin, Landau, Verwey, Overbeek (DLVO) theory for the stability of colloid suspensions, fail to predict the system behaviour except for very dilute electrolyte solutions (close to ideality). As a consequence, the quantitative description of systems containing higher concentrations or more complex combinations of charged solutes, such as biological fluids, electrochemical solutions, the precipitation of colloids, the self-assembly of surfactants and the foaming of seawater have been inaccessible.

The restriction of the Debye-Hückel theory to dilute systems was clearly stated by its authors, but others nonetheless applied the theory as if it were a general one. Efforts focused on adding parameters and extensions in order to make this oversimplified model fit, rather than on the development of new approaches.

The classical theories are mainly based on electrostatic intuition. These models account for the non-ideality of electrolyte behaviour only at very dilute concentration, and the introduction of fitting parameters such as the ionic radii is needed to square with experimental values at higher concentrations. That is, ion-specificity is not built into these models, and this is because they are not accounting for the Van der Waals forces, or they are not treating them adequately (Ninham and Yaminsky, 1997). Van der Waals forces include all of the 'electrodynamic' forces: the collective and coordinated interactions of moving electrons (Parsegian, 2006), and are further subdivided into interactions between permanent dipoles ('Keesom' forces); interactions between a permanent dipole and the transient dipole induced in a nonpolar molecule by the permanent dipole itself ('Debye' forces); and interactions between transient dipoles of nonpolar but polarisable bodies ('London' dispersion forces) (Parsegian, 2006). Dispersion forces depend on the particular ion: they are ion-specific and they are coupled to the electrostatic forces, therefore a separate mathematical treatment of the two (that implies they are additive) is not satisfactory. In addition the potential needs to be calculated for many-body interactions, which are not pairwise additive: the many-body problem must be tackled. Although the inclusion of many-body quantum electrodynamics in the classical theories is widely agreed upon, this is not an easy task, and several groups are employing different approaches, mainly continuum treatments and molecular dynamics simulations (MD).

Concerted efforts to understand the fundamental origins of the Hofmeister series and SIE in general have emerged (Arslanargin et al., 2016; T. L. Beck, 2011; Duignan, Baer and Mundy, 2016; Duignan, Baer, Schenter et al., 2017a,b; Duignan, Parsons et al., 2013a,b, 2014a,b,c; Jungwirth and B. Winter,

2008; Ninham, Duignan et al., 2011; Ninham and Yaminsky, 1997; Pollard and T. L. Beck, 2016, 2017; Shi and T. Beck, 2017).

This brief summary does not capture just how dynamic the theoretical work in the field currently is. In fact, there exists a plurality of positions on what details are most relevant in the theory, and even on where we are in our progress (that is, what remains to be understood). These are reflected in a number of publications and the following list is a brief selection: Boström et al. (2005), dos Santos et al. (2010), Gurau et al. (2004), Jungwirth and Cremer (2014), Kunz, Lo Nostro et al. (2004), Leontidis (2002, 2016), Lo Nostro and Ninham (2012), Parsons, Boström, Lo Nostro et al. (2011), Pegram and Record (2008), Schwierz, Horinek and Netz (2010), Schwierz, Horinek, Sivan et al. (2016), Y. Zhang and Cremer (2006, 2010) and Y. Zhang, Furyk et al. (2005). Each approach offers benefits and time will reveal the realm in which these different treatments are best applied. Nevertheless, the outlook looks promising (Lo Nostro and Ninham, 2016; Okur et al., 2017).

1.4 AN EXPERIMENTALIST'S POINT OF VIEW

Developing an understanding of SIE is a fundamental affair that has been actively investigated for a long time. It is compelling because of the widespread importance of electrolyte solutions across science and technology.

I would like to reflect here on my experience with SIE as a university student. During my early studies, I acquired an understanding of electrolyte solutions that drew mainly on electrostatic intuitions, and on quantities difficult to define such as hydration, hydrophobic forces or water structure. Only at an advanced stage I was exposed to the relevance of SIE: despite being acquainted with the high level of specificity that chemistry implicates, the encounter was a wondrous one. Somehow I had assumed that SIE were not that relevant and that our understanding of SIE was crystalline. I therefore came to the conclusion that, across the uncountable experimental applications and uses of electrolyte solutions, a number of other scientists could be in my same situation. That is, that their deep knowledge of the specificities of the particular system at hand might not necessarily be accompanied by an appreciation of the generality of the phenomenon of SIE.

The lack of coverage of SIE in introductory courses translates into cohorts of natural scientists graduating with little awareness of the matter, and this is so potentially disadvantageous that there are publications advocating for an introduction of the concept across the disciplines where electrolyte solutions are important (Friedman, 2013). If even the meaning of measurements of quantities like pH has to be revisited, as the measurement outcome is extremely ion-specific (Salis, Pinna et al., 2006), it is advisable to inform the

students at the start of their curricula, rather than to request a change in their *forma mentis* later. There are indeed cases where the effect of ions on a system are small with regards to the overall result, and in these cases the specific nature of the ions can be ignored, but this should be determined *a posteriori*.

1.5 MOTIVATIONS FOR THIS WORK

As the phenomenology of SIE is very complex, and the theorisation difficult, it is very hard to identify how the various interactions in solution balance, and what the overarching rules are. Everything seems to be equally relevant. This makes the work of theorists and experimentalists very difficult. The present work aims at improving this condition, in the first place by attempting an identification of the dominant variables that affect SIE in different experimental situations, and secondly by providing data that can offer a broader testing ground than those available so far in the literature.

The trigger for the research encompassed by this thesis was activated a few years ago by debate on the origin of SIE. The main point of discussion was on the fundamental origin of SIE. Do they originate from the ions alone, from the interactions of the ions with the solvent, from the interaction of the ions with a surface, or a mix of all of the above?

A way to address the above questions is by investigating the solvent-dependency of SIE, in order to ascertain the importance of the solvent. Whereas different types of ions and surfaces have been thoroughly analysed in relation to SIE, the same detailed investigation has not yet been applied to solvents.

Some knowledge that the SIE are evident in non-aqueous solvents was available prior to this work, but a comprehensive investigation into SIE in non-aqueous solvents had not been conducted (Bilaničová et al., 2008; Henry and Craig, 2008; Peruzzi, Ninham et al., 2012; Z. Yang, 2009). This work commenced seeking answers to the following questions: is water a special solvent in regards to manifestation of SIE? If not, how do SIE manifest in non-aqueous solvents — are the same trends as in water evident? Are there properties of the solvents or the ions directly or simply correlated to the SIE trends? Are the SIE trends experiment-dependent?

A deliberate choice was made to carry out these investigations in a qualitative manner, by focussing on the *trends* in SIE. This is because, this being among the first systematic exploratory studies of SIE in non-aqueous solvents, we deemed that it would be more useful to acquire a broad general picture rather than detailed quantitative information on a circumscribed system.

Ultimately, the expectation was that an improved knowledge of SIE in non-aqueous systems would advance our understanding of SIE in aqueous systems. As such, a theory that makes quantitative prediction of SIE in aqueous systems would also undergo the additional challenge of being tested against observations in non-aqueous solvents.

1.6 NON-AQUEOUS ELECTROLYTES

Although aqueous electrolytes have received the largest interest, non-aqueous electrolyte solutions are relevant in a number of applications, particularly those encompassing electrochemical and electroanalytical aspects. This is because non-aqueous solvents offer a variety of advantages over aqueous solutions, that include different solvating properties, larger electrochemical windows and the prevention of hydration and hydrolysis (Zuman and Wawzonek, 1978). Drawbacks are the toxicity of many non-aqueous solvents, and in some cases the high volatility and flammability.

Examples include battery technology (Aurbach et al., 2004; Li et al., 2013; M. Winter and Brodd, 2004); supercapacitors, where acetonitrile (MeCN) and propylene carbonate (4-methyl-1,3-dioxolan-2-one) (PC) are the solvents of choice (Béguin et al., 2014; M. Winter and Brodd, 2004); electrodeposition of metals (Jorné and Tobias, 1975; Simka et al., 2009); semiconductors (Fulop and Taylor, 1985; Lincot, 2005; Nicholson, 2005) including nanowires, as in R. Chen et al. (2003); conductive polymers (Ko et al., 1990) and fuel cells (M. Winter and Brodd, 2004). Non-aqueous solvents are also employed in analytical techniques such as non-aqueous capillary electrophoresis (Bjørnsdottir et al., 1998; Riekkola, 2002) and liquid chromatography (Jane et al., 1985) and are relevant in the rates of chemical reactions involving ionic transition states, such as S_N2 reactions (Parker, 1962). Non-aqueous solvents such as dimethyl sulfoxide (DMSO) and formamide (FA) are also important in life sciences, the first in polymerase chain reaction (PCR) and as a cryoprotecting agent for the preservation of cells, tissues and organs; the latter as a DNA denaturant. Methanol (MeOH) and ethanol (EtOH) are relevant in energy production. The systematic effect of different ions in the aforementioned applications has been studied only in some cases, such as in Lo Nostro, Mazzini et al. (2016).

1.7 OUTLINE OF THE THESIS

In the following chapters, I articulate the studies I performed on SIE in non-aqueous solvents.

These open with a review of the available literature in Chapter 2: in this chapter I identify the trends of SIE in a coherent way.

Chapter 3 is concerned with the fundamental trends of SIE in different non-aqueous solvents by investigating the electrostrictive volume, a standard bulk property of solutions.

I consequently review the use of the 'volcano plots' and the law of matching water affinities (LMWA) concept in Chapter 4, and extend these to non-aqueous solvents, for standard thermodynamic properties such as the energies of solution, but also for real-concentration ones: the activity coefficients and the solubility of electrolytes.

The exposition of my experimental work begins in Chapter 5, with the general procedures and the materials employed, and the issues encountered; the results obtained in the size-exclusion chromatography (SEC) of electrolytes experiments follow in Chapter 6; finally, the quartz crystal microbalance (QCM) investigations of the anion-specific conformation of polymer brushes are presented in Chapter 7.

I discuss all the results obtained in this work collectively in Chapter 8 to give a general picture of this exploratory qualitative work on SIE in non-aqueous solvents, and to outline its general implications.

In Chapter 9, I summarise the conclusions and delineate possible further work.

The appendices contains supplementary material in support of the discussion.

2 LITERATURE REVIEW

This chapter is reproduced with revisions and changes from:

V. Mazzini and V. S. J. Craig (2016), 'Specific-ion Effects in Non-aqueous Systems', *Curr. Opin. Colloid Interface Sci.* 23, pp. 82–93, DOI: 10.1016/j.cocis.2016.06.009.

2.1 INTRODUCTION

A reasonable starting point for this work is to review and analyse the available knowledge on SIE in non-aqueous solvents. This chapter therefore contains a review of the published literature on the matter, with the specific goal of looking for *trends* in the SIE in non-aqueous systems. The analysis is performed with the following questions in mind:

1. Is a consistent trend in the strength of SIE seen in different experiments for the same non-aqueous solvent?
2. Do the trends in the strength of SIE in the non-aqueous solvents match those observed in water?
3. Are the trends observed in non-aqueous solvents consistent with the Hofmeister or lyotropic series?
4. Can the SIE observed be related to the properties of the solvent?

The present review is limited to works that *explicitly* investigate SIE in non-aqueous solvents, as tracing publications that have only tangentially touched on the topic complicates the search due to the sprawled body of work on non-aqueous electrolytes.

In addition, only phenomena in neat solvents are covered. There is a considerable number of publications regarding electrolytes in mixed solvents, but this goes beyond the scope of this thesis, which addresses neat solvents only, as it is investigating the role of the solvent in SIE. I regard mixed solvents as adding an additional level of complexity on the matter of SIE in non-aqueous solvents, that is beyond the scope of this work.

The terminology that is going to be used is presented in Section 2.3. The properties of the solvents investigated are listed in Table 2.

A review summarising the general trends on the topic of SIE in non-aqueous solvents has not previously been compiled, as pointed out recently

by Kunz (2014), though Marcus has made a substantial contribution, in addition to his large personal scientific production, in reviewing and tabulating the existing works regarding electrolytes in non-aqueous solvents (Jenkins and Marcus, 1995; Marcus, 2015; Marcus and Hefter, 2004; Marcus, Hefter and Pang, 1994). The gap is addressed here, with the aim to obtain insight into the general manifestation of SIE in non-aqueous solvents. This is made challenging by the scarcity and patchiness of the data on the behaviour of salts in non-aqueous solvents, which is partly due to the low solubility of electrolytes in many of them.

The majority of the data that are discussed in this chapter are contained in a recent book from Marcus (2015). This is a carefully compiled work that includes critically tabulated data. It is a recent and updated collection of the state-of-the-art knowledge about aqueous and non-aqueous electrolyte solutions, and that makes it an invaluable reference for anyone interested in the topic.

2.2 MANIFESTATIONS OF SIE

The outcome of most measurements and experiments involving electrolyte solutions is dependent on the particular ions present (Kunz, 2010; Lo Nostro and Ninham, 2012). The effect is most often observed as a modulation in the magnitude of a property (i.e. surface tension, conductivity, activity of enzymes) or as a difference in the concentration of electrolyte required to induce a particular change (such as in the precipitation of colloids and proteins). However and notably, in some cases, different ions of the same charge induce the opposite effect. Often the strength of the effect varies regularly across the anions and cations, even in systems that are dissimilar.

A large number of experimental works limit themselves to reporting the presence of SIE in a small set of electrolytes, without then attempting a more systematic study. Often, the recognition of SIE is used as a self-standing explanation for the observed trend, as if the underlying mechanisms were fully understood. In a number of cases, the presence of a series is improperly claimed, as the electrolytes compared differ both in cations and anions, or only two salts have been considered. In order to produce work that is actually helpful in understanding SIE, the electrolytes studied must share a common ion, otherwise it is not possible to separate the contribution of the anions and cations. Then, the minimum number of electrolytes required to identify a series is three ions, but a larger range is highly desirable.

Assuming that the series produced by the anions and cations are independent is naive: SIE trends often change depending on the counterion present, and even reverse (see Section 2.3). Therefore, the anion series ob-

served when the common cation is Li^+ can be very different from the anion series when Cs^+ is the common counterion. Thus it is desirable to investigate the full matrix of combinations of cations and anions. Cations and anions always come at least as a pair and it is not possible to work on a real world experimental system that has a single isolated charge: electrical neutrality has to be maintained in the system. Therefore, resorting to the above methods is the only way to decipher the variations imparted by one of the two ions.

To the exculpation of us experimentalists, it has to be acknowledged that often limits are imposed by the experiment, or the solubility of the salts themselves, and therefore it is often quite difficult to achieve a characterisation of a broad variety of electrolytes.

2.3 TERMINOLOGY

The ordering of the salts that emerged from Hofmeister's work (1888) has since been referred to as the 'Hofmeister series', and the phenomenon as 'Hofmeister effects' or 'specific-ion effects'. Also the term 'lyotropic series' has been used (Calligaris and Nicoli, 2006; Fridovich, 1963; Larsen and Magid, 1974; Leontidis, 2016; Schott, 1984), although the phrase was originally introduced by Voet (1937) only for the behaviour of hydrophilic colloids in the presence of salts.

The series observed and reported are not always the same as the one found by Hofmeister for the precipitation of egg albumins, but often vary and even invert depending on the experiment and experimental conditions. That is the series can reverse due to changes in pH, concentration, temperature, counterion and surface charge (Heyda et al., 2010; Lyklema, 2009; Parsons, Boström, Maceina et al., 2010; Parsons and Ninham, 2011; Robertson, 1911; Schwierz, Horinek, Sivan et al., 2016; Senske et al., 2016). Therefore, nowadays the Hofmeister series is not precisely defined and the appellative is sometimes even used when the series is not followed. The ordering is seen to vary slightly from one publication to the next (Leontidis, 2002; Salis and Ninham, 2014; Vlachy, Jagoda-Cwiklik et al., 2009; Wiggins, 1997; Y. Zhang and Cremer, 2006), but despite this the overall trends of the series are agreed upon. There are also examples where the SIE on a system are categorised by authors as a Hofmeister series when in fact the magnitude of the effect shows a V-shaped ordering (with the minimum or the maximum usually occupied by chloride for the anions) rather than a monotonic trend (Schwierz, Horinek and Netz, 2010; Tóth et al., 2008; Varhač et al., 2009; Žoldák et al., 2004), which of course is inconsistent with the very definition of a monotonic series.

The variations observed in the ordering of SIE between different experiments and even the same experiment under different conditions hinder theorists' attempts at achieving a physical description and a mathematical formulation for SIE. It is often tacitly attributed to the influence of ions on the solvent— usually water (Collins and Washabaugh, 1985; Hribar et al., 2002)—and/or surfaces.

In this work, the phrase 'specific-ion effects' is used as an umbrella-term to describe *all* circumstances in which the type of ion has a pronounced influence on a measurable property of a solution; while the definition of 'Hofmeister effects' is reserved for the subset of SIE in which the strength of the effects of the ionic species follows the Hofmeister series. Also, the lyotropic series (Voet, 1937) is here recognised as a different series to the Hofmeister series, noting that, although sometimes these terms are used interchangeably, they are not equivalent as remarked by Marcus in his recent book (Marcus, 2015). The ordering of ions according to their lyotropic number was introduced by Voet (1937), based on their effects on several properties of colloidal suspensions: the smaller the lyotropic number the more effective the ion is at promoting flocculation, for instance.

The Hofmeister and lyotropic series are depicted in Fig. 1. This figure attempts to account for the variability seen in reports of the Hofmeister series in the literature. The ordering of ions that is highly consistent across different studies forms the backbone of the series and is shown in the centre. The positions of other ions are indicated by a bar to show the range of positions in the series that have been reported for that ion. The various distinctions and adjectives that have been used in the literature to group the ions according to their behaviour (such as 'kosmotropes/ chaotropes') are reported in the figure as well, and apply for most ions in the Hofmeister series. An evident exception is guanidinium, $C(NH_2)_3^+$, which is a poorly hydrated chaotrope and a 'structure breaker' (Mason, Neilson et al., 2003), while being the most effective protein denaturant; a different special case is constituted by the tetraalkylammonium cations: the particular correlation between their ion properties and the Hofmeister trend is discussed further below. The divide between the major groupings is usually set at chloride for anions and at sodium for cations: this is depicted by the horizontal grey bar in Fig. 1. Notably, cations and anions of analogous properties such as size, surface charge densities, etc., have *opposite* effects on protein stability and precipitation. That is, small, kosmotropic anions salt-out proteins, whereas small, kosmotropic cations generally salt-in proteins (with the already noted exceptions for cations). For a detailed discussion of the complex balance of the specific interactions of ions with the different sites of a protein (backbone, charged side-chains, hydrophobic and polar surface groups), see Okur et al. (2017) and Salis and Ninham (2014).

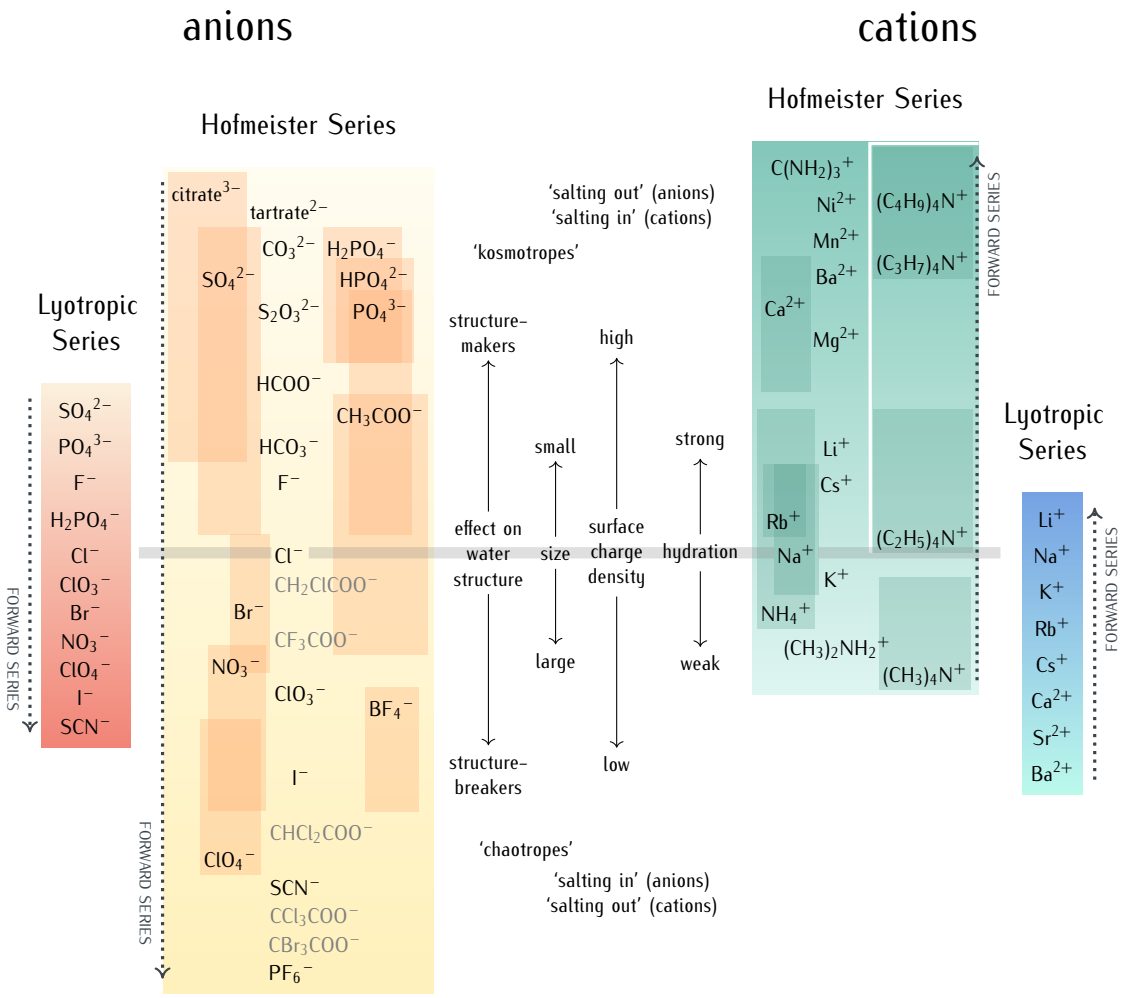

Figure 1: The Hofmeister and lyotropic series of ions in water. The forward direction for each series is indicated by the corresponding arrow. For the Hofmeister ions the forward series is the one of decreasing effectiveness at precipitating proteins out of solution. For the lyotropic ions, the forward series corresponds to increasing lyotropic number. The Hofmeister series were obtained by combining those reported in several references: for anions, Cacace et al. (1997), Collins and Washabaugh (1985), Hamaguchi and Geiduschek (1962), Hanstein (1979), Kunz (2010), Kunz, Henle et al. (2004), Maiti et al. (2009), Pinna et al. (2005), von Hippel and Schleich (1969), von Hippel and Wong (1964), Y. Zhang and Cremer (2010) and Zhao (2016); for cations, Arakawa and Timasheff (1984), Cacace et al. (1997), Carpenter and Lovelace (1935), Fischer and Moore (1907), Jain and Ahluwalia (1996), von Hippel and Schleich (1969), von Hippel and Wong (1964) and Zhao (2016). The ion is positioned in its most agreed upon ranking, and bars indicate the variations in position among different publications. The relative positioning of the haloacetates is well-known, but their positioning with respect to the 'classic' anions of the series is certain only in a few cases. This uncertainty is reflected by presenting these ions in grey text rather than black. The ethyl- to butylammonium cations ordering is known with respect to the tetramethylammonium ion, but not to the other cations in the series with certainty. A white line has therefore been drawn around these ions to mark the discontinuity. Ions at one end of the series are often attributed with having the opposite effect to ions at the other end of the series. As such there is a point in the series where the influence of ions reverses. The grey horizontal line traces the divide that corresponds to this property reversal. Exceptions to this classification are Rb^+ and Cs^+, which are larger and less hydrated than Na^+ and K^+; the guanidinium ion ($C(NH_2)_3^+$) and the tetraalkylammonium cations which are discussed in the text. The ions of the lyotropic series, as defined by Voet (1937), are integrated with those from Marcus (2015).

The salting-out ability of the tetraalkylammonium series decreases from $(CH_3)_4N^+$, generally a salting-out cation (although this can change depending on conditions, see Jain and Ahluwalia (1996) and von Hippel and Wong, 1964), to $(C_4H_9)_4N^+$, which is a very effective salting-in agent (Jain and Ahluwalia, 1996; Mason, Dempsey et al., 2009). This behaviour is analogous to the anions series, where smaller ions are more effective salting-out agents. But the water structure-making ability of the tetraalkylammonium cations also progressively increases with the length of the alkyl chains (and therefore the cation size), due to 'hydrophobic hydration' (Marcus, 1994; Zhao, 2016), in contrast to what happens for the inorganic anions and cations. Therefore, the relationship between the size (and surface charge density) of the tetraalkylammonium cations and their effect on water structure (and on protein stability) is the opposite of the one observed for inorganic cations. Few accounts of the relative positioning of the tetraethyl- to tetrabutylammonium ions with respect to the main cations of the series are available: these ions are therefore separated by a white line in Fig. 1, but their positioning follows their general behaviour (Marcus, 1994; Zhao, 2016): $(C_2H_5)_4N^+$ is considered as neutral to salting-in, and $(C_4H_9)_4N^+$ is extremely salting-in; $(CH_3)_4N^+$ has generally a salting-out effect, and can be more or less potent than NH_4^+ depending on the experiment (Hyde et al., 2017).

The ordering of ions in the Hofmeister and lyotropic series is similar, but it is not identical. They are most similar for anions. Notable are the inversions of fluoride with dihydrogenphosphate, chlorate with bromide, and nitrate and iodide with perchlorate between the series. For cations, the two series run in *opposite* directions, and whereas the divalent cations ordering is mirrored from the Hofmeister to the lyotropic series, the ordering of the alkali metal cations is not: the lyotropic series follows the cation size from caesium to lithium, whereas the Hofmeister series (in its most commonly proposed order) runs as: potassium > sodium > rubidium > caesium > lithium. Notably, the lyotropic numbers are not available for the tetraalkylammonium cations, and therefore these ions cannot be positioned within the lyotropic series. These distinctions between the Hofmeister and the lyotropic series will be used later in the identification of SIE trends in non-aqueous solvents.

The lyotropic numbers are mostly determined by considering the stability of colloidal systems, whereas the Hofmeister series describes a much broader range of complex phenomena seen across biological systems, colloidal dispersions, surface properties and solution structure. As noted by Voet, the lyotropic series correlates quite well with a single property of the ions, their enthalpy of hydration, at least for the cations. The Hofmeister series does not correlate directly with a single property of the ions, and this is because of the complex interplay of the properties of the ion, the interaction of ion and solvent and, in the case of an interfacial interaction, the characteristics of the interface. Such complexity is one of the reasons why a

theory of Hofmeister effects has not been achieved after more than a century from its first report.

In the ensuing chapters, we are going to also encounter cases where the ordering is ion-dependent, but neither the Hofmeister nor lyotropic series is evident, as for anions, the viscosity B-coefficients (*see* B_η) (VBC) (Bilaničová et al., 2008; Collins and Washabaugh, 1985), the limiting molar ionic conductivity (LMC) (Marcus, 2015), and for the ion pairing of tetraalkylammonium salts in ethanol (Giesecke, Mériguet et al., 2015).

In the cases where the series runs opposite to the conventional order, that have been known as either the reverse, inverse or indirect Hofmeister series, the term 'reverse' is employed here.

The great success of the Hofmeister series is that it is so regularly observed in systems that are very different: a great many systems adhere to the Hofmeister paradigm (Kabalnov et al., 1995; Lagi et al., 2007; Lonetti et al., 2005; Oncsik et al., 2015; Piculell and Nilsson, 1989; Roberts et al., 2002; Ru et al., 2000; Salomäki et al., 2004; Schott, 1995; Vrbka et al., 2004; Washabaugh and Collins, 1986; Wiggins, 1997). The negative consequence of this is that, on occasion, observations of SIE are described as Hofmeister effects when the strength of the influence of the ions does not follow the Hofmeister series, this somewhat clouds the field.

2.4 CHARACTERISTICS OF NON-AQUEOUS SOLVENTS

Non-aqueous solvents are liquids other than water. This work is concerned with the subset of non-aqueous solvents that are capable of dissolving salts. These solvents usually have high dielectric constant in order to be able to separate the charges of the electrolyte. But many other subtle and interwoven characteristics come into play to define what is a good solvent for electrolytes: the capability of donating/accepting hydrogen bonding, the physical size of the solvent molecules, the specific chemical groups in the solvent molecule that interact with the anion and the cation. Extensive descriptions are available in Izutsu (2009) and Marcus (2015).

Table 2 lists the properties of the solvents included in this thesis. Among those, the empirical parameters expressing solvent acidity and basicity (donor and acceptors numbers) need illustration.

The Gutmann Donor Number DN is a measure of the basicity of a solvent. It represents the ability of solvent molecules to donate a free electron pair from their donor atoms (O, N or S). It is quantified as the negative of the standard molar enthalpy of reaction $-\Delta H^{\ominus}$ of the solvent with the Lewis acid antimony pentachloride $SbCl_5$, in dilute solution in the inert solvent 1,2-dichloroethane at 25 °C (Marcus, 2015). These values are expressed in $kcal\,mol^{-1}$ units, as a difference from the reference solvent 1,2-dichloroethane, for which DN is set to 0.

Table 2: Physical properties of the solvents investigated.

solvent	M_i/g mol^{-1}	ρ/g cm^{-3}	ϵ_R	μ/D	η/mPa s	α/Å^3 [a]	κ_T/GPa^{-1}	DN [b]	AN [b]	pK_{SH} [b]	hydrogen bonding [c]
water	18.015	0.9970^{25}	80.100	1.8546	0.890	1.49 [d]	0.459	18	54.8	14.0	3D H-bond
MeOH	32.042	0.7914^{20}	33.0	1.7	0.544	3.26	1.214	30	41.5	17.2	linear H-bond
EtOH	46.068	0.7893^{20}	25.3	1.69	1.074	5.13	1.119	32	37.1	19.1	linear H-bond
PrOH	60.095	0.7997^{25}	20.8	1.55	1.945	6.96		30	33.7	19.4	linear H-bond
2PrOH	60.095	0.7809^{25}	20.18	1.56	2.04	6.98		36	33.5	21.1	linear H-bond
EG	62.068	1.1135^{20}	41.4	2.36	16.06	5.72	0.364	20	43.4		3D H-bond
FA	45.041	1.1334^{20}	111.0	3.73	3.34	4.22	0.399	24	39.8	16.8	3D H-bond
NMF	59.067	1.011^{19}	189.0	3.83	1.678	6.01	0.577 [e]	27	32.1	10.74	linear H-bond
DMF	73.094	0.9445^{25}	38.25	3.82	0.794	7.93	0.627 [e]	26.6	16	29.4	aprotic
DMA	87.120	0.9372^{25}	38.85	3.7	1.927	9.69		27.8	13.6	23.9	aprotic
MeCN	41.052	0.7857^{20}	36.64	3.925	0.369	4.44	1.10 [f]	32	18.9	33.3	aprotic
ACE	58.079	0.7845^{25}	21.01	2.88	0.306	6.47	1.262	17	12.5	32.5	aprotic
DMSO	78.133	1.1010^{25}	47.24	3.96	1.987	8.03	0.523 [g]	29.8	19.3	33.3	aprotic
EC	88.062	1.3214^{39}	89.78	4.81 [h]	1.925^{40} [i]	6.6	0.435 [j]	16.4			aprotic
PC	102.089	1.2047^{20}	66.14	5.36 [h]	2.5120 [i]	8.55	0.590	15.1	18.3		aprotic

Data from the CRC Handbook of Chemistry and Physics (Lide, 2010), unless otherwise noted.

M_i: molar mass; ρ: density at the t in °C indicated by the superscript; ϵ_R: dielectric constant; μ: dipole moment; η: viscosity at 25 °C; α: experimental static polarisability; κ_T: isothermal compressibility at 20 °C; DN: electron pair donicity (Gutmann donor number); AN: (Gutmann-Mayer acceptor number); pK_{SH}: solvent autoprotolysis constant.

[a] Bosque and Sales, 2002; [b] Izutsu, 2009; [c] Jenkins and Marcus, 1995; [d] Weiss et al., 2012; [e] Easteal and Woolf, 1985; [f] Easteal and Woolf, 1988; [g] Marcus and Hefter, 1997; [h] Chernyak, 2006; [i] Petrella and Sacco, 1978; [j] Naejus et al., 1998; [k] Barthel, Neueder and Roch, 2000; [l] Sassi et al., 2007.

The hydrogen bond donicity and electron pair acceptance of a solvent is correlated to its capability to contribute protons for hydrogen bonding. It is therefore limited to protic and protogenic solvents (solvents with a methyl group adjacent to a C=O, C≡N, or NO_2 group). The Gutmann–Mayer acceptor numbers AN of a solvent (Lewis acid) are evaluated from the nuclear magnetic resonance (NMR) chemical shift of the ^{31}P atom of triethylphosphine oxide $Et_3P{=}O$ in dilute solution in the solvent of interest. The AN values are dimensionless numbers, the higher the number, the higher the solvent acidity (Marcus, 2015).

Other scales have been defined, such as the solvent acidity scales are Kosower's Z values, Dimroth and Reichardt's E_T scale, Kamlet and Taft's α_{KT} parameter. conversely, solvent basicity scales include Kamlet and Taft's β_{KT} parameter (Izutsu, 2009).

The combination of properties of these solvents is very diverse. Based on the combinations of some of the properties general classifications have been introduced (Izutsu, 2009), which are not adopted here.

2.5 METHODOLOGY

In the ensuing sections, a range of studies into SIE in non-aqueous solvents are presented, grouped by solvent, and the SIE trends that emerge are discussed. It is immediately apparent that SIE are as ubiquitous in non-aqueous solvents as they are in water.

For each study the observed trend of SIE for the cations and anions has been extracted and displayed in a colour-coded table to assist in the interpretation of the data. The order of each table column runs from largest value at the top to smallest at the bottom. The series are compared to those defined in Fig. 1. A pale yellow cell background indicates a forward Hofmeister series, orange a reverse Hofmeister series, lilac a lyotropic series and purple a reverse lyotropic series. No colour is used where a series does not follow either the Hofmeister or lyotropic series. Where an individual ion is not included in the colour scheme for a particular series, this indicates that this ion is not in its correct location in the series. In some columns, the ammonium cation and the tetraalkylammonium cations (NH_4^+, $(CH_3)_4N^+$, $(C_2H_5)_4N^+$, $(C_3H_7)_4N^+$, $(C_4H_9)_4N^+$), which I will collectively refer to as the 'ammonium class' in the discussion, are offset to the right, so that they may be easily considered separately from the alkali metal cations. This has been done as these two classes of cations show consistent behaviour when considered separately but not an overall trend when considered together.

The trends in SIE observed for a range of properties of *aqueous* electrolyte solutions are shown in Table 3. These include (Marcus, 2015):

Table 3: Trends in SIE observed in water. Data from Marcus (2015).

water				
MRT	RDD*	MHC	LMC	VBC
cations				
Li^+	Li^+	$(C_4H_9)_4N^+$	Rb^+	$(C_4H_9)_4N^+$
Na^+	Na^+	$(C_3H_7)_4N^+$	Cs^+	$(C_3H_7)_4N^+$
K^+	$(C_4H_9)_4N^+$	$(C_2H_5)_4N^+$	NH_4^+	$(C_2H_5)_4N^+$
NH_4^+		$(CH_3)_4N^+$	K^+	Li^+
		Li^+	Na^+	$(CH_3)_4N^+$
		Na^+	$(CH_3)_4N^+$	Na^+
		K^+	Li^+	NH_4^+
		Rb^+	$(C_2H_5)_4N^+$	K^+
		Cs^+	$(C_3H_7)_4N^+$	Rb^+
			$(C_4H_9)_4N^+$	Cs^+
anions				
F^-	ClO_4^-	$SCN^- = ClO_4^-$	SO_4^{2-}	HPO_4^{2-}
SO_4^{2-}	I^-	F^-	CO_3^{2-}	$H_2PO_4^-$
Cl^-	Br^-	I^-	Br^-	CO_3^{2-}
Br^-	Cl^-	Cl^-	Cl^-	CH_3COO^-
NO_3^-		Br^-	I^-	SO_4^{2-}
I^-			NO_3^-	F^-
			ClO_4^-	Cl^-
			SCN^-	SCN^-
			HPO_4^{2-}	Br^-
			F^-	NO_3^-
			$HCOO^-$	$HCOO^-$
			CH_3COO^-	ClO_4^-
			$H_2PO_4^-$	I^-

* from electrolytes, ionic values not available.

- The NMR molecular reorientation time (MRT) of the solvent in the presence of ions, calculated as the ratio $\tau_{S(I)\,or}/\tau_{S\,or}$, of the molecular reorientation time constant in the presence of ions to the time constant of the neat solvent.

- The relative limiting static dielectric decrement (RDD) of an ion solution as its concentration approaches zero, calculated as the ratio of the limiting static dielectric decrement caused by the ion to the relative permittivity of the pure solvent $-\delta_{(I)}/\varepsilon_S\ (c_E \to 0)$, with units $dm^3\,mol^{-1}$.

- The constant pressure standard partial molar heat capacity of the ion (MHC), C_{PI}^{∞} in $J\,K^{-1}\,mol^{-1}$ which is the difference between the specific heat of the solution of the ion and that of the pure solvent, in the limit of infinite dilution.

- The limiting molar ionic conductivity (LMC) λ_I^{∞} ($S\,cm^2\,mol^{-1}$).

- The viscosity B-coefficients (*see* B_η) (VBC) of the Jones-Dole viscosity equation (Jones and Dole, 1929).

Table 4: Trends in SIE observed in MeOH. Data from Marcus (2015).

methanol				
MRT	RDD*	MHC	LMC	VBC
cations				
Li^+	Na^+	$(C_4H_9)_4N^+$	$(CH_3)_4N^+$	$(C_4H_9)_4N^+$
Na^+	$NH_4^+ = (C_4H_9)_4N^+$	$(C_3H_7)_4N^+$	Cs^+	Na^+
K^+	Li^+	$(C_2H_5)_4N^+$	$(C_2H_5)_4N^+$	Li^+
		$(CH_3)_4N^+$	NH_4^+	K^+
		K^+	Rb^+	$(C_3H_7)_4N^+$
		Cs^+	K^+	$(CH_3)_4N^+$
		Na^+	$(C_3H_7)_4N^+$	Cs^+
		Li^+	Na^+	$(C_2H_5)_4N^+$
			Li^+	
			$(C_4H_9)_4N^+$	
anions				
Br^-	Cl^-	ClO_4^-	ClO_4^-	Cl^-
I^-	Br^-	SCN^-	I^-	Br^-
SCN^-	I^-	I^-	SCN^-	I^-
ClO_4^-	ClO_4^-	Br^-	NO_3^-	NO_3^-
		Cl^-	Br^-	ClO_4^-
		F^-	Cl^-	

* from electrolytes, ionic values not available.

This table is an important point of comparison for the measurements made in non-aqueous solvents. In fact, some of these measurements follow a known series and therefore are of particular interest.

It must be noted that water is somewhat soluble in all the non-aqueous solvents and its presence may have some influence on the experimental results. The degree to which water has been excluded is not apparent in many of the studies and therefore cannot be addressed here.

2.6 Methanol

Putting water aside, MeOH is an excellent solvent for electrolytes (see Fig. 84). Whilst other solvents have higher dielectric constants than MeOH, they are inferior solvents for electrolytes. The excellent solubility of electrolytes can be attributed to the small size of its molecule: indeed the small size of the water molecule is clearly as important in conferring it the title as 'universal solvent' as is its high dielectric constant. In addition, the values of AN and DN, close to water, must be considered (Table 2). Essentially, MeOH has a sufficiently high dielectric constant to lower the electrostatic energy penalty of separating charges that is essential for dissolution of salts and a small molecular size which promotes dissolution.

Table 5: Additional trends in SIE observed in MeOH.

methanol		
NMR ion nuclear relaxation rates *	NMR hydroxyl proton chemical shift at 40 °C †	vapour pressure depression ‡
cations		
Rb^+	$Rb^+ = K^+ = Cs^+$	Cs^+
Na^+	$(CH_3)_4N^+$	Rb^+
Cs^+	Na^+	K^+
Li^+	$(C_2H_5)_4N^+$	Na^+
	$(C_4H_9)_4N^+$	
	Li^+	
anions		
Br^-	ClO_4^-	ClO_4^-
Cl^-	I^-	Cl^-
	SCN^-	Br^-
	Br^-	I^-
	Cl^-	
	CN^-	
	CF_3COO^-	
	CH_2ClCOO^-	
	CH_3COO^-	
	F^-	

* from Melendres and Hertz, 1974; † from R. N. Butler and Symons, 1969; ‡ from Barthel, Neueder and Lauermann, 1985.

The order of the strength of SIE observed for studies in MeOH are given in Table 4. Starting with the cations, it is evident that they display no consistent ordering across the experiments. The series are indeed very different from one experiment to the next and therefore the lack of agreement is unlikely due to experimental error. Rather the cation series depends sensitively on the type of experiment being performed. In comparison to the series observed for the analogous experiments in water (Table 3), the overall ordering of the ions is different in MeOH, with the exception of MRT. And even for the MRT experiment, only three cations have been measured in MeOH, so there is not sufficient evidence to conclude that this agreement with the series in water is not just incidental. Where only three ions have been measured no strong conclusions can be drawn.

Next, all the data can be considered, including the additional experiments listed in Table 5, to determine if there is evidence that the Hofmeister series is followed. For the alkali metal cations, four experiments show agreement with the Hofmeister series (see Fig. 1), these are the MRT, the MHC, the NMR ion nuclear relaxation rates (Melendres and Hertz, 1974) and the vapour pressure depression (Barthel, Neueder and Lauermann, 1985). The former two only involve three cations and therefore must be discounted. It is notable that a Hofmeister trend is also observed for NMR ion nuclear relaxation rates in water (Melendres and Hertz, 1974). In contrast, for tetraal-

Table 6: Trends in SIE observed in FA. Data from Marcus (2015).

formamide			
MRT	RDD*	LMC	VBC
cations			
Na^+	$(C_4H_9)_4N^+$	NH_4^+	$(C_4H_9)_4N^+$
K^+	Na^+	Cs^+	Na^+
Rb^+	Li^+	$(CH_3)_4N^+$	Li^+
Cs^+		Rb^+	Rb^+
		K^+	K^+
		$(C_2H_5)_4N^+$	$(C_2H_5)_4N^+$
		Na^+	Cs^+
		Li^+	NH_4^+
		$(C_3H_7)_4N^+$	$(CH_3)_4N^+$
		$(C_4H_9)_4N^+$	
anions			
Cl^-		NO_3^-	NO_3^-
Br^-		$SCN^- = Cl^- = Br^-$	Cl^-
I^-		I^-	Br^-
		ClO_4^-	I^-
		CH_3COO^-	SCN^-

* from electrolytes, ionic values not available.

kylammonium cations, the MHC shows a reversed Hofmeister series, which is also observed in water. LMC follows a lyotropic series for the alkali metal ions both in water and MeOH, and a forward Hofmeister series for the ammonium cations. The ordering of the latter group of cations is consistent also between the VBC experiments in water and MeOH, corresponding to a reverse Hofmeister series.

Examining the anions, an altogether different situation emerges. Firstly, it is clear that there is a more consistent general order of the anions across the experiments. Moreover, the anions are often ordered in accordance with the Hofmeister series (or present only slight deviations from it), noting that in some cases it is in the reverse order. Significantly for MHC the Hofmeister series is followed in MeOH but not in water. Clearly SIE in MeOH are often associated with the Hofmeister series, perhaps moreso than for water.

2.7 Formamide

FA, like water, is protic and forms a three-dimensional hydrogen bonded network, and therefore makes a particularly interesting comparison when considering SIE, where the hydrogen bonding network is often counted as playing a determining role. The order of the strength of SIE observed for studies in FA are given in Table 6.

In considering the cations it is apparent that no consistent ordering of the cation series across the experiments is observed. For alkali metal cations, the LMC, VBC and MRT measurements yield results that are inconsistent with the Hofmeister series. The alkali metal cations show a lyotropic series with regards to LMC (and MRT). The RDD follows a SIE ordering which is neither Hofmeister nor lyotropic, but it must be noted that the ordering of cations is the inverse of the ordering seen in water. In comparing the LMC measurements between water and FA, the overall cation trend is not in agreement. But if the ammonium class of cations (shown offset to the right in the table) is considered separately to the alkali metal ions, both of the trends considered separately are in good agreement.

When considering the anions, it is apparent that the ordering of the ions obtained from conductivity studies is not consistent with the Hofmeister series. However the ordering obtained from VBC and MRT measurements follows the Hofmeister series, although the nitrate ion is not appropriately placed in the VBC data and the MRT data only includes three ions. Many experiments do find a single ion misplaced in the series yet the overall effect is still generally considered as a Hofmeister series, so that precedent is followed here as well. It must be noted that VBC does not follow the Hofmeister series in water.

Overall it can be concluded that both the cations and the anions show some evidence of SIE consistent with those seen in aqueous systems.

2.8 *N*-METHYLFORMAMIDE

N-methylformamide (NMF) is a highly polar, water miscible organic solvent with applications in chemistry and biology. The experimental data showing the trends in the strength of the SIE for NMF is presented in Table 7.

No consistent trend in the cation series is observed across a range of experiments. For some experiments there is a suggestion that the Hofmeister series for cations is followed, but there is an insufficient number of ions measured to make a strong case for this. Interestingly, the forward Hofmeister ordering of cations in RDD coincides with the one observed in FA (Table 6), and is the *reverse* of the trend seen in water. More often occurring is the lyotropic series for alkali metal cations. The LMC of alkali metals cations follows a lyotropic series, whereas the ammonium class of cations follows a forward Hofmeister series: both trends taken separately agree with those of the same property in water. Notably for the VBC experiments the odd situation occurs, in which the ammonium cations have the same order as they do in water, whereas the alkali metal ions show a trend that is the exact reverse (lyotropic) of that seen in water (reverse lyotropic).

Table 7: Trends in SIE observed in NMF. Data from Marcus (2015).

N-methylformamide				
MRT	RDD*	MHC	LMC	VBC
cations				
Li^+ Na^+ K^+ Rb^+ Cs^+	$(C_4H_9)_4N^+$ Na^+ Li^+	K^+ Cs^+ Na^+ Li^+	$(CH_3)_4N^+$ $(C_2H_5)_4N^+$ NH_4^+ Cs^+ Rb^+ K^+ Na^+ $(C_3H_7)_4N^+$ $(C_4H_9)_4N^+$ Li^+	$(C_3H_7)_4N^+$ $(C_2H_5)_4N^+$ Cs^+ K^+ Na^+ Li^+ $(CH_3)_4N^+$ NH_4^+
anions				
Cl^- = Br^- I^-		I^- Br^- Cl^-	SCN^- I^- Br^- ClO_4^- Cl^-	Cl^- Br^- I^-

* from electrolytes, ionic values not available.

There is scarce data to consider for the anions in NMF. In this case the LMC shows a different trend to that seen in water and neither are Hofmeister like. The remaining experimental data suggests a correlation with the Hofmeister series for MRT and VBC and a reverse Hofmeister trend for MHC, albeit on an insufficient number of ions to draw the conclusion confidently.

2.9 *N*,*N*-DIMETHYLFORMAMIDE

N,*N*-dimethylformamide (DMF) is miscible with water and the majority of organic solvents, as such it is used extensively as a solvent for chemical reactions. A summary of the trends in the strength of the SIE in DMF for a range of experiments is presented in Table 8.

No persistent trend is seen in the strength of SIE for the cations or the anions in DMF. The ion-specific trends for alkali metal cations for MHC and the reduction of SO_2, follow forward and reverse Hofmeister series respectively. When comparing the LMC trends in water and DMF we find that in both solvents the ammonium class of cations follows the Hofmeister series and the other ions separately follow the lyotropic series, but the overall trend exhibited in the two solvents is different. The tetraalkylammonium cations in MHC (only two ions, therefore the identification is not strongly supported) and VBC follow a reverse Hofmeister series as in water, but the alkali metals trend in MHC differs and corresponds to a forward Hofmeister rather than

Table 8: Trends in SIE observed in DMF. Data from Marcus (2015) unless otherwise indicated in the table.

N,N-dimethylformamide			
MHC	LMC	VBC	Reduction of SO_2 *
cations			
$(C_3H_7)_4N^+$	NH_4^+	K^+	Li^+
$(C_2H_5)_4N^+$	$(CH_3)_4N^+$	Na^+	Na^+
K^+	$(C_2H_5)_4N^+$	$(C_4H_9)_4N^+$	K^+
Rb^+	Cs^+	$(C_3H_7)_4N^+$	$(C_2H_5)_4N^+$
Na^+	Rb^+	$(C_2H_5)_4N^+$	
Cs^+	K^+		
Li^+	Na^+		
	$(C_3H_7)_4N^+$		
	$(C_4H_9)_4N^+$		
	Li^+		
anions			
Cl^-	SCN^-		
Br^-	NO_3^-		
ClO_4^-	Cl^-		
I^-	Br^-		
	ClO_4^-		
	I^-		

* from Gardner et al., 1981.

reverse lyotropic series. In contrast the trends seen for the anions in MHC and LMC experiments have no relation to those in water nor to the Hofmeister or lyotropic series.

Although the scarce data do not allow for any strong conclusion to be made, it emerges from the available information that the introduction of another methyl group on the NMF molecule drastically changes the SIE manifestation. More data is required to systematically compare FA, NMF and DMF.

2.10 Dimethyl sulfoxide

DMSO is frequently used as a chemical solvent as it is less toxic than DMF and NMF and is miscible with water and a wide range of organic solvents.

Trends in the strength of the SIE observed in DMSO are shown in Table 9. No dominant trend is seen in the ordering of the cations or the anions across a range of experiments in DMSO and only the MHC measurements show clear evidence of a Hofmeister series, with the tetraalkylammonium ions also showing Hofmeister trends for LMC and VBC. Whilst the trends for the MRT and MHC in DMSO are completely different from the ones shown in water (where they show respectively a reverse Hofmeister and a reverse lyotropic ordering), the trends for the LMC and VBC experiments are in fuller

Table 9: Trends in SIE observed in DMSO. Data from Marcus (2015).

dimethyl sulfoxide			
MRT	MHC	LMC	VBC
cations			
Na^+	Na^+	$(CH_3)_4N^+$	$(C_4H_9)_4N^+$
K^+	K^+	$(C_2H_5)_4N^+$	Li^+
Rb^+	Cs^+	Cs^+	$(C_3H_7)_4N^+$
Cs^+	Li^+	Rb^+	K^+
		K^+	Na^+
		Na^+	Rb^+
		Li^+	Cs^+
		$(C_4H_9)_4N^+$	$(C_2H_5)_4N^+$
			$(CH_3)_4N^+$
anions			
Br^-	I^-	ClO_4^-	Br^-
I^-	ClO_4^-	SCN^-	I^-
	Br^-	NO_3^-	NO_3^-
	F^-	Br^-	Cl^-
	Cl^-	I^-	SCN^-
		Cl^-	ClO_4^-

agreement with water when the tetraalkylammonium ions and alkali metals are considered independently. Note that this differs from the correlation seen for VBC measurements in NMF, in which the alkali metal cations were in the reverse order.

The little data available for the anions show no consistent ordering, no recognisable series, or analogy with the trends in water.

2.11 ADDITIONAL SOLVENTS

In this section, the data for the solvents EtOH, PC and ethylene carbonate (1,3-dioxolan-2-one) (EC) are presented and discussed. As these solvents do not dissolve a wide range of electrolytes, the information is necessarily limited.

Other solvents, for which even less information is available, are not discussed in detail, but the series observed in these solvents are included in the summarising Table 13 to give a picture as comprehensive as possible. These solvents consist of the protic 1-propanol (propan-1-ol) (PrOH), ethylene glycol (ethane-1,2-diol) (EG), nitromethane ($MeNO_2$) and the aprotic acetone (propan-2-one) (ACE) and MeCN.

Table 10: Trends in SIE observed in EtOH. Data from Marcus (2015).

ethanol		
MHC	LMC	VBC
cations		
$(C_4H_9)_4N^+$	$(CH_3)_4N^+$	Na^+
$(C_3H_7)_4N^+$	$(C_2H_5)_4N^+$	$(C_4H_9)_4N^+$
$(C_2H_5)_4N^+$	Cs^+	$(C_3H_7)_4N^+$
K^+	Rb^+	Li^+
Cs^+	K^+	K^+
Na^+	$(C_3H_7)_4N^+$	Rb^+
Li^+	NH_4^+	$(C_2H_5)_4N^+$
	Na^+	Cs^+
	$(C_4H_9)_4N^+$	$(CH_3)_4N^+$
	Li^+	
anions		
I^-	ClO_4^-	Br^-
Br^-	SCN^-	ClO_4^-
Cl^-	I^-	
F^-	NO_3^-	
	Br^-	
	CH_3COO^-	
	Cl^-	

2.11.1 Ethanol

The SIE observed in experiments using EtOH as a solvent are summarised in Table 10. Considering the cations first, there is no consistent trend in the strength of SIE exhibited across the experiments, although there is a majority of cases where the Hofmeister series appears.

MHC data for the alkali metal cations display the same ordering as in DMSO, NMF and DMF, and they differ from water in the alkali metals series ordering. In EtOH the LMC data for the alkali metal cations follows a lyotropic series which is consistent with the ordering obtained in water, whereas a reverse lyotropic series is seen for alkali metal ions in the VBC data, which is in agreement with water as well. Consistency is also observed for the tetraalkylammonium cations between water and EtOH in LMC (note that NH_4^+ does not follow the series in EtOH) and VBC. The LMC and VBC trends therefore agree in water for the ammonium ions and the alkali metal ions considered separately, as already observed for other solvents.

For the anions, the conductivity and MHC data is consistent with the Hofmeister series but inconsistent with the trend obtained in water. That is, the LMC and MHC data in EtOH shows a reverse Hofmeister series for the anions that is not observed in those measurements in water.

Table 11: Trends in SIE observed in PC and EC. Data from Marcus (2015).

propylene carbonate			ethylene carbonate
MHC	LMC	VBC	VBC
cations			*cations*
$(C_4H_9)_4N^+$	$(CH_3)_4N^+$	Li^+	Na^+
$(C_3H_7)_4N^+$	$(C_2H_5)_4N^+$	K^+	Li^+
$(C_2H_5)_4N^+$	Cs^+	$(C_4H_9)_4N^+$	K^+
$(CH_3)_4N^+$	Rb^+	$(C_3H_7)_4N^+$	Rb^+
Na^+	K^+	$(C_2H_5)_4N^+$	Cs^+
K^+	$(C_3H_7)_4N^+$		$(C_4H_9)_4N^+$
Cs^+	Na^+		
Rb^+	$(C_4H_9)_4N^+$		
Li^+	Li^+		
anions			*anions*
ClO_4^-	SCN^-	Br^-	Br^-
Br^-	NO_3^-	I^-	Cl^-
Cl^-	ClO_4^-	ClO_4^-	I^-
I^-	I^-		ClO_4^-
	Cl^-		
	Br^-		

2.11.2 Propylene carbonate and ethylene carbonate

PC and EC are aprotic polar solvents that are effective at solubilising a wide range of electrolytes owing to their strong dipole moments. PC differs from EC only for the presence of a methyl group on the lactone ring. Both the solvents are of interest for their low volatility and toxicity, making them potential 'green' solvents for battery applications.

Scarce experimental data is available, and is summarised in Tables 11 and 12.

Considering the cations in PC, the SIE show no persistent trend across a range of experiments. However for both LMC and VBC measurements the trends are consistent with those obtained in water, if and only if, the tetraalkylammonium cations and the alkali metal cations are treated as separate classes. A reverse Hofmeister series is seen for MHC experiments for the tetraalkylammonium cations, in agreement with water, but the alkali metal cations follow a Hofmeister rather than a reverse lyotropic series. The same has been observed for all the alkali metal cations in the non-aqueous solvents discussed to this point.

For the anions there is no consistent trend observed across experiments, but there is evidence of a Hofmeister series for the LMC experiment, as already noted in EtOH (but *not* in water), and also for the VBC experiment (although only three ions are available) and the solubility of potassium salts in PC and EC (Table 12).

Table 12: Additional trends in SIE observed for PC and EC.

propylene carbonate		ethylene carbonate
solubility of K^+ salts *	FT-IR intensity of C=O stretching band *	solubility of K^+ salts †
anions		*anions*
SCN^-	Cl^-	I^-
I^-	SCN^-	ClO_4^-
ClO_4^-	Br^-	NO_3^-
Br^-	I^-	Br^-
CNO^-	ClO_4^-	Cl^-
Cl^-	CNO^-	F^-
F^-		

* from Peruzzi, Lo Nostro et al., 2015; † from Peruzzi, Ninham et al., 2012.

The cation data in EC are only available for one experiment, VBC, which shows a reverse lyotropic ordering of alkali metal ion, in accordance to the observed series in water and other solvents. Anion effects in EC show instead Hofmeister ordering, that agrees with the PC ordering for both the experiments available.

EC solvates mainly through ion-dipole interactions, which are stronger for small anions, therefore dispersion forces must contribute to the solubility of electrolytes in a significant way.

2.12 OTHER INVESTIGATIONS

Experiments in EG and FA show that SIE do not follow the Hofmeister series. The Diels-Alder reaction performed in these solvents in the presence of urea, guanidinium, perchlorate, chloride and quaternary ammonium salts shows a very different salt-dependence than when performed in water (Breslow and Guo, 1988).

Despite these results it is clear that both the Hofmeister series and the lyotropic series are evident in a wide range of solvents and that neither can be considered to be unique to water. Consistent with this are the experiments of Bilaničová et al. (2008), who studied the effects of different anions on the activity of the *Pseudomonas cepacia* lipase in 2-methyl-2-butanol. The enzyme was obtained by lyophilising a concentrated salt solution in water, at pH 7, and it was then dissolved in 2-methyl-2-butanol. The activity of the enzyme was the highest in a completely dry medium (reaction carried in the presence of molecular sieves), and the activity follows a Hofmeister series: $SO_4^{2-} > H_2PO_4^-/HPO_4^{2-} > Cl^- > Br^- = I^- = SCN^-$.

Investigations of SIE were performed also in liquid chromatography experiments. Smuts et al. (2014) used a cyclofructan-6-based chiral stationary phase doped with barium to resolve chiral phosphoric and sulfonic acids. The effect of the counterion of the barium salt added to the mobile phase on retention and enantioselectivity was investigated. It was found that they increase in the order CH_3COO^- < methanesulfonate (MSA$^-$) < CF_3COO^- < $ClO_4{}^-$, which is in agreement with the Hofmeister series. They also compared the selectivity and retention by changing the mobile phase from MeOH to EtOH. They found that the latter offers higher retention and improves enantioselectivity. They explain the phenomenon with the fact that the lower dielectric constant of EtOH forces closer ion pairs with the barium cation adsorbed on the stationary phase, which causes a longer retention and closer interaction with the chiral stationary phase. Sanganyado et al. (2014) investigated the effect of Hofmeister anions on the enantioresolution, enantioselectivity and retention factor of basic chiral pharmaceuticals in polar ionic mode liquid chromatography. Retention follows the ion-specific series: CH_3COO^- > $HCOO^-$ > $NO_3{}^-$.

An ion specific non-Hofmeister series is observed for the kinetics of the reaction of iodination of acetone (Lo Nostro, Mazzini et al., 2016), following the trend HBr < HCl < $HClO_4$ < HF < H_2SO_4 < H_3PO_4.

A technique that has been recently introduced for studying ion association in solution is electrophoretic NMR. The study of the association of monovalent Hofmeister anions paired with the $(CH_3)_4N^+$ cation in the deuterated solvents D_2O, DMSO, MeCN, MeOH, EtOH, shows complex ion-specificity that does not follow the Hofmeister or lyotropic series. These series and are strongly solvent-dependent (Giesecke, Mériguet et al., 2015). Complex non-Hofmeister series are also encountered for the cation association with disperse polyethylene oxide in MeOH solution (Giesecke, Hallberg et al., 2016). The authors identify that ion-polymer binding only happens for cations with a surface charge density below 0.10 $Å^{-2}$ to 0.15 $Å^{-2}$. Interestingly, no relevant changes in the series are observed for different cation-counterion pairings (the counterions investigated are AcO^-, I^- and $ClO_4{}^-$) have been investigated as counterions. This is in disagreement to the LMWA principle, which is extensively reviewed later in Section 4.4.

2.13 AN OVERALL VIEW

The SIE trends across a range of experiments for a range of solvents are summarised in Table 13. This table also includes the data for solvents that have not been discussed in the previous sections because of the little amount of data available: PrOH, EG, $MeNO_2$, ACE and MeCN.

Whilst in some cases the data is limited, the survey reveals some interesting information. The SIE observed are different for different solvents. It would be desirable to relate the SIE to the properties of the solvent, however at this stage the complexity and extensive variation seen in SIE across a range of solvents and a range of experiments does not allow for simple generalisations. Additionally, in many experiments the confidence with which the SIE can be labelled as a Hofmeister series or a lyotropic series is diminished due to the limited availability of data.

The LMC and VBC experiments are particularly interesting as the data is the most extensive across the range of solvents for these experiments. In comparing the trends observed in the non-aqueous solvents to those in water, it is apparent that the ammonium cations should be treated separately to the alkali metal cations, as in no case did the overall ordering of the ions coincide between water and a non-aqueous solvent, but in many cases the ordering did coincide when the classes were treated separately. Considering the LMC of cations, in general the ammonium class of cations follows the Hofmeister series and the alkali metal cations follow the lyotropic series. It should be highlighted here that the lyotropic numbers are not available for the ammonium class of cations, therefore the ordering of these ions can only be identified as either 'Hofmeister series' or 'other'. For the anions, a reverse Hofmeister series is observed when a series is evident, but not in all cases. It is expected that the LMC will be strongly influenced by the size and solvation of an ion and for this reason the tetraalkylammonium cations might be expected to behave differently to other ions because of their size (i.e. the increase in size due to the addition of methyl groups in the four lateral chains is not compensated by the change in solvation or other properties of the ion, as discussed in Section 2.3). As with the LMC experiments, the VBC experiments show agreements with both the sub-series of cations. The VBC experiments reveal that the cations follow the same trends as in water for both of the series considered separately for EtOH, DMF (two ions only), DMSO, PC (two ions) and EC. However, for three solvent, the VBC ordering of the ammonium cations agrees with that in water, whereas the ordering of the alkali metal cations does not: in MeOH and FA, the alkali metal cations follow a different trend (other than a lyotropic or Hofmeister series), and for NMF, the alkali metal cations series is reversed compared

Table 13: Summary of the SIE series seen for a range of experiments in water and non-aqueous solvents. Protic solvents are in bold, aprotic solvents are italicised. Series with three or less ions have been indicated in parentheses.

cations

solvent	MRT	RDD	MHC		LMC		VBC	
			$R_4N^{+\dagger}$	$M^{+\ddagger}$	R_4N^+	M^+	R_4N^+	M^+
water	R-HS	other	R-HS	R-lyo	HS	lyo	R-HS	R-lyo
MeOH	R-HS (3)	other	R-HS	HS	HS	lyo	R-HS (3)	other
EtOH	/	/	R-HS	HS	HS	lyo	R-HS	R-lyo
FA	R-lyo	other§	/	/	HS	lyo	R-HS (3)	other
NMF	R-lyo	other§	/	HS (3)	HS	lyo	R-HS	lyo
DMF	/	/	? (2) R-HS	HS	HS	lyo	R-HS	/ (2)
DMSO	R-lyo	/	/	HS	HS (3)	lyo	R-HS	R-lyo
PC	/	/	R-HS	HS	HS	lyo	R-HS	/ (2)
EC	/	/	/	/	/	/	/	R-lyo
PrOH	/	/	R-HS	/ (2)	HS	lyo	/	/
EG	R-lyo	/	/	/	HS	lyo	/	/
$MeNO_2$	/	/	/	R-lyo	HS	lyo	/	/
ACE	/	/	/	/	HS	lyo	R-HS	/ (2)
MeCN	/	/	? (2) R-HS	other	HS	lyo	R-HS	other

anions

solvent	MRT	RDD	MHC	LMC	VBC
water	HS	R-HS	other	other	other
MeOH	HS (3)	HS	R-HS	R-HS	HS
EtOH	/	/	R-HS	R-HS	/ (2)
FA	HS (3)	/	/	other	HS
NMF	HS (3)	/	R-HS (3)	other	HS (3)
DMF	/	/	other	other	/
DMSO	/ (2)	/	other	other	other
PC	/	/	other	R-HS	HS (3)
EC	/	/	/	/	HS (3)
PrOH	/	/	R-HS	R-HS	/
EG	HS (3)	/	/	HS	/
$MeNO_2$	/	/	other	R-HS	/
ACE	/	/	/	other	other
MeCN	/	/	HS	R-HS	HS

† ammonium cations, where R=H, (CH_3), (C_2H_5), (C_3H_7) or (C_4H_9).
‡ alkali metals.
§ reverse series of the one in water for RDD.

to that in water. That is, in NMF the forward lyotropic series is observed, whereas the *reverse* lyotropic series is observed in water. NMF and FA also show reversed SIE series with respect to water in the RDD experiment. The cause of series reversal in water has attracted some interest and has been related to salt concentration and surface charge (Parsons, Boström, Maceina et al., 2010). This investigation reveals that the solvent itself can also cause series reversal. It remains an interesting and important challenge to explain these phenomena.

A similar situation exists for the MHC data: the ammonium cations consistently follow a reverse Hofmeister ordering across solvents, but the alkali metal cations show a lyotropic trend only in water and $MeNO_2$, and by contrast the rest of the non-aqueous solvents follows a forward Hofmeister series.

For anions, the ordering observed in water is seldom reflected by the non-aqueous solvents. It is very interesting that both in the LMC and VBC case, a wider agreement of series is seen for cations rather than anions. This highlights that, with respect to those properties, the solvents behave similarly with cations and less so with anions. One might expect the opposite as stronger SIE are usually observed for anions.

2.14 SUMMARY

There is evidence of the Hofmeister series (forward or reverse) for the anions in *all* solvents except DMF, DMSO, $MeNO_2$ and ACE and for the cations in *all* solvents apart from EC. Though it is notable that the Hofmeister series is not uniformly observed for a particular experiment across the solvents and no particular effect of the solvent being protic is evident. Notably, in MeOH the anions follow the Hofmeister series in the MHC, LMC and VBC experiments even though this is not the case for these experiments in water. Also the other non-aqueous solvents can show a Hofmeister series in one of these experiments, where it has not been observed in water. Whereas for the cations, Hofmeister or lyotropic series are evident in a number of experiments with good consistency across solvents. Clearly the situation is very complex, and explanations for this situation are difficult to find. However, recognition that these series exist in non-aqueous solvents brings into focus the depth of complexity of SIE evident when a wider range of solvents are observed and highlights that there is a substantial degree of similarity in SIE present across a range of solvents, albeit with some outstanding differences.

The available evidence indicates that all solvents on occasion will exhibit the Hofmeister series and the lyotropic series and no particular property of a solvent can be correlated to the Hofmeister effect or the lyotropic series.

Therefore, we can conclude that neither series can be attributed to the properties of a solvent. The significant challenge is then to determine why particular experiments reveal the Hofmeister series or lyotropic series in one solvent and not another solvent. Resolution of this may well require a deep understanding of the full range of SIE. This question is addressed in the following chapters.

It also emerges that, in order to achieve a comprehensive picture of this phenomenon in non-aqueous solvents, many more experiments must be performed and theoretical investigations pursued. This is no small task and requires a renewed interest in the fundamental and systematic investigation of the properties of non-aqueous electrolyte solutions. It is desirable that theorists engaged in tackling the complexity of SIE extend their considerations to include non-aqueous solvents. I argue that explanations for SIE in aqueous systems can be rigorously tested by assessing their utility in explaining SIE observed in other solvents.

3 ELECTROSTRICTION

This chapter is reproduced with minor changes from:

V. Mazzini and V. S. J. Craig (2017), 'What Is the Fundamental Ion-specific Series for Anions and Cations? Ion Specificity in Standard Partial Molar Volumes of Electrolytes and Electrostriction in Water and Non-aqueous Solvents', *Chem. Sci.* 8 (10 2017), pp. 7052–7065, DOI: 10.1039/C7SC02691A.

3.1 MOTIVATION

A major point of debate is the fundamental origin of SIE, as highlighted in Section 1.5. The questions framing the debate are: What are the fundamental interactions for the manifestation of SIE? Do they originate from the ion alone, or the ion-solvent interaction, or the ion-ion interaction (i.e. at higher ion concentrations), or the ion-surface interaction, or a mix of the above?

Here I attend to the above questions by investigating properties of a very simple system, in the conviction that the ion-specificity (if present) manifested in this setting is a close expression of the fundamental mechanisms. The simplest electrolyte solution setting can be individuated in an infinitely dilute solution. Therein, only ion-solvent interactions can be assumed to take place, and ion- ion interactions are excluded. In addition, we can look at a property of the solution for which no interacting surfaces intervene: a bulk property. Therefore the interference of interacting surfaces is removed, and we are left with a system where only ion-solvent interactions are in place. This is the best possible setting for studying the role of the solvent on SIE, and also to gather information on whether SIE are manifest in the limit of infinite dilution, and in the absence of surface or ion-ion interactions.

Finally, in order for this general investigation of solvent effects on SIE trends to be meaningful, data must be available for a large number of solvents: the standard partial molar volume of electrolytes in solution and the derived electrostriction are properties that respond to all of the above requirements. They are available in the critically compiled collections by Millero (1971, 1972a) for aqueous electrolytes and by Marcus and Hefter (2004) for electrolytes in non-aqueous solvents.

3.2 PARTIAL MOLAR VOLUMES AND ELECTROSTRICTION

The partial molar volume of a species 'i' in solution represents the change in volume of the solution upon addition of one mole of solute at constant temperature, pressure, and other components of the solution (Lewis and Randall, 1961; Millero, 1972b):

$$\overline{V}_i = \left(\frac{\partial V}{\partial n_i}\right)_{T,\ P,\ n_{j\neq i}} \qquad [1]$$

where $\overline{V}_i$ is the partial molar volume of the solute in solution; V the total volume of the solution and n_i the number of moles of solute present in solution. The partial molar volume is an important quantity because it can be demonstrated that the partial molar volumes of the components of a solution are additive:

$$V = \sum_i n_i \overline{V}_i \qquad [2]$$

The partial molar electrostrictive volume of the species 'i' in solution ($\overline{V}_{i\,el}$), can be calculated in the following way (Marcus, 2011):

$$\overline{V}_{i\,el} = \overline{V}_i - \overline{V}_{i\,intr} \qquad [3]$$

Where $\overline{V}_i$ is the experimentally derived partial molar volume of the species 'i' in solution and $\overline{V}_{i\,intr}$ is the intrinsic molar volume of the species 'i', which is not directly measurable by experiment. If the *standard partial molar volume* $\overline{V}_i^\circ$ is used in the calculation, the electrostrictive volume at infinite dilution $\overline{V}_{i\,el}^\circ$ (also known as $\overline{V}_{i\,el}^\infty$, standard partial molar electrostrictive volume) is obtained, which reflects *only* the interactions between the solute and the solvent (and not solute-solute effects). These standard quantities are the subject of the present chapter.

The dependence of the standard partial molar volume $\overline{V}_i^\circ$ on solvent properties has been investigated by Hamann and Lim (1954) in water and three other solvents: there exists an inverse linear relationship between the standard partial volume of the electrolytes and the compressibility of the solvent. Later, Marcus, Hefter and Pang (1994) applied a stepwise multivariable linear least-squares regression to the standard partial molar volumes of ions in solution in order to relate them to solvent and ion properties. They found that the cube of the ion radius is the major contributor to the standard partial molar volume in solution. Secondly, the electron pair-sharing capability of the ion plays a role. The solvent compressibility and self-association are also found to play a role, but no correlation is observed with solvent dipole moment and relative permittivity. Marcus has also investigated the

ion specificity of electrostriction (Marcus, 2013): he analysed the correlation between the standard molar ionic electrostriction and the surface tension increment generated by ions. He found a reasonable correlation for cations but not for anions.

The connection between SIE and partial standard molar volumes of ions in solution can be made in two ways. Jenkins and Marcus (1995) demonstrate that a relationship between the viscosity *B*-coefficient of the Jones-Dole equation and the molar volume of the ion in solution exists. On the other hand, the ion specificity of the viscosity *B*-coefficient has been known for a long time, starting with the work of Cox and Wolfenden (1934). Additionally Collins (1997) accommodated it intrinsically in the formulation of his 'LMWA'. This suggests that the link between electrostriction, which derives from the standard molar volumes of electrolytes, and SIE is straightforward. If such a connection can be elaborated in non-aqueous solvents, additional insight into the nature of SIE will be gained, as partial molar volumes are useful for the understanding of the interactions occurring in aqueous and non-aqueous solutions (Millero, 1972b). The standard molar quantities are therefore perfectly suited for the purpose of studying SIE in non-aqueous solvents.

Much careful work has been done in the experimental determination of partial molal volumes of electrolytes in solution, therefore abundant information is already available in the literature, and has been extensively reviewed (Marcus and Hefter, 2004; Millero, 1971). As the experimental observable used for the calculation of the electrostrictive volume is the density of the solution, this type of experiment can be quite simple to perform in order to acquire data where missing (given the right experimental apparatus is available — see Appendix G.1.1). Attempts to calculate electrostriction theoretically have also been made (Desnoyers et al., 1965; Kasprowicz and Kielich, 1967; Marcus and Hefter, 1999; Padova, 1963).

The electrolyte exerts a constricting pressure on the order of hundreds of MPa on the surrounding solvent molecules (Marcus, 2011), thus reducing the volume the solvent occupies. Figure 2 shows the dependence of the electrostrictive volume on molal concentration in water (calculated using the density data of electrolyte solutions from Söhnel and Novotný, 1985): its magnitude is different for each electrolyte. The electrostriction is larger at small concentrations as the effect saturates when all of the solvent is electrostricted.

As electrostriction happens when a salt is dissolved in a solvent, the volume of the resulting solution is usually different from the sum of the volumes of the individual components, and generally smaller. This phenomenon is attributed to the fact that, under the huge electric field exerted by an ion, the solvent contracts (or more rarely expands). This results in the partial molar volume of the electrolyte being different from the 'intrinsic'

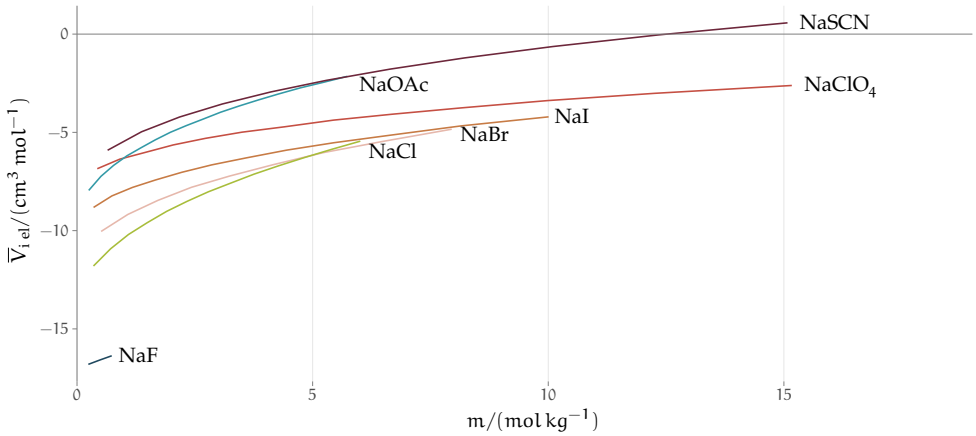

Figure 2: Concentration dependence of the electrostrictive volume in water for a range of electrolytes. The density of the electrolyte solutions used for the calculation of the electrostrictive volume are taken from Söhnel and Novotný (1985).

volume of the electrolyte by a quantity which is the electrostrictive volume. A scheme showing the dependence of the electrostrictive volume upon the reciprocal magnitude of the standard molar volume and the intrinsic molar volume is shown in Fig. 3. This phenomenon has always been connected to the electrostatic field density of the ion. Detailed treatment of partial molar volumes and electrostriction has been performed in previous reviews (Marcus and Hefter, 2004; Millero, 1972b).

3.3 METHODS

The molar electrostrictive volume is calculated here according to Eq. [3], using the standard partial molar volume in order to obtain the standard partial molar electrostrictive volume (hence in the limit of infinite dilution):

$$\overline{V}^{\ominus}_{i\,el} = \overline{V}^{\ominus}_{i} - \overline{V}_{i\,intr} \qquad [4]$$

Where $\overline{V}^{\ominus}_{i}$ is the standard partial molar volume of the species 'i' in solution, and $\overline{V}_{i\,intr}$ is the intrinsic molar volume of the species 'i'. The criteria used for selecting the values of standard and intrinsic molar volumes of electrolytes are detailed in Section 3.3.1.

In this chapter, the electrostrictive volume of electrolytes in water and 11 non-aqueous solvents, five of which are protic (MeOH, EtOH, FA, NMF, EG) and the remaining aprotic (DMSO, PC, EC, ACE, MeCN, DMF) is discussed. These non-aqueous solvents cover a wide range of relative permittivities ϵ_R and compressibilities κ_T, as shown in Table 2.

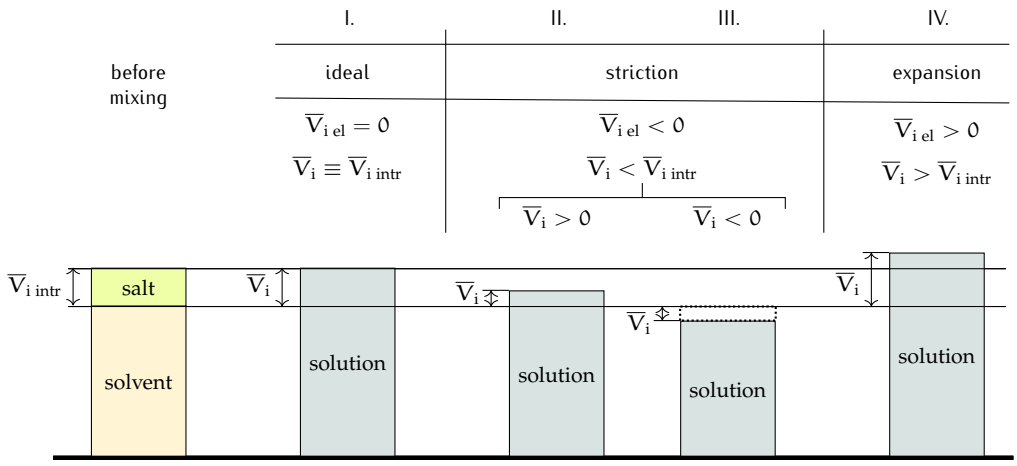

Figure 3: Schematic of the range of possible outcomes for the final solution volume when a salt is dissolved in a solvent, depending on the effect of electrostriction. In this picture, the depicted volume of salt corresponds to one mole (therefore it represents the intrinsic molar volume). This picture particularly helps in visualising the case where the molar volume of the salt in solution is negative.

Electrolytes containing the following monovalent anions and cations are considered in this chapter (here listed according to the Hofmeister series):

$$AcO^- > F^- > Cl^- > Br^- > I^- > ClO_4{}^- > SCN^-$$
$$K^+ > Na^+ > Rb^+ > Cs^+ > Li^+$$

Where AcO^- stands for the acetate anion, CH_3COO^-. It must be noted that for this set of anions, the difference between Hofmeister and lyotropic series is only reflected in the position of I^- and $ClO_4{}^-$. Conversely, the ordering of the cations is very different in the two series (see Fig. 1).

3.3.1 Data sources and selection criteria

This section details the criteria used for selecting the values to analyse and to employ in Eq. [4].

The values of the standard molar volumes, $\overline{V}_i^\circ$, are taken from Millero's review (Millero, 1971) in the case of water (with the exception of SCN^-, for which the conventional volume indicated by Marcus (Table 2, 2011) has been used), and from Marcus and Hefter's review (Marcus and Hefter, 2004) in the case of non-aqueous solvents. Not all the $\overline{V}_i^\circ$ values of electrolytes in non-aqueous solvents have been experimentally determined (and reviewed), but, using an extra-thermodynamic assumption, Marcus and Hefter (2004) calculated the $\overline{V}_i^\circ$ values of the single ions in solution, which are additive. The missing values (where possible) have therefore been calculated by using the ionic standard partial molar volumes. These values are affected by a sig-

nificant error, $\pm 2\,cm^3\,mol^{-1}$ for the ion $\Rightarrow \pm 4\,cm^3\,mol^{-1}$ for the electrolyte, and the associated error bars are plotted in the standard and electrostrictive volumes plots. Where no error bars are plotted, the standard partial molar volume of that electrolyte is the recommended, experimentally measured, (many independent sources obtained consistent results) value according to the reviews of Millero (1971) for water and Marcus and Hefter (2004) for non-aqueous solvents. The same applies for the plots of the electrostrictive volumes, which are derived from the standard molar volumes according to Eq. [4].

The intrinsic molar volume of the electrolytes, $\overline{V}_{i\,intr}$, cannot be experimentally measured. Several methods to estimate it have been proposed (for a review of them, see section 3.2 Marcus, 2011), but no general agreement on the best method exists. Some of these methods rely on the ionic radii to estimate the intrinsic molar volume of an electrolyte. As these values are sensitive to the assumptions of the model chosen, this approach is not followed here. According to Marcus (2011), reasonable estimates (independent of the ionic radii) of the intrinsic molar volume of an electrolyte in solution are the ones proposed by Pedersen et al. (1984), who extrapolated the intrinsic volume of the molten electrolyte down to room temperature (assuming the expansivity coefficient is constant), and by Marcus (2010), who calculated the intrinsic volume for highly soluble salts, by extrapolating their partial molar volumes in concentrated solution up to a concentration where all the water present is completely electrostricted. If this information is not available, an acceptable estimation of the intrinsic molar volume can be obtained from the crystal molar volume $\overline{V}_{cryst}$ (Eq. [5]), which was first used by Padova (1964):

$$\overline{V}_{cryst} = \frac{M_i}{\rho_{salt}} \qquad [5]$$

where $\overline{V}_{cryst}$ is the molar volume of the crystalline electrolyte, M_i the molar mass of the electrolyte and ρ_{salt} is the density of the salt. This method requires that the coordination number of the cations and anions is the same in solution as in the crystal lattice. This estimate is the most prone to error, as it is well known that coordination numbers are not the same for the same ion across different solvents (Marcus, 2016).

Therefore, for the purpose of this work, the estimates calculated by Pedersen et al. (1984) were used when available, otherwise the ones given by Marcus (2010) were used, and $\overline{V}_{cryst}$ was employed as the last resort. These criteria were used to determine $\overline{V}_{i\,intr}$ for all the electrolytes considered. The intrinsic molar volumes of the electrolytes used in this work are shown in Fig. 4. The one-letter labels ('M', 'S' or 'C') drawn in the intrinsic and

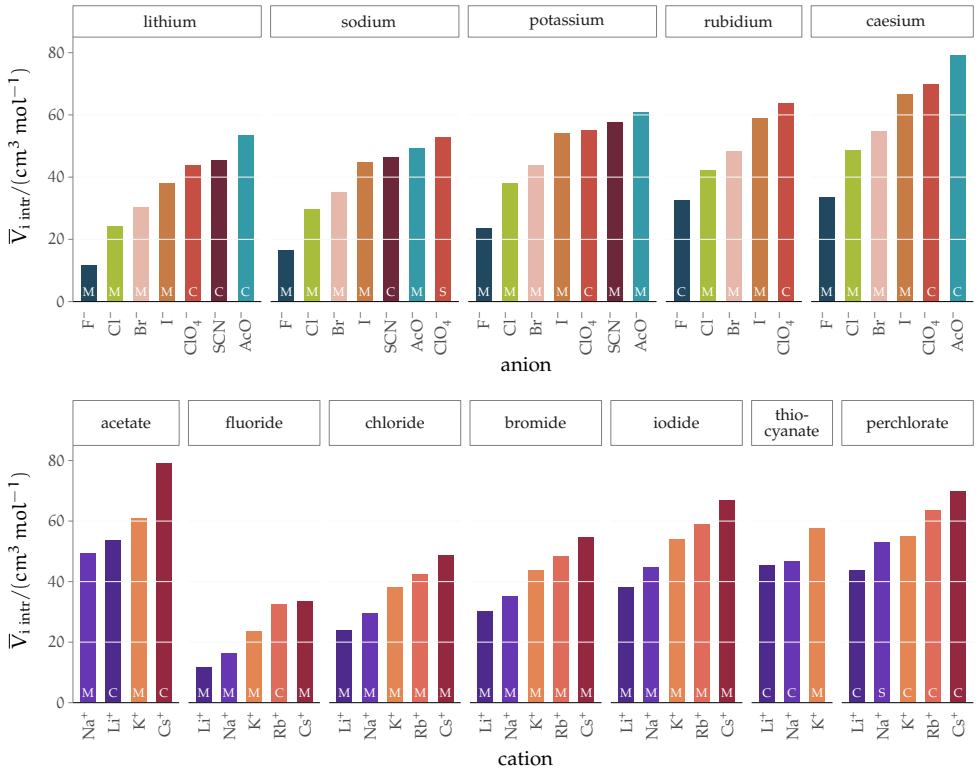

Figure 4: Intrinsic molar volumes $\overline{V}_{i\,intr}$ of the electrolytes grouped by cation (top) and by anion (bottom). The white labels inside the plot bars indicate the method of estimation of the intrinsic molar volume. M: extrapolation from molten salts, from Pedersen et al. (1984); S: from 'soluble salts' (Marcus, 2010); C: crystal volume, as in Eq. [5].

in the electrostrictive volume plots specify the method used to estimate the intrinsic molar volume of that electrolyte.

The *ionic* intrinsic molar volumes are even more elusive quantities to calculate, as they require again an extra-thermodynamic assumption to split the electrolyte volumes into their ionic constituents, thus introducing new sources of error. In addition, although ionic quantities are convenient, they do not reflect the physical reality as cations or anions are never on their own in solution. The present analysis is therefore restricted only to the electrolytes as a whole.

3.4 RESULTS AND DISCUSSION

3.4.1 Standard molar volumes

The standard partial molar volumes $\overline{V}_i^{\ominus}$ are shown for water in Fig. 5. Note that all the values used in the calculations and the calculated electrostrictive values are provided in Table 31 of Appendix A. The plots of the stand-

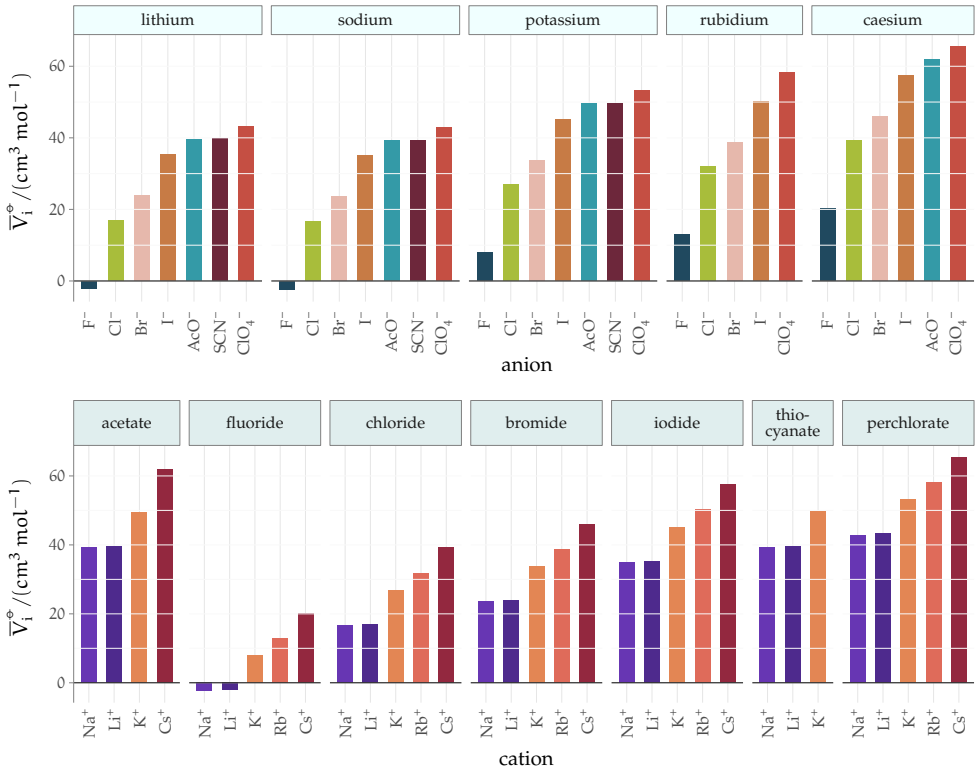

Figure 5: Standard molar volumes $\overline{V}_i^\phi$ of the electrolytes in water grouped by cation (top) and by anion (bottom).

ard partial molar volumes in all the remaining solvents are provided in Appendix A.2 (Figs. 33 to 43).

The series observed in each solvent for electrolytes sharing a common ion are outlined in Tables 14 and 15.

In order to make the large amount of information in the table more accessible, the cells have been colour-coded to indicate when the ordering of the ions corresponds to a series. The colour coding legend is given in the table caption. Where an overall series is found but an ion is incorrectly placed in the series, no colour is used for the incorrectly placed ion. It is apparent that the standard molar volumes follow the Hofmeister series for the anions, and the reverse lyotropic series for the cations. Note that as data is only available for two anions in EC, no series can be recognised but the ordering of the two ions is in line with the Hofmeister series and therefore consistent with the other solvents. The only exception observed for the anions is the ion-specific ordering observed in ACE: it follows an order that does not correspond to any known series. With regard to the cations, data is only available for two cations in ACE so no series can be recognised, but the ordering of the two ions is consistent and in line with the the reverse lyotropic series and therefore confers with the results for other solvents. An exception to the reverse lyotropic series observed is for cations paired with iodide in EG. Additionally, the order of the sodium and lithium cations is reversed in water compared to all of the other solvents, indicating that for one of these

Table 14: Specific-ion effects series exhibited in the standard molar volume of electrolytes $\overline{V}_i^{\ominus}$: anions arranged by a common cation.

cation	protic solvents						aprotic solvents					
	water	MeOH	EtOH	FA	NMF	EG	PC	EC	DMSO	ACE	MeCN	DMF
Li^+	F^- Cl^- Br^- I^- AcO^- SCN^- ClO_4^-	F^- Cl^- Br^- I^- SCN^- ClO_4^-	F^- Cl^- Br^- I^- AcO^-	F^- Cl^- Br^- I^- SCN^- ClO_4^-	Cl^- Br^- I^- SCN^- ClO_4^-	F^- Cl^- Br^- I^-	Cl^- Br^- I^- ClO_4^-	I^- ClO_4^-	F^- Cl^- Br^- I^- ClO_4^-	Cl^- ClO_4^- Br^- I^-	Cl^- Br^- I^- SCN^- ClO_4^-	Cl^- Br^- I^- ClO_4^-
Na^+	F^- Cl^- Br^- I- AcO^- SCN^- ClO_4^-	F^- Cl^- Br^- I^- SCN^- ClO_4^-	F^- Cl^- Br^- I^- AcO^-	F^- Cl^- Br^- I^- SCN^- ClO_4^-	Cl^- Br^- I^- SCN^- ClO_4^-	F^- Cl^- Br^- I^-	Cl^- Br^- I^- ClO_4^-	I^- ClO_4^-	F^- Cl^- Br^- I^- ClO_4^-	Cl^- ClO_4^- Br^- Br^- I^-	Cl^- Br^- I^- SCN^- ClO_4^-	Cl^- Br^- I^- ClO_4^-
K^+	F^- Cl^- Br^- I^- AcO^- SCN^- ClO_4^-	F^- Cl^- Br^- I^- SCN^- ClO_4^-	F^- Cl^- Br^- I^- AcO^-	F^- Cl^- Br^- I^- SCN^- ClO_4^-	Cl^- Br^- I^- SCN^- ClO_4^-	F^- Cl^- Br^- I^-	Cl^- Br^- I^- ClO_4^-	I^- ClO_4^-	F^- Cl^- Br^- I^- ClO_4^-		Cl^- Br^- I^- SCN^- ClO_4^-	Cl^- Br^- I^- ClO_4^-
Rb^+	F^- Cl^- Br^- I^- ClO_4^-	F^- Cl^- Br^- I^- ClO_4^-	F^- Cl^- Br^- I^-	F^- Cl^- Br^- I^- ClO_4^-		F^- I^- Cl^- Br^-	Cl^- Br^- I^- ClO_4^-		F^- Cl^- Br^- I^- ClO_4^-		Cl^- Br^- I^- ClO_4^-	Cl^- Br^- I^- ClO_4^-
Cs^+	F^- Cl^- Br^- I^- AcO^- ClO_4^-	F^- Cl^- Br^- I^- ClO_4^-	F^- Cl^- Br^- I^- AcO^-	F^- Cl^- Br^- I^- ClO_4^-	Cl^- Br^- I^- ClO_4^-	F^- Cl^- Br^- I^-	Cl^- Br^- I^- ClO_4^-		F^- Cl^- Br^- I^- ClO_4^-		Cl^- Br^- I^- ClO_4^-	Cl^- Br^- I^- ClO_4^-

For each cation, the anions are listed from smallest (top) to largest (bottom) standard molar volume. The cell background is coloured if that order of ions corresponds to a known SIE series. Pale yellow corresponds to a direct Hofmeister series.

Table 15: Specific-ion effects series exhibited in the standard molar volume of electrolytes $\overline{V}_i^{\circ}$: cations arranged by a common anion.

anion	protic solvents						aprotic solvents					
	water	MeOH	EtOH	FA	NMF	EG	PC	EC	DMSO	ACE	MeCN	DMF
AcO^-	Na^+ Li^+ K^+ Cs^+		Li^+ Na^+ K^+ Cs^+									
F^-	Na^+ Li^+ K^+ Rb^+ Cs^+	Li^+ Na^+ K^+ Rb^+ Cs^+	Li^+ Na^+ K^+ Rb^+ Cs^+	Li^+ Na^+ K^+ Rb^+ Cs^+		Li^+ Na^+ K^+ Rb^+ Cs^+			Li^+ Na^+ K^+ Rb^+ Cs^+			
Cl^-	Na^+ Li^+ K^+ Rb^+ Cs^+	Li^+ Na^+ K^+ Rb^+ Cs^+	Li^+ Na^+ K^+ Rb^+ Cs^+	Li^+ Na^+ K^+ Rb^+ Cs^+	Li^+ Na^+ K^+ Cs^+	Li^+ Na^+ K^+ Rb^+ Cs^+	Li^+ Na^+ K^+ Rb^+ Cs^+		Li^+ Na^+ K^+ Rb^+ Cs^+	Li^+ Na^+	Li^+ Na^+ K^+ Rb^+ Cs^+	Li^+ Na^+ K^+ Rb^+ Cs^+
Br^-	Na^+ Li^+ K^+ Rb^+ Cs^+	Li^+ Na^+ K^+ Rb^+ Cs^+	Li^+ Na^+ K^+ Rb^+ Cs^+	Li^+ Na^+ K^+ Rb^+ Cs^+	Li^+ Na^+ K^+ Cs^+	Li^+ Na^+ K^+ Rb^+ Cs^+	Li^+ Na^+ K^+ Rb^+ Cs^+		Li^+ Na^+ K^+ Rb^+ Cs^+	Li^+ Na^+	Li^+ Na^+ K^+ Rb^+ Cs^+	Li^+ Na^+ K^+ Rb^+ Cs^+
I^-	Na^+ Li^+ K^+ Rb^+ Cs^+	Li^+ Na^+ K^+ Rb^+ Cs^+	Li^+ Na^+ K^+ Rb^+ Cs^+	Li^+ Na^+ K^+ Rb^+ Cs^+	Li^+ Na^+ K^+ Cs^+	Rb^+ Li^+ Na^+ K^+ Cs^+	Li^+ Na^+ K^+ Rb^+ Cs^+	Li^+ Na^+ K^+	Li^+ Na^+ K^+ Rb^+ Cs^+	Li^+ Na^+	Na^+ Li^+ K^+ Rb^+ Cs^+	Li^+ Na^+ K^+ Rb^+ Cs^+
SCN^-	Na^+ Li^+ K^+	Li^+ Na^+ K^+		Li^+ Na^+ K^+	Li^+ Na^+ K^+						Li^+ Na^+ K^+	
ClO_4^-	Na^+ Li^+ K^+ Rb^+ Cs^+	Li^+ Na^+ K^+ Rb^+ Cs^+		Li^+ Na^+ K^+ Rb^+ Cs^+	Li^+ Na^+ K^+ Cs^+		Li^+ Na^+ K^+ Rb^+ Cs^+	Li^+ Na^+ K^+	Li^+ Na^+ K^+ Rb^+ Cs^+	Li^+ Na^+	Li^+ Na^+ K^+ Rb^+ Cs^+	Li^+ Na^+ K^+ Rb^+ Cs^+

For each anion, the cations are listed from smallest (top) to largest (bottom) standard molar volume. The cell background is coloured if that order of ions corresponds to a known SIE effects series. Purple corresponds to a reverse lyotropic series.

ions there is a solvent interaction that is not seen in other solvents. It is evident from this evaluation of the standard molar volumes of electrolytes in a wide range of solvents that the SIE can be ordered into a fundamental series that is independent of the solvent. Moreover, the standard molar volume is a bulk property. This infers that the series arises solely from the properties of the ions and is almost completely independent of the solvent and extant at low concentration and in the absence of surfaces. The implications of this are discussed further in Section 3.4.4.

3.4.2 Electrostriction in water and non-aqueous solvents

SIE are often attributed to the influence that the ions exert on the solvent, most often water. This has led to terms such as structure-making/structure-breaking and chaotropic and kosmotropic. These arguments generally follow a consideration of the size of an ion and its electrostatic charge. The charge on an ion produces a large electric field and this exerts a pressure on the surrounding solvent molecules that results in electrostriction. Therefore, also electrostriction is explored here as a measure of ion specificity in a wide range of solvents.

The molar electrostrictive volumes calculated from Eq. [4] for water are shown in Fig. 6. The electrostrictive volumes in all the remaining solvents are provided in Appendix A.3 (Figs. 44 to 54).

The first observation is that the electrostrictive volumes for ions sharing a common counterion are different: the magnitude of electrostriction is therefore ion-specific in all of the solvents considered. The series observed in each solvent for electrolytes sharing a common ion are outlined in Tables 16 and 17. For the anion series (shown in Table 16), surprisingly consistent behaviour is observed across the different solvents. The trend observed is predominantly a Hofmeister series across all protic and aprotic solvents. The exceptions are: a reversal of the series in EtOH, a reversal of the series for the caesium salts in NMF and a lyotropic series for the sodium salts in water. The assignment of the series for the sodium salts in water is equivocal, as the electrostrictive values for sodium perchlorate and sodium iodide are very close. If their order is reversed, this system is also consistent with the Hofmeister series. No known ion-specific ordering is observed in ACE, for sodium salts in MeOH, for lithium and caesium salts in EtOH, and for lithium salts in FA. The preponderance of the Hofmeister series produced from the electrostrictive volumes for anions across a wide range of solvents is in accordance with the domination of the Hofmeister series for anions derived from the standard molar volumes, adding weight to the argument that the anions fundamentally give rise to a Hofmeister series independent of the solvent.

Table 16: Specific-ion effects series exhibited in the electrostrictive volume of electrolytes $\overline{V}^{\circ}_{i\,el}$: anions arranged by a common cation.

cation	protic solvents						aprotic solvents					
	water	MeOH	EtOH	FA	NMF	EG	PC	EC	DMSO	ACE	MeCN	DMF
Li^+	AcO^-	F^-	F^-	F^-	Br^-	F^-	Cl^-	I^-	Cl^-	Cl^-	Cl^-	Br^-
	F^-	Cl^-	Br^-	Br^-	SCN^-	Br^-	Br^-	ClO_4^-	F^-	ClO_4^-	Br^-	Cl^-
	Cl^-	SCN^-	I^-	SCN^-	I^-	Cl^-	I^-		Br^-	I^-	SCN^-	I^-
	Br^-	I^-	AcO^-	Cl^-	Cl^-	I^-	ClO_4^-		I^-	Br^-	I^-	ClO_4^-
	SCN^-	Br^-	Cl^-	I^-	ClO_4^-				ClO_4^-		ClO_4^-	
	I^-	ClO_4^-		ClO_4^-								
	ClO_4^-											
Na^+	F^-	F^-	F^-	Cl^-	Br^-	F^-	Cl^-	ClO_4^-	Cl^-	Cl^-	Cl^-	Cl^-
	Cl^-	$Cl^- = I^-$	I^-	Br^-	I^-	Cl^-	I^-	I^-	Br^-	ClO_4^-	Br^-	Br^-
	Br^-	ClO_4^-	Br^-	F^-	Cl^-	Br^-	ClO_4^-		F^-	I^-	I^-	I^-
	AcO^-	Br^-	Cl^-	I^-	ClO_4^-	I^-	Br^-		I^-	Br^-	ClO_4^-	ClO_4^-
	ClO_4^-	SCN^-	AcO^-	ClO_4^-	SCN^-				ClO_4^-		SCN^-	
	I^-			SCN^-								
	SCN^-											
K^+	F^-	I^-	F^-	Cl^-	Br^-	F^-	Cl^-	I^-	Cl^-		Cl^-	Br^-
	AcO^-	F^-	I^-	Br^-	I^-	Cl^-	I^-	ClO_4^-	Br^-		Br^-	Cl^-
	Cl^-	Cl^-	Br^-	F^-	Cl^-	I^-	Br^-		F^-		SCN^-	I^-
	Br^-	SCN^-	Cl^-	I^-	SCN^-	Br^-	ClO_4^-		I^-		I^-	ClO_4^-
	I^-	Br^-	AcO^-	SCN^-	ClO_4^-				ClO_4^-		ClO_4^-	
	SCN^-	ClO_4^-		ClO_4^-								
	ClO_4^-											
Rb^+	F^-	F^-	F^-	F^-		I^-	Cl^-		F^-		Cl^-	Br^-
	Cl^-	I^-	I^-	Cl^-		F^-	I^-		Cl^-		Br^-	Cl^-
	Br^-	Cl^-	Br^-	Br^-		Cl^-	Br^-		Br^-		I^-	I^-
	I^-	Br^-	Cl^-	I^-		Br^-	ClO_4^-		I^-		ClO_4^-	ClO_4^-
	ClO_4^-	ClO_4^-		ClO_4^-					ClO_4^-			
Cs^+	AcO^-	I^-	F^-	Cl^-	I^-	F^-	I^-		Cl^-		Cl^-	Br^-
	F^-	F^-	I^-	Br^-	Br^-	I^-	Cl^-		Br^-		Br^-	Cl^-
	Cl^-	Cl^-	Br^-	I^-	Cl^-	Cl^-	Br^-		F^-		I^-	I^-
	I^-	Br^-	AcO^-	F^-	ClO_4^-	Br^-	ClO_4^-		I^-		ClO_4^-	ClO_4^-
	Br^-	ClO_4^-	Cl^-	ClO_4^-					ClO_4^-			
	ClO_4^-											

For each cation, the anions are listed from largest (top) to smallest (bottom) electrostrictive volume. The cell background is coloured as indicated in the legend below if that order of ions corresponds to a known SIE series.

Hofmeister | reverse Hofmeister | lyotropic

Table 17: Specific-ion effects series exhibited in the electrostrictive volume of electrolytes $\overline{V}_{i\,el}^{\ominus}$: cations arranged by a common anion.

anion	protic solvents						aprotic solvents					
	water	MeOH	EtOH	FA	NMF	EG	PC	EC	DMSO	ACE	MeCN	DMF
AcO^-	Cs^+ Li^+ K^+ Na^+		Li^+ Cs^+ K^+ Na^+									
F^-	Rb^+ Na^+ K^+ Li^+ Cs^+	Rb^+ Na^+ Cs^+ Li^+ K^+	Li^+ Rb^+ Na^+ K^+ Cs^+	Rb^+ Na^+ Li^+ K^+ Cs^+		Rb^+ Li^+ Na^+ K^+ Cs^+			Rb^+ Li^+ Na^+ K^+ Cs^+			
Cl^-	Na^+ K^+ Rb^+ Cs^+ Li^+	Na^+ Rb^+ K^+ Cs^+ Li^+	Li^+ Na^+ K^+ Rb^+ Cs^+	Na^+ Cs^+ K^+ Rb^+ Li^+	Cs^+ K^+ Na^+ Li^+	Na^+ K^+ Li^+ Rb^+ Cs^+	Li^+ Cs^+ Na^+ Rb^+ K^+		Li^+ K^+ Na^+ Cs^+ Rb^+	Li^+ Na^+	Rb^+ Cs^+ K^+ Na^+ Li^+	Rb^+ K^+ Cs^+ Na^+ Li^+
Br^-	Na^+ K^+ Rb^+ Cs^+ Li^+	Na^+ Rb^+ K^+ Cs^+ Li^+	Li^+ Na^+ K^+ Rb^+ Cs^+	Na^+ Cs^+ Rb^+ Li^+ K^+	Li^+ Cs^+ K^+ Na^+	Li^+ Na^+ K^+ Rb^+ Cs^+	Li^+ Cs^+ Rb^+ Na^+ K^+		Li^+ Na^+ K^+ Rb^+ Cs^+	Li^+ Na^+	Rb^+ Cs^+ K^+ Na^+ Li^+	Li^+ Rb^+ K^+ Cs^+ Na^+
I^-	Na^+ Cs^+ K^+ Rb^+ Li^+	Cs^+ Na^+ Rb^+ K^+ Li^+	Li^+ Na^+ K^+ Rb^+ Cs^+	Cs^+ Na^+ Rb^+ K^+ Li^+	Cs^+ K^+ Na^+ Li^+	Rb^+ K^+ Na^+ Li^+ Cs^+	Cs^+ Rb^+ K^+ Li^+ Na^+	K^+ Li^+ Na^+	Cs^+ K^+ Li^+ Na^+ Rb^+	Li^+ Na^+	Rb^+ Na^+ Cs^+ K^+ Li^+	Cs^+ Rb^+ K^+ Na^+ Li^+
SCN^-	K^+ Na^+ Li^+	K^+ Na^+ Li^+		Li^+ K^+ Na^+	Li^+ K^+ Na^+						K^+ Li^+ Na^+	
ClO_4^-	Na^+ Rb^+ Cs^+ K^+ Li^+	Na^+ Rb^+ Cs^+ K^+ Li^+		Na^+ Cs^+ Rb^+ Li^+ K^+	Na^+ Cs^+ Li^+ K^+		Na^+ Cs^+ Rb^+ Li^+ K^+	Na^+ Li^+ K^+	Na^+ Cs^+ Li^+ Rb^+ K^+	Li^+ Na^+	Na^+ Rb^+ Cs^+ K^+ Li^+	Na^+ Rb^+ Cs^+ Li^+ K^+

For each anion, the cations are listed from largest (top) to smallest (bottom) electrostrictive volume. The cell background is coloured as indicated in the legend below if that order of ions corresponds to a known SIE series.

Hofmeister | reverse Hofmeister | lyotropic | reverse lyotropic | new series 1 | reverse new series 1 | new series 2

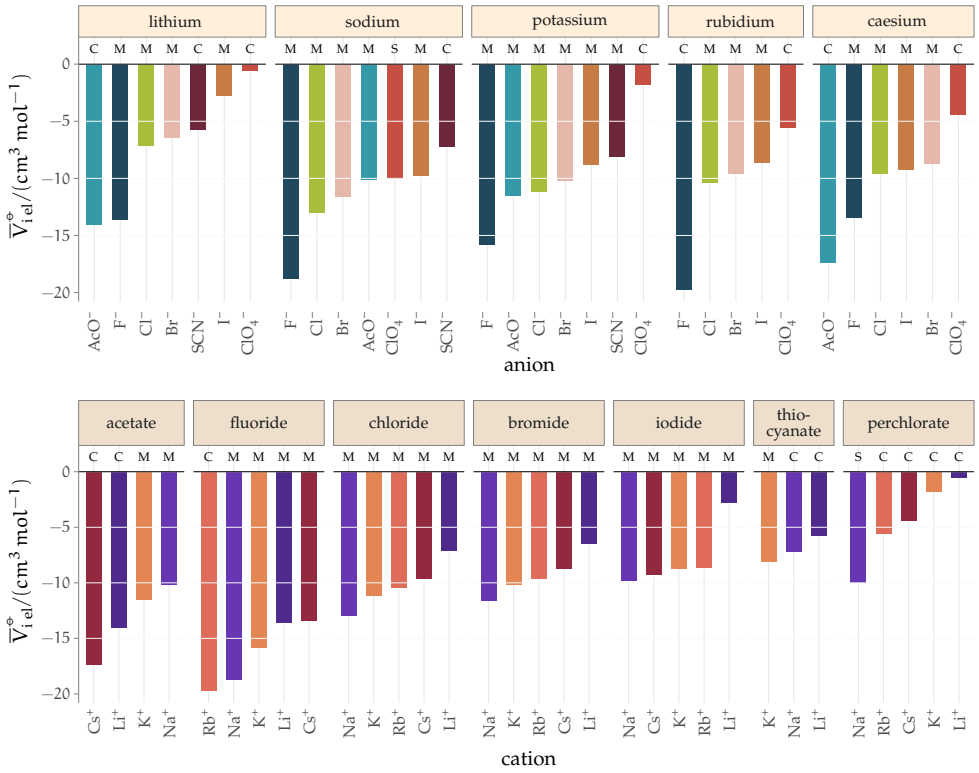

Figure 6: Molar electrostrictive volume $\overline{V}^{\circ}_{i\,el}$ of alkali metal salts in water at infinite dilution grouped by cation (top) and by anion (bottom). The labels above the plot bars indicate the method of estimation of the intrinsic molar volume used in the calculations. M: extrapolation from molten salts, from Pedersen et al. (1984); S: from 'soluble salts' (Marcus, 2010); C: crystal volume, as in Eq. [5].

The situation for the cations is very different (Table 17). All the known series plus an additional two are observed. Although the lyotropic series (forward or reverse) is the most common, the variety of behaviour is large and does not seem to correlate to any property of the solvent or the counterion. The difference with respect to Table 16 is striking. It has to be noted that the differences in electrostriction values across cations are much smaller than those for anions and therefore the uncertainty in the estimate of the standard molar volume is more significant.

The wide range of behaviour seen reflects the complexity we have observed in measurements of ionic molar heat capacity (MHC), limiting molar conductivity (LMC) and viscosity *B*-coefficient (VBC) across a range of solvents reported in Chapter 2 (Table 13).

3.4.3 Electrostriction normalised by electrolyte size

The electrostriction values above are strongly influenced by the size of the ions themselves. It is therefore desirable to evaluate the degree of electrostriction relative to the size of the ion. This can be done by normalising the elec-

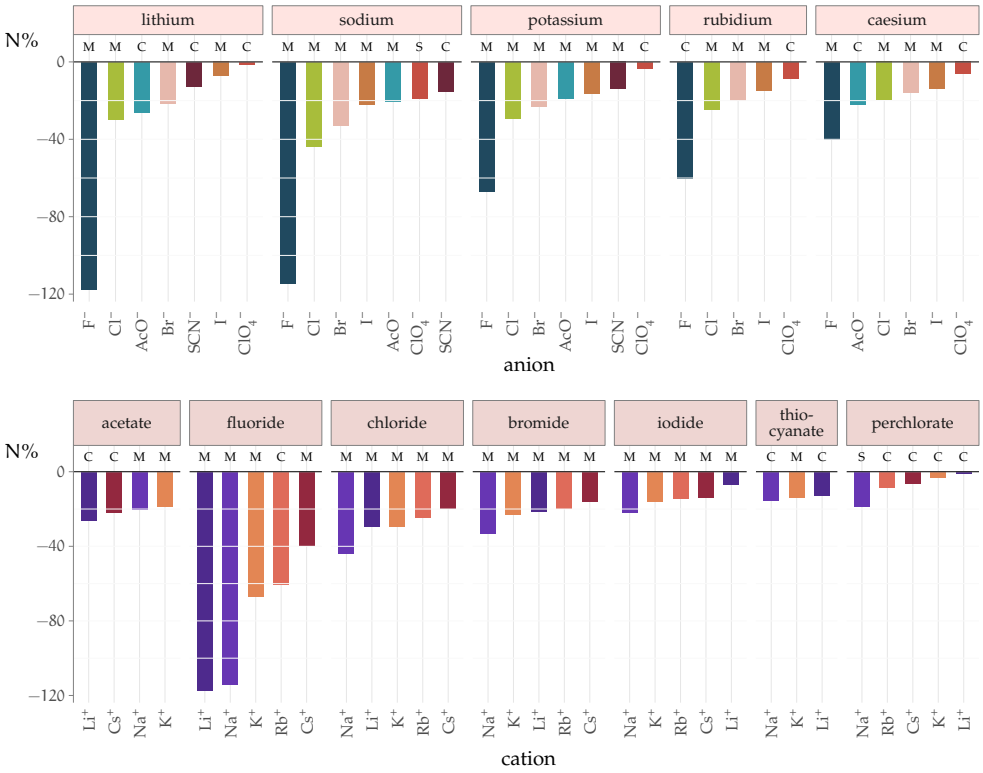

Figure 7: Normalised molar electrostrictive volume N% of alkali metal salts in water at infinite dilution grouped by cation (top) and by anion (bottom). The labels above the plot bars indicate the method of estimation of the intrinsic molar volume used in the calculations. M: extrapolation from molten salts, from Pedersen et al. (1984); S: from 'soluble salts' (Marcus, 2010); C: crystal volume, as in Eq. [5].

trostrictive volumes calculated above by the intrinsic molar volume of the electrolyte: in this way, the relative degree of electrostriction compared to the ion size is evaluated.

This equates to the following calculation:

$$\begin{aligned} \mathrm{N\%\ (electrostriction)} &= \frac{\overline{V}^{\circ}_{\mathrm{i\ el}}}{\overline{V}_{\mathrm{i\ intr}}} \times 100 = \frac{\overline{V}^{\circ}_{\mathrm{i}} - \overline{V}_{\mathrm{i\ intr}}}{\overline{V}_{\mathrm{i\ intr}}} \times 100 = \\ &= \left(\frac{\overline{V}^{\circ}_{\mathrm{i}}}{\overline{V}_{\mathrm{i\ intr}}} - 1 \right) \times 100 \end{aligned} \qquad [6]$$

Where $\overline{V}^{\circ}_{\mathrm{i}}$ is the standard partial molar volume of the species 'i' in solution, and $\overline{V}_{\mathrm{i\ intr}}$ is the intrinsic molar volume of the species 'i'.

The new quantity N% is dimensionless and represents a 'normalised' electrostriction under the condition that all the electrolytes had the same intrinsic molar volume (without accounting for changes in charge density, polarisability, etc.). This quantity is equal to 0 when the intrinsic and standard volumes are exactly the same (i.e. no electrostriction of the solvent has happened, as in case I. of Fig. 3); negative when electrostriction takes place: the larger the electrostriction, the more negative the normalised quantity be-

comes. Two sub-cases can be identified when N% is negative: $-100\% < N\% < 0$ when the molar volume of the electrolyte is positive (case II. of Fig. 3), whereas $N\% < -100\%$ for case III. of Fig. 3, when the molar volume of the electrolyte is smaller than 0 and therefore the final solution volume is even smaller than the original pure solvent volume. Finally, N% is positive when expansion of the solvent happens as in case IV. of Fig. 3.

The resulting plots for electrolytes in water are in Fig. 7. The plots for all the remaining solvents are in the Appendix A.4 (Figs. 55 to 65). Tables 18 and 19 summarise the series observed in the different solvents, grouping electrolytes by cation and anion, respectively.

The effect of the normalisation is an even more homogeneous picture for the anion behaviour (Table 18 versus Table 16), where the Hofmeister series is nearly universal, with the only exception being lithium salts in ACE.

Significantly for the cations shown in Table 19: the reverse lyotropic series is preponderant, as it was for the standard partial molar volumes (Table 14). The most variability in behaviour across solvents is observed for polyatomic ions, for which the Hofmeister series and reverse Hofmeister series are observed and an altogether new series occurs as well. Polyatomic ions have permanent multipole moments due to the asymmetrical distribution of charge, therefore it is unsurprising that electrostriction does not follow the same series evident for the monoatomic anions. If the polyatomic anions are set aside, the reverse lyotropic series is nearly universal. This is a dramatic change from the pre-normalised electrostrictive volumes summarised in Table 17. The preponderance of the reverse lyotropic series produced from the normalised electrostrictive volumes for cations across a wide range of solvents is in accordance with the domination of the reversed lyotropic series for cations derived from the standard molar volumes, adding weight to the argument that the cations fundamentally give rise to a reversed lyotropic series independent of the solvent.

Table 18: Specific-ion effects series exhibited in the normalised electrostrictive volume of electrolytes, N%: anions arranged by a common cation.

cation	protic solvents						aprotic solvents					
	water	MeOH	EtOH	FA	NMF	EG	PC	EC	DMSO	ACE	MeCN	DMF
Li^+	F^- Cl^- AcO^- Br^- SCN^- I^- ClO_4^-	F^- Cl^- Br^- I^- SCN^- ClO_4^-	F^- Cl^- Br^- I^- AcO^-	F^- Br^- Cl^- SCN^- I^- ClO_4^-	Br^- Cl^- SCN^- I^- ClO_4^-	F^- Cl^- Br^- I^-	Cl^- Br^- I^- ClO_4^-	I^- ClO_4^-	F^- Cl^- Br^- I^- ClO_4^-	Cl^- Br^- ClO_4^- I^-	Cl^- Br^- I^- SCN^- ClO_4^-	Cl^- Br^- I^- ClO_4^-
Na^+	F^- Cl^- Br^- I- AcO^- ClO_4^- SCN^-	F^- Cl^- Br^- I^- SCN^- ClO_4^-	F^- Cl^- Br^- I^- AcO^-	F^- Cl^- Br^- I^- ClO_4^- SCN^-	Cl^- Br^- I^- ClO_4^- SCN^-	F^- Cl^- Br^- I^-	Cl^- Br^- I^- ClO_4^-	I^- ClO_4^-	F^- Cl^- Br^- I^- ClO_4^-	Cl^- ClO_4^- Br^- I^-	Cl^- Br^- I^- SCN^- ClO_4^-	Cl^- Br^- I^- ClO_4^-
K^+	F^- Cl^- Br^- AcO^- I^- SCN^- ClO_4^-	F^- Cl^- Br^- I^- SCN^- ClO_4^-	F^- Cl^- Br^- I^- AcO^-	Cl^- F^- Br^- I^- SCN^- ClO_4^-	Br^- Cl^- I^- SCN^- ClO_4^-	F^- Cl^- Br^- I^-	Cl^- I^- Br^- ClO_4^-	I^- ClO_4^-	F^- Cl^- Br^- I^- ClO_4^-		Cl^- Br^- I^- SCN^- ClO_4^-	Cl^- Br^- I^- ClO_4^-
Rb^+	F^- Cl^- Br^- I^- ClO_4^-	F^- Cl^- Br^- I^- ClO_4^-	F^- Cl^- Br^- I^-	F^- Cl^- Br^- I^- ClO_4^-		I^- F^- Cl^- Br^-	Cl^- I^- Br^- ClO_4^-		F^- Cl^- Br^- I^- ClO_4^-		Cl^- Br^- I^- ClO_4^-	Cl^- Br^- I^- ClO_4^-
Cs^+	F^- AcO^- Cl^- Br^- I^- ClO_4^-	F^- Cl^- Br^- I^- ClO_4^-	F^- Cl^- Br^- I^- AcO^-	Cl^- Br^- F^- I^- ClO_4^-	Br^- Cl^- I^- ClO_4^-	F^- Cl^- I^- Br^-	Cl^- I^- Br^- ClO_4^-		F^- Cl^- Br^- I^- ClO_4^-		Cl^- Br^- I^- ClO_4^-	Cl^- Br^- I^- ClO_4^-

For each cation, the anions are listed from largest (top) to smallest (bottom) normalised electrostrictive volume. The cell background is coloured as indicated in the legend above if that order of ions corresponds to a known SIE series.

Hofmeister | lyotropic

Table 19: Specific-ion effects series exhibited in the normalised electrostrictive volume of electrolytes, N%: cations arranged by a common anion.

anion	protic solvents						aprotic solvents					
	water	MeOH	EtOH	FA	NMF	EG	PC	EC	DMSO	ACE	MeCN	DMF
AcO^-	Li^+ Cs^+ Na^+ K^+		Li^+ Na^+ K^+ Cs^+									
F^-	Li^+ Na^+ K^+ Rb^+ Cs^+	Li^+ Na^+ K^+ Rb^+ Cs^+	Li^+ Na^+ K^+ Rb^+ Cs^+	Li^+ Na^+ Rb^+ K^+ Cs^+		Li^+ Na^+ K^+ Rb^+ Cs^+			Li^+ Na^+ K^+ Rb^+ Cs^+			
Cl^-	Na^+ Li^+ K^+ Rb^+ Cs^+	Li^+ Na^+ K^+ Rb^+ Cs^+	Li^+ Na^+ K^+ Rb^+ Cs^+	Na^+ Li^+ K^+ Rb^+ Cs^+	Li^+ Na^+ K^+ Cs^+	Li^+ Na^+ K^+ Rb^+ Cs^+	Li^+ Na^+ K^+ Rb^+ Cs^+		Li^+ Na^+ K^+ Rb^+ Cs^+	Li^+ Na^+	Li^+ Na^+ K^+ Rb^+ Cs^+	Li^+ Na^+ K^+ Rb^+ Cs^+
Br^-	Na^+ K^+ Li^+ Rb^+ Cs^+	Na^+ Li^+ K^+ Rb^+ Cs^+	Li^+ Na^+ K^+ Rb^+ Cs^+	Na^+ Li^+ K^+ Rb^+ Cs^+	Li^+ Na^+ K^+ Cs^+	Li^+ Na^+ K^+ Rb^+ Cs^+	Li^+ Na^+ K^+ Rb^+ Cs^+		Li^+ Na^+ K^+ Rb^+ Cs^+	Li^+ Na^+	Li^+ Na^+ K^+ Rb^+ Cs^+	Li^+ Na^+ K^+ Rb^+ Cs^+
I^-	Na^+ K^+ Rb^+ Cs^+ Li^+	Na^+ Li^+ K^+ Rb^+ Cs^+	Li^+ Na^+ K^+ Rb^+ Cs^+	Na^+ Cs^+ Rb^+ K^+ Li^+	Li^+ Cs^+ Na^+ K^+	Rb^+ Na^+ K^+ Li^+ Cs^+	Li^+ Na^+ K^+ Rb^+ Cs^+	K^+ Li^+ Na^+	Li^+ Na^+ K^+ Cs^+ Rb^+	Li^+ Na^+	Na^+ Li^+ K^+ Rb^+ Cs^+	Li^+ Na^+ K^+ Rb^+ Cs^+
SCN^-	Na^+ K^+ Li^+	Na^+ Li^+ K^+		Li^+ K^+ Na^+	Li^+ K^+ Na^+						Li^+ Na^+ K^+	
ClO_4^-	Na^+ Rb^+ Cs^+ K^+ Li^+	Na^+ Li^+ Rb^+ K^+ Cs^+		Na^+ Cs^+ Rb^+ Li^+ K^+	Na^+ Li^+ Cs^+ K^+		Na^+ Li^+ Rb^+ Cs^+ K^+	Li^+ Na^+ K^+	Na^+ Li^+ Rb^+ Cs^+ K^+	Li^+ Na^+	Na^+ Li^+ Rb^+ K^+ Cs^+	Li^+ Na^+ Rb^+ Cs^+ K^+

For each anion, the cations are listed from largest (top) to smallest (bottom) normalised electrostrictive volume. The cell background is coloured as indicated in the legend below if that order of ions corresponds to a known SIE series.

Hofmeister | reverse Hofmeister | lyotropic | reverse lyotropic | reverse new series 1 | new series 3

3.4.4 General implications

From this work a number of conclusions regarding SIE can be drawn.

It is apparent that the ordering of SIE for the standard molar volumes and the normalised electrostriction of electrolytes at infinite dilution is *independent* of the solvent. This ordering follows a Hofmeister series for anions and a reversed lyotropic series for cations, which corresponds to smaller 'harder' cations and anions having a smaller intrinsic volume $\overline{V}_i^{\circ}$ and causing a larger normalised electrostriction N% than large, 'soft' cations and anions. As a consequence, the grouping usually associated with the Hofmeister series is respected for anions. That is the 'structure makers' or 'kosmotropes' which are ions small in size and with high surface charge density and small polarisability give rise to the largest electrostriction. This does not hold for the cations, where the Hofmeister series ordering is lost and an ordering that follows the reverse lyotropic series which is determined by the cation size is instead in place.

This solvent-independence of electrostriction in the limit of infinite dilution demonstrates that, at a fundamental level, such as for bulk properties of very diluted solutions, the ordering of SIE are solely a property of the ions and the only essential ingredient for SIE to happen is the presence of electrolytes. As most experimental observations of SIE are made at moderately high to high electrolyte concentrations, this may lead to the erroneous conclusion that these effects are only manifest at high concentrations. In fact neither surfaces nor higher concentrations are needed. Of course the solvents do matter in that they mediate the strength of the effects. This finding is corroborated by the trends found in Chapter 2 for bulk properties such as the limiting molar conductivity (LMC) and the viscosity *B*-coefficient (VBC), where a lyotropic series is predominant for the alkali metals cations and a Hofmeister series for the anions. Whereas other experiments involving ions at high concentration and surfaces result in a perturbation to the fundamental series observed here, as illustrated in Table 13 of Chapter 2. These perturbations likely arise due to a complex interaction of ion pairing, dispersion forces, and solvation both in the bulk and at interfaces. Furthermore, the balance of these effects will depend on temperature as well as the specifics of the solvent and surfaces (Leontidis, 2017). An improved understanding of the suite of SIE observed may therefore be gained by considering them as perturbations to the fundamental series observed here in the simplest systems.

The homogeneity in behaviour of electrostrictive phenomena must not shadow the fact that ion solvation mechanisms differ greatly across solvents. Electrostriction is only one consequence of ion solvation and does not capture the local ion-solvent interactions or the structure of the solvent around

solvated ions. The chemical properties, molecular size and polarisability of the solvents vary widely. The interactions between ions and solvent are reflected in selective ion- solvent interactions. These have been shown to vary greatly for solvents of different polarisability, leading to different trends in solvation (Arslanargin et al., 2016; Pollard and T. L. Beck, 2017). The thermodynamics of solvation across solvents and the effect of ions on solvent structure and on solvent dynamics needs to be considered to obtain a comprehensive physical picture. Some of these matters are addressed in the following chapters.

How might this information be useful in furthering our understanding of SIE? This analysis tells us that calculations and simulations of SIE in dilute solutions should be able to reproduce the Hofmeister series for anions and the lyotropic series for cations without specifically accounting for the solvent, supporting an approach already being employed (Duignan, Baer and Mundy, 2016). The details of the solvent will matter in determining the magnitude of the effect. The interpretation I propose for this evidence is that, when the system becomes more complex, for instance because a surface comes into play, or because the electrolyte concentration is increased, those fundamental SIE are perturbed and both surfaces and the solvent come into play and determine their final ordering.

3.5 CONCLUSIONS

In this chapter, the trends of SIE for standard molar volumes and standard electrostrictive volumes have been analysed. In order to compare across ions and solvents, a normalisation of the electrostrictive volumes has been performed. This work evidences the presence of SIE at low concentration, a notion that has often been disregarded in the literature, where many authors associate SIE only with higher salt concentrations (Parsons and Salis, 2016). This is perhaps due to the magnitude of these effects being small for many measurements at low concentration, and in some systems SIE may only be revealed once electrostatic effects have been quenched by screening.

Electrostriction is an ion-specific effect in all of the electrolyte solutions considered. This confirms that, with respect to SIE, water is not a 'special' solvent. This also rejects the idea of an exclusive association between the existence of SIE and the presence of a hydrogen-bonding network: aprotic solvents show ion specificity as well, indeed ions in all solvents show ion specificity. Further, the complexity conferred by ion specificity is necessary for life, but ion specificity is not restricted to aqueous solutions.

These findings support the hypothesis that the ordering of SIE is fundamentally due to properties of the ions themselves and that this fundamental

ordering is exhibited experimentally under appropriate circumstances. This is exemplified by the partial molar volume and normalised electrostriction of anions following a Hofmeister series whilst the cations follow a reverse lyotropic series. The quantitative connection between these series and the individual properties of the ions is not trivial and remains the realm of active efforts in this field. This outcome is important for the understanding of SIE. In models of bulk properties of solvents in the limit of infinite dilution, the specific nature or the granularity of the solvent should not determine the order of the SIE.

4 VOLCANO PLOTS

This chapter is reproduced with minor changes from:

V. Mazzini and V. S. J. Craig (2018), 'Volcano Plots Emerge from a Sea of Non-aqueous Solvents: The Law of Matching Water Affinities Applies across All Solvents.' Submitted.

4.1 INTRODUCTION

Understanding of SIE, and especially phenomena such as the reversal of the Hofmeister series, has benefited greatly from the empirical 'law of matching water affinities (LMWA)', enunciated by Collins (1997). This law predicts that, in aqueous solutions, ion pairs are formed by cations and anions with matching size (charge density). Collins explains that 'the small ions of opposite charge form contact ion pairs because of electrostatic attraction; the large ions of opposite charge form contact ion pairs because this releases weakly hydrated water, which becomes strongly interacting water in bulk solution' (Collins, 2012). This is an extension of the 'like seeks like' rule. Collins used 'volcano plots' as one of the theoretical foundations for the LMWA. The term 'volcano plot' arises from the shape of the plot which resembles a cinder cone in profile. Such plots were first published by Morris in response to a suggestion from Fajans, who first enunciated a 'competition principle' regarding the dissolution of crystalline electrolytes and their interaction in solution.

In this chapter the relationship between volcano plots and the LMWA is examined, and the volcano plots are extended to non-aqueous solvents, firstly to test the existence of such volcano relationships in non-aqueous solvents, and secondly to test the hypothesis that trends in ion specificity only depend on the ions and not on the solvent.

Although SIE are often interpreted as arising from the interaction of ions with water, the evidence presented in the previous chapter shows that universal ion-specific trends are observed across a wide range of solvents, implying that trends in ion-specificity arises from the ions *independently* of the solvent (although, the solvent mediates the magnitude of the effect).

4.2 ENERGIES RELATED TO THE SOLVATION PROCESS

As the present chapter deals with the thermodynamics of solvation, I introduce here the definitions of the quantities that are going to be discussed: the energies and the entropy related to the solvation of ions and the dissolution of electrolytes.

The enthalpy of solvation $\Delta_{\text{abs. soln.}}H$ is the heat exchanged when a substance is transferred from a vacuum (or the gas phase) to the solvent at constant pressure (McNaught and Wilkinson, 1997). This quantity includes contributions from the formation of a cavity in the solvent, the reorientation of the solvent molecules and the formation of both electrostatic and dispersion interactions between the solute and the solvent. The Gibbs free energy of solvation is calculated using its fundamental thermodynamic definition: $\Delta_{\text{abs. soln.}}G = \Delta_{\text{abs. soln.}}H - T\Delta_{\text{abs. soln.}}S$, where $\Delta_{\text{abs. soln.}}S$ is the entropy of solvation of the species and $\Delta_{\text{abs. soln.}}H$ is the enthalpy of solvation. In each case the relevant change is the change between the species in solution and the species in the ideal gas phase; T is the absolute temperature in K. $T = 298.15\,\text{K}$ for all the quantities discussed here.

The standard enthalpy $\Delta_f H^\ominus$, entropy $\Delta_f S^\ominus$, and Gibbs free energy $\Delta_f G^\ominus$ of *formation* refer instead to the formation of the species of interest (in our case either aqueous electrolyte, gaseous ions or crystalline salt) from the constituent elements in their respective *standard* states.

The *absolute standard molar enthalpy of solvation* of a salt $\Delta_{\text{abs. soln.}}H^\ominus$ is the change in enthalpy when one mole of gaseous ions are dissolved in an infinitely large quantity of solvent. It is calculated as the sum of the $\Delta_{\text{abs. soln.}}H^\ominus$ of the constituent ions and is referred to as 'absolute enthalpy of solvation' in the following sections for brevity.

The *standard molar enthalpy of dissolution* of the crystalline salt $\Delta_{\text{soln.}}H^\ominus$ is calculated as the difference between the standard molar enthalpy of formation of the infinitely dilute aqueous electrolyte $\Delta_f H^\ominus(\text{MX, aq})$ and the standard molar enthalpy of formation of the pure electrolyte $\Delta_f H^\ominus(\text{MX, cr})$ (which in this case refers to crystalline salts, as none of the alkali metal halides are gaseous or liquid in standard conditions). It will be referred to as 'enthalpy of dissolution' in the following sections.

Analogous definitions stand for the absolute standard molar Gibbs free energy of solvation of a salt $\Delta_{\text{abs. soln.}}G^\ominus$ and the standard molar Gibbs free energy of dissolution of the crystalline salt $\Delta_{\text{soln.}}G^\ominus$.

These two quantities are represented on the axes of the 'classic' volcano plots. Figure 8 illustrates the relationship between the different states and relative solvation energies.

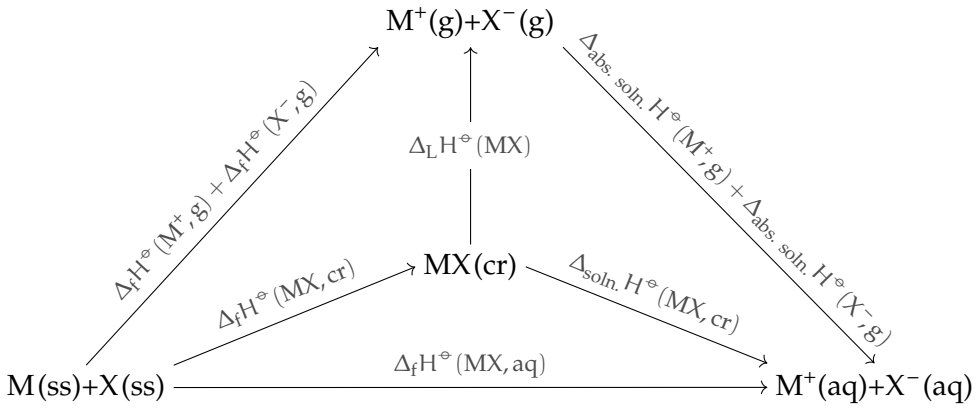

Figure 8: The Born-Haber cycle for the quantities of interest in the classic enthalpy volcano plot. (ss) indicates the standard state, (cr) the crystalline solid, (g) the gaseous state and (aq) the hydrated ion at infinite dilution. $\Delta_f H^\ominus$ is the standard molar enthalpy of formation; $\Delta_L H^\ominus$ is the lattice enthalpy of the crystalline salt; $\Delta_{soln.} H^\ominus$ is the standard molar enthalpy of dissolution; $\Delta_{abs.\ soln.} H^\ominus$ is the standard molar enthalpy of solvation of the gaseous ion.

4.3 THE ORIGIN OF VOLCANO PLOTS

To my knowledge, the appellative 'volcano plot' in this context was first used by Conway (1977), who likely borrowed this term from electrocatalysis plots related to the *kinetics* of reactions (Quaino et al., 2014). Conway also published volcano plots in the field of electrochemical catalysis (Conway, 1987).

The classic 'volcano plots' that are discussed here were published by Morris (1969) to illustrate Fajans's 'competition principle'. This was formulated by Fajans (and coworkers) in his early work in German (Fajans, 1921; Fajans and Karagunis, 1930), and later summarised in the light of additional experimental evidence (Fajans and Johnson, 1942). The competition principle stems from the observation that the solubility of alkali metal halides in *water* does not simply follow the inverse of their lattice energies (Fajans, 1921), but the smallest solubility is observed for the salts composed of ions that have absolute hydration energies most similar in value (their difference being therefore closest to zero), and increases with increasing differences in the hydration energy of the ions. Fajans proposed a mechanism in which the cations and anions in a crystal lattice that is dissolving compete for the surrounding solvent molecules: salts are more soluble if the solvent interacts strongly with either the anion or cation and the other ion is 'pushed away', than if both the anion and cation are equally *competing* for interactions with the solvent.

They later observed (Fajans and Karagunis, 1930) that the trend observed for the solubility of alkali metal halides salts also holds for enthalpies, osmotic coefficients and the tendency to form solid hydrates for alkali metal

halides. Their measurements of the refractive index of electrolyte solutions showed that the same competition principle can be extended to electrolytes in solution, and they infer the formation of association ion pairs for ions of similar absolute free energy of hydration (Fajans and Johnson, 1942). The fact that anions and cations of the same size do not have the same absolute hydration enthalpy (anions have a larger hydration enthalpy than cations of the same size), demonstrates, according to Fajans and Johnson, that what generates the volcano trends is the difference in hydration enthalpy rather than the difference in ionic radii of the ions constituent the salt. Therefore, according to the authors, the two quantities cannot be used interchangeably and it is the *hydration energy that causes the volcano trend*. They attribute the difference in hydration enthalpy of the anions and cations to an asymmetry in the properties of the water molecule. However, when analysing trends in the osmotic coefficients with concentration, they observe that the difference in the hydration enthalpies is not valid over the whole concentration range and also that *a simple property cannot explain the behaviour of electrolytes*.

Later, when Morris published the volcano plots, he supported the explanation proposed by Fajans and made no additional remarks regarding the origin of the volcano trend (Morris, 1969).

4.3.1 Early literature citing volcano plots

Before the 'revival' of volcano plots initiated by Collins (1997), who included them as evidence of the 'law of matching water affinities (LMWA)' (discussed later in Section 4.4), the significance of the 'striking' volcano relationship had been discussed explicitly by Conway (1977). He showed that, on a semi-quantitative level, the enthalpy of dissolution of a salt crystal in water can be expressed as a function of the reciprocal sums of the anionic and cationic radii, r_- and r_+:

$$\Delta_{\text{hydr.}}H(\text{salt}) = \frac{-A}{r_+ + r_-} - \frac{(ze)^2}{2}\left(1 - \frac{1}{\epsilon_R}\right)\left(\frac{1}{r_+} + \frac{1}{r_-}\right) = \quad [7]$$

$$= \frac{-A}{r_+ + r_-} - \frac{(ze)^2}{2}\left(1 - \frac{1}{\epsilon_R}\right)(r_+ + r_-)\frac{1}{r_+ r_-} \quad [8]$$

Where A is the is the Madelung constant for the crystal lattice and ze is the formal charge ($z = 1$ for the alkali metal halides). Equation [8] has a maximum for cationic and anionic radii that are closest in value, that is, when their difference is closest to zero. Conway therefore dismisses the 'mechanistic' interpretation given by Fajans and Johnson (1942) and supported by Morris (1969), labelling the argument of the preferential competition of the ion for the solvent as unnecessary, as the volcano shape *arises naturally as the*

result of the mathematical form of the dissolution enthalpy (or Gibbs free energy) function (Conway, 1977).

Later, Jenkins and Pritchett (1984) use a fitting of the volcano plot to determine absolute single ion values of several thermodynamic properties. They also assume a volcano-like relationship between the dissolution enthalpies/Gibbs free energies (y-axis) and the difference of the ionic viscosity *B*-coefficient B_η (x-axis).

The volcano plots of Morris (1969) have been invoked on a number of occasions to explain the solubility of compounds in water (Crawford and Klapötke, 1999; Vishnu and Mishra, 1981; J.-H. Yang et al., 2007).

4.4 THE LAW OF MATCHING WATER AFFINITIES

The volcano plots of Morris (1969) were cited by Collins (1997) as a thermodynamic foundation of his empirical 'law of matching water affinities (LMWA)'. The LMWA states that, in solution, oppositely charged ions (as well as charged groups) that have similar affinity for water spontaneously lose part of their hydration shells to associate and form a contact ion-pair (two ions interacting directly with no water molecules in-between).

Collins built his argument on the volcano plots, on thermodynamic observations such as the entropy of water molecules near an ion, and on experimental evidence (viscosity *B*-coefficient, NMR, gel sieving chromatography, neutron and x-ray diffraction, etc.). Collins states that oppositely charged ions in solution tend to form contact (or 'inner-sphere') ion pairs when they have 'matching water affinity'. Here *water affinity* refers to the strength of interaction of the ion or charged moiety with water, and can be expressed via a range of properties of ions in solution. For volcano plots, Collins uses the absolute Gibbs free energy of hydration of the gaseous ion as a measure of its affinity for water. The water affinity is directly related to the charge density on the ion (which is proportional to size for spherical monoatomic ions). The smaller the ion, the greater the charge density. Collins argued that ions tend to associate when their interactions are stronger than their interaction with water (they are both small) or when their interaction with water is less favourable than the water-water interaction (when both ions are large). Ions with comparable ('matched') hydration enthalpies or free energies form salts that are the least soluble. It is argued that this is because ions with matched charge densities have comparable interactions with water and tend to form inner-sphere ion pairs in solution. Therefore, according to Collins, charged and also noncharged moieties in solution will prefer to associate with moieties of matching absolute free energies of hydration. This is an extension of the 'like dissolves like' principle. This framework has proved successful for

rationalising a variety of observations, such as ion pumps, the interactions of ions with proteins, and ion selectivity in ion exchange chromatography.

The LMWA was re-stated and expanded in four subsequent papers (Collins, 2004, 2006, 2012; Collins, Neilson et al., 2007). After the publication of the LMWA, the terms and concepts 'volcano plots' and LMWA are cited indistinguishably. A similar 'like seeks like' principle has been formulated by Lyklema (2003) when reviewing SIE on the stability of colloids: small cations are more effective at destabilising colloids that have small negatively charged surface sites (i.e. Li^+ is more effective than Rb^+ in precipitating TiO_2, with surface sites of deprotonated hydroxyl groups) and vice versa (AgI colloids are precipitated at lower concentrations of RbI than LiI). An older and analogous concept is the hard-soft principle of acids and bases (HSAB) (Pearson, 1963). This states that 'hard' (nonpolarisable) acids prefer to bind to 'hard' bases, and 'soft' (polarisable) acids prefer to bind to 'soft' bases. This influences a large number of phenomena in solution, such as the rates of nucleophilic substitution reactions and the formation and stabilisation of metal-ligand complexes (Pearson, 1963).

4.5 BRIEF REVIEW OF RECENT VOLCANO PLOT STUDIES

The LMWA concept has been embraced by the scientific community. The papers introducing the LMWA concept (Collins, 1997, 2004, 2006, 2012; Collins, Neilson et al., 2007) have had a large impact, in fields spanning from (bio)chemistry and (bio)physics to pharmacology, physiology, food science, materials science, polymer science and microbiology. There is no doubt that the LMWA has been a very helpful framework across disciplines, advancing the understanding of SIE both experimentally and theoretically, as recognised by many authors (Kunz and Neueder, 2009; Pollard and T. L. Beck, 2016; Schmidtchen, 2010).

An important further step is the extension of the LMWA to charged surfactant headgroups relevant in biology and colloid science (carboxylate, phosphate, sulfate, sulfonate) by Vlachy, Jagoda-Cwiklik et al. (2009). A Hofmeister ordering of these headgroups based on computational and experimental data was proposed, and the LMWA was used to rationalise the interaction of such groups with aqueous ions. Using this generalised approach, the behaviour of polyelectrolytes, surfactants and lipids were predicted with success. Subsequent experiments from the same group supported this approach (Vlachy, Drechsler et al., 2009).

The general predictions of the LMWA have been confirmed by various experiments. In water, x-ray absorption spectroscopy indicates that sodium binds more strongly than potassium to the acetate anion (Uejio et al., 2008).

Also, investigations with NIR (near infra-red) spectroscopy find that the depletion of water from hydration shells of alkali metal ions varies among ions in accordance with the LMWA (Kojić et al., 2014). Moreover, picosecond dynamics of water at a proteins' surface (and hence the protein stability) is altered by anions following the opposite trend to the dynamics of bulk water, which is in agreement with the LMWA (Aoki et al., 2016). However, 2DIR spectroscopy (Sun et al., 2013) reveals the existence of contact ion pairs in solution between SCN^- and Ca^{2+} or Mg^{2+}. This is in opposition to the LMWA.

The LMWA has been employed to rationalise a number of behaviours in electrolyte solution. These include the retention of proteins on cation-exchange absorbents (DePhillips and Lenhoff, 2001), the interaction of polyelectrolytes with halide ions (Lukšič, Bončina et al., 2012), the rheological behaviour of copolymers (Obiweluozor et al., 2014) and the salt-dependence of the interaction potential between a colloidal polystyrene particle and a flat glass surface (Ao et al., 2011). The reactivity in aqueous solution (Trompette, 2015) and ionic liquids (Lin et al., 2016) also belongs to the list. In addition, the LMWA framework supports the observed solubility of anionic surfactants (Klein et al., 2009), the influence of counterions and coions on the cmc of mixed anionic-cationic surfactant systems (Hao, Deng et al., 2012; Hao, N. Yang et al., 2016; Nan, He et al., 2013; Nan, Xu et al., 2015), the phase behaviour of cationic lipids (Tarafdar et al., 2013), and the phase behaviour, stability and morphology of naturally occurring marine surfactants (T. Zhang et al., 2016). The aggregation behaviour of dyes in aqueous solution (Mooi and Heyne, 2012; Mooi, Keller et al., 2014) and their interaction with surfactants (Srivastava and Ismail, 2014) can be qualitatively accommodated by the LMWA as well.

Regarding peptides and proteins, contrasting experimental evidence has been reported. Anion interactions with charged sites of proteins (Fox et al., 2015), and also the interaction of divalent and trivalent cations with a negatively charged protein in the native membrane environment (Batoulis et al., 2016), confirm the LMWA. On the other hand, the empirical rule falls short of explaining the effects of monovalent cations on enzymatic activity (Medda, Salis et al., 2012), or the concentration dependence of the cation effectiveness in promoting hemoglobin aggregation (Medda, Carucci et al., 2013). In addition, while the association strength of monovalent cations with carboxylate moieties of a polypeptide follows the LMWA (with the exception of NH_4^+ and Li^+), the divalent ions do not follow it at all (Kherb et al., 2012).

Theorists have been looking to provide foundations for the LMWA (Asthagiri et al., 2000; Gao, 2011; Merchant and Asthagiri, 2009; Shi and T. Beck, 2017). They all agree that continuum models and classical models are insufficient to quantitatively describe electrolyte solutions, although they can

partially capture their behaviour. For instance, the weak pairing of differently sized ions is attributed to a 'shadowing' effect of the larger ion, which prevents the smaller ion from favourably interacting with the solvent (Lund et al., 2010). Other groups (Duignan, Parsons et al., 2014c; Parsons, Boström, Lo Nostro et al., 2011) propose the inclusion of dispersion interactions to reach a quantitatively descriptive and physically meaningful picture, that accounts for the LMWA.

A number of MD are in agreement with the predictions of the LMWA (Fennell et al., 2009; C.-W. Liu et al., 2014; Soniat et al., 2016; Xie et al., 2016). The predictions of the LMWA have also been used as benchmarking for MD simulations (Lukšič, Fennell et al., 2014), and to make reasonable guesses of values for which experimental data are absent (Moreira and Firoozabadi, 2010). Some results are in disagreement with the LMWA, as in the case of MD simulations that only find solvent-shared ion pairs and no contact ion pairs (Hess and van der Vegt, 2009), and the substantial deviation found when ions are of a similar size to the water molecule (Q. Zhang et al., 2014).

4.5.1 Other reports of volcano trends

Other authors have reported volcano or volcano-like trends. They are listed below and summarised in Table 20.

Dzubiella et al. (2009) in Kunz's book about SIE (Kunz, 2009), follow the same reasoning as Conway (1977), and argue that the ion-dependence of many collective properties of electrolytes that are obtained as the difference of an ion-pair property and a single-ion property will show a peak or valley with respect to the difference of the radii of the single ions. For instance, the enthalpy of dissolution of an electrolyte is obtained as the difference between the sum of the absolute enthalpies of hydration of the gaseous ions (properties of the single ions) and the lattice enthalpy (a property of the ion pair) and the enthalpy of dissolution does indeed show a maximum when plotted against the difference of the radii of the constituent ions. The position of the peak will change for different properties. In their simplified model, they increase the radius of the cation by a quantity of the order of the lengthscale of the O–H bond in the water molecule (0.08 nm), to account for the fact that the cations are solvated by the oxygen of water, which has a non-vanishing radius. The plot of the enthalpy of dissolution of electrolytes against the difference of the radii of the constituent ions (anion minus cation) has a maximum in correspondence to such difference amounting to 0.08 nm (Dzubiella et al., 2009). Despite the model being basic and therefore not being capable of quantitative agreement with experimental values, the authors reach the same conclusions as Conway (1977): due to its functional form, the enthalpy of hydration of an electrolyte is bound to have a max-

Table 20: Volcano plots reported in the literature. The symbols are defined in the text.

reference	x-axis	y-axis	additional information
Morris, 1969	$\Delta_{\text{abs. hydr.}}H^{\ominus}(X^-,g) - \Delta_{\text{abs. hydr.}}H^{\ominus}(M^+,g)$	$\Delta_{\text{hydr.}}H^{\ominus}(MX,cr)$	to illustrate Fajans's competition principle
	$\Delta_{\text{abs. hydr.}}G^{\ominus}(X^-,g) - \Delta_{\text{abs. hydr.}}G^{\ominus}(M^+,g)$	$\Delta_{\text{hydr.}}G^{\ominus}(MX,cr)$	
Dzubiella et al., 2009	$r_{M^+} - r_{X^-}$	$\Delta_{\text{hydr.}}H^{\ominus}(MX,cr)$	fitted by parabolas
Kherb et al., 2012	$\Delta_{\text{abs. hydr.}}H^{\ominus}(CH_3COO^-) - \Delta_{\text{abs. hydr.}}H^{\ominus}(M^{z+})$	$K_d(RCOO^-M^{z+})$	inverted volcano for monovalent cations, except NH_4 and Li^+; *no* volcano trend for divalent cations
Gujt et al., 2014	$\Delta_{\text{abs. hydr.}}G^{\ominus}(M^+) - \Delta_{\text{abs. hydr.}}G^{\ominus}(X^-)$	S	
		K_a	
Batoulis et al., 2016	z/r	efficacy in clustering a membrane protein	*no* volcano trend obtained when z, crystal radius, volume, polarizability or softness are plotted on the x-axis
	B_η		
	$\Delta_{\text{abs. hydr.}}G^{\ominus}/CN$		
Soniat et al., 2016	$\Delta_{\text{abs. hydr.}}G^{\ominus}(X^-) - \Delta_{\text{abs. hydr.}}G^{\ominus}(M^+)$	ϕ	inverted volcano
Arslanargin et al., 2016	$\Delta_{\text{abs. hydr.}}H^{\ominus}(X^-) - \Delta_{\text{abs. hydr.}}H^{\ominus}(K^+)$	$\Delta_{\text{hydr.}}H^{\ominus}(KX,cr)$	opposite trend than KX in water

imum when the difference in radii between anion and cation has a certain value. This value corresponds to zero in Conway's model, and to 0.08 nm in the analysis of Dzubiella et al., as they account for the different sizes of the solvating groups of the water molecule.

Kherb et al. (2012) show an inverted volcano for the association strength of monovalent cations with the carboxylate moieties of a polypeptide (although NH_4^+ and Li^+ are exceptions), but the divalent ions do not follow a volcano trend. Gujt et al. (2014) find a volcano relationship between the association constants of eight alkali halides calculated from their conductivity at low concentration and the difference of the Gibbs free energies of hydration of the cation and anion. Soniat et al. (2016) show the volcano relationship between the osmotic coefficients ϕ of the alkali halides and the difference in hydration free energies of the constituent ions (this had been noted early on by Fajans as well). Batoulis et al. (2016) study the oligomerisation by different cations (mostly divalent and trivalent) of a protein in a native membrane environment. They find that plots of the protein clustering efficacy of cations versus the ion charge-to-radius ratio, or hydration energy, or water viscosity *B*-coefficient show a volcano trend in which Sr^{2+} marks the maximum. They conclude that the most effective ions at clustering are the ones that have hydration energy closer to the acetate groups hydration energy in the protein. Arslanargin et al. (2016), study the solvation of potassium halides in EC and PC, by means of statistical mechanics and simulations. They plot the enthalpy of dissolution of the crystal against the difference of the ionic hydration enthalpies they have computed, and the trend they obtain is ion-specific and in line with a volcano trend (see Section 4.5.3 for further discussion on those trends).

4.5.2 Limitations of the LMWA

The intuition built into the LMWA is formidable, but it is a simplistic model with intrinsic limitations (Kunz, 2010; Parsons, Boström, Lo Nostro et al., 2011; Shi and T. Beck, 2017). As such, it is important that the shortcomings and inconsistencies are acknowledged if a predictive understanding of the behaviour of ions and charged sites in solution is to be achieved.

A number of authors have pointed out weaknesses in the foundations of the LMWA. The first criticism is the usage of volcano plots to explain ion-ion interactions in solution. The quantities plotted on the volcano plots are standard thermodynamic quantities. As such they refer to ions at infinite dilution and hence the application to ion-ion interactions is tenuous. The connection between the two physical situations of infinite dilution and finite concentrations has not been justified. An additional incongruence is the explanation for the interaction among large ions in solution. The justification

for the LMWA assumes that the interactions among large ions and water are less favourable than water-water interactions, however the hydration energy of large ions is large and favourable (negative), therefore this argument cannot be sustained. Large ions must be preferentially interacting for another reason, most likely due to attractive dispersion forces.

These observations were first brought forward by Lo Nostro and Ninham (2012), and reiterated and expanded by Duignan, Parsons et al. (2014c), who proposed a different volcano plot based on the B coefficients from Bromley's theory (Bromley, 1973) (not to be confused with the Jones-Dole viscosity *B*-coefficient B_η. They obtained a 'reversed volcano' with a clearer physical meaning than the explanations behind the LMWA. Salis and Ninham (2014) attempted a reconciliation of the quantitative and qualitative views, as the theoretical basis for the LMWA is questionable but its predictions are correct, however, as yet, the quantitative theoretical approach proposed by Ninham and collaborators has not been as broadly received. They argue that a theory that correctly treats electrostatics and quantum mechanical dispersion forces can quantitatively predict the behaviour and association of both charged and non-charged ions and sites in solution. This theory develops a wider framework which includes interactions between ions and uncharged surfaces, in which the LMWA is contained as a sub-case. They propose that small ions prefer to lose water molecules and interact directly as the small size gives rise to large interaction energies (in agreement with the LMWA); whereas large ions interact strongly by dispersion forces (in contrast to the LMWA which has these ions interacting weakly). When ions of different sizes interact, neither dispersion forces nor electrostatic interactions are highly favourable. The latter argument also explains the adsorption of large ions onto uncharged surfaces and uncharged protein moieties by means of dispersion interactions.

4.5.3 The LMWA and nonaqueous solvents

The LMWA was proposed for water, and only three cases in the literature where its concepts are discussed for non-aqueous solvents could be identified.

Long et al. (2013) suggest the extension of the LMWA to a non-aqueous solvent (MeOH), which requires a name change to the LMSA (law of matching solvent affinities). They use LMSA to rationalise the ion-specific growth of a polyelectrolyte in water-MeOH mixtures. However, in this work the salt concentration is low, the system behaviour is complex and water-MeOH interactions have not been considered.

Lin et al. (2016) have investigated aqueous tetraalkylammonium ionic liquids as both solvents and catalysts for non-enzymatic regioselective acyla-

tions of glucose. In the reaction mechanism they propose, they also make use of the LMWA to explain the better performance of tetrabutylammonium acetate with respect to tetramethylammonium acetate.

With regards to aprotic solvents, Arslanargin et al. (2016) show that the trend of the dissolution enthalpy of crystals versus the computed hydration enthalpies of potassium halides in PC and EC is ion-specific, and the trend in these solvents has a maximum for KF, whereas in water KI shows the maximum dissolution enthalpy.

4.6 RESULTS AND DISCUSSION

Noting that volcano plots have been used to explain the LMWA, which implies water as the solvent, I wish to verify their existence in non-aqueous solvents. If verified, I wish to determine whether the trends in non-aqueous solvents are the same as in water. A number of electrolyte solution properties (y-axis) are therefore plotted against the difference of a property of the constituent ions (x-axis) in this section, starting from the 'classic' volcano plots.

Alternative interpretations of volcano plots exist. One approach places interactions of the ions with the solvent at the centre, attributing the volcano plot trends to the ion-solvent interaction, represented by the solvation energy (Collins, 1997, 2004, 2006, 2012; Collins, Neilson et al., 2007; Morris, 1969; Schmidtchen, 2010). Alternatively, volcano plots are attributed to the characteristics of the ions: size, and the associated polarisability, surface charge density, etc. (Conway, 1977; Dzubiella et al., 2009). In the first case, solvent dependent trends that alter the volcano plots substantially between solvents are to be expected. In addition, the volcano plots should be observed also for electrolytes containing polyatomic anions with geometries that are neither spherical nor tetrahedral, such as thiocyanate and acetate.

4.6.1 Definition of a volcano plot

It is important to clarify the definition of a volcano plot that is going to be applied in the ensuing sections. The term volcano plot refers to a scatter plot where the data trend follows an overturned 'V': it monotonically increases in a linear (the adjective is loosely applied) fashion up to a maximum, and then decreases, monotonically and linearly, with a slope of similar absolute value to the ascending section. A volcano trend is recognised here when two conditions are met. Firstly, a scatter plot of a particular property of an electrolyte shows a maximum with respect to the difference in a particular property of the anions and cations making up the electrolyte. This may for

example be the difference in size. Secondly, the peak of the volcano (i.e. the maximum) occurs in a quite narrow interval of values of the difference in a particular property of the ions. The plot is therefore quite symmetrical with respect to a vertical axis that goes through the maximum, thus resembling the shape of a volcanic cinder cone in profile. When evaluating volcano plots formed from electrolytes, the trend can be observed with a common cation for a number of anions (anion trend) or with a common anion for a number of cations (cation trend).

4.6.2 Methods and data sources

The dissolution energies of electrolytes in non-aqueous solvents were obtained via two stages. Firstly, the energies of *dissolution* of the crystalline electrolytes in water were obtained as the difference of the hydration energies of the ions composing the electrolyte minus the formation energy of the crystalline electrolyte. The relationship of these thermodynamic quantities is illustrated in Fig. 8.

$$\Delta_{\text{hydr.}} H^{\circ}(MX, cr) = \Delta_f H^{\circ}(MX, aq) - \Delta_f H^{\circ}(MX, cr)$$

These thermodynamic data are tabulated in the NBS tables (Wagman et al., 1982).

Secondly, the dissolution energies of the salts in non-aqueous solvents were calculated by adding to $\Delta_{\text{hydr.}} H^{\circ}(MX, cr)$ the energy of transfer to the non-aqueous solvent of interest :

$$\Delta_{\text{soln.}} H^{\circ}(MX, cr) = \Delta_{\text{hydr.}} H^{\circ}(MX, cr) + \Delta_{\text{transfer}} H^{\circ}(MX, aq \rightarrow slv)$$

The energies of transfer to non-aqueous solvents were taken from Marcus (2015), where the ionic energies of transfer are tabulated. The ionic radii of ions (for ions in water) are from Marcus (2015). The *ab-initio* radii have been calculated by Parsons and Ninham (2009). The osmotic and activity coefficients of electrolytes have been calculated by the author using a collection of the available data in the literature. The collected data is available in Appendix C. The solubility of electrolytes in water and non-aqueous solvents are collected from the current literature and are tabulated in Appendix D.

4.6.3 Classic volcano plots

The 'classic' treatment of volcano plots performed by Morris (1969), is here extended to non-aqueous solvents. This consists of plotting the standard enthalpy $\Delta_{\text{soln.}} H^{\circ}$ (or Gibbs free energy $\Delta_{\text{soln.}} G^{\circ}$) of dissolution of a crystal-

line salt versus the difference in absolute solvation enthalpies $\Delta_{\text{abs. soln.}}H^{\ominus}$ (or Gibbs free energies $\Delta_{\text{abs. soln.}}G^{\ominus}$) of the gaseous ions composing the salt. The relationship among these quantities is shown as a Born-Haber cycle in Fig. 8. Starting with the trends for alkali metals halides, here I analyse and present the Gibbs free energies in detail and supply the same analysis for enthalpies in Figs. 67 and 68 of Appendix B. Figures 9a and 9b show, for alkali metal halides, the Gibbs free energy of dissolution of the salt versus the difference in the absolute Gibbs free energies of solvation of the constituent ions for a range of solvents, where the lines follow the cation trends (constant anion).

It is immediately apparent that the volcano trend is maintained across *protic* non-aqueous solvents, the only apparent influence of the solvent being a shift in the y-axis. Notably the shift shows a definite trend across the alcohols from MeOH to BuOH, whereas the data for EG and FA are similar to water.

This demonstrates that, for bulk standard thermodynamic properties, the same trends arise in protic solvents as in water, showing that the phenomenon is *not exclusive* to water. This is all the more surprising as the properties of these solvents differ substantially, in particular their relative ability to solvate anions (see Table 2). The interaction strength of cations with the solvent is quantified by the Gutmann donor number, DN, and the interaction strength of anions with the solvent is quantified by the Gutmann-Mayer acceptor number, AN (see Table 2). In both cases larger numbers indicate stronger solvation.

It is apparent that the $\Delta_{\text{transfer}}G^{\ominus}$ is small between the solvents EG, FA and water (all three solvents have a 3D hydrogen bonding network), whereas the $\Delta_{\text{transfer}}G^{\ominus}$ becomes greater for the alcohols as the hydrophobicity and size of the solvent molecules increase.

In aprotic solvents, for *cation* trends, the volcano trend is maintained, but the peak position is shifted towards positive x-values and the 'arms' corresponding to the different cation series are vertically displaced. This indicates a substantial difference in solvation between iodide, bromide and chloride. That is, the protic solvents seem to be equally good solvents for monovalent anions, with the exception of fluoride which is poorly solvated, but aprotic solvents differentiate between the anions such that the solvation is ordered: iodide > bromide > chloride > fluoride. Small anions (Cl^-, F^-) or anions containing a localised negative charge on the oxygen atom (CH_3COO^-) are good hydrogen-bond acceptors and therefore are strongly solvated in protic solvents (high AN, see Table 2), but are weakly solvated in aprotic solvents. In contrast, large anions such as I^- and $ClO_4{}^-$, that are weak hydrogen-bond acceptors, can also be solvated through dispersion interactions in aprotic solvents, and therefore the difference in solvation energies between protic and aprotic solvents is not as large (Izutsu, 2009). The enhanced reactiv-

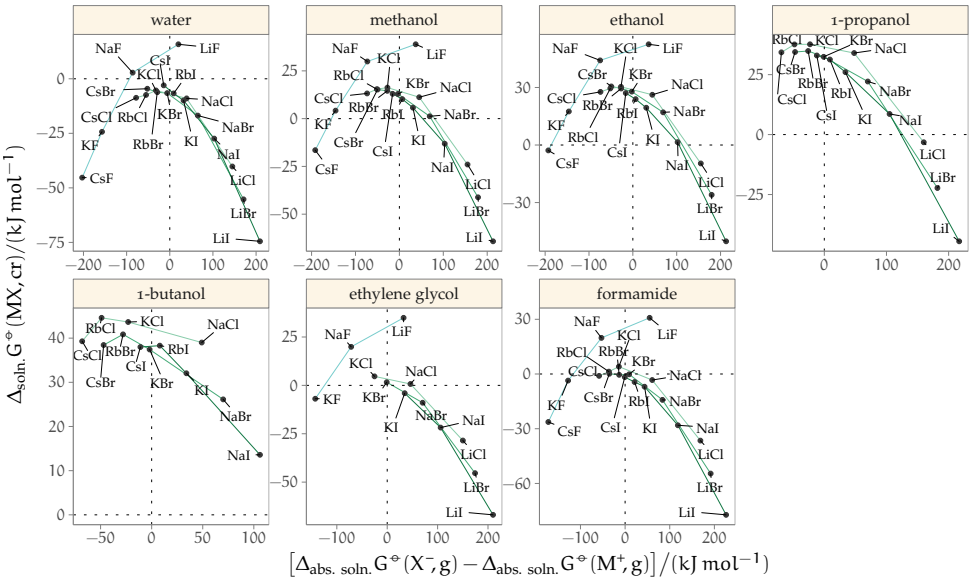

(a) Protic solvents

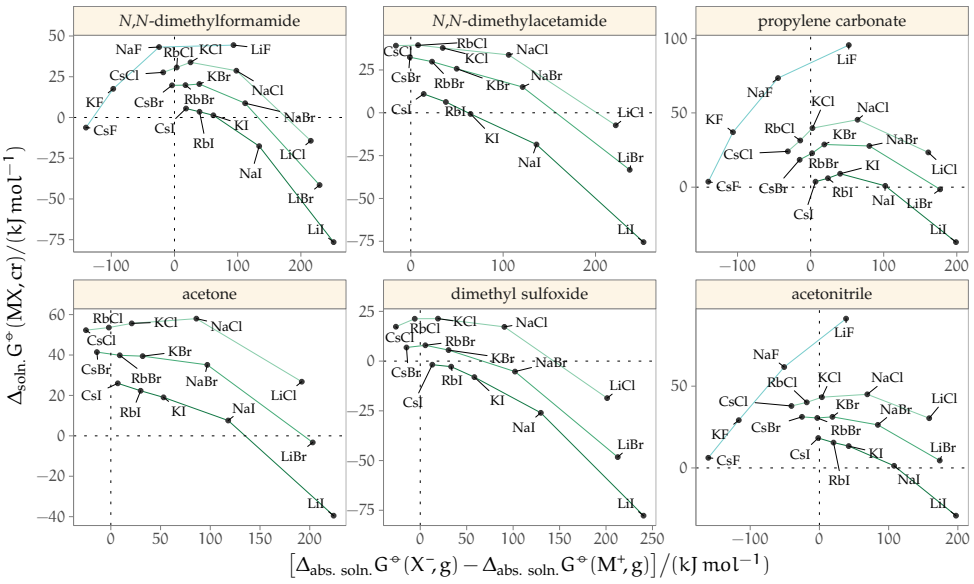

(b) Aprotic solvents

Figure 9: Gibbs free energy of dissolution of salts ($\Delta_{soln.}G^{\ominus}$) versus the difference in the absolute free energies of solvation $\Delta_{abs.\ soln.}G^{\ominus}$ of the constituent ions for a range of solvents. Coloured lines are drawn to help identify the cation trends (constant anion).

ity of anions in non-aqueous solvents, derived from their poor degree of solvation, ('naked' anions), is advantageous in several organic synthesis reactions (Parker, 1962).

In contrast, whereas the *anion* trends for protic solvents also follow the volcano trend (Appendix B, Figs. 74 and 76), the volcano shape is lost in aprotic solvents (see Appendix B, Figs. 75 and 77). As the data regarding fluoride salts are not available in aprotic solvents, it is not possible to observe the complete trend.

From these observations some general rules of thumb can be proposed. Firstly, the ion-specific trends observed in water are observed in protic solvents. Secondly, in aprotic solvents the ion-specific trends observed in water are likely to hold for the cation trends (constant anion) but not for the anions (constant cation).

For anion trends in particular, it often happens that the electrolyte occupying the peak position of the volcano changes, when changing from one solvent to another. This has been reported by Arslanargin et al. (2016) in the case of the dissolution enthalpies of the potassium fluoride–chloride–bromide series in water and PC: it increases from fluoride to bromide in water, whereas it decreases from fluoride to bromide in PC. The larger data set used here shows that the situation is complex across all solvents and such behaviour also happens in protic solvents (e.g. in PrOH).

The observed volcano shape for the enthalpies of dissolution of anions can be justified as follows: in aprotic solvents, the enthalpy of dissolution of anions gets less favourable (more endothermic, and therefore more positive) as the anion size decreases with respect to the cation size, because the dispersion contributions to the ion-solvent interactions become smaller. An 'exploded' volcano plot of enthalpies is shown in Figs. 69 and 70 of Appendix B to facilitate the analysis of the single anion trends for different cations. As anions are quite polarisable, the dispersion interactions play an important role in their solvation. This increasing dissolution enthalpy with decreasing anion size gives rise to the 'right arm' of the volcano. The solvation of the anion becomes more favourable only when specific bonding interactions with the solvent, such as hydrogen bonds, intervene. These interactions are what gives rise to the left slope of the volcano, which is not observed if the solvent is not capable of these interactions. Therefore, a true volcano shape is only going to be observed for protic solvents, which have hydrogen bonding abilities and are therefore good anion solvators (Böes et al., 2006), or in cases where the solvent can form specific interactions with the anion.

4.7 INTERPRETATION OF VOLCANO PLOTS IN SOLVENTS

4.7.1 The origin of volcano plots

Some authors (Collins, 1997, 2004, 2006, 2012; Collins, Neilson et al., 2007; Morris, 1969; Schmidtchen, 2010) attribute the origin of the volcano trend to the interactions of the ions with the solvent, following the original idea of Fajans's competition principle (Fajans and Johnson, 1942). Other authors instead see it as a consequence of the properties of the ions alone, such as size (Conway, 1977; Dzubiella et al., 2009). In an attempt to clarify the situation, two tests are performed here.

Firstly, we can use the difference of the radii of the ions composing the electrolyte in place of the difference of their absolute solvation energies. As can be seen in Figs. 10 and 11 (cation trends) and in Appendix B in Figs. 78 to 81 (anion trends), the same volcano trend is obtained.

It must be highlighted here that the ionic radii used in the plots are those for the ions in *water*, as this is the only solvent for which estimates of the solvated ion sizes are available. In a different solvent, these are likely to be different, as they depend on the ion coordination number, which changes across solvents (Marcus, 2016). But these aqueous radii correlate well with the *ab-initio* radii calculated by Parsons and Ninham (2009) and they are available for a larger number of ions than the *ab-initio* radii. The aqueous radii values used provide an estimate that is sufficient for non-aqueous solvated ions, especially as the cation-anion difference has been used and its trend can be expected to vary even less than the absolute values of the radii itself. As the volcano shapes are retained when using the differences in the ionic radii in place of the ionic solvation energies difference, the hypothesis that it is the properties of the ions alone that give rise to the volcano trend appears equally valid. Moreover as the radii are a more fundamental characteristic, it can be argued that the radii are ultimately the origin of the volcano trend. An argument that was proposed by Fajans and Johnson (1942) in favour of solvation enthalpies rather than radii, is the fact that the maximum of the volcano occurs when the former is closer to zero. This was also used to justify the 'matching solvent affinity' idea and the competition principle itself.

But the maximum is not at zero in all solvents represented in Fig. 9. In addition, the fact that the maxima occur at non-zero radii differences (Figs. 10 and 11) can be interpreted as a solvent-specific characteristic, as the region of the solvent that most strongly interacts with the ion will differ for cations and anions (i.e., for a certain solvent with anion-solvating and cation-solvating groups of a certain size, ions will be best solvated when their size difference is closest to the difference in distances of solvation of the anion

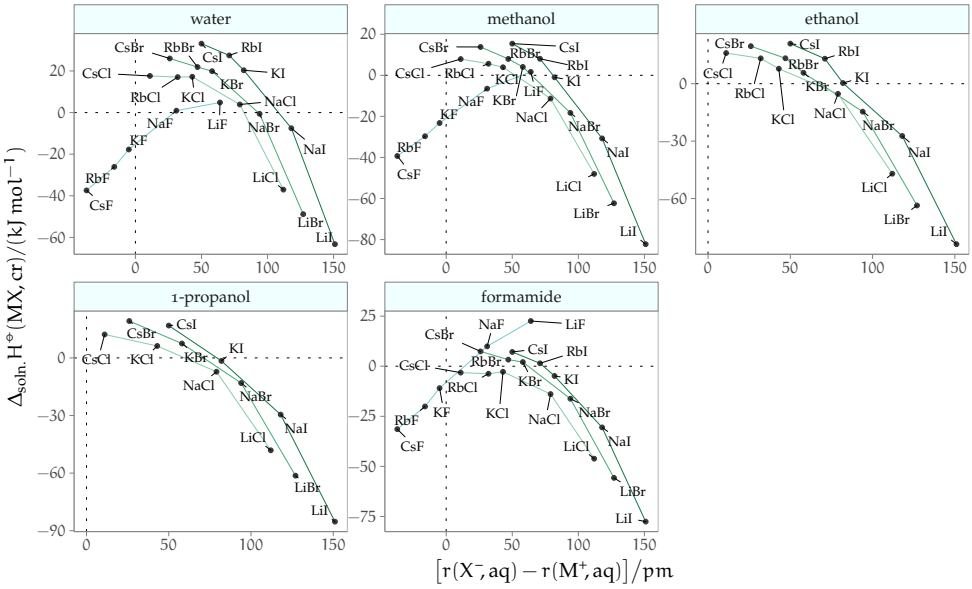

(a) Protic solvents

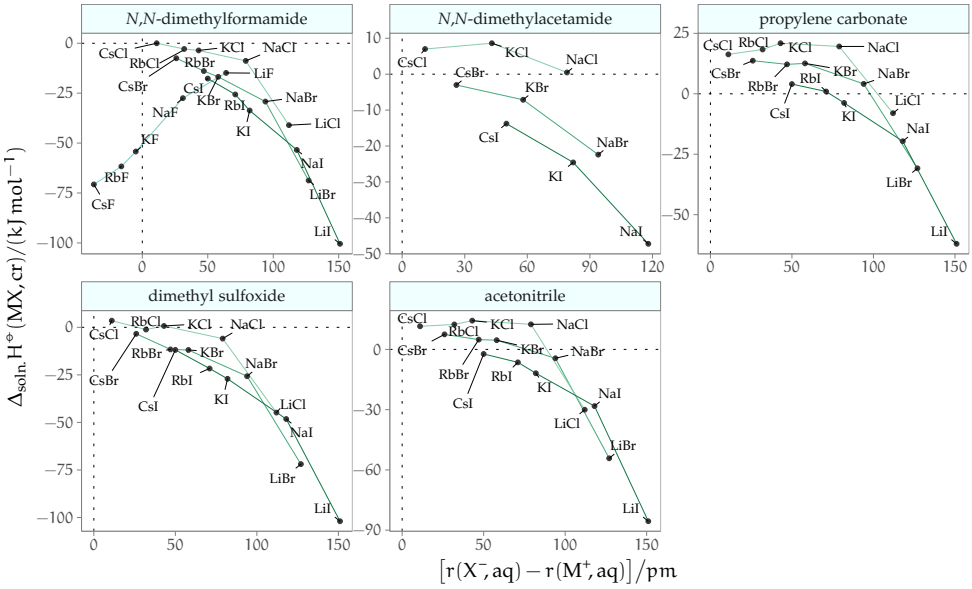

(b) Aprotic solvents

Figure 10: Enthalpy of dissolution of salts $\Delta_{soln.}H^{\ominus}$ versus the difference of the radii r of the constituent ions for a range of solvents. Coloured lines are drawn to help identify the cation trends.

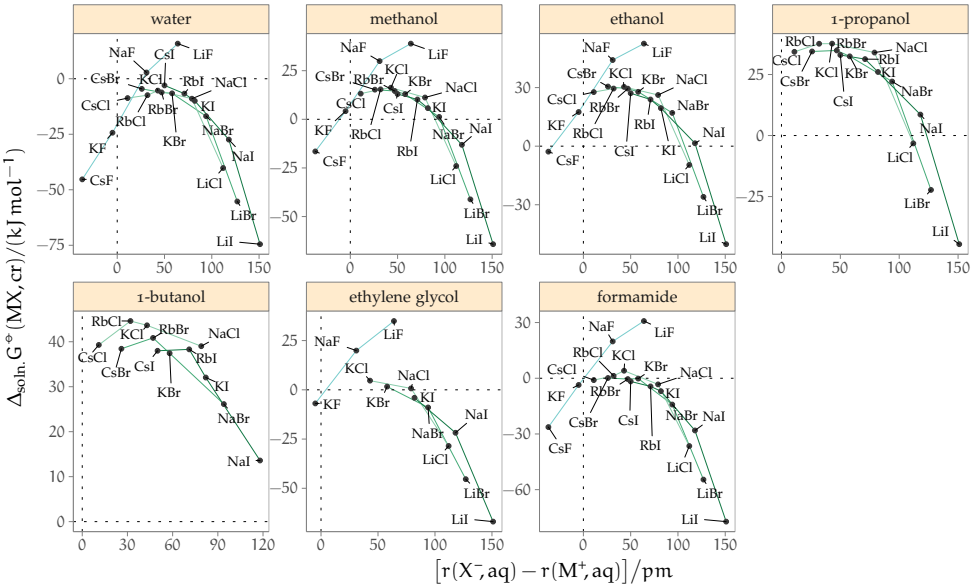

(a) Protic solvents

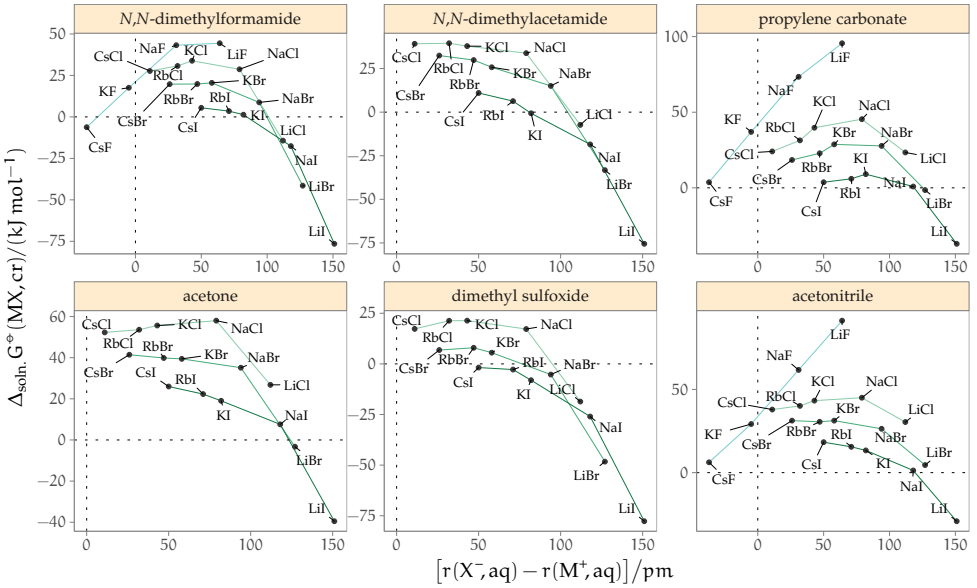

(b) Aprotic solvents

Figure 11: Gibbs free energy of dissolution of salts $\Delta_{soln.}G^{\ominus}$ versus the difference of the radii r of the constituent ions for a range of solvents. Coloured lines are drawn to help identify the cation trends.

and cation). The position of the maximum therefore reflects the asymmetry of the solvent molecules. This could be further tested by estimating the solvated radii of ions in non-aqueous solvents.

A second test that can be made is to look at the trends for electrolytes containing polyatomic ions of different geometries: tetrahedral, such as ClO_4^-, trigonal planar (NO_3^-) and linear (SCN^-). For polyatomic ions the ion is not spherical, therefore the radius of the ion is a poorly defined measure. Therefore, for polyatomic ions, plots against the difference in radii of the anion and cation are less likely to show a volcano trend whereas plots against the differences in enthalpy or Gibbs free energy of solvation should still exhibit a volcano trend, if the origin of the volcano trend is truly the energetics of the interaction of the ions with the solvent, as these measures remain reliable for polyatomic ions. However, for polyatomic ions, volcano plots are generally not observed, either when the solvation energies or the radii are used to construct the x-coordinate (abscissa). Exceptions are electrolytes containing ions with tetrahedral geometry, such as perchlorates, which do show an extremal behaviour that is in accordance with a volcano plot. Volcano plots of electrolytes containing an alkali metal cation and a polyatomic anion are shown in Figs. 12 to 15 (connecting lines highlighting cation trends). Although not all electrolytes are available, there is little evidence of a volcano trend in both cases. For polyatomic ions volcano plots are not observed either when the solvation energies or the radii are used to construct the x-coordinate (abscissa).

The above two tests indicate that the radii hypothesis is preferable over the solvation energies hypothesis, as they give equal results in terms of volcano plots, and the former is a simpler, more fundamental concept. Further, volcano trends are not observed for most salts containing polyatomic ions, whereas they would be expected under the solvation energies hypothesis. Finally and importantly, the solvation energies depend on the size of the ion. It is important to clarify here, that when I ascribe the effect to the 'radius' or 'size' of the ion, all other properties of the ion that are convoluted with size (polarisability, etc.) are included. If the volcano plot can truly be ascribed to the ion alone, then it would be most interesting to acquire the solvated radii of ions in non-aqueous solvents. Using these radii, an analysis of the position of the maximum in volcano plots in different solvents might reveal important details of solvation such as the distance of solvation of ions in different solvents and differences between cations and anions.

Details about the trends of polyatomic ions

Volcano plots of electrolytes containing polyatomic anions are shown in Figs. 12 to 15 (cation trends), and in Appendix B in Figs. 72 and 73 (cation trends). The perchlorates show extremal behaviour and are therefore in

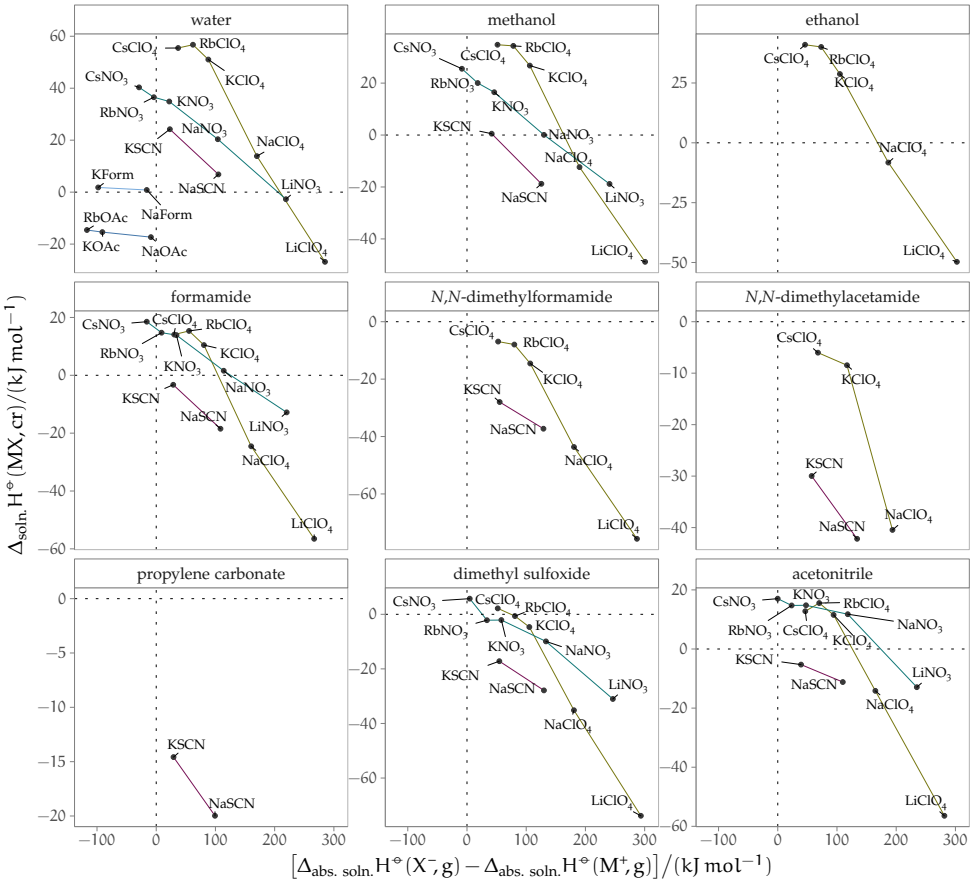

Figure 12: Salts containing polyatomic anions. Enthalpy of dissolution $\Delta_{soln.}H^{\ominus}$ versus the difference in the absolute enthalpies of solvation of the constituent ions $\Delta_{abs.\ soln.}H^{\ominus}$. Coloured lines are drawn to help identify the cation trends.

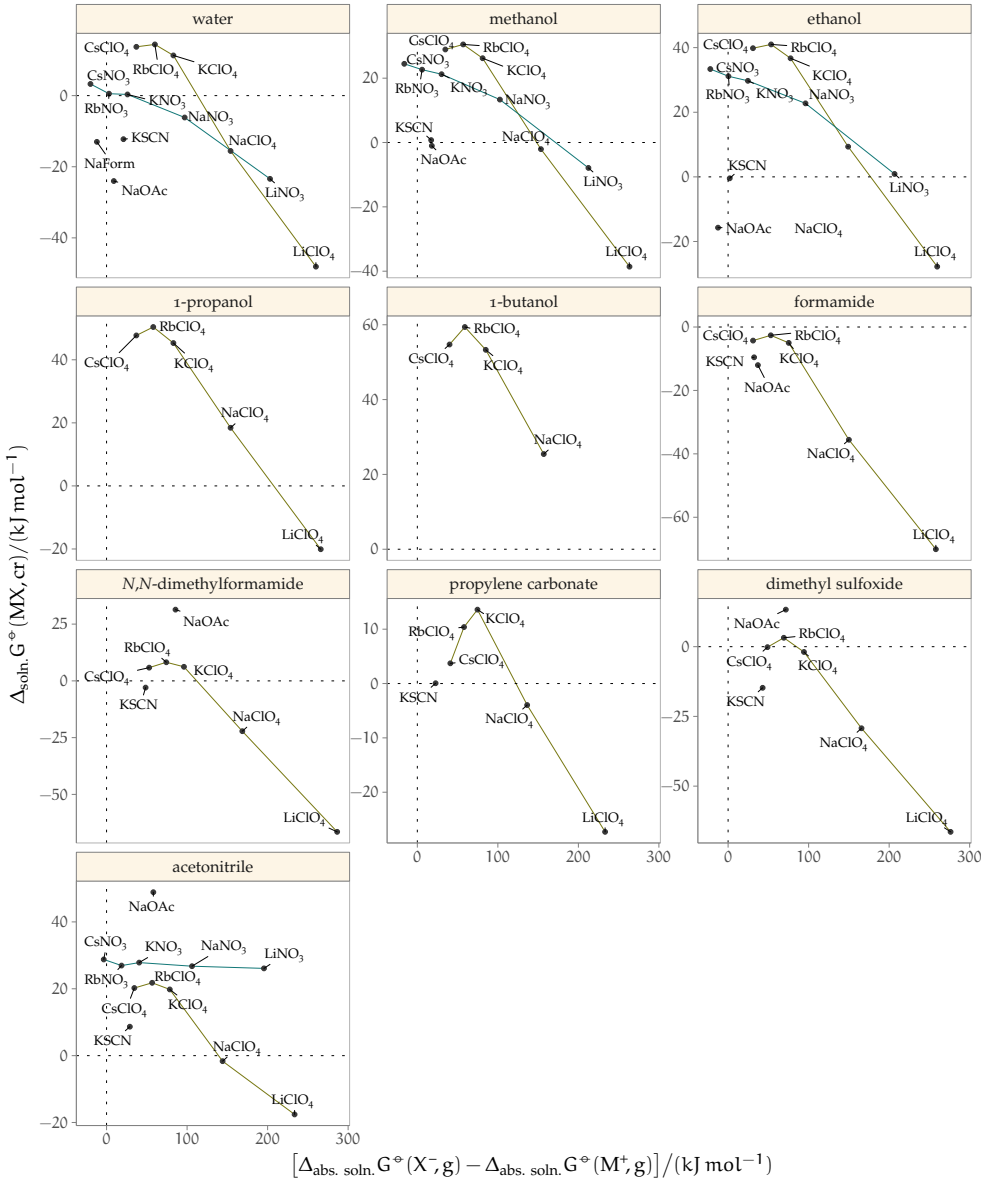

Figure 13: Salts containing polyatomic anions. Gibbs free energy of dissolution $\Delta_{soln.}G^{\ominus}$ versus the difference in the absolute Gibbs free energies of solvation of the constituent ions $\Delta_{abs.\ soln.}G^{\ominus}$. Coloured lines are drawn to help identify the cation trends.

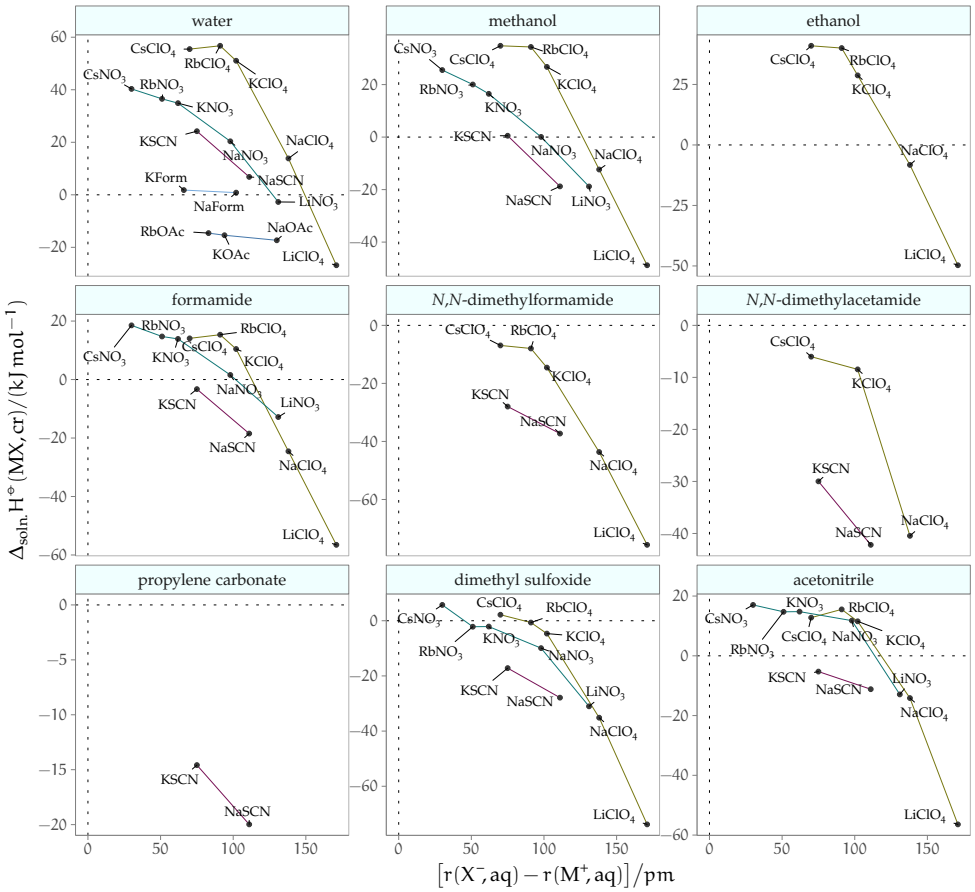

Figure 14: Salts containing polyatomic anions. Enthalpy of dissolution $\Delta_{soln.}H^{\ominus}$ versus the difference of the radii r of the constituent ions. Coloured lines are drawn to help identify the cation trends.

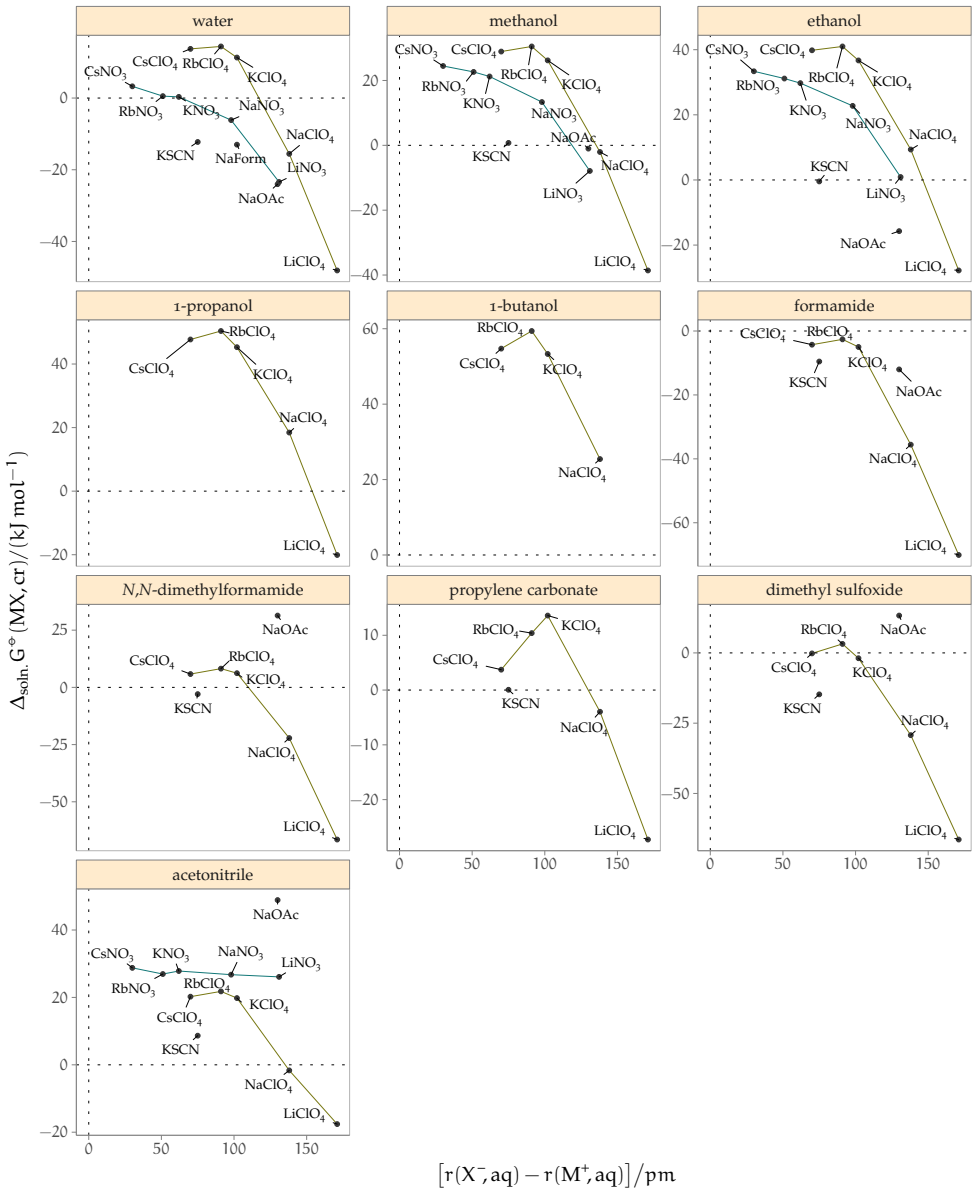

Figure 15: Salts containing polyatomic anions. Gibbs free energy of dissolution $\Delta_{soln.}G^{\ominus}$ versus the difference of the radii r of the constituent ions. Coloured lines are drawn to help identify the cation trends.

agreement with a volcano trend. The maximum for these series is not positioned close to a zero x-value as occurs in the classic volcano plots of alkali metal halides, but is shifted towards positive values. Plots against the difference in solvation energies and against the difference in radii show the same trend, thus indicating no preferential dependence of the volcano on solvation energies rather than radii. For thiocyanates, formates and acetates too little data is available to make an assessment, but the data is plotted for completeness.

4.7.2 Consequences

As espoused in Section 4.6.3, the existence of volcano plots in other solvents infers that, across solvents, the ion-specific trends observed in water will be observed in other protic non-aqueous solvents, and that the trends observed in water are more likely to hold for cations in non-aqueous solvents than for anions. This is a very interesting piece of information, which poses questions about the role of the solvent properties (hydrogen bonding, polarisability) in anion solvation. The trends in standard solution thermodynamic quantities behave differently than the electrostriction trends discussed in Chapter 3, despite both being bulk properties of solutions. For electrostrictive volumes, we have seen that both cations and anions follow the same ion-specific series across all solvents. Here, the homogeneity in ion-specific behaviour holds for cations in protic and aprotic solvents and anions in protic solvents, but not for anions in aprotic solvents. How do the two results reconcile? Despite solution energies and electrostrictive volumes being both bulk properties at standard concentration, they are very different in nature, with the first being more sensitive to ion-solvent specific interactions. This also shows that experiments can probe different aspects of ion-solvent interaction, and therefore the series observed can reveal different details of solvation.

This information is also useful in terms of predicting the unknown ion-specific trends in non-aqueous solvents where the corresponding trends are known in water. It must be stressed here, that all of the above analysis and observations are valid for *standard, bulk* quantities. I explore whether this holds at real concentrations below.

4.8 VOLCANO PLOTS IN THE 'REAL WORLD'

As stated in Section 4.5.2, in the LMWA foundations standard thermodynamic quantities were used to explain electrolyte behaviour at finite concentrations. The use of ion-ion interactions arguments to explain data at infinite dilution is not justified, as the activity of a species at infinite dilution is by

definition 1, and therefore ion pairing is excluded. Despite this, the LMWA holds very well in water and explains a number of phenomena that occur in solution at finite concentrations of electrolyte (and often in very complex systems, where surfaces, macromolecules, high concentrations and so on are present). The quantities analysed so far contain no information about the behaviour of ions at real concentrations (but still they are useful in informing the ion-solvent interactions in non-aqueous solvents!). An attempt at investigating the volcano trends at finite concentrations in water and non-aqueous solvents is therefore made here, by considering the solubility and activity coefficients of electrolytes in non-aqueous solvents. The ultimate goal is to test whether volcano plots are evident in these systems and the LMWA reasoning (or the theory proposed by Ninham and collaborators) can be extended to non-aqueous solvents.

4.8.1 The solubility of electrolytes

In order to ascertain if a volcano trend is exhibited in the solubility S of electrolytes, the molal solubilities of alkali metal halides against the difference of their radii are plotted in Figs. 84 and 85 of Appendix B.

A reversed volcano plot is observed in water, and, despite the scarce availability of information, it is retained in MeOH and the homologous series of alcohols, although the solubility decreases rapidly along the series (the data are therefore plotted using a semi-logscale). Also, there is a suggestion of an inverted volcano trend in the other protic non-aqueous solvents. In aprotic solvents, the left slope of the inverted volcano is missing. That is, where the fluorides series and chloride series are present, their solubility does not increase going towards smaller x-values. This is interesting and confirms what was observed previously in regards to the solvation of anions by aprotic solvents: it does not matter how much the ions are 'mismatched', the solvation of the fluoride and chloride anions in aprotic solvents is so unfavourable that the solubility of their salts is very low. This also demonstrates that the thermodynamics of the volcano plots at infinite dilution is not directly connected to the electrolyte solubility. This is also shown by the fact that, whereas the trend of KF – KCl – KBr dissolution energies observed in water is the opposite of the trend in PC (Arslanargin et al., 2016), the solubilities in the two solvents follow unrelated trends: KCl < KBr < KF < KI in water, and KF < KCl < KBr < KI in PC.

4.8.2 Activity coefficients

Activity coefficients γ are the ideal quantifier for ion-ion interactions in solution. For this analysis, I have also collected the activity and osmotic coef-

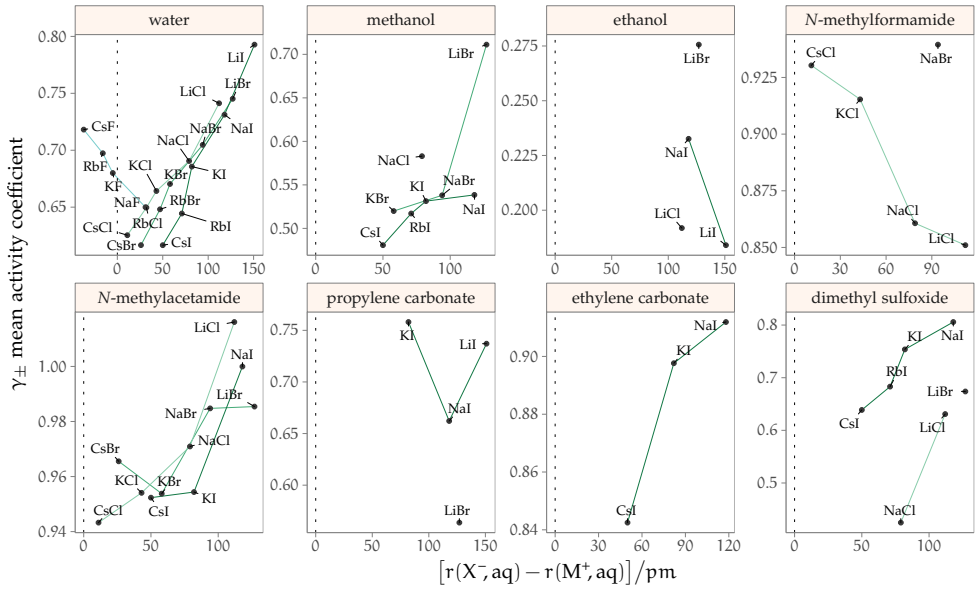

Figure 16: Inverted volcano plots of the activity coefficients γ versus the difference of the radii r of the constituent ions. The electrolyte concentration is 0.4 mol kg^{-1}, except for: MeOH (0.07 mol kg^{-1}); PC (0.18 mol kg^{-1}); EC and NMA, (0.09 mol kg^{-1}); DMSO and NMF (0.05 mol kg^{-1}). Coloured lines are drawn to help identify the cation trends.

ficients available in the literature for non-aqueous solvents. The data have been fitted (where no fitting was performed in the original paper) in order to interpolate to an intermediate concentration value so that as many electrolytes as possible can be compared. Unfortunately, the data available for non-aqueous solvents is scarce.

Plots of the activity coefficients plotted versus the ionic radii difference are shown in Fig. 16 (Fig. 83 in Appendix B highlights the anion trends). The osmotic coefficients are shown in Appendix B, Fig. 71 (lines highlighting cation trends), and Fig. 82 (lines following anion trends). In addition, Figs. 72 and 73 show the plots for electrolytes containing a polyatomic anion.

It is important to clarify that the coefficients plotted for each solvent are for a specific salt concentration, which is not preserved across solvents due to different electrolyte solubility.

For alkali metal halides in water, we observe the inverted volcano as proposed by Duignan (with Bromley's B-coefficients) and mentioned by Fajans and Soniat et al. (2016). This same trend seems to show in MeOH, *N*-methylacetamide (NMA), DMSO and in EC (although just three points are available in this solvent). The trend in NMF is reversed. This is interesting because a reversal of the trend in NMF with respect to the other solvents is also observed for the viscosity *B*-coefficient (VBC) of the alkali metal cations series (Table 13).

The scarcity of data is problematic, but the trends observed in water seem to be respected. The lack of data does not allow any conclusions to be drawn regarding the differences between protic and aprotic solvents. It

seems though, that the 'LMSA' as proposed by Long et al. (2013) can be substantiated in these non-aqueous solvents, except for NMF.

For electrolytes containing polyatomic anions, the data are too scarce to allow for any consideration, but they are nonetheless shown for completeness.

4.9 CONCLUSIONS

This analysis of volcano plots in solvents delivers a number of interesting details.

Firstly, the volcano plots of Morris are observed to be valid across protic and aprotic solvents, with the same trends as in water, with the exception of anion trends in aprotic solvents.

Secondly, it is argued that fundamentally the volcano trends arise from ion size, and this also gives rise to the solvent affinity.

Thirdly, it is demonstrated that volcano trends are manifest not only under standard conditions of infinite dilution but also at real concentrations.

The work presented above is consistent with the following interpretation: ions, or charged moieties in any solvent, form ion pairs that are in close contact when their size difference is most similar to the size difference of the cation- and anion-solvating groups of that solvent. The opposite is the case for ions of different sizes, that are poorly associated and retain their solvation shells. This is valid for anions and cations in water and protic solvents, and for cations that share the same anion in aprotic solvents. This is not strictly valid when comparing anions that share a common cation in aprotic solvents. Putting this last category aside, where the particulars of the solvation of the anions is more strongly solvent-specific and dominates, the formulation of a more general principle for the interaction of electrolytes in solvents that further develops the LMWA to encompass all solvents can be proposed: SIE are dominated by, and largely originate from, the relative *effective* size of the anion and cation. The effective size being the size of the ion and the distance of closest approach of the solvating group. The matching of effective ion size (MEIS) is therefore a useful and important general concept in understanding and predicting ion-specificity across solvents. That is, when the effective ion size of the cation and anion are matched, the ions lose part of their solvation shell to associate in solution, whereas when the effective ion size of the cation and anion are mismatched the ions do not associate. From this analysis the SIE cannot be pinned to a single property of the ion, as it is impossible to deconvolve the effect of size, electrostatic charge, polarisability, instantaneous dipoles (dispersion). Despite that, it is striking that the volcano trend is maintained across solvents. The presence

of common trends across solvents has been noted on occasion before, for instance, in Criss and Mastroianni (1971), who, by analysing the cationic viscosity *B*-coefficient in water, MeOH and MeCN, also inferred that water is not a different solvent in its interactions with ions. However, further experimental work is required in order to determine the specificity of the solvent influence at finite concentrations.

These observations demonstrate that, as noted in Chapters 2 and 3 already, water is not a special solvent with respect to SIE, in that non-aqueous solvents exhibit similar phenomena.

Theoretical work is needed in order to understand the details of ion-solvent interactions and explain the qualitative trends presented here, and ultimately to develop a quantitative predictive theory of SIE that applies across multiple solvents.

5 EXPERIMENTAL PROCEDURES

This chapter summarises all the shared methodologies and materials that have been used for the experiments performed. Also the general experimental problems associated with working with non-aqueous electrolytes are discussed.

Most of the material is reproduced with minor changes from:
V. Mazzini, G. Liu et al. (2018), 'Probing the Hofmeister Series beyond Water: Specific-ion Effects in Non-aqueous Solvents', *J. Chem. Phys.* 148, 22, p. 222805, DOI: 10.1063/1.5017278.

5.1 EXPERIMENTAL MATERIALS

5.1.1 Electrolytes

The experimental part of this thesis focuses on monovalent 1 : 1 electrolytes as in previous chapters, but the selection of electrolytes has been restricted to only the sodium salts. Therefore these experiments are probing *specific-anion* effects.

The reason for this choice is primarily practical. The aim is to test different solvents and therefore only a limited number of salts can be tested in order for the measurements to be completed in a timely manner. In water, anions induce the most marked differences in the magnitude of SIE. The assumption that this would hold for non-aqueous solvents as well is soundly grounded, as the physical characteristics of the ions are not changing. The seven anions considered are listed below according to their Hofmeister ordering:

$$CH_3COO^- > F^- > Cl^- > Br^- > I^- > ClO_4{}^- > SCN^-$$

The common cation is Na^+. Molecular models of the salts and solvents are shown in Fig. 17.

Preparation of electrolytes — drying

The electrolytes were already available, and their specifications are listed in Table 21. The salts were used to prepare the samples without any further purification beyond drying, which was performed periodically. Preliminary

Table 21: Chemical specifications of the electrolytes used in the experiments.

electrolyte	supplier	product number	specifications
NaOAc	SIGMA®	S – 3272	electrophoresis reagent ⩾ 99%
NaF	Ajax Chemicals	1230 – 500G	Univar® conforms to ACS
NaCl	SIGMA-ALDRICH®	S7653 – 5KG	BioXtra, ⩾ 99.5% (AT)
NaBr	Riedel-de Haën	02119	extra pure, Ph. Eur.
NaI	MERCK®	106523	ACS reagent, Ph. Eur., ⩾ 99.5%
$NaClO_4$	SIGMA®	410241 – 500G	ACS reagent, 98 + %
NaSCN	ALDRICH®	251410 – 500G	ACS reagent, ⩾ 98%

Table 22: Oven drying protocol for the electrolytes.

electrolyte	oven type	t/°C	time/h
NaOAc	vacuum	120	10
NaF	furnace	130	24
NaCl	furnace	130	24
NaBr	vacuum	140	12
NaI	vacuum	70	12
$NaClO_4$	vacuum	140	12
NaSCN	vacuum	120	12

experimental tests were performed with the salts as they were, without drying.

The drying procedure was performed either in a furnace or in a vacuum oven, and a chemicals purification handbook (Armarego and Chai, 2009) was consulted for the recommended drying temperatures. Each salt was transferred into a small Petri dish (diameter 4 cm), and the Petri dish was placed in the oven with the lid ajar. Clumps were broken with a mortar and pestle before being transferred to the Petri dish where needed, as was the case for highly hygroscopic salts. The drying conditions are listed in Table 22 for each of the salts. After drying, the salts were quickly transferred into dry 40 ml glass vials equipped with polypropylene caps that had been washed repeatedly with Type I ultrapure water (according to the ASTM D1193 – 06 standard, produced with an ELGA *PURELAB® Chorus I* apparatus) and dried overnight in an oven at 80 °C. The vial was allowed to cool in a desiccator over silica gel and under vacuum before placing the dried salt inside. A piece of folded weighing paper, flushed with dry nitrogen, was used as a funnel for the transfer to the dry vial. After filling, a strip of *Parafilm M®* film was applied around the vial cap, and all the vials were then stored in a desiccator over silica gel. The NaSCN and NaI vials were also wrapped in aluminium foil in order to prevent light degradation. The hygroscopic salts were dried periodically as required.

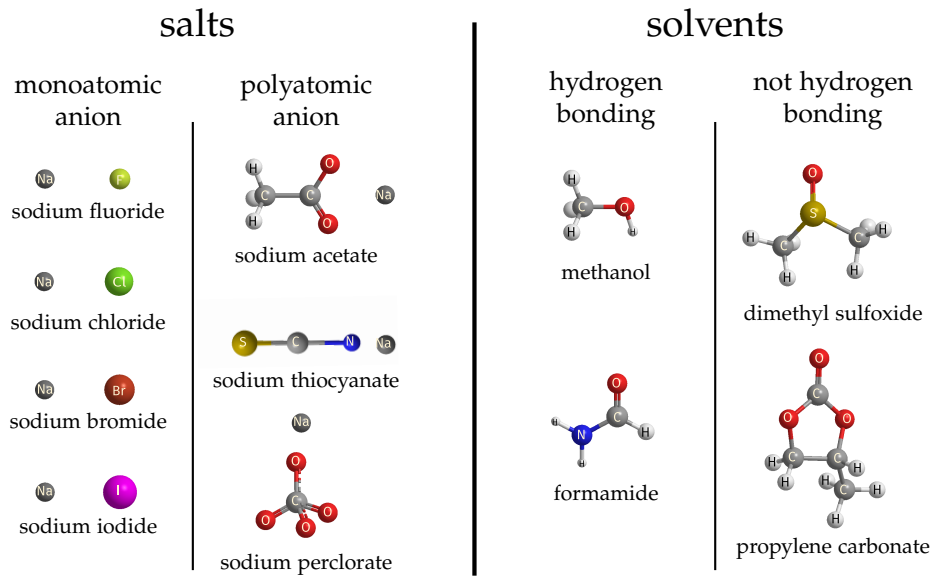

Figure 17: Stick-and-ball molecular models of the experiments salts and solvents.

A short digression on hygroscopicity

I deem it interesting to report the following observation. Sodium salts of 'kosmotropic' anions, which are the ones that are strongly hydrated in aqueous solution, are not hygroscopic at all. The powdered sodium salts of 'chaotropic' anions, are instead progressively more hygroscopic going down the Hofmeister series, to the point that NaSCN is a deliquescent salt. This is counter-intuitive as one would expect the opposite. The reason for this is that the crystal lattice free energy has to be taken into consideration, and this is much larger for 'matched' ions such as Na^+ and F^- than for 'mismatched' ones. This free energy follows Collins' LMWA (Collins, 1997), discussed in Section 4.4.

5.1.2 Solvents

In selecting the solvents to use, it was decided to experiment on two representatives from each class of hydrogen-bonding capability (protic/aprotic). The reason for choosing two aprotic and two protic solvents, rather than two high permittivity or low permittivity ones for instance, is that hydrogen bonding abilities have been indicated as one of the fundamental enablers of SIE (Thomas and Elcock, 2007). As the present work is ultimately investigating the origin of SIE, it is important to explore this connection.

We have seen in the previous chapters that proticity does not matter at a fundamental level on SIE. With this in mind, it is important to ascertain what happens when the system complexity increases with the addition of interacting surfaces and higher concentrations. Does proticity matter in these non-bulk, non-ideal conditions?

Table 23: Technical specifications of the solvents investigated.

solvent	supplier	product number	specifications
MeOH	RCI Labscan Limited	AH1118 – G2.5L	anhydrous, water max. 50 ppm
FA	SIGMA-ALDRICH®	47670 – 1L – F	puriss. p.a., ACS reagent, ⩾ 99.5, %, ⩽ 0.1% water, ⩽ 0.02% free acid (HCOOH)
	Fluka®	34724 – 1L – R	HYDRANAL®, water max. 200 ppm
DMSO	SIGMA-ALDRICH®	276855 – 2L	anhydrous, ⩾ 99.9%
PC	SIGMA-ALDRICH®	310328 – 2L	anhydrous, 99.7%

For the above reasons, the solvents chosen are MeOH and FA as protic representatives, and DMSO and PC as aprotic ones. The experiments have also been performed in water in order to have a comparison. The physical properties that these solvents span are very diverse, as Table 2 shows; molecular models representations of the salts and solvents are shown in Fig. 17.

Preparation

High purity, anhydrous solvents were purchased in order to avoid complications with drying the solvents *in-situ*. In fact, tests in the drying of solvents with 3 Å molecular sieves revealed that the solvent conductivity often increases upon the addition of molecular sieves (especially for MeOH). An increase in conductivity means that ions (of unknown species) have been released into the solvent. These ions represent an undesired contamination that could interfere with the effects of the ions of interest. Therefore the addition of molecular sieves for drying the solvent, or for keeping the solvent dry was obviated. The water content was periodically checked through Karl Fischer (KF) titration. The technical specifications of the solvents are reported in Table 23. Preliminary tests were often carried out with non-dry solvent from bottles already available in the laboratory. It seems that small quantities of water do not affect the SIE trends, as no differences in the ordering of ion effects were observed between experiments performed with standard solvents and those performed with anhydrous solvents.

the description of the technique is in Section 5.3.1, page 95.

5.2 PREPARATION OF THE SALT SOLUTIONS

The electrolyte solutions were prepared in molality m ($mol\,kg^{-1}$) concentration units. Molality was preferred over concentration c in $mol\,dm^{-3}$ because the solution density changes with the salt present (see Fig. 99 in Appendix G), and this effect is relatively more significant at lower salt concen-

trations. As the preparation of solutions by molality involves weighing both solute and solvent, it does not present the above mentioned complication.

A KERN® ABJ − 220 − 4M analytical balance was therefore used. A Petri dish was employed as support for the vial and to distribute its weight on a larger surface of the balance plate. The vials where the solutions were going to be prepared were washed with Type I ultrapure water, dried in an oven overnight and kept in a plastic desiccator over silica gel and under vacuum before use. Typically 20 g to 25 g of solution (depending on its density) were prepared each time in a 25 ml vial. This quantity was preferred over larger quantities in order to facilitate storage in desiccators. Also, to avoid problems associated with storage (e.g. contamination, evaporation of the solvent), it was preferred to re-prepare the solution more often rather than storing it for a long time.

The salt was first weighed directly into the vial, followed by the addition of the solvent (as close as possible to the desired weight). Both salt and solvent weight were noted in order to calculate the solution concentration with the maximum accuracy achievable. The weighing procedure was performed in air, as quickly as possible. The usage of a glove bag was considered and trialled but the problems associated with the scale instability overcame the advantage of weighing in a dry atmosphere. The relative humidity in the laboratory was on average low (around 25 %), therefore swift operation and the monitoring of water content through Karl Fischer (KF) titration were preferred for practicality.

Parafilm M® was applied around the vial cap immediately after preparation to help prevent moisture ingress. When dissolution was not instantaneous, a vortex mixer and sonication were used to help the dissolution process. In some cases, such as for iodide salts, sonication was applied only briefly to avoid oxidation of the iodide to iodine (revealed by the appearance of a yellow colour). This is particularly true for DMSO solutions of NaI: no sonication was applied at all in this case.

5.2.1 Solubility of the salts

The solubility of the electrolytes in the different solvents is listed in Table 24. Most of the information was available in the literature. A salt concentration that was accessible for most electrolytes in the different solvents is $0.05\,\mathrm{mol\,kg^{-1}}$. Therefore this was set as the electrolyte concentration for the chromatography experiments. QCM measurements were performed with electrolyte solutions of $10^{-3}\,\mathrm{mol\,kg^{-1}}$ concentration. This lower concentration was sufficient to produce detectable changes in the polymer brush behaviour, whilst higher concentrations had little effect on the magnitude of the changes observed (see Fig. 29 in Chapter 7).

Table 24: Literature solubility $\mathcal{S}$ data for the electrolytes investigated.

methanol			
electrolyte	$\mathcal{S}/\mathrm{mol\,kg^{-1}}$	$t/°C$	reference
NaOAc	1.95*	15	H. Stephen and T. Stephen, 1963
NaF	0.099*	20	H. Stephen and T. Stephen, 1963
NaCl	0.24†	25	Pinho and Macedo, 2005
NaBr	1.63†	25	Pinho and Macedo, 2005
NaI	5.20*	25	H. Stephen and T. Stephen, 1963
$NaClO_4$	4.194	25	Chan et al., 1996
NaSCN	4.939	24.7	Hála, 2004
formamide			
electrolyte	$\mathcal{S}/\mathrm{mol\,kg^{-1}}$	$t/°C$	reference
NaOAc	$\geqslant 0.05$‖		
NaF	0.026‡	25	Scrosati and Vincent, 1980
NaCl	1.61§	25	Scrosati and Vincent, 1980
NaBr	3.43§	25	Scrosati and Vincent, 1980
NaI	4.00§	25	Scrosati and Vincent, 1980
$NaClO_4$	$\geqslant 0.05$‖		
NaSCN	17.7§	25	Scrosati and Vincent, 1980
dimethyl sulfoxide			
electrolyte	$\mathcal{S}/\mathrm{mol\,kg^{-1}}$	$t/°C$	reference
NaOAc	0.0078‡	25	J. N. Butler, 1967
NaF	insoluble	25	J. N. Butler, 1967
NaCl	0.08	25	J. N. Butler, 1967
NaBr	0.55	25	J. N. Butler, 1967
NaI	1.0	25	J. N. Butler, 1967
$NaClO_4$	1.8	25	J. N. Butler, 1967
NaSCN	0.12‡	25	J. N. Butler, 1967
propylene carbonate			
electrolyte	$\mathcal{S}/\mathrm{mol\,kg^{-1}}$	$t/°C$	reference
NaOAc	<0.05‖		
NaF	5×10^{-5}	25	Harris, 1958
NaCl	3×10^{-6}	25	Harris, 1958
	1.7×10^{-4}‡	25	Muhuri et al., 1993
NaBr	0.08	25	Harris, 1958
	3.6×10^{-3}‡	25	Muhuri et al., 1993
NaI	1.11	25	Harris, 1958
$NaClO_4$	2.5‡	25	Muhuri et al., 1993
NaSCN	$\geqslant 0.05$‖		

* Calculated by the author, original given as 'percentage by weight' Wt.%.
† Calculated by the author, original given as mass fraction w_{salt}.
‡ Units: $\mathrm{mol\,dm^{-3}}$.
§ Calculated by the author, original given as $\mathrm{g\,kg^{-1}_{solvent}}$.
‖ no literature data available, the value listed comes from experience and refers to room temperature.

Table 25: Summary of the electrolytes investigated per solvent.

electrolyte	MeOH	FA	DMSO	PC
NaOAc	✓	✓		
NaF	✓			
NaCl	✓	✓	✓	
NaBr	✓	✓	✓	
NaI	✓	✓	✓	✓
$NaClO_4$	✓	✓	✓	✓
NaSCN	✓	✓	✓	✓

The electrolytes investigated for each solvent are summarised in Table 25. Although there are literature reports (Harris, 1958) that NaBr is soluble in PC at a concentration of $5 \times 10^{-2}\,\mathrm{mol\,kg^{-1}}$, it was not possible to achieve its solubilisation at that concentration nor at the lesser concentration of $10^{-3}\,\mathrm{mol\,kg^{-1}}$. Note the solubility of salts varies greatly across solvents and is in most cases lower than in water. This limits the range of electrolytes and the concentrations available for investigation.

5.2.2 Storage of solutions

The iodine and thiocyanate solutions vials were covered in aluminium foil to prevent light degradation of the anions. All the vials containing solutions were kept in a glass desiccator over silica gel and granular phosphorous pentoxide, P_4O_{10}, which were changed regularly. Additionally, the desiccator was placed under a slight vacuum.

5.3 THE INFLUENCE OF TRACE QUANTITIES OF WATER

When investigating SIE in polar non-aqueous solvents, which are to some extent hygroscopic, the possible interference of water is a concern. It is known that water can selectively solvate ions in mixtures with non-aqueous solvents (J. N. Butler et al., 1971). Preferential solvation is found to be negligible for mixtures of solvents of similar polarity and/or hydrogen-bonding capability (Marcus, 2004), therefore we can expect trace concentrations of water in MeOH and FA to be distributed randomly in solution and within the solvation shells of the ions. In the case of solvents that differ in polarity or hydrogen-bonding properties to water, such as DMSO and PC, water preferentially solvates the anions, while the cations exhibit little to no preferential solvation (Marcus, 2005). This matters particularly for the experiments in this work as they are probing *specific-anion* effects.

Table 26: Water to ion ratio $R = n_{H_2O}/n_I$ per 1 kg of solution calculated for the salt concentration indicated in parentheses (in $mol\,kg^{-1}$).

w_{water}% *	n_{H_2O}/mol	R (0.1)	R (0.05)	R (0.001)
0.01	0.006	0.03	0.06	3
0.03	0.02	0.08	0.2	8
0.10	0.06	0.3	0.6	28
0.20	0.1	0.5	1	56
0.35	0.2	1	2	98
0.50	0.3	1.4	3	140
1.00	0.6	3	6	281

* $w_{water}\% = m_{H_2O}/m_{sample} \times 100$;

Water should not be present in solution in concentrations comparable with those of the ions that are investigated, and if possible, it should be one-order of magnitude lower (Zuman and Wawzonek, 1978). In any case, experimenting in SIE in non-aqueous solvents implies embarking in a constant battle against water.

Analytical methods for water determination include KF titration as employed in this work, but also gas chromatography is generally applicable, and UV spectra can provide additional information (Zuman and Wawzonek, 1978).

A first, simplistic approach can be as follows: assuming that water distributes primarily in the solvation shell and assuming a hydration number of 6, the concentration of water required to form a complete hydration shell around the ions present in a solution is calculated. Let us define the ratio $R = n_{H_2O}/n_I$ as the number of water molecules per ion (counting both cations and anions). For electrolyte concentrations of $10^{-1}\,mol\,kg^{-1}$, $5 \times 10^{-2}\,mol\,kg^{-1}$ and $10^{-3}\,mol\,kg^{-1}$, Table 26 shows R for different water concentrations w_{water}%. At the electrolyte concentration used in the chromatography experiments ($5 \times 10^{-2}\,mol\,kg^{-1}$), $w_{water} \geqslant 1\,\%$ is necessary in order for each salt ion (anion and cation) to be fully surrounded by a solvation shell of water molecules. The w_{water}% in the samples tested by KF titration was always less than 0.13 %. This shows that for salts at a concentration of $5 \times 10^{-2}\,mol\,kg^{-1}$ and above the water concentration is too low to dominate the solvation shell. For a water content of 0.1 % by weight, which was the highest water content measured by KF titration, in the 'anhydrous' experiments, there is approximately one molecule of water for every 550 molecules of MeOH. Similarly the ratio of solvent molecules to water molecules is 400 in FA, 230 in DMSO and 175 in PC. It is evident from Table 26 that, as the electrolyte concentration decreases, lower concentrations of water are required to fully occupy the solvation shell of the ions present. This encourages the use of higher ($> 5 \times 10^{-2}\,mol\,kg^{-1}$) electrolyte concentrations, but the lower solubility of electrolytes in many non-aqueous solvents limits the available concentration.

However, the ability to form a solvation shell around each ion is not the most appropriate measure of the extent to which water affects the properties of the non-aqueous system: the activity, rather than the concentration, of water in the solvent is the quantity of consequence. For instance, the physical properties of ionic liquids, such as melting point, viscosity and density are known to change significantly even in presence of trace amounts of water (Huddleston et al., 2001; Seddon et al., 2000). Therefore the reasoning made above must be taken with caution. Prudence demands that the influence of water on the properties of non-aqueous systems be tested experimentally.

In order to address the question more pragmatically, I have performed some tests to determine the effect of the addition of small amounts of water on the experiment outcome. I have performed tests both for SEC runs and QCM experiments, and the results are reported and discussed in Appendix F. The contents in Appendix F are best understood after one is acquainted with the concepts and terminology introduced in Chapter 6 and Chapter 7, which follow. The main information sought through these tests is whether the presence of traces of water can substantially alter the qualitative SIE trends of the experiment. The results are varied, and while in MeOH no effect on the overall trend is observed, ions in PC (but not DMSO) may be relevantly influenced by small amounts of water. The conclusion is that further detailed studies of the influence of water on the behaviour of non-aqueous systems are necessary, and the experimental results presented in Chapters 6 and 7 need to be considered with awareness of the problematic.

The determination of how much water is important is unlikely to be a simple consideration. Rather it will depend on the information being sought. It is known, for instance, that the influence of water depends on it being available as a proton donor. Experiments show that traces of water are highly reactive with radical anions in MeCN, whereas the same content of water has almost no effects in DMF and DMSO. Therefore, in the latter two solvents water is solvated in a way that forbids it from acting as a proton donor: it is argued that this is because of hydrogen bonding (Zuman and Wawzonek, 1978).

It will therefore be important to determine the concentration of water that leads to a measurable change as well as the concentration of water required to alter the observed ion-specific trends.

5.3.1 The Karl Fischer titration method for water determination

Karl Fischer (KF) titration is a selective method for the determination of the amount of water in a sample, provided no side reactions occur (Bruttel and

Schlink, 2006). The method is based on the Bunsen reaction (employed for the titration of SO_2 in aqueous solution):

$$SO_2 + I_2 + 2\,H_2O \longrightarrow H_2SO_4 + 2\,HI$$

and involves the oxidation of sulfuric anhydride by iodine in an anhydrous solvent, often MeOH, in the presence of a base, noted RN (for instance pyridine or imidazole), capable of neutralising the acids produced. The overall reaction in methanolic solution takes place in two stages: the formation of monomethyl sulfite from MeOH and sulfuric anhydride first, followed by its oxidation by iodine with consumption of water, according to the reactions listed below (Verhoef and Barendrecht, 1976).

$$CH_3OH + SO_2 + RN \longrightarrow [RNH]^+\,SO_3CH_3^-$$

$$H_2O + I_2 + [RNH]^+\,SO_3CH_3^- + 2\,RN \longrightarrow [RNH]^+\,SO_4CH_3^- + 2\,[RNH]^+\,I^-$$

The molar ratio of the titration reaction is different from the aqueous Bunsen reaction and is $H_2O : I_2 : SO_2 : RN : CH_3OH = 1 : 1 : 1 : 3 : 1$ (Smith et al., 1939).

In this work, a *Metrohm* 870 *KF Titrino Plus* KF titration unit equipped with a *Metrohm* 803 *Ti Stand* was used for water determination. This is a volumetric KF titration instrument, which automatically performs the titration for best results and safest practice.

One-component KF reagents for titration were used. This means that the titrant (Fluka® HYDRANAL®-Composite 5, approximate titre 5 mg of H_2O per ml of titrant) contains all the reactive components needed for the titration reaction, and the working medium where the sample is dissolved is composed of dry MeOH (Fluka® HYDRANAL®-Methanol Rapid). The one-component titrating solution presents the disadvantage that its titre decreases by about 5% per year, so calibration was carried out frequently using a small amount ($\approx$ 0.01 g) of Type I ultrapure water.

The water determination procedure was as follows: the sealed titration cell of the instrument is filled with the working medium from the reagent bottle to the minimum level required and the 'conditioning' procedure is carried out (i.e. the water present in the vessel is eliminated by adding titrant until a constant and low titrant drift is reached — this corresponds to the amount of environmental moisture that inevitably enters the titration vessel). Once conditioning is performed, a beaker containing an empty 2 ml glass syringe (that had previously been rinsed with a small amount of sample) and the sample vial is placed on the analytical scale and zeroed. The beaker is then taken from the scale and the syringe is filled with sample from the vial, and the whole sample withdrawn is injected in the KF titration cell. The syringe and sample vial are placed back in the beaker and weighed in order to de-

termine the weight of the sample injected in the cell. This amount is input through the instrument dial pad and the titration commenced. The titration is carried out automatically, the end point is detected by electrometric methods. When the titration is complete, the instrument outputs the water content as mass fraction of water in the sample w_{water}%.

MeOH, DMSO, FA, PC do not undergo any side-reaction with the KF reagents, therefore the titration can be carried out following the standard procedure.

It must be borne in mind that, as the materials used are quite dry, a large sample is required (at least 1 g). Actually, the ideal titration accuracy is reached when 20 % to 80 % of the 5 ml titration burette is used. For dry solutions such as the ones used in this work, such as a solution containing a w_{water} of 0.05 %, 10 g of sample would be needed in order to use 1 ml of titrant (the titrant titre is approximately 5 mg H_2O per ml of titrant)! If this were done, another problem would arise as the large sample volume dilutes the titration medium, which could affect the titration reaction. A compromise must therefore be made between checking the water content with acceptable accuracy and disturbing the titration or wasting sample. Therefore 1 g to 2 g of sample was used for each KF titration. The titration was repeated at least two times, or more if the results were not in agreement.

5.4 MATERIAL INCOMPATIBILITIES WITH THE SOLVENTS

When working with solvents other than water, another important experimental challenge arises because many widely applied experiments have not been performed with non-aqueous solvents. Most of our current experimental understanding is for water solutions. This means that, in addition to the limitations listed above for the solubility of electrolytes and the additional precautions needed to avoid water contamination, unforeseen materials incompatibility issues can arise. Materials such as glass, stainless steel and perfluorinated polymers have no chemical resistance issues with the solvents employed here. However it is a different scenario when dealing with other types of polymers, especially elastomers. These can be found in connecting tubing, pump tubing, gaskets, O-rings, vial cap liners and so on. DMSO in particular is an excellent solvent for many different types of plastics.

In order to avoid unwanted contamination from the dissolution of materials in the non-aqueous solvents employed, polymers and elastomers with excellent chemical resistance were used in all the experiments. These include Saint-Gobain Tygon® 2001 for the QCM peristaltic pump tubing, DuPont™ Karlez® 6380 for the QCM O-ring and internal cell gasket, Teflon® tubing for

the QCM sample cell connections; polytetrafluoroethylene (PTFE) and fluorinated ethylene propylene (FEP) tubing for the SEC experiments.

6 CHROMATOGRAPHY OF SALTS

This chapter is reproduced with minor changes from:
V. Mazzini, G. Liu et al. (2018), 'Probing the Hofmeister Series beyond Water: Specific-ion Effects in Non-aqueous Solvents', *J. Chem. Phys.* 148, 22, p. 222805, DOI: 10.1063/1.5017278.

6.1 RATIONALE

An important contribution in the study of SIE is the characterisation of electrolytes of biological interest by size-exclusion chromatography (SEC), performed by Washabaugh and Collins (1986).

Given the great insight that this relatively simple experiment has given, I have replicated it for sodium salts of Hofmeister anions (see Section 5.1.1) in MeOH, FA, DMSO and PC, in order to acquire information on the solvation and surface-interaction status of anions in non-aqueous solutions.

This experiment, although quite simple in theory, has proved challenging. This is because it involves a technique and a stationary phase that was developed for aqueous solutions. Therefore additional work was needed to adapt the technique to non-aqueous solvents.

6.2 SIZE-EXCLUSION CHROMATOGRAPHY IN WATER

The ion specificity observed in the experiments of Washabaugh and Collins (1986) was the opposite of what would be expected if the ions in solution behaved ideally. Ideal ions are expected to interact with their hydration shells with the same strength (independently of the ion), and they are expected not to interact with the column (uncharged) stationary phase. In ideal conditions, small electrolytes are expected to elute in order of decreasing size and to leave the column after the void volume, but before one column volume of eluent has been passed. (See Table 27 for the size of the molecules). As the ions investigated are of similar size to the eluent, it is expected that their retention factor would be close to 1 (the eluent retention factor).

Rather, Washabaugh and Collins (1986) found that the electrolytes do not behave ideally, and are eluted in order of increasing size, in agreement with the Hofmeister series. In addition, some of the electrolytes elute later than

Table 27: Molar masses, radii and volumes of the ions and solvents studied. Ionic *ab initio* radii, r_I, from Parsons and Ninham (2009); ionic volumes, V_I, calculated as $4/3\pi {r_I}^3$; Van der Waals volumes of the solvent molecules, V_{VdW}, calculated using the '*Geometrical Descriptors*' plugin from the *MarvinSketch* software (ChemAxon, 2017); Van der Waals radii, r_{VdW}, calculated by the author from V_{VdW}.

anion	M_I / g mol^{-1}	r_I / Å	V_I / Å^3
Na^+	22.99	0.61	0.95
F^-	19	1.02	4.4
Cl^-	35.45	1.69	20.2
Br^-	79.9	1.97	32.0
I^-	126.9	2.12	39.9
ClO_4^-	99.45	2.17	42.8
SCN^-	58.08	2.18	43.4
AcO^-	59.04	2.2	44.6
solvent	M_I / g mol^{-1}	r_{VdW} / Å	V_{VdW} / Å^3
water	18.01	1.8	24.24
MeOH	32.04	2.1	36.84
FA	45.04	2.1	41.7
DMSO	78.13	2.6	72.69
PC	102.09	2.8	87.98

one column volume of eluent. The explanation proposed was that small anions such as fluoride are strongly hydrated and travel in solution with their sphere of hydration tightly bound, resulting in a larger hydrodynamic volume and a shorter retention time than expected. On the other hand, larger polarisable ions such as bromide, iodide or thiocyanate are capable of directly interacting with the stationary phase, behaving as 'sticky' ions. This latter finding was also demonstrated by Washabaugh and Collins by showing the temperature-dependence of the retention times of the electrolytes containing large, polarisable ions.

Washabaugh and Collins (1986) also introduced the classification of ions into 'kosmotropes' ('that turn towards order', as referred to their ordering of the surrounding water molecules) and 'chaotropes' (thought to disorder the surrounding water molecules), based on their chromatographic behaviour. The anions that elute before Cl^- on a *Sephadex*® G – 10 column are kosmotropes, whereas the ones that elute after Cl^- are chaotropes. This terminology quickly became popular in several fields regarding electrolytes (the term chaotrope was already in use and had been introduced by Hamaguchi and Geiduschek (1962), but Washabaugh and Collins coined 'kosmotrope' to describe the ions that behave in the opposite way). These terms have become almost synonyms with the phrases 'structure-maker' and 'structure breaker', that had been used since the 1950s, but 'kosmotrope' and 'chaotrope' do not imply a long-range effect on the structure of water, whereas the former terms do. The use of all these terms is currently undergoing revision.

These experiments contributed to the formulation of the law of matching water affinities (LMWA) (Collins, 1997, 2004; Collins, Neilson et al., 2007) and also provided evidence for the importance of dispersion forces on the behaviour of ions in water (Kunz, Belloni et al., 2004; Ninham, Duignan et al., 2011; Parsons, Boström, Lo Nostro et al., 2011; Salis and Ninham, 2014).

6.3 DESCRIPTION OF THE TECHNIQUE

Size-exclusion chromatography (SEC) is a type of liquid column chromatography that uses the stationary phase as a sieve in order to separate analytes according to their solvodynamic volume. Through calibration, the molecular weight of each separated fraction can be indirectly estimated.

'chromatography' indicates a family of laboratory techniques employed in the separation of mixtures

SEC can be employed for preparative or analytical purposes. It is popular for the fractionation of proteins and for the characterisation of polymer mixtures.

It is the only type of chromatography where no interaction is sought between the analyte and the stationary phase. The column therefore acts merely as a sieve. The separation or characterisation of a substance of a particular solvodynamic radius (which includes the size of the molecule or ion and any tightly bound solvent), is therefore obtained on a purely entropic basis. Separation is based on differences in the average path an analyte traverses inside the column. This is correlated to the size of the analyte with respect to the porosity of the stationary phase. More accurately, the analyte partitions between the moving eluent phase outside the pore space, and the pools of stationary eluent inside the pores (Striegel et al., 2009). If the molecule is sufficiently large that it is excluded from accessing the pores of the stationary phase, its path will be short and it will exit the column together with the eluent front. Alternatively, if the analyte can access the pores, there will be a fraction of its molecules inside the pores at any time, and therefore its elution volume will be greater the smaller the analyte size. The longest paths are available when the solute can access all the porosity. In practical terms this is when the solute is as small as the molecules of solvent.

The eluted analyte is characterised by its retention factor K_{SEC} (Striegel et al., 2009; Tayyab et al., 1991):

$$K_{SEC} = (V_R - V_o)/V_i \quad [9]$$

where V_R is the retention volume of the analyte peak, V_o is the void volume of the column (the volume of the interstitial mobile phase), and V_i is the internal pore volume of the column (the stagnant volume of solvent trapped inside the stationary phase pores). A $K_{SEC} = 0$ indicates that the analyte is completely excluded from accessing the stationary phase pores, whereas

$K_{SEC} = 1$ indicates that the analyte accesses all volumes accessible to the solvent. Molecules with intermediate sizes will display a retention factor between 0 and 1, proportional to their size. A $K_{SEC} > 1$ is indicative of specific absorption to the stationary phase packing and is a non-ideal condition that violates the assumption of exclusively entropic separation.

Experimentally, the void volume V_0 is measured by running a sample that is larger than the cut-off porosity of the stationary phase. A common choice for determining V_0 is Blue Dextran. This is what was used where possible. The internal pore volume V_i can be measured by subtracting V_0 from the elution volume of a molecule of similar size to the eluent. As the detection of such a molecule is often difficult (in the past radioactive labelling was used), a molecule larger than the eluent but much smaller than the analyte is used, or the total geometric volume V_t of the column is used as an estimate of the internal volume. This is simply the volume of the cylinder with the same height and radius of the stationary phase of the column. In this second case, K_{SEC} is approximated as K_{AV} (available) where:

$$K_{AV} = (V_R - V_0)/(V_t - V_0) \quad [10]$$

As this estimate does not account for the volume occupied by the packing material and of the molecules of solvent tightly bound to the packing, this method results in an underestimation of the real retention factor of the analyte.

Both K_{SEC} and K_{AV} are independent of the stationary phase height and are therefore useful in comparing different packings of the same stationary phase. In addition, K_{SEC} contains information about the physical distribution of the analyte in the column.

The calibration of the column can be performed by a series of solutes that behave 'ideally', are of known molecular weight and are monodisperse. These can be proteins, peptides, polymers, olygomers based on the technique being used and the molecular weights of interest. For established SEC procedures, calibration kits are commercially available. In the present work I have attempted to calibrate the column but with no success.

The detection of the analyte can be performed by monitoring chemical or physical properties of the eluate, depending on the properties of the analytes and of the eluent; popular techniques include differential refractometry, spectroscopy (mostly UV-vis, but also Fourier-transform infrared spectroscopy (FT-IR) and NMR), viscometry.

6.4 EXPERIMENT DETAILS

The chromatographic arrangement and experiment procedures used by Washabaugh and Collins (1986) were followed where possible. Though, substantial differences could not be avoided in our experiments, and are summarised in Section 6.4.6. The usage of non-aqueous solvents presents a number of challenges including the measurement of the void volume and internal volume. A detailed description of the methods we have used to determine these volumes are included in Section 6.4.5.

6.4.1 Preparative tests

The same stationary phase as the one used by Washabaugh and Collins (1986) was used: *Sephadex*® G-10, epichlorohydrin-crosslinked dextran with an exclusion limit of 700 Da. The gel is marketed for use in water, therefore it was necessary to test its swelling and resistance to non-aqueous solvents. This was done by suspending one gram of *Sephadex*® in each of five vials and adding an excess of anhydrous solvent or neat water. The swelling order after three days was as follows: PC $\ll$ MeOH $<$ water $<$ FA $\leqslant$ DMSO. Therefore the height of the column stationary phase was expected to vary in the presence of different solvents. In PC very little swelling was observed. The swelling of the stationary phase is a critical parameter as it determines the column exclusion limit. With regards to stability of the *Sephadex*® suspensions, after 3 years of storage in the dark, no degradation was observed upon visual inspection.

As an automated system such as the *GE Healthcare ÄKTA-Lab* was not available, and it was anyway uncertain what effect non-aqueous solvents would have on several parts of the apparatus such as the gaskets, it was chosen to perform the chromatographic runs manually on an apparatus I assembled.

6.4.2 Experiment apparatus and preparation

A 44 cm-long glass column was used, with an internal diameter of 1.63 cm (measured by caliper: 1.627 cm; measured by filling with a certain height of water and weighing the water: 1.630 cm), equipped with a 24/29 *Quickfit*® cone and a *Teflon*® tap.

A schematic of the arrangement is in Fig. 18. The apparatus was mounted and run inside a fumehood.

A stainless steel connector and a *Teflon*® connector were made in-house in order to connect the large bore glass outlets of the eluent reservoir and of

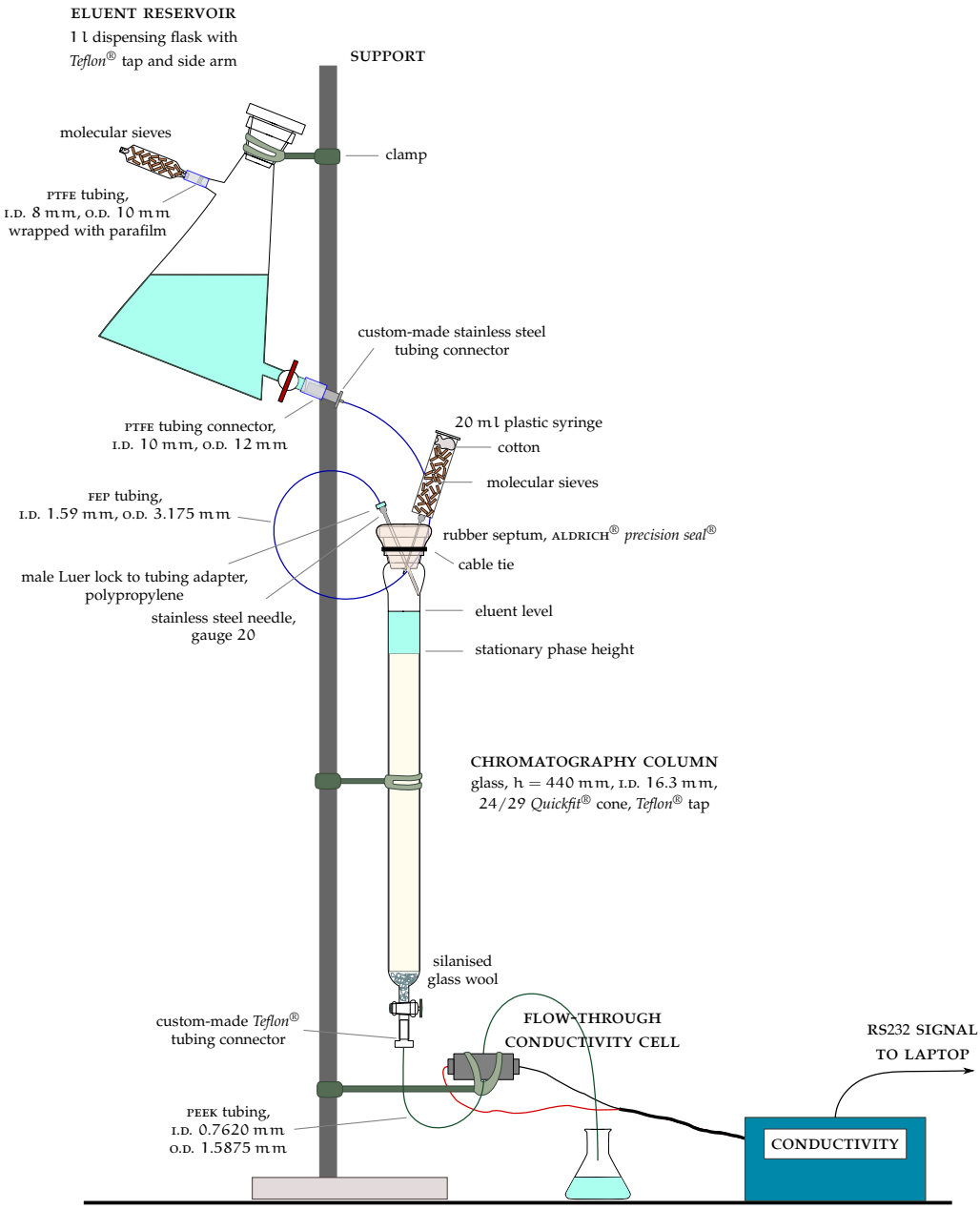

Figure 18: Scheme of the chromatography experiment setup.

the column to tubing. All the tubing was made of high chemical resistance polymers: FEP or PTFE, or polyether ether ketone (PEEK).

Detector

In order to detect the sample peak, we monitored the conductivity of the eluate and ran each sample separately. The detection by conductivity made it impossible to use a NaCl solution as eluent, as in Washabaugh and Collins's work (1986), because our tests showed that the conductivity signal to noise ratio of the sample peak was too small. Washabaugh and Collins (1986) had used a NaCl solution as eluent in order to minimise the ion-exchange effects of the hydroxyl groups on the *Sephadex*® surface.

Our trials in MeOH show that the peak position is not substantially affected when using pure eluent in place of a salt solution. For the initial trials, the conductivity of the eluate was checked with a dip-in probe connected to a *TPS smartCHEM-LAB* multi-parameter laboratory analyser. The laboratory conductivity sensor, also supplied by *TPS*, had a cell constant $k = 1.0$. This sensor needs to be immersed in at least 15 ml of sample in order to measure its conductivity. Once it was ascertained that the non-aqueous chromatography experiment was feasible, it was evident that a resolution of 15 ml in monitoring the eluate conductivity was too low. A custom-built flow-through conductivity cell was therefore made in-house. The design of this custom-made cell aimed at obtaining a detector with a small dead volume to have a good resolution, with sufficient sensitivity, and that would be resistant to the range of different solvents that we were going to use. This flow-through cell consists of a hollow PEEK cylinder, sealed at the two extremities by two threaded stainless steel electrodes. The design of the conductivity cell is reproduced in Fig. 92 of Appendix E. The inlet and outlet to the cell are perpendicular to the main cavity of the cylinder, so that the solution flows parallel to the electrodes surface. The total volume of the chamber is about 1 ml. The cell is mounted with the electrodes in a horizontal position and the inlet tube at the bottom, so that the internal chamber completely fills with the eluate without leaving air pockets. The electrodes send the signal to the *TPS smartCHEM-LAB* unit, which records the conductivity in auto-logging mode, every 30 s. The conductivity readings from the *TPS smartCHEM-LAB* unit are sent through an RS232 to USB 2.0 port adapter to a laptop, where they are processed by the *Termite* 3.3 RS232 terminal (Compu Phase, 2015). Despite this cell being of rudimental construction and despite the inferior performance of stainless steel with respect to platinised platinum (the material of choice for conductivity cell electrodes), it shows a linear response at low conductivity as shown in Fig. 19. The sensitivity is about one fourth of the *TPS* dip-in probe in the linear region.

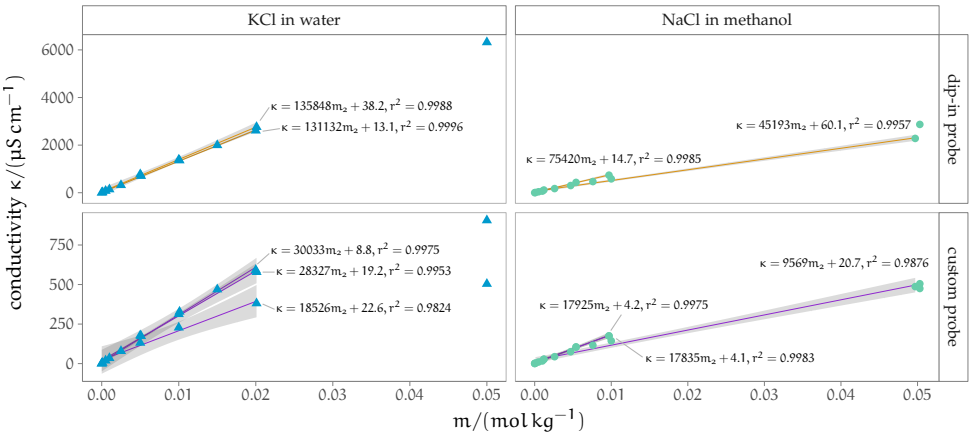

Figure 19: Calibration curves for the custom made conductivity probe against the *TPS* probe. The shadings around the fitting lines represent a 95% confidence interval.

Column silanisation

The column was silanised before packing. Given its dimensions, it was not possible to carry out the silanisation inside a desiccator. The column was prepared for the silanisation procedure by washing it with a 10% NaOH solution, thoroughly rinsing it with Type I ultrapure water, and drying in an oven at 85 °C overnight (the glass wool, the tap and a stopper for the top *Quickfit*® cone were washed and dried in the oven as well). The following morning, the column was taken out of the oven and assembled and stoppered swiftly. A quick procedure for silanising was carried out as follows in a fumehood: a few drops of chlorotrimethylsilane (ALDRICH®) were introduced with a 1 ml plastic syringe while the column was still warm and the stopper quickly put back. The chlorotrimethylsilane quickly evaporated to react with the silanol groups of the glass.

The column was kept stoppered and sealed with *Parafilm M*® until packing.

Column packing

The packing of the column was performed in MeOH as it was the first eluent I intended to test. Also, as MeOH is less viscous than FA and DMSO, I expected packing to be faster in this solvent as the flow rate would be higher. All of the operations were performed rapidly in order to let as little moisture as possible into the column. None of the solvents and solutions used were filtered or degassed. All of the operations were performed in a fumehood. The packing of the column was performed with the conductivity probe already connected to the column. This was done especially to avoid disturbing the packing as the insertion of the PTFE column outlet-to-tubing adapter required some force.

The *Sephadex*® G-10 (≈ 53 g) was dried in an oven at 85 °C in a 250 ml conical flask for 8 h, the flask was then put in a desiccator to cool. An excess of dry MeOH (≈ 150 ml was subsequently added to the *Sephadex*®, the flask was sealed with aluminium foil and *Parafilm M*®, and left to swell overnight in a desiccator. As the column did not have a frit, a small amount of silanised glass wool was placed in the bottom throat of the column to prevent the *Sephadex*® from going through the tap. The glass wool was tapped gently, trying to avoid compacting it too much, with a long glass rod to form a surface as even and horizontal as possible. Part of the supernatant MeOH was discarded from the *Sephadex*® suspension in order to obtain a thick slurry (≈ 75% settled *Sephadex*®), which was kept in suspension by delicately swirling the flask. The column was filled with approximately 8 cm of neat dry eluent, the glass wool was tapped delicately with a long glass rod to eliminate the trapped air bubbles; the tap was then opened and the slurry poured down a glass rod slowly in one motion. The glass rod was used to direct the slurry flow towards the inner wall of the column and prevent splashing and bubble incorporation in the slurry. As soon as the slurry pouring was finished, a cone 24 drying tube filled with molecular sieves was applied at the top, to avoid the entrance of moisture, whilst allowing air through in order to let the eluent flow. The tap was kept open and anhydrous MeOH added at the top of the column (by removing and then replacing the drying tube) to pack the stationary phase. More than one column volume (≈ 50 ml) of solvent was eluted before closing the tap. When the tap was closed, the drying tube on top was substituted with a stopper and sealed externally with *Parafilm M*®. *Parafilm M*® was also applied around the closed column tap.

6.4.3 Experiment procedure

The day after packing in MeOH, the height of the stationary phase was measured, amounting to 32.3 cm. For the first sample run, an *Aldrich Precision Seal*® rubber septum (low in solvent extractables) for 24/40 joints was put on the top cone and the sleeve was bent over and secured with a cable tie. The rubber septum was always kept in place until the end of all of the experimental runs in all of the eluents. It was replaced with a new one when the number of punctures was compromising the seal. The septum was punctured with the needle (25G) of a 20 ml plastic syringe, from which the plunger had been removed and that had been filled with molecular sieves (kept in place by cotton wool at the end of the syringe), in order to equalize the column to atmospheric pressure. Another needle (20G) was used to connect the reservoir tubing and feed the eluent to the column.

At the end of each day, the two needles would be removed and capped, and the rubber septum covered with *Parafilm M*® as an additional protection from moisture.

The eluent reservoir was refilled, when needed, with fresh anhydrous solvent from the storage bottle. Cannulation with dry nitrogen from the solvent storage bottle was tested in order to fill the eluent reservoir and keep the eluent as anhydrous as possible, but as the cannulation procedure is extremely time-consuming for large volumes of solvent, it was decided to instead transfer the solvent classically by using an oven-dried 250 ml beaker as a transferring vessel. All of the operations were performed rapidly in a fumehood.

The eluent reservoir was washed and dried periodically, especially when changing eluent in the column. The reservoir was sealed with *Parafilm M*® at the end of each day to avoid the entrance of moisture and preserve the molecular sieves. Also the column rubber septum and tap were wrapped in aluminium foil and *Parafilm M*® overnight. The PTFE adapter for the conductivity cell tubing at the outlet of the column was never disconnected.

The concentration of each electrolyte sample was $5 \times 10^{-2}\,\mathrm{mol\,kg^{-1}}$.

Sample loading

In order to load the sample, the eluent level in the column was lowered until it reached the top of the stationary phase. The column tap was then closed and the rubber septum was punctured with a 1 ml *Hamilton*® syringe mounting a 25G needle, which had just been rinsed with 0.5 ml of sample, and filled with fresh sample. The syringe was emptied very slowly while its needle tip was kept close to the column wall so that the falling sample drops would not disturb the column packing. The tap was opened immediately afterwards, the *Hamilton*® syringe extracted from the rubber septum, and the sample was left to absorb on the stationary phase. As soon as the sample was completely loaded, the eluent supply was restored by opening the reservoir tap, and the eluent level above the stationary phase was restored to a marked level as quickly as possible, but still while being very careful to avoid disturbance of the column bed at the beginning of the addition. At the same time that the eluent supply was reopened, the conductivity-metre auto-logging was started, in order to record the conductivity of the eluate as a function of time.

Elution

In order to keep the column flow quite constant, the solvent reservoir tap was adjusted so that there would always be a certain height of eluent above the stationary phase. This height was approximately 6 cm.

During elution, the flow rate was monitored by measuring the time required to fill a 5 ml measuring cylinder with eluate (the cylinder was put in place of the waste container, after the conductivity probe). For best accuracy, during the anhydrous runs, the flow rate was measured continuously by alternating two measuring cylinders, that were dried after each use.

The conductivity was recorded on a laptop connected as described in Section 6.4.2. One conductivity reading was registered every 30 s, which corresponded to different amounts of eluted volume depending on the flow rate of the column. The flow rate-dependence on the solvent is shown in Table 28. The conductivity was manually plotted in real time in order to monitor the experiment.

When the light sensitive NaI and NaSCN where eluted, the column was wrapped in aluminium foil.

Sometimes bubbles would form or be trapped in the conductivity sensor chamber due to the inlet tubing leaking, causing oscillations in the conductivity reading. Because of the material and the narrow bore of the outlet tubing, they would not leave the measuring chamber spontaneously and they had to be manually removed by pulling out the outlet tubing from the chamber and letting the air bubble exit.

Usually only one sample was chromatographed per day due to the slow flow rate of the column.

6.4.4 Eluent change

The same *Sephadex*® column packing was used for all eluents, which were changed in sequence in the order MeOH – FA – DMSO – PC (– DMSO because PC and water only have a narrow miscibility range) – H_2O. All electrolytes that were soluble in that eluent were run on the column, and then the solvent was changed. The change from one eluent to the next was performed by passing eluent mixtures at increasing volume content of the new eluent. A typical solvent change would be made in four steps, and at least one column volume (40 ml) of mixture was eluted in each step: first a 3 : 1 (old eluent : new eluent) mixture, followed by a 1 : 1 (old : new) solution, then a 1 : 3 (old : new) mix, and finally at least one column volume of neat new eluent. The gradual solvent change was done to minimise stress on the stationary phase due to swelling or shrinking in the new solvent.

Sephadex® swells differently in the solvents, and the height of the packing and the other column parameters are listed in Table 28. The column height was stable during the experiments in each solvent.

FLOW RATE DEPENDENCE ON ELUENT TYPE As the flow was gravity-driven, it is also interesting to comment on the flow rate in the different

Table 28: Characteristics of the column in different solvents, listed in the order they were changed on the *Sephadex*® packing.

solvent	h	F	SD/%	V_o	V_t	$V_t - V_o$	V_i	V_o/V_i
MeOH	32.3	1.2	4.4	27.1	67.4	40.3	24.6*	1.10
FA	34.1	0.15	4.6	25.9	71.2	45.3	28.7*	0.90
DMSO	36.1	0.21	11.0	28.5	75.3	46.9	29.3*	0.97
PC	24.7	0.32	4.6	21.5*	51.5	30.0	18.0*	1.19
water	32.1	0.22	4.2	25.8	67.0	41.2	25.7	1.01

h is the stationary phase height in cm; F the average flow rate in $\mathrm{ml\,min^{-1}}$; volumes are expressed in ml.
* calculated, not measured experimentally.

eluents. It is remarkably fast in MeOH. The variation of the flow rate is informative because it gives an idea of the control achievable by gravity elution. It was chosen not to use a Mariotte bottle to control the flow rate for a number of reasons, including technical difficulties and the unknown response of the stationary phase to the different eluents, including the back-pressure that had to be overcome.

In changing eluent from PC back to DMSO (in preparation for water), the flow of intermediate eluent composition mixtures was extremely slow, taking more than five days to elute the three intermediate mixtures. When back to neat DMSO, the column had not swollen back even to the height it had in MeOH (being 3 mm shorter), and the flow rate was $0.04\,\mathrm{ml\,min^{-1}}$ (taking 2 h 12 min to elute 5 ml of DMSO. When eluting the DMSO : water mixtures, the column was equally slow until the 1 : 1 mixture, which started to elute faster at 5 ml in 1 h. The final column height in water was not greater than the height in MeOH, as expected from the preliminary swelling tests, possibly because it did not recover from the extreme shrinking in PC. This is likely to have had an effect on the exclusion limit of the stationary phase, which might therefore have been smaller than 700 Da. Unfortunately it was compulsory to run water last, as the column had to be as anhydrous as possible for the previous runs, and therefore the order of PC and water could not be inverted.

Another open question is about whether all of the old solvent is removed from the *Sephadex*® stationary phase when the new eluent is added. This is a question that I have not addressed in my tests, and I assume that complete replacement of the solvent in the column takes place. The miscibility of the solvents favours this.

6.4.5 Column benchmarking

The measurement of the void volume V_o and internal volume V_i of the column presented additional challenges. Blue Dextran is soluble only in water, DMSO and FA. In those cases, it was used as per usual protocols and

detected both visually and by UV-vis spectroscopy on collected fractions of the eluate (fraction volume $\approx 1\,\mathrm{ml}$), by monitoring the peak at 630 nm. In the case of MeOH, instead, a sample of PVP-360 (polyvinylpirrolidone of average molecular weight = 360 000 Da), at concentration $w_{PVP} = 0.0028$ was used and detected by UV absorbance at 210 nm. In PC, despite PVP-360 being soluble, it was not possible to detect it and only an estimate of V_o was made based on the elution profiles of the electrolytes peaks. It is possible that this is because PC itself absorbs at 210 nm, or because of residual iodide in the column that was not possible to remove (NaI behaves as highly sticky in PC).

Several molecules were tested in a trial column packing in MeOH in order to calibrate the column: DiI, 1,1′-dioctadecyl-3,3,3′,3′-tetramethyl-indocarbocyanine perchlorate, ($M_i = 933.87\,\mathrm{g\,mol^{-1}}$), methylene blue ($M_i = 319.85\,\mathrm{g\,mol^{-1}}$) and crystal violet ($M_i = 407.98\,\mathrm{g\,mol^{-1}}$). All of these molecules showed non-ideal behaviour and formed large bands with very long elution times. Also glucose ($M_i = 180.1559\,\mathrm{g\,mol^{-1}}$) was trialled as a molecule for calibration, and I attempted its detection by differential refractivity index measurement (by measuring distinct fractions in a non-flow through instrument), but it was not possible to detect it accurately. This is possibly due to the low concentration of the glucose solutions, given its low solubility in MeOH.

In water, D_2O (sample size 1 ml) was successfully used for determining V_i and detected by measuring the T_2 NMR relaxation time of the eluate fractions with a *XIGO Nanotools Acorn Area* instrument. This technique could have also been used for the other eluents, by running their corresponding deuterated solvent, but this approach was only discovered after the last eluent change to water, and it was not feasible to change back to the non-aqueous solvents (mainly because of the possibility of water contamination). An estimate of the internal volume for the column in the other solvents was therefore calculated as a proportion of their geometric volume V_t, by using the internal volume to geometric volume ratio V_i/V_t found for water. This is of course an estimate of the internal volume that is an approximation, but I think that it is more informative than using the geometric volume. In fact, in the column $(V_t - V_o)$ is about 60% larger than V_i, therefore the difference between the two cannot be ignored when one wants to interpret the partition coefficient in terms of the distribution of the sample between the void volume and the internal pore volume. It follows that K_{AV} is not an acceptable estimate of K_{SEC} when one is looking for information about the sample distribution. See Table 28 for the values in the various solvents.

Another observation that must be made about the values in Table 28 is about the void volume V_o to total geometric volume V_t ratio: the first is usually reported to be around $30\% - 35\%$ of the swollen stationary phase (Tay-

yab et al., 1991), but in this case it amounts to 40%. This could be an intrinsic property of *Sephadex*® G-10, as it is highly crosslinked.

In addition, the ratio V_o/V_i expresses the porosity of the stationary phase, and it is the smallest in PC, followed by MeOH, then water, FA and DMSO. The size of the substances that are excluded from the internal porosity is therefore affected by this parameter, with the *Sephadex*® swollen in PC excluding smaller molecules from its internal pores than the *Sephadex*® in DMSO, which has a larger exclusion limit than water.

6.4.6 Differences from Washabaugh and Collins's experiment

This section summarises the substantial differences between our experiment procedure and the one detailed by Washabaugh and Collins (1986).

- The stationary phase height in this work was approximately 30 cm rather than 85.5 cm, although Washabaugh and Collins made tests on a shorter column and obtained the same results.

- The column temperature was controlled by Washabaugh and Collins at 30 °C through a circulating water bath. In my experiments this was not controlled, rather the experiments were conducted in an air conditioned room at approximately 22 °C.

- I did not filter or degas the eluent and samples.

- The detection of the sample peak was performed by conductivity, thus a neat eluent was used rather than a 0.1 $\mathrm{mol\,dm^{-3}}$ solution of NaCl.

- The flow rate was gravity driven rather than set by using a Mariotte bottle, and this resulted in flow rates that were more variable from solvent to solvent. Washabaugh and Collins set the flow rate at 0.5 $\mathrm{ml\,min^{-1}}$.

- The concentration of the sample was $5 \times 10^{-2}\,\mathrm{mol\,kg^{-1}}$ rather than 0.1 $\mathrm{mol\,dm^{-3}}$ because of the lower solubility of salts in the non-aqueous solvents.

- The internal volume of the column was measured by running a D_2O sample rather than tritiated water. It was also only determined in water.

6.5 RESULTS AND DETAILED DISCUSSION

This section contains an in-depth discussion of the chromatograms. The results in regards to the solvent effects on SIE and the overarching trends are discussed in the ensuing section, Section 6.6.

Chromatograms were measured for a range of electrolytes in water, MeOH, FA, DMSO and PC in order to investigate the influence of the solvent on the ion specificity of elution. More than 100 chromatography runs were performed in total.

For all of the chromatograms, the baseline conductivity of the pure solvent has been subtracted and the values of the conductivity rescaled relative to the maximum conductivity being set to 1. This maximum conductivity equals 467 µS cm^{-1} in water, 22.44 µS cm^{-1} in MeOH, 103.5 µS cm^{-1} in FA, 53.1 µS cm^{-1} in DMSO and 4.91 µS cm^{-1} in PC. Although these values have been measured with the custom-made conductivity cell we built and cannot therefore be regarded as accurate absolute values, they do give an idea of the different conductivities in the various solvents. Also the average neat solvent conductivity (baseline) changed: 3 µS cm^{-1} in water, 0.2 µS cm^{-1} in MeOH, 40 µS cm^{-1} in FA, 0.05 µS cm^{-1} in DMSO and 0.02 µS cm^{-1} in PC. Again, these values are approximate estimates of the real values, but it is noticeable that FA has a much higher conductivity. This is due to the fact that in the presence even of low quantities of moisture, FA hydrolyses to ammonium formate. Very dry FA had been purchased, but the presence of traces of moisture in the chromatography path cannot be completely excluded.

Based on the sizes of the ions (Table 27), the ordering of elution expected in ideal conditions is $CH_3COO^- - SCN^- - ClO_4^- - I^- - Br^- - Cl^- - F^-$, although the shapes of the polyatomic ions thiocyanate, perchlorate and acetate are expected to have an influence on their solvodynamic radius and therefore may influence their positioning.

Water is the only solvent in which I have measured the internal volume, V_i, accurately in addition to the void volume, V_0. For all of the non-aqueous solvents, only the geometric volume of the packing has been measured and the internal volume has been estimated by using the ratio of internal volume to geometric volume found for water — noting that the swelling of the column is solvent dependent (see Section 6.4.5). Such an estimate of the internal volume is not accurate due to the different levels of swelling and different molar volumes of the different solvents. However, I think it is still a better estimate than the geometric volume, particularly for interpreting the elution of electrolytes. Therefore, I have used the estimate of the internal volume for the calculation of K_{SEC}. Regardless, my primary interest is in the ion-specific trends in each solvent and these are not impacted by the calculation of K_{SEC}. The (measured) geometric volume and void volume, and the calculated in-

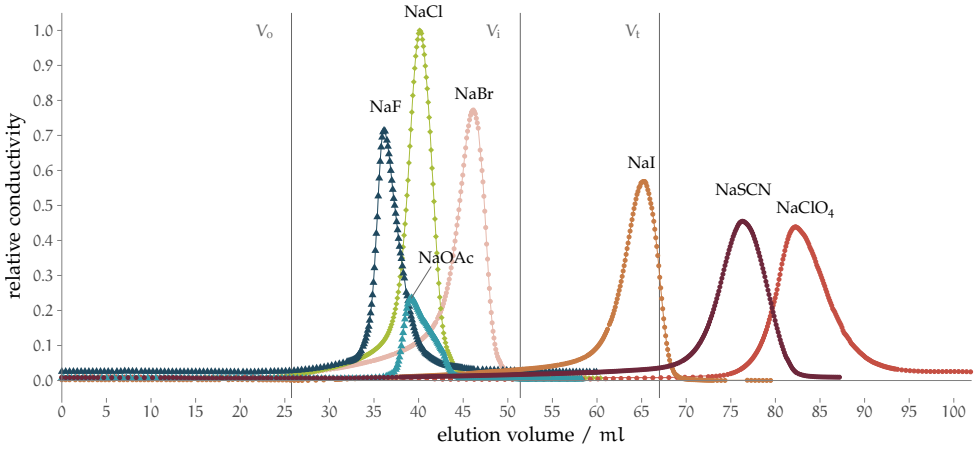

Figure 20: Size exclusion chromatograms for a range of electrolytes in water. The conductivity of the pure solvent has been subtracted and the signal has been normalised to the highest peak such that the relative conductivity ranges between 0 and 1 and is dimensionless. The elution volume is expressed in millilitres of eluent and is compared to the void volume, V_o, the internal volume V_i and the geometric volume V_t.

ternal volume are indicated in each of the non-aqueous chromatograms, and their values are listed in Table 28.

It is also worth to observe that the peaks have different areas. The area correlates with the conductivity of the electrolyte.

Studies on the effect of the addition of small quantities of water on the SEC elution order have been performed and are discussed in Appendix F.1.

Water

Although water is the eluent that was used last, I report it first in order to use it as a point of comparison. The elution order in water (Fig. 20) follows the Hofmeister series with the exception that the order of SCN^- and ClO_4^- is inverted. This is in agreement with the earlier experiments of Washabaugh and Collins (1986), to which these experiments add information for acetate and perchlorate. Notably, the ordering of the anions does not follow the 'naked' size of the anions, but rather the reverse trend is observed. This is consistent with the small ions being strongly hydrated, and the larger polarisable ions being strongly attracted to the stationary phase and only eluting after a full column volume of water has passed. That is, retention in the column is observed for the strongly chaotropic anions. Acetate, which is a large ion but has a charged group of low polarisability, elutes where expected based on its size, therefore ideally. Whereas fluoride, which is substantially smaller than acetate, elutes before it. This indicates a very large and strongly bound hydration sphere for fluoride. Notably the shape of the acetate elution peak exhibits a shoulder and in this respect it differs from the other peaks which are symmetrical. This may be due to some of the acetate being present as the undissociated acid.

Although we observe the same elution order as Washabaugh and Collins (1986), some discrepancies in the experiment results are present: in their case, bromide was eluting after the tritiated water (internal volume) peak with a K_{AV} of 1.2, thus supporting the hypothesis that Cl^- behaves ideally and is the watershed 'neutral' ion between chaotropes and kosmotropes. This was also supported by the calibration performed by Washabaugh and Collins with the aminoacid glycine and its polymers up to hexaglycine ($M_i = 75\,g\,mol^{-1}$ to $360\,g\,mol^{-1}$), although as both the aminoacid and the oligopeptides exist in solution as zwitterions, doubts about their aptness as calibrating references arise, given that they are ionic themselves. In our case, though, also bromide elutes within the first column volume, with a K_{AV} of 0.8. This might be an indication of the fact that the different experiment conditions are considerably influencing the observed retention factors.

Also the NaI peak shape is notably different, with it being slightly fronting in my experiments, versus noticeably tailing in Washabaugh and Collins's. Fronting and tailing peaks are asymmetrical peaks, that do not have the ideal Gaussian peak profile, and where the skewed part either precedes (fronting) or trails behind (tailing) the peak. Fronting is usually associated with column overloading or a flawed packing of the stationary phase, whereas tailing indicates specific interaction with the stationary phase (the analyte is retained anomalously), or extra-column effects. However, in SEC, the fronting, tailing and splitting of peaks can also be induced by reversible association of the analyte in solution, such as in the formation of dimers. Theoretical studies on protein association in SEC predict that, when the association and dissociation rates are comparable to the convection rate, a merged, broad peak forms, with either fronting when dimers dominate or tailing when monomers dominate (Yu et al., 2006). In fronting, as the dimers move ahead of the monomers, they dissociate into monomers themselves, which migrate more slowly, thus producing a self-sharpening advancing wave. When both the association and dissociation kinetics are slow, split peaks form. For ions in solution, the associated species have to be identified. It is possible that they are contact or solvent-shared ion pairs in solution (Yu et al., 2006).

The behaviour and series we observe in water is of reference to the behaviours observed in the non-aqueous solvents, which are discussed below.

Methanol

The elution order in MeOH (Fig. 21) follows precisely the same order as water. The overall elution volumes are much greater and all of the electrolytes required an elution volume greater than the internal volume, suggesting that all of the ions except acetate and fluoride interact with the column i.e. are 'sticky', but the degree with which they interact with the column remains

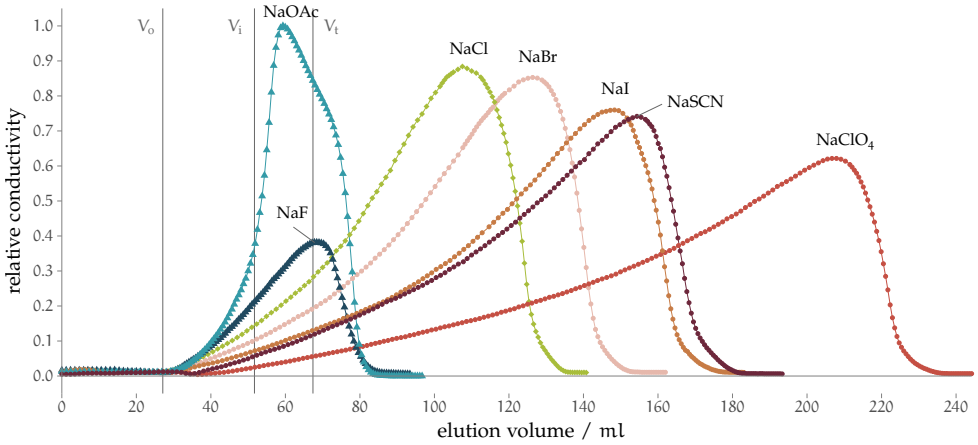

Figure 21: Size exclusion chromatograms for a range of electrolytes in MeOH. The conductivity of the pure solvent has been subtracted and the signal has been normalised to the highest peak such that the relative conductivity ranges between 0 and 1 and is dimensionless. The elution volume is expressed in millilitres of eluent and is compared to the void volume, V_o, the internal volume V_i and the geometric volume V_t.

size-dependent in the same way as in water. For both water and MeOH the observation is that the smaller the ion the weaker the interaction with the column.

The peak shapes are much different than for water: broader and fronting. Whilst the broader peak shape and late elution are consistent with the sticky behaviour (with MeOH being a poorer solvent for the anions in comparison to water), the fronting phenomenon is not something I am able to explain with certainty. A hypothesis might be that there is ion exchange happening in the column, but for this to be true we should observe fronting in all solvents, which is not the case. As the column packing was in good conditions (confirmed by the peak shape of the PVP used for benchmarking and by the Blue-Dextran runs in FA and DMSO performed later), also fronting due to defects (cracks, channels, inhomogeneities) in the stationary phase packing is to be excluded. In addition, if this were the case fronting should also have been observed in the other eluents which were run after MeOH. Another explanation is that the ions are solvated by a continuously evolving number of MeOH molecules, thus leading to complexes which have long enough life to cause a distribution of molecular paths. This is corroborated by the presence of a tridimensional hydrogen bonding network in MeOH. A final, more plausible hypothesis is that the ions migrate in an association equilibrium of solvated contact ion pairs and solvent-shared ion pairs. The association of cation and anion is plausible given the low dielectric constant of MeOH. Yu et al. (2006) have shown that fronting peaks are formed when the association and dissociation rates are comparable to the convection rate in the column, and fronting peaks are favoured when the dimers prevail. It must also be noted that the flow rate was particularly fast in this eluent, it being about 4

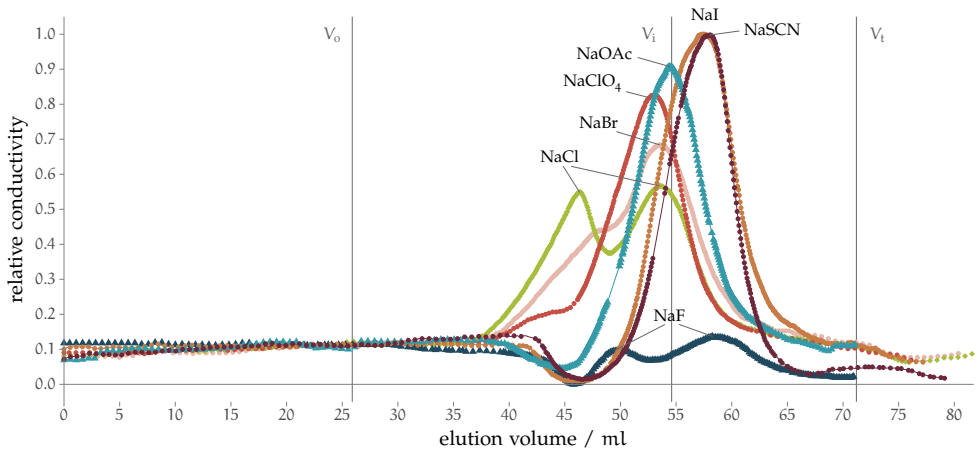

Figure 22: Size exclusion chromatograms for a range of electrolytes in FA. The conductivity of the pure solvent has been subtracted and the signal has been normalised to the highest peak such that the relative conductivity ranges between 0 and 1 and is dimensionless. The elution volume is expressed in millilitres of eluent and is compared to the void volume, V_o, the internal volume V_i and the geometric volume V_t.

to 6 times the flow rate in the other eluents, and more than double the one that Washabaugh and Collins (1986) used.

Does this finding of 'sticky' behaviour for all anions imply that for a protein that could hypothetically be dissolved in pure MeOH, all of the salts would have a salting-in effect? Then, electrolytes could actually be used to increase the solubility of proteins in MeOH.

Formamide

When FA is the eluent, the chromatogram changes dramatically (Fig. 22). The elution volumes for all ions are very similar, indicating much weaker ion specificity. FA is the eluent in which the stationary phase has the largest porosity (see Table 28). This could be offered as an explanation for the lower selectivity, but the expectation is that the pore sizes are still far larger than the ion sizes. The precise elution order is difficult to quantify because of the small differences in the elution times and the presence of double peaks.

Two curious features are in fact present in this chromatogram: double peaks (for F^-, Cl^- and partially Br^- and $ClO_4{}^-$, which show a shoulder) and a dip in the baseline conductivity before a number of peaks (AcO^-, F^-, I^-, SCN^-). The two features are not correlated to the ion type, as they appear in different combinations for different species.

It is likely that double peaks are the result of different association equilibria of the ions. FA undergoes keto-enol tautomerism, and also contains impurities of ammonium formate (and formic acid), which increase its conductivity as discussed previously. Although it has been observed that some anions do stabilise the enol form of FA, I expect the solvodynamic radii of the keto and enol forms to be very similar, therefore they should not be

able to give a split peak. A different plausible species in solution might originate from the association of the anion with the ammonium of the free ammonium formate, and this would be expected especially for softer anions. In fact, based on the LMWA, the softer anions might have favourable interactions also with ammonium, but this does not explain the presence of double peaks for chloride and bromide which are kosmotropes. In addition, while for the chaotropes the second peak is a shoulder, for the kosmotropes the twin peaks have almost identical areas. It is not easy to estimate whether there is enough ammonium formate in solution to create a second peak as big as the one from NaX, although the LMC of NH_4^+ is higher than that of Na^+ (Table 6 in Chapter 2), therefore a smaller concentration of the former gives a larger peak signal. This is corroborated by the fact that the peak conductivity is about double the conductivity of the baseline, therefore there is not a huge difference. It is not possible, though, to account for the concentrations of each ion in solution as their conductivities are different. It is likely therefore that there are two distinct causes for the formation of double peaks, one which leads to double peaks for kosmotropes and the other for chaotropes. further analysis would be required to determine the chemical composition of the two different peaks. If the chemical species are the same, then the two peaks are likely the result of different associated entities in solution, and the structure of the solution should be investigated. Although these should have very long lifetimes. This is also suggested by research that shows that peak splitting is favoured at a high linear velocity (not our case), for a short column length (which is the case for this experiment), or for relatively slow association and dissociation rates (Yu et al., 2006).

The dip in the baseline conductivity is another puzzle, for which I do not have an explanation. It happens both for double peaks (F^-) and for single peaks (I^- and SCN^-). As already explained, FA has a higher baseline conductivity due to the presence of ammonium formate, the product of the hydrolysis of FA in the presence of trace quantity of water. The dip indicates that the concentration of ammonium formate is depleted right before the peak passes. It corresponds to a difference in conductivity of about $5\,\mu S\,cm^{-1}$ (this quantity is measured with the custom-made conductivity probe, therefore it is not a good estimate of the true value, and is likely smaller by about a fourth) from a baseline that averages a $40\,\mu S\,cm^{-1}$ conductivity. If the $HCOONH_4$ and NaX actually undergo a double exchange of ions to some extent, then the conductivity of HCOONa is lower than $HCOONH_4$, and could therefore explain the dip in the baseline. But again, while the close association in solution of the ammonium with the chaotropic ions I^- and SCN^- is expected, it is not as justified with acetate and fluoride, for which a dip in the baseline before the peak is observed as well.

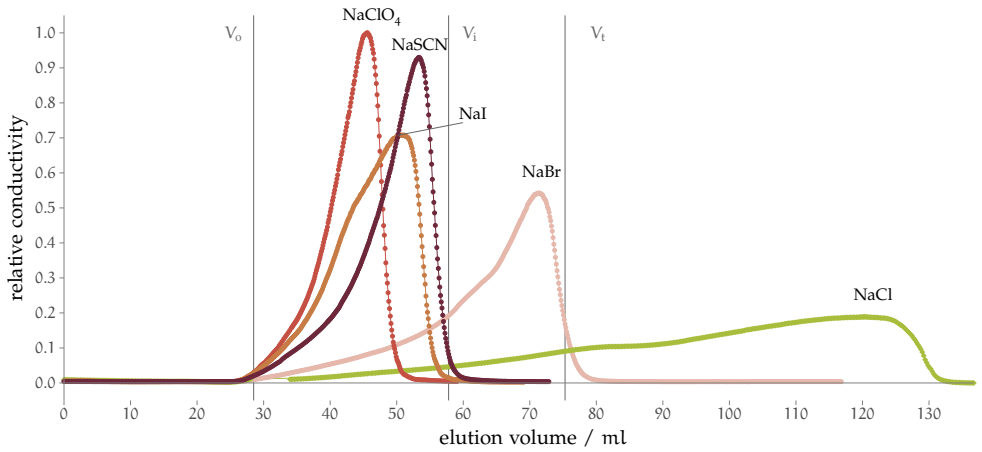

Figure 23: Size exclusion chromatograms for a range of electrolytes in DMSO. The conductivity of the pure solvent has been subtracted and the signal has been normalised to the highest peak such that the relative conductivity ranges between 0 and 1 and is dimensionless. The elution volume is expressed in millilitres of eluent and is compared to the void volume, V_o, the internal volume V_i and the geometric volume V_t.

Independently of the presence of these two unique chromatogram features, the overall behaviour in FA indicates that the solvation of kosmotropic and chaotropic anions in is much more similar in this solvent than in the other solvents investigated, and that also there is little or no interaction of the ions with the *Sephadex*® surface. The latter suggests that all ions are strongly solvated, which is in agreement with the high dielectric constant and dipole moment of this solvent (Table 2 Chapter 1).

Dimethyl sulfoxide

The chromatogram for DMSO (Fig. 23) shows the reversal of the elution pattern observed in protic solvents.

As such, the order observed is that expected based on the size of the anion alone. Whilst the order suggests that size is controlling the elution, long elution times for chloride and bromide indicate that they are interacting strongly with the stationary phase. These sticky ions are now kosmotropic anions in contrast to water and MeOH where they presented as sticky. In this case the smaller less polarisable ions have a greater affinity for the stationary phase.

We are observing for the first time a reversal of the Hofmeister series due to *solvent effects* (reversal has already been observed to happen in relation to surface charge, concentration and pH, see Section 2.3).

All of the peak shapes indicate fronting, as was the case in MeOH, but in this case the peak is more skewed for bromide and chloride, which is the opposite of what happens in MeOH. This suggests that DMSO is also a quite poor solvent for practically all of the anions, that tend to exhibit association. Chloride and bromide, in addition, have more have favourable

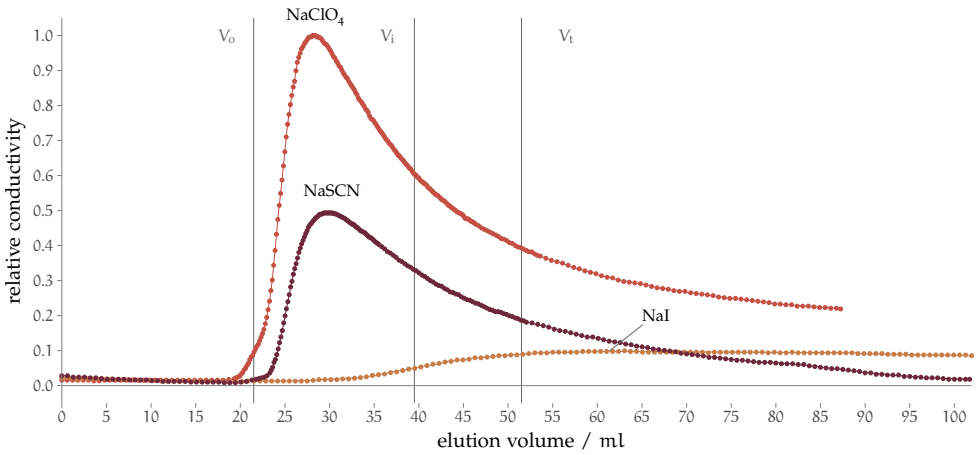

Figure 24: Size exclusion chromatograms for a range of electrolytes in PC. The conductivity of the pure solvent has been subtracted and the signal has been normalised to the highest peak such that the relative conductivity ranges between 0 and 1 and is dimensionless. The elution volume is expressed in millilitres of eluent and is compared to the void volume, V_o, the internal volume V_i and the geometric volume V_t.

interactions with the stationary phase and behave as sticky ions. This is also in agreement with the fact that aprotic solvent are less good solvents for anions, as indicated by their donor number. Interestingly though, in DMSO some ions are eluting within one column volume, which does not happen in MeOH. Both the dipole moment and dielectric constant of DMSO are higher, so this is probably why it is more successful in solvating the anions overall.

Propylene carbonate

The range of electrolytes that could be studied in PC is limited (Fig. 24). The available data suggests similar behaviour to that observed in DMSO. However, in this case, iodide behaves as strongly sticky. Its interaction with the column was so strong that it altered the baseline for a number of runs afterwards. Although NaBr was not run in the anhydrous final runs, a test with a saturated sample during the trial runs (Fig. 94 Chapter 5) shows that it behaves as even stickier than NaI, thus confirming the reverse trend of anions for DMSO.

6.6 SUMMARY

I have successfully performed SEC of sodium electrolytes in four non-aqueous solvents. SEC sheds light on the ion-solvent and ion-surface interaction in solution.

The elution behaviour for the various electrolytes is summarised in Fig. 25. Here the value of K_{SEC} is shown for the various electrolytes (ordered from top to bottom as the Hofmeister series i.e. the fundamental series for anions) in

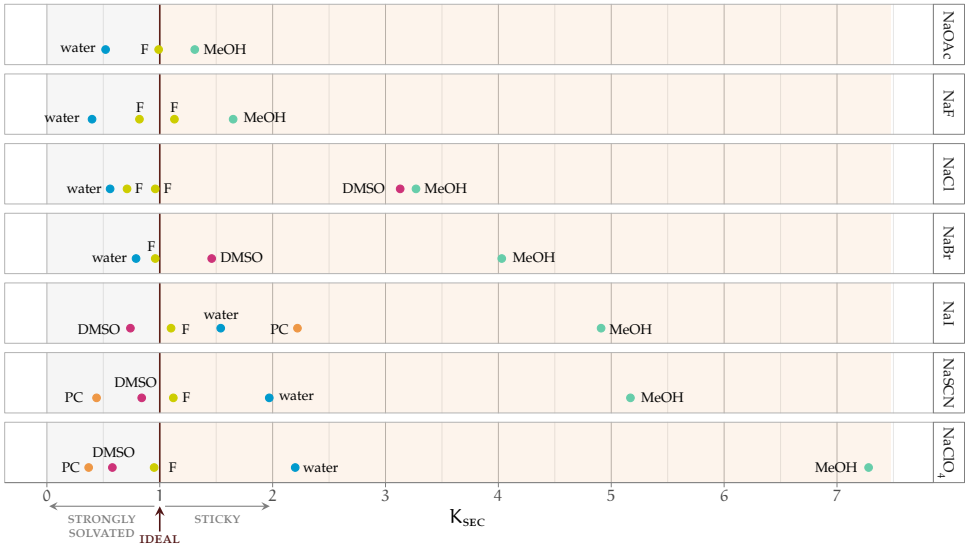

Figure 25: Summary of the retention factors, K_{SEC}, of each electrolyte when eluted with different solvents. The electrolytes are listed from top to bottom according to the Hofmeister series (kosmotropic to chaotropic). The labels on the bottom left indicate the thresholds characterising different behaviours of the ions in solution. This plot elucidates the K_{SEC} trends in different solvents: MeOH and water show the same ordering, FA shows no selectivity, PC and DMSO show an ordering that is opposite to MeOH and water.

the different solvents. When presented in this manner, if K_{SEC} values increase when going down the series, a Hofmeister series is evident. If the K_{SEC} values decrease when going down the series, a *reverse* Hofmeister series is evident. It is apparent that the ion specificity in the SEC for water and MeOH follows the Hofmeister series, whereas the reverse Hofmeister series is observed for PC and DMSO. The K_{SEC} values for FA vary little, as such no series is evident.

Overall water and MeOH behave very differently to DMSO and PC. One might therefore ascribe the difference to the protic and aprotic nature of the solvents respectively. However, the protic solvent FA appears to present an intermediate case. In which case, the binary interpretation of protic versus aprotic is not sensible. Rather, the effects of the solvents may be due to their polarisability— noting that the aprotic solvents are larger and more polarisable. The overall picture that emerges is that in solvents of low polarisability (water and MeOH, see Table 2), the polarisable ions interact strongly with the stationary phase, whereas in solvents of higher polarisability (DMSO and PC) the more polarisable ions preferentially interact with the solvent — and therefore do not interact strongly with the stationary phase. FA, which has a polarisability greater than that of water and MeOH, but less than DMSO and PC, presents an intermediate situation in which the ion specificity is weak and the ordering is unclear.

This is the first instance where a Hofmeister series reversal is due to solvent effects. In particular, the solvent *polarisability* appears as the solvent

property that the reversal depends on. This aligns with studies that stress the importance of dispersion interactions for the behaviour of ions in solution (Duignan, Parsons et al., 2014c; Ninham and Yaminsky, 1997; Parsons, Boström, Lo Nostro et al., 2011). The solvent properties therefore add to other already known elements in solution that affect the overall SIE trend manifestation.

Strangely, while the elution order observed here for aprotic solvents approximately agrees with the conductivity data (LMC) discussed in Chapter 2, the data trends in protic solvents either do not agree (water and FA, although in FA interestingly we have three ions that display identical LMC: SCN^-, Cl^- and Br^-), or is reversed as in MeOH, that shows a reverse Hofmeister series in LMC but a direct one in SEC. This indicates that the experiment perturbs the solvents differently based on the solvent, so it is solvent-specific. Of course the two experiments of LMC and SEC are very different, as the mobility of an ion is only determined by its solvated size, whereas in chromatography we also have the interaction with a surface at play. The solvent-surface competition for the anion seems to matter more for protic solvents, i.e. to be more 'disruptive' of the Hofmeister series.

These experiments show that, at real concentrations and in the presence of surfaces, the solvent properties do matter for the anions series observed. In particular, the solvent polarisability is the major cause of perturbation of the fundamental Hofmeister series for anions.

The more general implications of the solvent effects on the ion-specific ordering are best discussed with a global view, together with the QCM experiment results presented in Chapter 7. This holistic discussion is performed in Section 8.2.

7 ANION-SPECIFIC POLYMER CONFORMATION

The set of experiments described in this chapter analyses the conformation of positively charged polymer brushes in the presence of different Hofmeister anions. This chapter is reproduced with minor changes from:
V. Mazzini, G. Liu et al. (2018), 'Probing the Hofmeister Series beyond Water: Specific-ion Effects in Non-aqueous Solvents', *J. Chem. Phys.* 148, 22, p. 222805, DOI: 10.1063/1.5017278.

7.1 INTRODUCTION

An important area of ion specificity is the interaction of electrolytes with polymers and biopolymers. Surface-grafted polymer brushes of different chemical composition are often used as model systems to investigate such phenomena (Ayres, 2010; Kumar et al., 2002).

For this second experimental study on specific-anion effects, we chose a brush made of poly(2-methacryloyloxyethyl-trimethylammonium chloride (PMETAC), as it interacts with anions, that act as counterions for the terminal positively charged alkylammonium group. As a result of interacting with different anions, the polymer brush chains may desolvate and coil, or may extend and fully solvate in solution, thus leading to changes in the overall film thickness or viscoelastic properties, as well as wetting/dewetting properties. This polymer is of interest for smart, environment-responsive surface coatings (Andrieu-Brunsen et al., 2015; Moya and Irigoyen, 2013; Tan et al., 2011; Wei and Ngai, 2012). The repeating unit of the polymer is illustrated in Fig. 26.

It is known that in aqueous systems the counter-ion of the brush strongly influences the conformation of the brush (Biesalski et al., 2004; G. Liu and G.

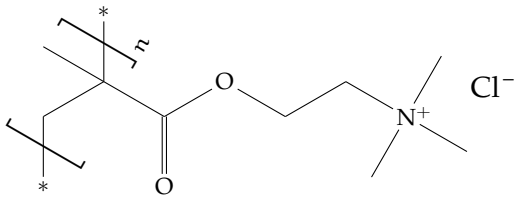

Figure 26: Poly(2-methacryloyloxyethyl-trimethylammonium chloride (PMETAC), skeletal structural formula.

Zhang, 2013). Azzaroni et al. (2005) studied the ion-specific properties and behaviour of positively charged PMETAC brushes in water. They showed, by coupling QCM with atomic force microscopy, infrared spectroscopy and contact angle measurements, that PMETAC brushes in water undergo total collapse in the presence of ClO_4^-. The response of PMETAC brushes in water to Hofmeister anions and cations has been characterised in detail by Kou, J. Zhang, Wang et al. (2015), who found that the Hofmeister anions interact with the charged sites on the brush to different degrees, in agreement with the LMWA (Section 4.4), which is consistent with the expectations based on dispersion interactions.

7.2 QCM FOR INVESTIGATING POLYMER CONFORMATION

A quartz crystal microbalance (QCM) is a surface-acoustic-wave-based analytical instrument (Johannsmann, 2015) that employs a quartz crystal resonator to detect mechanical and rheological changes in its environment. For experiments in solution this could be a change in the solvent, adsorption or desorption of material from the sensor surface or a change in conformation of molecules on the sensor surface.

The term 'microbalance' was introduced by Günter Sauerbrey (Sauerbrey, 1959). Although the name implies that the QCM is a device for measuring small (micro) masses, it actually measures an areal mass density in the units of mass per unit area. Fundamentally, the QCM is a *stress* balance, in that it detects periodic stresses exerted at its surface (Johannsmann, 2015).

7.2.1 Description of the technique

As crystalline quartz is piezolectric (that is, it generates an internal electrical current when mechanically deformed by an applied force), its acoustic resonance can be excited electrically (inverse piezoelectricity).

Whilst the main application of quartz resonators are in time and frequency control (i.e. quartz clocks, computer clock signal), the fact that the resonance frequency and resonance bandwidth depend on the environment the resonator is in contact with makes them suitable to be employed as frequency-based sensors.

The quartz crystal resonators we use are 330 µm thick, 15 mm diameter disks with a fundamental resonance frequency of 5 MHz, that have electrodes on both their faces in order to provide electrical contact. The crystal cut is chosen so that, when an AC-voltage is applied to the electrodes, an oscillating *shear* deformation is produced in the crystal (AT-cut, that oscillates in thickness-shear mode). If the frequency of the exciting voltage

matches one of the acoustic resonance frequencies of the disk, the amplitude of oscillation is large and the sensor draws a large electric current from the generator. The resonance frequencies are therefore easily found by scanning different input voltage frequencies and measuring the current drawn by the electrodes.

In the apparatus I employed, the quartz resonator is mounted on an O-ring so that it seals one side of a liquid sample cell. Only one face of the sensor is exposed to the sample cell environment.

It is crucial for surface-sensing in liquids that the resonator vibrates in shear-mode. A different oscillation where the disk expands would produce compressional waves. Compressional waves interact with liquid samples much differently: whereas shear waves rapidly decay in liquids and in gases (according to Johannsmann (2015), the penetration depth at 5 MHz in water is 250 nm), compressional waves propagate into fluids, and can be reflected and scattered by objects in the sample cell and return to the sensor surface. This means that information from the liquid bulk is mixed with the signal from the liquid at the sensor interface, and therefore the sensor does not just 'see' the fluid at its surface but well beyond that, therefore losing its surface-detection specificity. Compressional waves are a much more prominent problem in liquids than in gases because the latter have a low impedance to compressional waves. As some flexural vibrating modes cannot be eliminated form the resonator vibration because of energy trapping, efforts are made so that the effects of compressional waves are constant and therefore ignored when looking at frequency shifts.

The quartz sensor resonance frequency f_n and half-bandwidth Γ_n can be interrogated in different ways (Johannsmann, 2015), that are based either on oscillator circuits, impedance analysis, or ring-down techniques. The instrument used in this work employs the ring-down technique: a radio frequency (RF) pulse of frequency close to the expected sensor resonance frequency is used to excite the quartz sensor; the excitation is then shut off and the current produced by the free decay of the sensor oscillation is recorded. The signal is fitted by a decaying cosine function in time: the decay time, which is the time when the oscillations envelope has decayed by a factor of e, is equal to $(1/2\pi\Gamma_n)$; the cosine period is equal to $1/f_n$. This technique is at the base of the patented quartz crystal microbalance with dissipation monitoring (QCM-D) from *Q-sense*, used here: '-D' stands for 'with dissipation monitoring', and the dissipation factor is defined as $D_n = 2\Gamma_n/f_n$. The ring-down method can be faster than the other interrogation techniques. This method is analogous to the NMR free-induction decay, although they are different in that the ring-down method uses a narrow RF pulse to excite only the resonant crystal oscillation mode of interest, whereas in NMR a broader pulse is used to excite all of the different Larmor frequencies of the same

nucleus, that change based on its chemical environment. As this is not the case in QCM, it is more efficient to excite the resonance frequency of interest and repeat the process for the overtones, than to excite all of the crystal resonances at once and decompose them by Fourier transform.

The changes in the sensor environment can be therefore detected as both its resonant frequency, f_n, and its dissipation factor, D_n, shifts from the 'natural' ones. The first observable is sensitive to the stress at the sensor surface (which, if the situation satisfies certain conditions, is equivalent to the area-averaged mass per unit area); the second observable is instead related to the damping properties (the viscous dissipation) at the sensor surface.

As the fundamental mode of the quartz-crystal disks with keyhole-shaped electrodes (which are the type employed here) often behaves differently from the overtones — for reasons that are poorly understood (possibly poor energy trapping), only the overtones are usually considered. These crystals are also called overtone crystals for this reason.

7.2.2 Polymer conformation monitoring

So how can a QCM be used to monitor the conformation of polymer brushes?

A polymer brush is grafted to the gold electrode surface of the quartz sensor. The resonant frequency f_n, and the energy dissipation D_n, are recorded continuously. We typically use the third overtone as the first overtone is susceptible to drift, likely associated with the mounting of the resonator or the keyhole- shaped electrodes. When measuring in liquids, the load sensed by the resonator is not just the load of the polymer chains grafted to the surface, but also includes the mass of any solvent that is coupled to it (Craig and Plunkett, 2003). In systems like the one employed here, where a polymer film is covalently bound to the sensor, the mass of the film cannot change, but the coupled load can change in response to the configuration of the polymer and/or changes in the solvent.

Therefore, a swelling and solvation of the brush will produce a decrease in f_n (increased load due to coupling with the solvent that enters the brush) and an increase in D_n (increased dissipation of the extended and solvated polymer chains. When the brush collapses and desolvates, the opposite happens: less solvent is coupled to the brush, resulting in a positive Δf_n and a negative ΔD_n.

7.3 EXPERIMENT DETAILS

A *Biolin Scientific Q-sense E*1 QCM-D was used to measure the shifts in frequency (Δf_n) and dissipation (ΔD_n) of the polymer brush-coated resonator

in the presence of 10^{-3} mol kg^{-1} electrolyte solutions (varying by anion) in the solvents of interest. The preparation of the samples is described in Chapter 5.

7.3.1 PMETAC brush preparation

This procedure was performed by the group of Prof. Guangming Liu at the Department of Chemical Physics, Hefei National Laboratory for Physical Sciences at the Microscale, University of Science and Technology of China, Hefei, P. R. China. I received the sensors ready for QCM use.

The gold-coated resonators used in the QCM-D were cleaned by piranha solution (volume fractions $\varphi_{H_2O_2} = 0.3$, $\varphi_{H_2SO_4} = 0.7$) for 10 min at 60 °C, then rinsed with copious amounts of ultra-pure water, and dried under a nitrogen stream before use. The clean resonators were immersed in a 5×10^{-3} mol dm^{-3} solution of MUBB (ω-Mercaptoundecyl bromoisobutyrate) in anhydrous ethanol for ≈ 24 h at room temperature to form a uniform monolayer of initiator with a thickness of ≈ 1.2 nm, as determined by ellipsometry. PMETAC brushes were prepared using the SI-ATRP method (Edmondson et al., 2004). Typically, METAC (2-methacryloyloxyethyl-trimethylammonium chloride) (5.94 g, 2.86×10^{-2} mol), the free initiator 2-EBiB (ethyl 2-bromoisobutyrate) (2.7×10^{-2} g, 1.4×10^{-4} mol), and BPY (2,2′-dipyridyne) (4.4×10^{-2} g, 2.8×10^{-4} mol) were dissolved in 20 ml of MeOH/water mixture ($\varphi_{MeOH} = 0.8$, $\varphi_{H_2O} = 0.2$). Then, the initiator-modified substrates were placed inside the flask, and the solution was stirred at 25 °C under argon for 120 min to remove dissolved oxygen. Afterward, CuBr (2×10^{-2} g, 1.4×10^{-4} mol) and $CuBr_2$ (3×10^{-3} g, 1.4×10^{-5} mol) were quickly added under argon protection at 25 °C. The polymerization was allowed to proceed for a specific time to prepare the PMETAC brushes. At the end of polymerization, the resonators grafted with PMETAC brushes were washed with water and MeOH, and then soaked in a MeOH/water mixture ($\varphi_{MeOH} = 0.8$, $\varphi_{H_2O} = 0.2$) overnight to remove the ligand and unreacted monomer.

7.3.2 Experiment setup and procedure

The 'bare' sensor was a *QSensor QSX 301 Gold* 5 MHz quartz crystal resonator. The polymer brush was constituted by PMETAC.

I used two different PMETAC-coated sensors for our measurements, as the first deteriorated after some time. The dry thickness of the brush was 31.11 nm for the first sensor (used for MeOH, FA and DMSO) and 28.69 nm for the second one (used for DMSO, PC and water).

In order to avoid contamination, special high-chemical resistance O-rings and gaskets were used.

An *ISMATEC REGLO Digital* ISM596 peristaltic pump was connected to the outlet tubing of the QCM sample chamber to draw the solution from the storage vial into the measuring cell via the PTFE inlet tubing of the cell. This connecting order was chosen as the sample would only come in contact with *Teflon*® tubing before entering the measurement cell, and therefore possible contamination by coming in contact with the pump tubing was avoided.

All of the solvent exchange in the cell was performed at a pumping rate of $0.1\,\mathrm{ml\,min^{-1}}$, to avoid disturbing the brush conformation or inducing stress on the O-ring. The pump was stopped after each liquid exchange.

The vial containing the sample (or solvent) that was being sampled had to stay uncapped for the whole duration of the operation, as the feeding tubing to the sample cell had to be immersed inside the vial. In order to limit the exposure of the solutions to atmospheric moisture, the opening of the vial was covered with aluminium foil and sealed with *Parafilm M*® on top of the foil. In addition, the samples were only taken out of the storage desiccators for the time necessary to perform a measurement.

The measuring procedure was as follows: the baseline in pure solvent was acquired for at least 30 min (no solvent flow); 1 ml of the electrolyte solution was pumped into the chamber and left to equilibrate for at least 30 min; 5 ml of the neat solvent was pumped through the cell to rinse the cell, and this operation was repeated until the baseline was reached again.

This procedure was performed for each electrolyte both on the brush-coated sensor and on the bare sensor. Each electrolyte measurement was repeated for confirmation.

Difficulties were encountered, especially in solvents where the brush response was small: in FA a strong baseline drift was observed, and in DMSO the presence of bubbles rendered the acquisition problematic, creating the need for many repeated runs.

7.3.3 Correcting for solution density and viscosity effects

As the viscosity and density of an electrolyte solution vary depending on the concentration and type of electrolyte, the resonant frequency and dissipation of the quartz resonator will be affected by changes in the solution. As a result, the measured Δf_n and ΔD_n relative to the neat solvent, include both the signal of interest (changes in brush conformation in response to the electrolyte) and the response to the altered properties of the solution. The effect of NaBr concentration on the blank sensor in different solvents is shown in Fig. 27. The effect increases with concentration of the salt as expected, as the viscosity and density of the solutions increase, but the slopes differ by solvent and DMSO and FA are the ones showing the most dramatic increase.

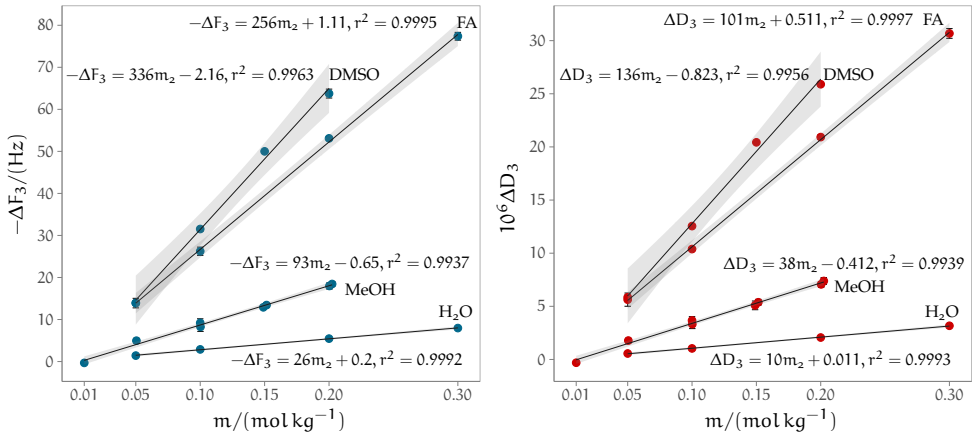

Figure 27: Effect of NaBr solutions at different concentrations on the shifts measured by the bare quartz resonator. The shadings around the fitting lines represent a 95% confidence interval. The *normalised* frequency shift ΔF_3 is plotted rather than Δf_3, and the frequency shift axis is reversed.

No correlation with the solvent density or compressibility is apparent. Pc was not tested due to the low solubility of NaBr in this solvent.

Please note that, in all the plots showing QCM results, the y-axis of the frequency shift plot has been reversed, so that the frequency and the dissipation shift have the same sign when the polymer brush swells or collapses (positive shift for swelling, negative shift for collapse). In addition, the *normalised* frequency shift ΔF_3 is plotted rather than Δf_3.

In order to isolate the response of the film, the Δf_n and ΔD_n caused by the same solution on a blank sensor were recorded and subtracted from the shifts measured in the presence of the polymer brush. This correction method is simplistic as it assumes the effects to be additive, but it is a simple and accessible way of estimating the change in sensor environment. Figure 28 shows both the brush-coated sensor and the bare sensor shifts in the presence of the different $10^{-3}\ mol\,kg^{-1}$ electrolytes, and demonstrates a clear distinction between the two responses.

7.3.4 Choice of the electrolyte sample concentration

The net response of the PMETAC brush to solutions at different concentrations of NaBr (this experiment is not anhydrous) is plotted in Fig. 29. Increasing concentrations of salt do not have a marked effect on the response magnitude of the brush. A low electrolyte concentration was therefore chosen for the experiments in order to avoid saturating the brush response.

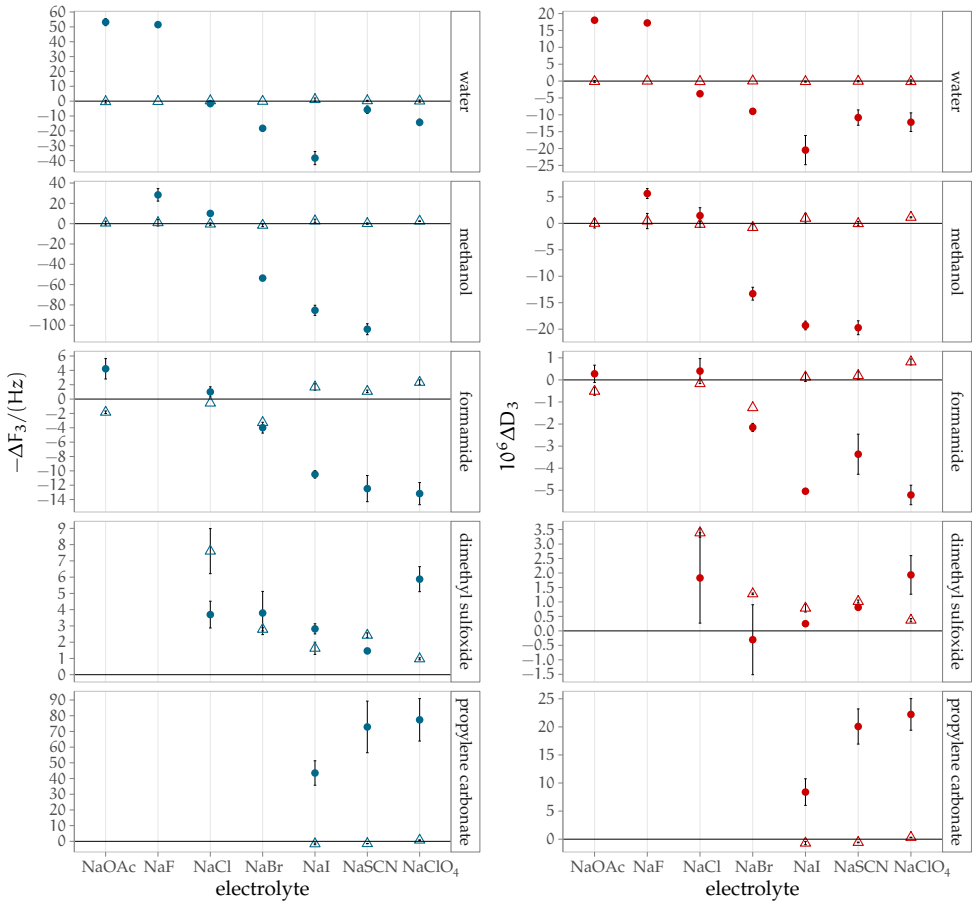

Figure 28: Comparison of shifts recorded in presence of the brush-coated sensor (full circles) and the bare quartz sensor (empty triangles). This shows the significance of the brush signal. The *normalised* frequency shift ΔF_3 is plotted rather than Δf_3, and the frequency shift axis is reversed.

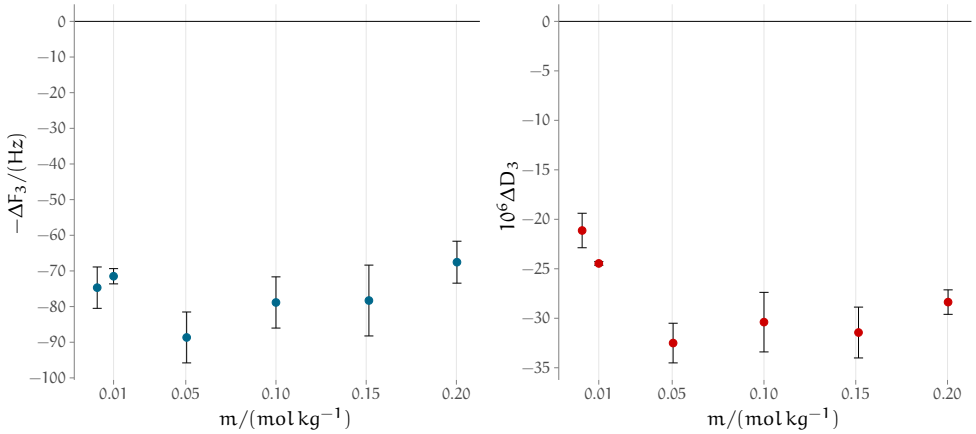

Figure 29: Effect of different concentrations of NaBr on the net PMETAC shifts in MeOH. The *normalised* frequency shift ΔF_3 is plotted rather than Δf_3, and the frequency shift axis is reversed.

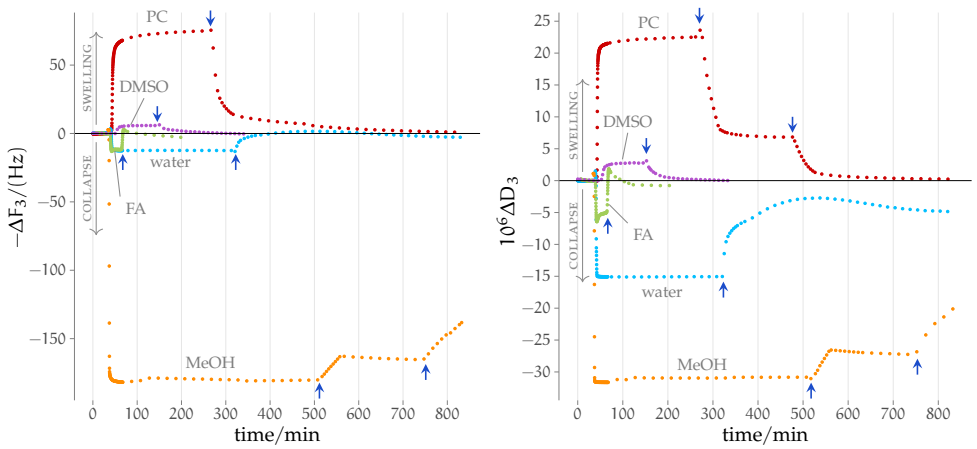

Figure 30: Comparison of the effect of $10^{-3}\,\mathrm{mol\,kg^{-1}}$ $NaClO_4$ on the PMETAC brush in different solvents. The corresponding conformational change of the brush is indicated on the plots. The blue arrows indicate when the pure solvent has been flushed. The *normalised* frequency shift ΔF_3 is plotted rather than Δf_3, and the frequency shift axis is reversed.

7.4 RESULTS AND DISCUSSION

The effects of water contamination on the SIE polymer conformations are discussed in Appendix F.2. These are found to be more relevant for 'chaotropic' ions; however, the overall SIE trend is not altered.

7.4.1 Effect of $NaClO_4$ on PMETAC in different solvents

As an exemplification of the recorded brush response, Fig. 30 shows the QCM recording of the frequency and dissipation shifts of the PMETAC brush when a $10^{-3}\,\mathrm{mol\,kg^{-1}}$ solution of $NaClO_4$ is introduced in the sample cell. I have selected this electrolyte because the brush displays the most extreme solvent-response: its conformation is dramatically different in magnitude and sign, and collapse is observed in protic solvents while swelling happens in aprotic ones. The response observed in water is in agreement with literature results (Azzaroni et al., 2005; Kou, J. Zhang, Wang et al., 2015).

In MeOH, the brush does not re-swell when neat solvent is flushed into the cell (neat solvent application indicated by the arrows in Fig. 30). The exchange with different counterions was necessary in order for the brush to be swollen in neat MeOH. Also the kinetics of the brush response (time needed to return to the baseline signal after the brush deformation) changes depending on the solvent, with it being the slowest in PC and water.

7.4.2 Discussion of results in all solvents

The monitoring by QCM of the conformation of a brush grafted to a quartz crystal resonator can be interpreted as follows: if the oscillation frequency increases(loss in coupled mass) and the dissipation decreases (coupled mass decreasing), the brush is collapsing. If the opposite is observed, the brush is swelling with respect to its status in the neat solvent. The swelling of the brush has been justified as resulting from the ingress of external counterions into the brush, that break up the multiplets formed by the ion-pairs, that partly restrict the full stretching of the polymer chains (Chu et al., 2014). Multiplets are aggregates of ion pairs (e.g. 2 ion pairs or 3 ion pairs), that form in consequence of the presence of densely confined charges. The brush instead collapses because of direct anion-specific binding to the alkylammonium groups and neutralisation of the net charge (Azzaroni et al., 2005).

The results of the QCM measurements are summarised in Fig. 31. Here ΔF_3 and ΔD_3 provide for a consistent picture of how ions influence the conformation of the PMETAC polymer film in different solvents. The ions are ordered according to the fundamental series for anions (i.e. the Hofmeister series). It is clear that the protic solvents, water, MeOH and FA all exhibit SIE that follow the Hofmeister series. The series is reversed in the aprotic solvents DMSO and PC.

In FA and DMSO, the effects of the electrolytes are smaller compared to the other solvents. The PMETAC polymer brush carries a positive charge through the dissociation of the chloride cation from the alkylammonium groups. These charged groups promote the swelling of the film. Therefore a collapse of the film is associated with a decrease in the overall positive charge due to incorporation of anions into the film. Conversely swelling of the film infers an increase in the positive charge or osmotic pressure in the film associated with ingress of kosmotropic anions into the brush. The latter requires that the kosmotropic anions do not form contact ion pairs with the alkylammonium groups of the brush (Kou, J. Zhang, Z. Chen et al., 2017).

7.4.3 ΔD versus $-\Delta F$ plot

In order to investigate changes in the viscoelastic properties of the brush, a plot of ΔD_3 versus $-\Delta F_3$ can be constructed for all the electrolytes in the different solvents. This is shown in Fig. 32. To a good approximation, the points form a line of constant slope, indicating that the electrolytes do not substantially alter the viscoelasticity of the brush.

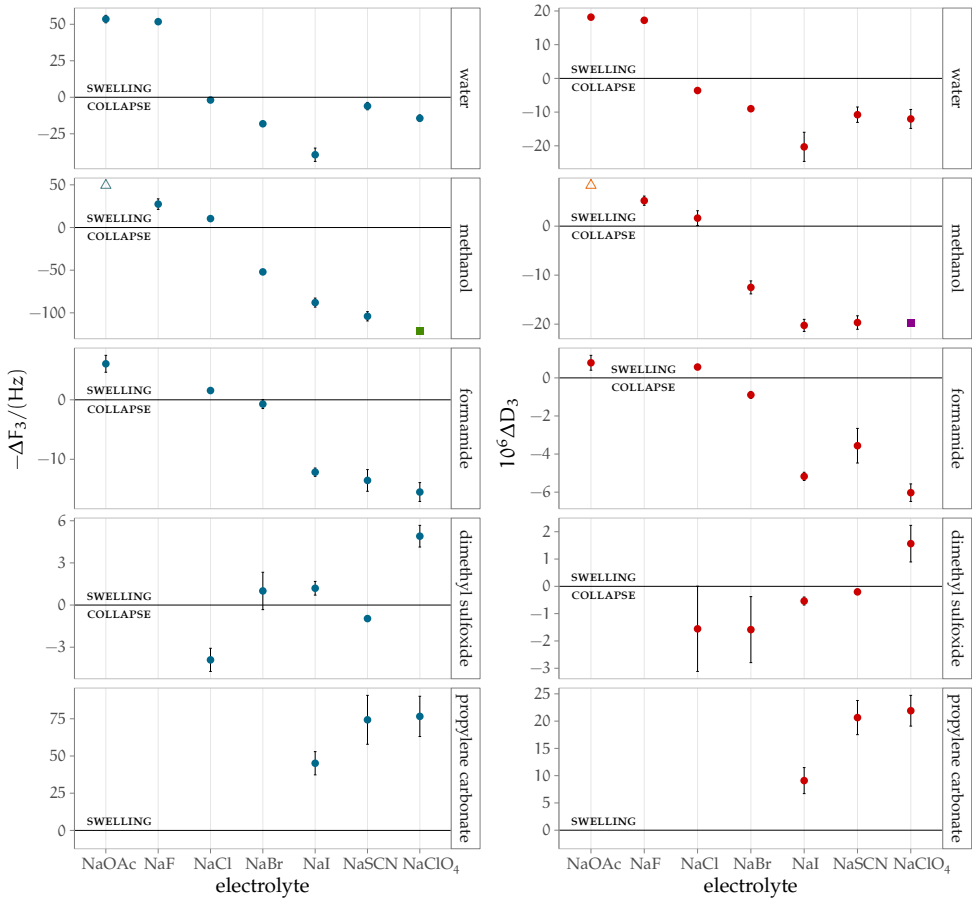

Figure 31: Summary of frequency and dissipation shifts produced by a 10^{-3} mol kg^{-1} electrolyte solution on a PMETAC brush in different solvents. The corresponding conformational change of the brush is indicated on the plots. In MeOH, the electrolytes NaOAc and $NaClO_4$ have not been measured in anhydrous conditions. For NaOAc, the value from 'as supplied' MeOH has been used and is represented by the empty triangle symbol. $NaClO_4$ has not been tested in dry conditions as the brush is difficult to re-swell afterwards, as seen by our non-anhydrous tests. The value is an estimate calculated from the non-anhydrous $NaClO_4$ measurement by using the ratio of the anhydrous to non-anhydrous response of NaSCN, and is indicated by a square symbol. The *normalised* frequency shift ΔF_3 is plotted rather than Δf_3, and the frequency shift axis is reversed.

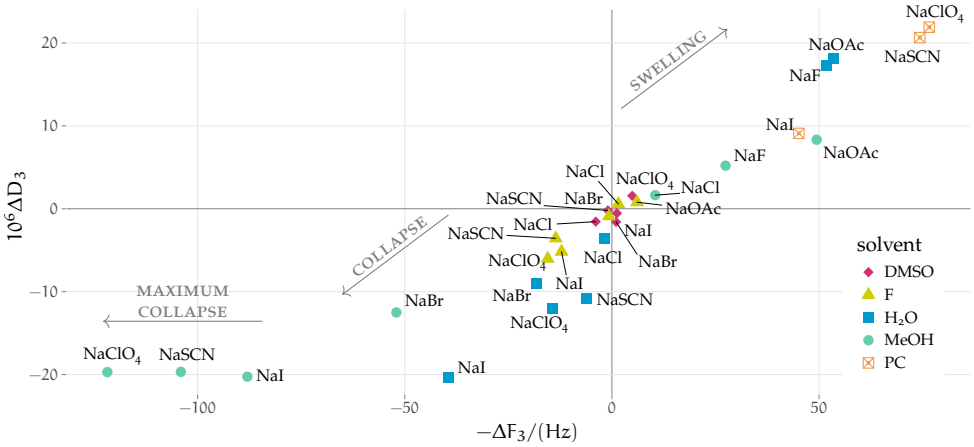

Figure 32: ΔD_3 versus $-\Delta F_3$ plot of the electrolytes in all of the solvents investigated. The *normalised* frequency shift ΔF_3 is plotted rather than Δf_3, and the frequency shift axis is reversed.

7.5 SUMMARY

In this chapter, the conformation of polymer brushes has been successfully investigated by QCM measurements. The ion-specific brush response to the different Hofmeister anions depends on the solvent environment: water, MeOH and FA display a forward Hofmeister series; DMSO and PC a reverse Hofmeister series.

Also this experiment shows that the solvent affects the manifestation of the fundamental Hofmeister trend for anions, causing an inversion exactly as is observed in the SEC experiments. In this case though, the watershed solvent is shifted from FA (which was the 'neutral' solvent in SEC measurements): the series in FA is still a Hofmeister one.

The surfaces interacting with the system are very different in these two experiments, with *Sephadex*® being covered in OH groups and largely neutral (a very small quantity of the hydroxyls can be expected to dissociate and become negatively charged), whereas PMETAC carries a net positive charge on an alkylammonium group. Despite the large difference in the surface properties and net charge, the Hofmeister series is observed in practically all cases, and a reversal happens in both experiments. This is remarkable agreement.

It is best to discuss the SIE trends measured here in conjunction with the SEC trends of Chapter 6, in order to analyse the connection of the experiment series with the solvent properties in a global perspective. Such treatment is performed Section 8.2.

8 AN OVERALL VIEW OF ANION TRENDS IN NON-AQUEOUS SOLVENTS

The findings from the previous chapters are here discussed to form a general picture of SIE in non-aqueous solvents. The experiment results require dedicated attention and I will discuss the general implications of these in Section 8.2, which is is reproduced with changes from:

V. Mazzini, G. Liu et al. (2018), 'Probing the Hofmeister Series beyond Water: Specific-ion Effects in Non-aqueous Solvents', *J. Chem. Phys.* 148, 22, p. 222805, DOI: 10.1063/1.5017278.

8.1 A GLOBAL DEPICTION OF SIE IN NON-AQUEOUS SOLVENTS

The investigations presented in this thesis have struggled against: a limited and patchy literature on SIE in non-aqueous electrolytes, that rendered general considerations difficult to formulate; the intrinsic difficulties presented by working in non-aqueous electrolytes; and the challenges in measuring a representative range of Hofmeister electrolytes, that includes difficulties associated with the solubilities of the electrolytes and the large number of experiments required to observe SIE trends.

Despite those difficulties, a general qualitative description of the role of the solvent on SIE is achieved, and the fundamental understanding of SIE is informed by this work. Also, some rules of thumbs are proposed for the behaviour of different non-aqueous electrolytes, depending on the conditions and interacting species (presence of a surface, ion-ion interactions).

The succession of Chapters 3 to 7 takes in consideration systems at increasing levels of complexity in terms of interacting entities.

The initial literature review of Chapter 2 gathers very complex and experiment-dependent SIE evidence. A number of important points emerge: SIE are observed in all solvents, and they follow a variety of different series, including the Hofmeister and lyotropic ones. This shows that the Hofmeister series is not exclusive to water. The absence of a clear overall pattern indicates that a rich level of complexity is present, and therefore SIE in non-aqueous solvents are at least as many-sided as they are in water. Despite the variability, there is evidence that the Hofmeister series and the reverse

lyotropic series are the most frequent trends for anions and cations, respectively.

This hint is confirmed by the electrostriction studies of Chapter 3, where I have individuated the fundamental SIE series for anions and cations: these are the forward Hofmeister series for anions and the reverse lyotropic series for cations. They are *independent* of the solvent, and are valid for infinitely dilute solutions and in the absence of interacting surfaces. Consequently, I proposed the interpretation that the SIE ordering is fundamentally a property of the ion, and, as one moves away from the ideal bulk conditions, the effects of ion-ion interactions at real concentration, of ion-surface interactions in the presence of surfaces and of various experiment conditions (e.g. temperature) perturb the fundamental series. This is an important step forward in the interpretation of the general SIE phenomenon, but at this point a question still hangs unanswered. How do the perturbations act? That is, what are the dominant interactions (or properties) of the system that establish a different perturbed order of the fundamental series?

A first step in answering this question is taken with the examination of the volcano plots for non-aqueous solvents in Chapter 4. Starting with *standard* solvation energies, the volcano trends appear broadly in all solvents, suggesting that the same interactions are at play and determine the ion-solvent interaction. This is remarkable given the widely different properties of the range of solvents examined, and consolidates the thesis of Chapter 3, that the ions determine the fundamental ordering of SIE. In addition, the data show that, whereas the cation and anion trends observed in water can be expected to hold for protic non-aqueous solvents, and the cation trends in water can be expected to hold also in aprotic solvents, this prediction does not apply to *anion* trends in aprotic solvents. In this last case, one could expect perturbations and reversal as a result of the solvent change from hydrogen-bonding to non-hydrogen bonding. The extension of the volcano plots to real concentrations (by studying non-aqueous activity coefficients and the solubility of electrolytes) shows that the infinite dilution findings are generally confirmed. This is important because the volcano plots at real-concentrations also take into account the cation-anion 'matching' effect. This study highlights the limited ability of aprotic solvents to solvate anions, which reveals crucial for the appearance of solvent-related perturbations in volcano plots. In this study, no relevant interacting surfaces are present, but ion-ion interactions are, thus adding an additional level of detail to the non-aqueous SIE picture.

The experimental work of Chapters 6 and 7 presents the highest complexity in the range of this thesis, as ion-solvent, ion-ion, and ion-interfaces interactions are present. This allows to bring into focus the dominant inter-

actions when interfaces are present: these are the dispersion contributions to the surface-solvent-ion competition, as extensively discussed in Section 8.2.

The overall interpretation proposed in this thesis is therefore that SIE are fundamentally a property of the ion, which follows the forward Hofmeister series for anions and the reverse lyotropic series for cations in ideal conditions, independently of the solvent. The interaction of ions with other ions or with surfaces, and other changes from the ideal conditions act as perturbations to this fundamental series.

The rules of thumb that derive from the findings above can be summarised as follows:

- for bulk properties of aqueous and non-aqueous electrolytes at infinite dilution, the fundamental series is to be expected (forward Hofmeister for anions and reverse lyotropic for cations);
- for bulk properties at real concentrations, the protic/aprotic nature of the solvent is the dominant characteristic that perturbs the anion series. The cation series is instead expected to be akin to that in water in both protic and aprotic solvents;
- for real concentrations and interacting surfaces, the dispersion interactions of both solvent and surface contribute to perturbing the fundamental anion series. These can cause reversal of the series, and solvents of intermediate polarisability might not exhibit clear SIE trends.

This provides a framework for understanding how ion-specific trends in non-aqueous solvents are related to ion-specific trends in water.

Another topic that I would like to touch upon is the role of the 'structure' of the solvent. This is a property that is ill-defined (Ninham and Lo Nostro, 2010), and extremely difficult to quantify experimentally. It also includes the structuring due to the presence of a hydrogen-bonding network, but it has a more general significance. That is, the electron distribution around a solvated ion will vary greatly from solvent to solvent, and consequently the potential that the ion is experiencing, which includes many-body interactions and higher order multipole contributions. The topological distribution around an ion in solution is challenging to investigate and is also the ultimate challenge for theory and modelling. The debate is still active as to the range to which the ions perturb the ordering of water molecules in solution (Funkner et al., 2012; Gurau et al., 2004; Paschek and Ludwig, 2011). This has not been addressed in my work, but deserves to be included in future investigations. On the other side, the fact that such general ion trends are observed is definitely remarkable given the great difference in properties of the solvents investigated.

In addition, I have tested the influence of water as an impurity with some targeted testing. I concluded that the presence of small quantities of wa-

ter ($< 0.2\,\%$) does not affect the SIE trend in the non-aqueous solvents examined, relatively to the experiments performed. I have collected evidence, though, that higher quantities of water influence the magnitude of SIE in non-aqueous solvents and the peak shape in SEC. This topic is a vast one and it demands to be addressed in depth.

A number of authors have made remarks about the risk of looking too hard for a simple explanation of the universal SIE trends. They note that no isolated property of an ion or a surface can be turned into a master key to unlock all the variations and manifestations of these phenomena (Kunz, 2009; Okur et al., 2017). That is, the observed and quite universal qualitative series are actually the result of subtle balances of a number of very specific competing interactions. Therefore a qualitative analogy across a number of experiments does not demonstrate that they are governed by the same rules. I hope that the general picture presented here does not come across as shoddy reductionism, as it is rather an attempt at organising this complexity in the broader context of non-aqueous solvents. I hope that the appreciation of the author for the detail and for the complexity of the SIE phenomena is clear throughout this work. I also look forward to improvements of the picture and interpretation presented.

The present work also highlights the need for additional targeted SIE experiments in non-aqueous solvents, in order to further define the picture introduced here.

A final important point to note is that the findings presented show that the protagonist role that has been attributed to water for the manifestation of SIE needs to be put into perspective. I have confirmed that SIE are not an exclusive feature of aqueous solutions, and that other non-aqueous solvents show the same trend. This is not to diminish the importance of water to human life, or to dismiss the intriguing charm of water — although I might not agree that it i s the most complex solvent, as stated in Kunz (2009), but rather the most extensively studied one. The usefulness and the allure of investigating non-aqueous electrolytes, not just as a niche sector functional to direct application, but as a broader knowledge horizon that has the potential of furthering the understanding of fundamental scientific queries, shows through.

If SIE are fundamental for enabling life processes, then could life based on a non-aqueous solvent be possible? Might it already be happening on a remote planet in the galaxy?

And this ultimately circles back to the understanding of water, the most important solvent for human existence.

8.2 THE GLOBAL EXPERIMENT PICTURE OF ANION TRENDS

The meaning of the ion-specific non-aqueous trends presented in detail in Chapters 6 and 7 are best discussed jointly with a general view.

I have performed experiments investigating SIE in two different systems using the same range of solvents, to shed light onto the effects of interacting surfaces and real concentrations on the fundamental anion series (the Hofmeister series, Fig. 1) individuated in Chapter 3.

The nature of the SEC and QCM experiments is very different. In the chromatography experiments the interacting surface is a polar, largely uncharged, stationary phase, whereas in the QCM experiments a polymer brush terminated in cationic alkylammonium groups constitutes the interacting surface. In addition, in SEC a dynamic property is evaluated, whereas the QCM experiment can be considered a static one. Despite the differences between these experiments, the trends in the SIE are consistent, as Table 29 illustrates.

Table 29: Summary of the anion-specific trends from experiment

experiment	water	MeOH	FA	DMSO	PC
SEC	HS	HS	no trend	R-HS	R-HS
QCM	HS	HS	HS	R-HS	R-HS

In almost the totality of solvent-experiment combinations, the Hofmeister series manifests, either in a forward or reverse ordering. This is in broad agreement with the conclusions from Chapter 3, where the forward Hofmeister series was identified as the fundamental series of anions in *all* solvents, for bulk properties of a solution at infinite dilution. However, a further degree of complexity is present here, compared to the fundamental Hofmeister series of Chapter 3: the series reverses in some solvents, and in one case no series can be determined at all. This is an indication that interacting solvent, surfaces as well as ion-ion interactions play a substantial role in perturbing the fundamental Hofmeister ordering. This additional degree of complexity was similarly encountered in Chapter 4, where the trends in the thermodynamics of solvation were examined with the volcano plot treatment. There, solvent-related perturbations were observed in the manifestation of a volcano trend for the standard solvation energies of electrolytes in different solvents, and it was concluded that the anion trends observed in water can be expected to be found unchanged in protic solvent, but not necessarily thus in aprotic solvents, where the order could be altered.

Taking a dichotomic view, and following the conclusions of Chapter 4, the experiment results could be interpreted as follows: the fundamental series (forward Hofmeister) is observed in the protic solvents, whereas it is reversed in the aprotic solvents. But this binary interpretation is an oversimpli-

fication that does not fully capture the gradation of ion-specific behaviours detected. In fact, in the QCM experiments the trend in FA followed the results obtained in water and MeOH (Fig. 31), whereas in the SEC experiments no clear trend was observed (Fig. 25). In addition, the amplitude of the brush response in the QCM experiment (Fig. 31) is large for water and MeOH, is smaller for FA, is the smallest but reversed in DMSO (where only two salts are inducing a net variation of the brush conformation) and becomes large again and reversed in PC. This is not simply a direct-to-reverse Hofmeister series switch when passing from protic to aprotic solvents: a progression is taking place.

The aprotic solvents are considerably more polarisable than the protic solvents, with FA being the most polarisable protic solvent (Table 2). The results can therefore be interpreted as resulting from a competition between the solvent and the surface for the anion. The evidence suggests that in protic solvents the more polarisable anions interact more strongly with the surface (and the less polarisable anions do not interact strongly with the surface), whereas in aprotic solvents the more polarisable anions do not interact with the surface as they are more favourably solvated. It follows that the trends observed are not due to the binary categorisation of solvents into protic and aprotic ones, but rather reflect changes in the polarisability of the solvent. These findings show that a binary view of the behaviour of protic versus aprotic solvent with respect to ions is not capturing the full complexity of the phenomenon. Rather there is a gradation of behaviours, and the surface properties (both of the charged surface groups and the non-charged sites) determine where the 'watershed' sits for the reversal of the observed trend. In the two investigations performed here, the watershed is at FA when *Sephadex*® is the interacting surface, whereas it is at DMSO when PMETAC brushes are the surface. It must also be noted that the type of experiment may influence the observed trends.

The experimental observations can therefore largely be explained by an evaluation of the dispersion forces between the ions and the solvent and the ions and the surface. Noting that these interactions will vary depending on the nature of the surface. This suggests that for a different class of surface (e.g. a metal oxide) the series may well be reversed.

Thus the basis for which the huge complexity of SIE observed across different solvents and in the presence of different surfaces emerges: solvents of different polarisability are competing for ions of different polarisability with surfaces that differ in polarisability and charge. This has the implication that, in order to model the SIE in different solvents, the polarisability of the solvent needs to be included, as the ion-solvent dispersion interactions play a fundamental role in SIE.

Table 30: Ionic *ab initio* static polarisabilties α_I from Parsons and Ninham (2009).

anion	$\alpha_I/Å^3$	cation	$\alpha_I/Å^3$
F^-	1.218	Li^+	0.028
Cl^-	4.220	Na^+	0.131
Br^-	6.028	K^+	0.795
I^-	8.967	Rb^+	1.348
ClO_4^-	4.790	Cs^+	2.354
SCN^-	7.428	$(CH_3)_4N^+$	7.448
AcO^-	5.607		

In Chapter 4 I concluded that the anion series observed in water is less likely to be preserved in aprotic solvents than the cation series. A probable cause of the non-preservation of the anion trend appears now in light of the experimental investigations: the dispersion interactions determined by the polarisability of the solvent, surface, and ion. The fact that this perturbation is observed for anions but not for cations in Chapter 4 now falls into place: anions are more polarisable than the alkali metal cations (Table 30) and therefore the dispersion interactions are more relevant for this class of ions.

Furthermore, another cause of series reversal has been identified, being solvent polarisability. This adds to the list of other causes of reversal reported in the literature: concentration, temperature, pH, counterion and surface charge (Lyklema, 2009; Parsons, Boström, Maceina et al., 2010; Robertson, 1911; Schwierz, Horinek, Sivan et al., 2016; Senske et al., 2016). Notably, we have not encountered any other reports of the reversal of the anion series across the solvents water, MeOH, FA, DMSO, PC, in the literature we reviewed (Table 13 of Chapter 2).

In view of these trends, a rule of thumb can be proposed: ion-specific trends in weakly polarisable solvents can be expected to follow those of water, ion-specific trends in strongly polarisable solvents follow the reverse trend, whereas solvents of intermediate polarisability may not exhibit a clear trend. Given the paucity of data on SIE in non-aqueous solvents compared to aqueous solvents, this rule of thumb may provide a useful starting point for engineering SIE in non-aqueous solvents. As such the polarisability of the substrates should also be important in affecting SIE trends and as such metal and metal oxide surfaces may well present different trends to those observed here.

It must be noted, though, that polarisability and hydrogen-bonding properties are different properties and are not connected by a simple relationship. I happened to use protic solvents of lower polarisability than the aprotic ones in my experiments. But there exist protic solvents of higher polarisability such as NMA and *t*-BuOH (Table 2) and aprotic solvents of low polarisability such as MeCN and $MeNO_2$. A first check of the rule of thumb here proposed

is therefore apparent: to test the experimental ionic trends in protic solvent of higher polarisability than FA and in aprotic solvents of lower polarisability than DMSO. Especially the aprotic solvents of low polarisability will be important in confirming or disproving the importance of polarisability over hydrogen-bonding postulated here.

Further, the studies reported here all employed Na^+ as the cation. It is known in some ion-specific phenomena that the particular pairing of ions is important (Craig, Ninham et al., 1993a,b; Kunz and Neueder, 2009; Lyklema, 2003). This aspect and the cation series *per se* in non-aqueous solvents have not been investigated here and remain a challenge for future investigations. The division of SIE in a cationic and anionic series is an artificial device that simplifies the organisation of the information, but has no real physical meaning as an ion cannot actually exist as an isolated charge. Therefore an ion in solution will also be affected by its counterion.

9 CONCLUSIONS

This thesis presents a wide-ranging investigation of specific-ion effects (SIE) in non-aqueous solvents. This is a qualitative study of the ordering of SIE in non-aqueous solvents compared to water. It consists of a comprehensive review of the literature, analysis and interpretation of a carefully selected subset of the literature data for non-aqueous electrolytes, and an experimental investigation of SIE in non-aqueous solutions.

In Chapter 1, I have clarified the terminology, that is particularly hazy in this field: in order to do so, I have compiled the Hofmeister series for cations and anions by merging the trends reported in a number of authoritative SIE references, and distinguished it from the lyotropic series, which is pertinent to a narrower category of SIE.

The analysis starts with the review of the available literature on non-aqueous solvents in Chapter 2. A general account of the ordering of SIE is compiled in different non-aqueous solvents. The results show the presence of SIE in non-aqueous solvents, which follow a variety of different series including the Hofmeister and lyotropic series, and display complex behaviour such as series reversal. This shows that the Hofmeister series is not a prerogative of aqueous solutions. In addition, no simple correlation of the ion-specific trend to the properties of the solvents is evident.

In Chapter 3 I have evaluated the standard electrostrictive volumes of Hofmeister electrolytes in a number of different solvents, and shown that, for bulk standard properties of electrolyte solutions, the SIE ordering is independent of the solvent. I have therefore inferred that SIE are fundamentally a property of ions, and that their universal fundamental ordering is the forward Hofmeister series for anions and the reverse lyotropic series for cations:

cations Li^+ Na^+ K^+ Rb^+ Cs^+

anions F^- Cl^- Br^- I^- ClO_4^- SCN^-

this also evidences the fact that water is by no means a 'special' solvent invested of exclusive SIE powers.

An additional literature data analysis is performed in Chapter 4, where I extend the volcano plots of standard solvation energies to non-aqueous solvents. These are related to the law of matching water affinities (LMWA) principle. The volcano plot trends arise in both protic and aprotic non-aqueous

solvents for cations, and in protic solvents for anions. I conclude that the evidence suggests that the ion size, rather than the ion-solvent interaction, is the origin of the volcano trend. This confirms the central role of the ion properties for SIE, presented in the previous chapter. Finally, I extended the volcano plots to real concentrations in water and non-aqueous solvents, confirming the standard volcano trends and proposed a rule of thumb for predicting ion-specific trends in new systems, stating that, across solvents, the ion-specific trends observed in water will likely be observed in other protic non-aqueous solvents, and that the trends observed in water will be more likely to hold for cations in non-aqueous solvents than for anions.

The experimental part of this thesis consists of two studies of the specific-anion effects in water and the non-aqueous solvents MeOH, FA, DMSO and PC. These tests particularly show how the trends are affected by the addition of an interacting surface. The first experiment is the size-exclusion chromatography (SEC) of sodium Hofmeister electrolytes on a *Sephadex*® stationary phase in the different solvents. I have found that, for the elution of electrolytes, water and MeOH show a forward Hofmeister series, whereas DMSO and PC exhibit a reverse Hofmeister trend. No trend can be identified for FA. In the second set of experiments, I investigated the conformation (swelling/-collapse) of a cationic polymer brush in the presence of electrolyte solutions in the same solvents. The ordering of anion effects follows a forward Hofmeister series for water, MeOH and FA in this case, and a reverse Hofmeister series for DMSO and PC. I have rationalised these experimental findings by noting that the nuances of the behaviours in the different solvents best correlate to the solvent polarisability. I have therefore concluded that dispersion forces are crucial in the competition of the surface and the solvent for interactions with the ions. These experiments are also the first reports of SIE series reversal due to the solvent.

In Chapter 8 I have discussed all the findings with a global view, assembling a coherent picture for the solvent effect in SIE. Overall, I propose an interpretation that places the fundamental origin of the SIE on the ions, that in ideal conditions (bulk properties and ion-solvent interactions only) follow the forward Hofmeister series for anions and the reverse lyotropic series for cations. The introduction of ion-ion interactions, interacting surfaces and so on can be consequently viewed as perturbations on these fundamental series. These are more likely to alter the fundamental (Hofmeister) ordering for anions in aprotic solvents. Anions in protic solvents and cations in protic and aprotic solvents can instead be expected to more likely follow the ordering observed in water. Finally, when interacting surfaces are present, their perturbation effect can be largely rationalised by considering their polarisability with respect to the solvent polarisability, as dispersion forces appear to

present the crucial interaction that guides the ion preference for interacting with either the solvent or the surface.

The information and data analysed here can serve as valuable testing ground for the theories and models of SIE, and strongly suggests that 'ion size' and dispersion forces are the principal features in determining the ion-specific trends.

9.1 FURTHER WORK

The conclusions achieved in this thesis are based on as much evidence I could gather. As I have pointed out, the conclusions and ideas presented here need to be further tested, and corrected, and refined. The avenues for further work are therefore abundant and span in all possible directions of the multifaceted world of non-aqueous electrolytes.

Experimentally, these include testing for the cation series in non-aqueous solvents. When different cation trends at common anion are achieved, these will help in obtaining a picture for the trends depending on the cation-anion match.

In order to further understand how polarisability and proticity prevail, more solvents of different polarisability should be tested, and especially aprotic solvents of low polarisability.

Also, additional experiments involving different surfaces are useful. In these also the liquid-air interface is new ground to be probed, as well as surfaces with very different dielectric properties such as metals and mineral oxides. The study of the liquid-air interface presents a challenge as moisture needs to be avoided.

Examples of possible experiments include spectroscopic and scattering studies, NMR studies, the self-assembly of surfactants, the solubility of gases. A list of experiments that I have attempted but have been unsuccessful is available in Appendix G.

On this note, also the influence of water on the SIE needs to be studied in more detail, as it could be particularly relevant in mixes with aprotic solvents.

Finally, the acquisition of more extensive fundamental thermodynamic data as the molar electrolyte volumes, activity or osmotic coefficients of electrolytes is particularly needed to extend the base of electrolytes investigated.

This work has focussed on qualitative trends, but ultimately a more quantitative treatment is required. Therefore, theoretical and modelling work should be applied in order to develop a theory able to predict ion trends for water as well as non-aqueous electrolytes.

A ELECTROSTRICTION DATA

A.1 TABULATION OF THE VOLUMES

Table 31: Values of all the volumes used in Chapter 3. $\overline{V}_{i\,intr}$ is the intrinsic molar volume; 'mode' indicates the estimate of $\overline{V}_{i\,intr}$ employed; $\overline{V}_i^{\ominus}$ indicates the standard molar volume, and 'minimum error' is the minimum error associated with $\overline{V}_i^{\ominus}$; $\overline{V}_{i\,el}^{\ominus} = \overline{V}_i^{\ominus} - \overline{V}_{i\,intr}$ is the electrostrictive volume; N% is the electrostrictive volume normalised by the intrinsic molar volume.

electrolyte	solvent	$\overline{V}_{i\,intr}$	mode*	$\overline{V}_i^{\ominus}$	minimum error†	$\overline{V}_{i\,el}^{\ominus}$	N%
RbF	water	32.6	C	12.9	R	−19.7	−60.5
NaF	water	16.4	M	−2.4	R	−18.8	−114.5
CsOAc	water	79.2	C§	61.8	R	−17.4	−22.0
KF	water	23.7	M	7.9	R	−15.8	−66.8
LiOAc	water	53.6	C‡	39.6	R	−14.1	−26.2
LiF	water	11.6	M	−2.0	R	−13.6	−117.6
CsF	water	33.6	M	20.2	R	−13.4	−39.9
NaCl	water	29.6	M	16.6	R	−13.0	−43.9
NaBr	water	35.1	M	23.5	R	−11.6	−33.0
KOAc	water	61	S	49.5	R	−11.5	−18.9
KCl	water	38	M	26.9	R	−11.2	−29.3
RbCl	water	42.3	M	31.9	R	−10.4	−24.6
KBr	water	43.9	M	33.7	R	−10.2	−23.2
NaOAc	water	49.4	S	39.3	R	−10.2	−20.5
$NaClO_4$	water	52.9	S	42.9	R	−10.0	−18.9
NaI	water	44.8	M	35.0	R	−9.8	−21.9
CsCl	water	48.8	M	39.2	R	−9.6	−19.7
RbBr	water	48.4	M	38.8	R	−9.6	−19.9
CsI	water	66.8	M	57.6	R	−9.2	−13.8
KI	water	54	M	45.2	R	−8.8	−16.2
CsBr	water	54.8	M	46.1	R	−8.8	−16.0
RbI	water	58.9	M	50.3	R	−8.6	−14.6
KSCN	water	57.7	S	49.6	R	−8.1	−14.0
NaSCN	water	46.6	C¶	39.4	R	−7.2	−15.5
LiCl	water	24.1	M	17.0	R	−7.2	−29.7
LiBr	water	30.3	M	23.8	R	−6.5	−21.4
LiSCN	water	45.5	C‖	39.7	R	−5.8	−12.6
$RbClO_4$	water	63.8	C	58.2	R	−5.6	−8.7
$CsClO_4$	water	69.8	C	65.5	R	−4.4	−6.3
LiI	water	38.1	M	35.3	R	−2.8	−7.2
$KClO_4$	water	55.0	C	53.1	R	−1.8	−3.3
$LiClO_4$	water	43.8	C	43.2	R	−0.6	−1.3
RbF	MeOH	32.6	C	−5	4	−37.6	−115.3
NaF	MeOH	16.4	M	−20	4	−36.4	−222.0
CsI	MeOH	66.8	M	33	4	−33.8	−50.6
NaCl	MeOH	29.6	M	−3.9	R	−33.5	−113.2
NaI	MeOH	44.8	M	11.3	R	−33.5	−74.8
RbI	MeOH	58.9	M	26	4	−32.9	−55.9
KI	MeOH	54	M	21.7	R	−32.3	−59.8
CsF	MeOH	33.6	M	2	4	−31.6	−94.0
LiF	MeOH	11.6	M	−20	4	−31.6	−272.4
KF	MeOH	23.7	M	−7.6	R	−31.3	−132.1
RbCl	MeOH	42.3	M	11	4	−31.3	−74.0
KCl	MeOH	38	M	7	R	−31	−81.6
$NaClO_4$	MeOH	52.9	S	22	4	−30.9	−58.4
NaBr	MeOH	35.1	M	4.3	R	−30.8	−87.7
CsCl	MeOH	48.8	M	18	4	−30.8	−63.1

Volumes and error in $cm^3\,mol^{-1}$.

* M: from molten salts (Pedersen et al., 1984); S: from soluble salts (Marcus, 2010); C: calculated from density of the crystal (Lide, 2010); † 'R' indicates a value recommended by the reviewer (Marcus et al., 2004; Millero, 1971). ‡ from Saunderson et al., 1961; § from Yode, 2015; ‖ from Lee, 1964; ¶ from VWR, 2014.

electrolyte	solvent	$\overline{V}_{i\,intr}$	mode*	$\overline{V}_i^{\ominus}$	minimum error†	$\overline{V}_{i\,el}^{\ominus}$	N%
KSCN	MeOH	57.7	S	28	4	−29.7	−51.5
NaSCN	MeOH	46.6	C¶	17	4	−29.6	−63.5
RbBr	MeOH	48.4	M	19	4	−29.4	−60.7
KBr	MeOH	43.9	M	14.7	R	−29.2	−66.5
CsBr	MeOH	54.8	M	26	4	−28.8	−52.6
LiCl	MeOH	24.1	M	−4.5	R	−28.6	−118.7
LiSCN	MeOH	45.5	C‖	17	4	−28.5	−62.6
LiI	MeOH	38.1	M	11	4	−27.1	−71.1
$RbClO_4$	MeOH	63.8	C	37	4	−26.8	−42.0
LiBr	MeOH	30.3	M	4	4	−26.3	−86.8
$CsClO_4$	MeOH	69.8	C	44	4	−25.8	−37.0
$KClO_4$	MeOH	55.0	C	33	4	−22.0	−40.0
$LiClO_4$	MeOH	43.8	C	22	4	−21.8	−49.8
LiF	EtOH	11.6	M	−35	4	−46.6	−401.7
RbF	EtOH	32.6	C	−8	4	−40.6	−124.5
NaF	EtOH	16.4	M	−23	4	−39.4	−240.2
KF	EtOH	23.7	M	−14	4	−37.7	−159.1
LiBr	EtOH	30.3	M	−5.2	R	−35.5	−117.2
CsF	EtOH	33.6	M	0	4	−33.6	−100
LiI	EtOH	38.1	M	5	4	−33.1	−86.9
LiOAc	EtOH	53.6	C‡	22	4	−31.6	−59.0
LiCl	EtOH	24.1	M	−4.9	R	−29	−120.3
NaI	EtOH	44.8	M	16.2	R	−28.6	−63.8
KI	EtOH	54	M	25.5	R	−28.5	−52.8
RbI	EtOH	58.9	M	32	4	−26.9	−45.7
CsI	EtOH	66.8	M	40	4	−26.8	−40.1
NaBr	EtOH	35.1	M	9	4	−26.1	−74.4
KBr	EtOH	43.9	M	18	4	−25.9	−59.0
NaCl	EtOH	29.6	M	5	4	−24.6	−83.1
RbBr	EtOH	48.4	M	24	4	−24.4	−50.4
KCl	EtOH	38	M	14	4	−24	−63.2
CsBr	EtOH	54.8	M	32	4	−22.8	−41.6
RbCl	EtOH	42.3	M	20	4	−22.3	−52.7
CsOAc	EtOH	79.2	C§	57	4	−22.2	−28.0
CsCl	EtOH	48.8	M	28	4	−20.8	−42.6
KOAc	EtOH	61	S	43	4	−18	−29.5
NaOAc	EtOH	49.4	S	34	4	−15.4	−31.2
RbF	FA	32.6	C	24	4	−8.6	−26.5
NaCl	FA	29.6	M	21.3	R	−8.3	−28.0
NaBr	FA	35.1	M	28.2	R	−6.9	−19.7
CsCl	FA	48.8	M	42.3	R	−6.5	−13.3
NaF	FA	16.4	M	10	4	−6.4	−39.0
KCl	FA	38	M	31.7	R	−6.3	−16.6
RbCl	FA	42.3	M	36	4	−6.3	−14.9
CsBr	FA	54.8	M	48.9	R	−5.9	−10.8
CsI	FA	66.8	M	61	4	−5.8	−8.7
LiF	FA	11.6	M	6	4	−5.6	−48.3
RbBr	FA	48.4	M	43	4	−5.4	−11.2
LiBr	FA	30.3	M	25	4	−5.3	−17.5
KBr	FA	43.9	M	38.8	R	−5.1	−11.6
NaI	FA	44.8	M	40	R	−4.8	−10.7
LiSCN	FA	45.5	C‖	41	4	−4.5	−9.8
LiCl	FA	24.1	M	19.9	R	−4.2	−17.4
RbI	FA	58.9	M	55	4	−3.9	−6.6
KF	FA	23.7	M	20	4	−3.7	−15.6
CsF	FA	33.6	M	30	4	−3.6	−10.7
KI	FA	54	M	50.6	R	−3.4	−6.3
KSCN	FA	57.7	S	55	4	−2.7	−4.7
$NaClO_4$	FA	52.9	S	51	4	−1.9	−3.6
NaSCN	FA	46.6	C¶	45	4	−1.6	−3.4
LiI	FA	38.1	M	37	4	−1.1	−2.9
$CsClO_4$	FA	69.8	C	71	4	1.2	1.7
$RbClO_4$	FA	63.8	C	65	4	1.2	1.9
$LiClO_4$	FA	43.8	C	47	4	3.2	7.3
$KClO_4$	FA	55.0	C	61	4	6.0	10.9
RbI	EG	58.9	M	26	R	−32.9	−55.9

Volumes and error in $cm^3\,mol^{-1}$.

* M: from molten salts (Pedersen et al., 1984); S: from soluble salts (Marcus, 2010); C: calculated from density of the crystal (Lide, 2010); † 'R' indicates a value recommended by the reviewer (Marcus et al., 2004; Millero, 1971). ‡ from Saunderson et al., 1961; § from Yode, 2015; ‖ from Lee, 1964; ¶ from VWR, 2014.

electrolyte	solvent	$\overline{V}_{i\,intr}$	mode*	$\overline{V}_i^{\ominus}$	minimum error†	$\overline{V}_{i\,el}^{\ominus}$	N%
RbF	EG	32.6	C	17	4	−15.6	−47.9
LiF	EG	11.6	M	−3	4	−14.6	−125.9
NaF	EG	16.4	M	2	4	−14.4	−87.8
KF	EG	23.7	M	11	4	−12.7	−53.6
NaCl	EG	29.6	M	20.9	R	−8.7	−29.4
LiBr	EG	30.3	M	22.2	R	−8.1	−26.7
KCl	EG	38	M	30	4	−8	−21.1
LiCl	EG	24.1	M	16.4	R	−7.7	−32.0
CsF	EG	33.6	M	26	4	−7.6	−22.6
KI	EG	54	M	46.5	R	−7.5	−13.9
NaBr	EG	35.1	M	27.6	R	−7.5	−21.4
KBr	EG	43.9	M	36.7	R	−7.2	−16.4
NaI	EG	44.8	M	38	4	−6.8	−15.2
RbCl	EG	42.3	M	36	4	−6.3	−14.9
RbBr	EG	48.4	M	43	4	−5.4	−11.2
LiI	EG	38.1	M	33.2	R	−4.9	−12.9
CsI	EG	66.8	M	62	4	−4.8	−7.2
CsCl	EG	48.8	M	45	4	−3.8	−7.8
CsBr	EG	54.8	M	52	4	−2.8	−5.1
LiCl	PC	24.1	M	7	4	−17.1	−71.0
CsI	PC	66.8	M	50	4	−16.8	−25.1
CsCl	PC	48.8	M	33	4	−15.8	−32.4
NaCl	PC	29.6	M	14	4	−15.6	−52.7
RbCl	PC	42.3	M	27	4	−15.3	−36.2
KCl	PC	38	M	23	4	−15	−39.5
LiBr	PC	30.3	M	15.3	R	−15	−49.5
RbI	PC	58.9	M	44	4	−14.9	−25.3
KI	PC	54	M	39.5	R	−14.5	−26.9
LiI	PC	38.1	M	24	4	−14.1	−37.0
NaI	PC	44.8	M	31	4	−13.8	−30.8
CsBr	PC	54.8	M	43	4	−11.8	−21.5
$NaClO_4$	PC	52.9	S	41.5	R	−11.4	−21.6
RbBr	PC	48.4	M	37	4	−11.4	−23.6
NaBr	PC	35.1	M	24	4	−11.1	−31.6
KBr	PC	43.9	M	33	4	−10.9	−24.8
$CsClO_4$	PC	69.8	C	61	4	−8.8	−12.7
$RbClO_4$	PC	63.8	C	55	4	−8.8	−13.7
$LiClO_4$	PC	43.8	C	37.1	R	−6.7	−15.3
$KClO_4$	PC	55.0	C	51	4	−4.0	−7.2
KI	EC	54	M	47	4	−7	−13.0
LiI	EC	38.1	M	35	4	−3.1	−8.1
$NaClO_4$	EC	52.9	S	52	4	−0.9	−1.7
$LiClO_4$	EC	43.8	C	43	4	−0.8	−1.9
NaI	EC	44.8	M	44	4	−0.8	−1.8
$KClO_4$	EC	55.0	C	55	4	0.0	0.0
LiCl	DMSO	24.1	M	4.5	R	−19.6	−81.3
KCl	DMSO	38	M	20	4	−18	−47.4
RbF	DMSO	32.6	C	15	4	−17.6	−54.1
LiF	DMSO	11.6	M	−6	4	−17.6	−151.7
LiBr	DMSO	30.3	M	13	4	−17.3	−57.1
NaCl	DMSO	29.6	M	12.5	R	−17.1	−57.8
CsCl	DMSO	48.8	M	32	4	−16.8	−34.4
RbCl	DMSO	42.3	M	26	4	−16.3	−38.5
NaBr	DMSO	35.1	M	19.5	R	−15.6	−44.4
KBr	DMSO	43.9	M	28.4	R	−15.5	−35.3
NaF	DMSO	16.4	M	1	4	−15.4	−93.9
RbBr	DMSO	48.4	M	33	R	−15.4	−31.8
CsBr	DMSO	54.8	M	39.8	R	−15	−27.4
KF	DMSO	23.7	M	9	4	−14.7	−62.0
CsF	DMSO	33.6	M	21	4	−12.6	−37.5
CsI	DMSO	66.8	M	54.2	R	−12.6	−18.9
KI	DMSO	54	M	42.2	R	−11.8	−21.9
LiI	DMSO	38.1	M	27	4	−11.1	−29.1
NaI	DMSO	44.8	M	33.7	R	−11.1	−24.8
RbI	DMSO	58.9	M	48.2	R	−10.7	−18.2
$NaClO_4$	DMSO	52.9	S	47	4	−5.9	−11.2
$CsClO_4$	DMSO	69.8	C	67	4	−2.8	−4.1

Volumes and error in $cm^3\ mol^{-1}$.

* M: from molten salts (Pedersen et al., 1984); S: from soluble salts (Marcus, 2010); C: calculated from density of the crystal (Lide, 2010); † 'R' indicates a value recommended by the reviewer (Marcus et al., 2004; Millero, 1971). ‡ from Saunderson et al., 1961; § from Yode, 2015; ‖ from Lee, 1964; ¶ from VWR, 2014.

electrolyte	solvent	$\overline{V}_{i\,intr}$	mode*	$\overline{V}_i^{\ominus}$	minimum error†	$\overline{V}_{i\,el}^{\ominus}$	N%
$LiClO_4$	DMSO	43.8	C	41	4	−2.8	−6.4
$RbClO_4$	DMSO	63.8	C	61	4	−2.8	−4.3
$KClO_4$	DMSO	55.0	C	55	4	0.0	0.0
LiCl	ACE	24.1	M	−70	4	−94.1	−390.5
$LiClO_4$	ACE	43.8	C	−42	4	−85.8	−195.8
LiI	ACE	38.1	M	−31	4	−69.1	−181.4
LiBr	ACE	30.3	M	−37	4	−67.3	−222.1
NaCl	ACE	29.6	M	−26	4	−55.6	−187.8
$NaClO_4$	ACE	52.9	S	2	4	−50.9	−96.2
NaI	ACE	44.8	M	13	4	−31.8	−71.0
NaBr	ACE	35.1	M	7	4	−28.1	−80.1
RbCl	MeCN	42.3	M	−3	4	−45.3	−107.1
CsCl	MeCN	48.8	M	4	4	−44.8	−91.8
RbBr	MeCN	48.4	M	4	4	−44.4	−91.7
KCl	MeCN	38	M	−6	4	−44	−115.8
CsBr	MeCN	54.8	M	11	4	−43.8	−79.9
NaCl	MeCN	29.6	M	−14	4	−43.6	−147.3
KBr	MeCN	43.9	M	1	4	−42.9	−97.7
NaBr	MeCN	35.1	M	−7	4	−42.1	−119.9
LiCl	MeCN	24.1	M	−17	4	−41.1	−170.5
RbI	MeCN	58.9	M	18.3	R	−40.6	−68.9
NaI	MeCN	44.8	M	4.3	R	−40.5	−90.4
CsI	MeCN	66.8	M	26.4	R	−40.4	−60.5
LiBr	MeCN	30.3	M	−10	4	−40.3	−133.0
KSCN	MeCN	57.7	S	18.7	R	−39	−67.6
KI	MeCN	54	M	15.7	R	−38.3	−70.9
LiSCN	MeCN	45.5	C‖	9	4	−36.5	−80.2
$NaClO_4$	MeCN	52.9	S	17	4	−35.9	−67.9
$RbClO_4$	MeCN	63.8	C	28	4	−35.8	−56.1
$CsClO_4$	MeCN	69.8	C	35	4	−34.8	−49.9
NaSCN	MeCN	46.6	C¶	12	4	−34.6	−74.2
LiI	MeCN	38.1	M	5	4	−33.1	−86.9
$KClO_4$	MeCN	55.0	C	25	4	−30.0	−54.5
$LiClO_4$	MeCN	43.8	C	15.3	R	−28.5	−65.1
CsI	NMF	66.8	M	55	4	−11.8	−17.7
LiBr	NMF	30.3	M	18.7	R	−11.6	−38.3
CsBr	NMF	54.8	M	44	4	−10.8	−19.7
LiSCN	NMF	45.5	C‖	36	4	−9.5	−20.8
KBr	NMF	43.9	M	35	4	−8.9	−20.3
CsCl	NMF	48.8	M	40	4	−8.8	−18.0
KI	NMF	54	M	45.5	R	−8.5	−15.7
NaBr	NMF	35.1	M	27.1	R	−8	−22.8
NaI	NMF	44.8	M	37.3	R	−7.5	−16.7
LiI	NMF	38.1	M	31	4	−7.1	−18.6
KCl	NMF	38	M	31	4	−7	−18.4
NaCl	NMF	29.6	M	22.7	R	−6.9	−23.3
LiCl	NMF	24.1	M	17.3	R	−6.8	−28.2
KSCN	NMF	57.7	S	51	4	−6.7	−11.6
$NaClO_4$	NMF	52.9	S	47	4	−5.9	−11.2
$CsClO_4$	NMF	69.8	C	64	4	−5.8	−8.4
$LiClO_4$	NMF	43.8	C	40	4	−3.8	−8.7
NaSCN	NMF	46.6	C¶	43	4	−3.6	−7.7
$KClO_4$	NMF	55.0	C	55	4	0.0	0.0
LiBr	DMF	30.3	M	0.2	R	−30.1	−99.3
RbBr	DMF	48.4	M	19	4	−29.4	−60.7
RbCl	DMF	42.3	M	13	4	−29.3	−69.3
KBr	DMF	43.9	M	14.9	R	−29	−66.1
KCl	DMF	38	M	9	4	−29	−76.3
CsBr	DMF	54.8	M	26	4	−28.8	−52.6
CsCl	DMF	48.8	M	20	4	−28.8	−59.0
NaCl	DMF	29.6	M	1	4	−28.6	−96.6
LiCl	DMF	24.1	M	−3.8	R	−27.9	−115.8
NaBr	DMF	35.1	M	7.3	R	−27.8	−79.2
CsI	DMF	66.8	M	40.7	R	−26.1	−39.1
RbI	DMF	58.9	M	34.6	R	−24.3	−41.3
KI	DMF	54	M	31.3	R	−22.7	−42.0

Volumes and error in $cm^3\,mol^{-1}$.

* M: from molten salts (Pedersen et al., 1984); S: from soluble salts (Marcus, 2010); C: calculated from density of the crystal (Lide, 2010); † 'R' indicates a value recommended by the reviewer (Marcus et al., 2004; Millero, 1971). ‡ from Saunderson et al., 1961; § from Yode, 2015; ‖ from Lee, 1964; ¶ from VWR, 2014.

electrolyte	solvent	$\overline{V}_{i\,intr}$	mode*	$\overline{V}_i^{\circ}$	minimum error†	$\overline{V}_{i\,el}^{\circ}$	N%
NaI	DMF	44.8	M	22.2	R	−22.6	−50.4
LiI	DMF	38.1	M	16	4	−22.1	−58.0
$NaClO_4$	DMF	52.9	S	33	4	−19.9	−37.6
$RbClO_4$	DMF	63.8	C	45	4	−18.8	−29.4
$CsClO_4$	DMF	69.8	C	52	4	−17.8	−25.5
$LiClO_4$	DMF	43.8	C	27	4	−16.8	−38.4
$KClO_4$	DMF	55.0	C	41	4	−14.0	−25.4

Volumes and error in $cm^3\ mol^{-1}$.
* M: from molten salts (Pedersen et al., 1984); S: from soluble salts (Marcus, 2010); C: calculated from density of the crystal (Lide, 2010); † 'R' indicates a value recommended by the reviewer (Marcus et al., 2004; Millero, 1971). ‡ from Saunderson et al., 1961; § from Yode, 2015; ‖ from Lee, 1964; ¶ from VWR, 2014.

BIBLIOGRAPHY FOR THE CURRENT APPENDIX

Lee, D. A.

1964 'Anhydrous Lithium Thiocyanate', *Inorg. Chem.* 3, 2, pp. 289–290, DOI: 10.1021/ic50012a039.

Lide, D. R.

2010 (ed.), *CRC Handbook of Chemistry and Physics*, 90th ed., CRC Press/Taylor and Francis, Boca Raton, FL.

Marcus, Y.

2010 'On the Intrinsic Volumes of Ions in Aqueous Solutions', English, *J. Solution Chem.* 39, 7, pp. 1031–1038, DOI: 10.1007/s10953-010-9553-6.

Marcus, Y. and G. T. Hefter

2004 'Standard Partial Molar Volumes of Electrolytes and Ions in Nonaqueous Solvents', *Chem. Rev.* 104, pp. 3405–3452, DOI: 10.1021/cr030047d.

Millero, F. J.

1971 'The Molal Volumes of Electrolytes', *Chem. Rev.* 71, 2, pp. 147–176, DOI: 10.1021/cr60270a001.

Pedersen, T. G., C. Dethlefsen and A. Hvidt

1984 'Volumetric Properties of Aqueous Solutions of Alkali Halides', English, *Carlsberg Res. Commun.* 49, 3, pp. 445–455, DOI: 10.1007/BF02907785.

Saunderson, C. and R. B. Ferguson

1961 'Crystal Data for Anhydrous Lithium Acetate', *Acta Crystallogr.* 14, 3, p. 321.

VWR

2014 *Sodium Thiocyanate Density*, ca.vwr.com/store/catalog/product.jsp?catalog_number=CAAA33388-A3.

Yode, R.

2015 'Cesium Acetate', in *Encyclopedia of Reagents for Organic Synthesis*, John Wiley & Sons, Ltd, ISBN: 9780470842898, DOI: 10.1002/047084289X.rn01845.

A.2 STANDARD MOLAR VOLUMES OF ELECTROLYTES

A.2.1 Protic solvents

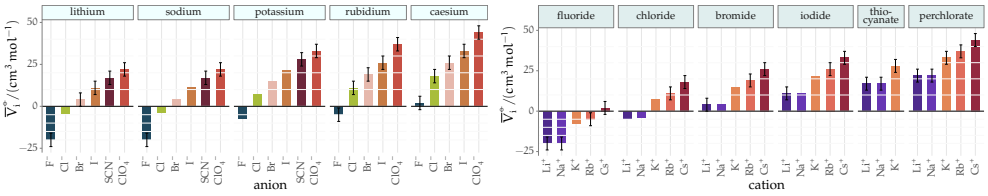

Figure 33: Standard molar volume $\overline{V}_i^{\circ}$ of alkali metal salts in MeOH grouped by cation (left) and by anion (right).

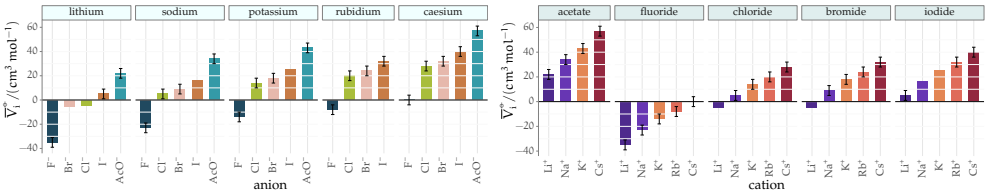

Figure 34: Standard molar volume $\overline{V}_i^{\circ}$ of alkali metal salts in EtOH grouped by cation (left) and by anion (right).

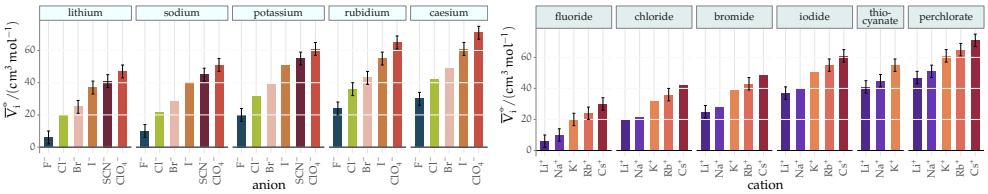

Figure 35: Standard molar volume $\overline{V}_i^{\circ}$ of alkali metal salts in FA grouped by cation (left) and by anion (right).

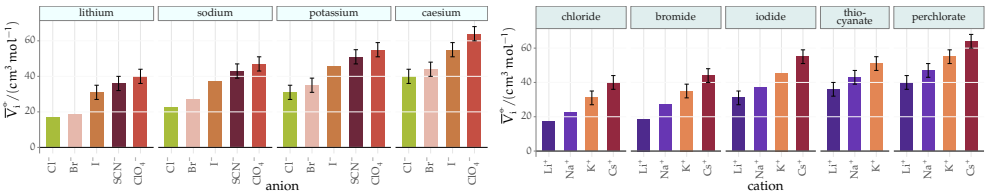

Figure 36: Standard molar volume $\overline{V}_i^{\circ}$ of alkali metal salts in NMF grouped by cation (left) and by anion (right).

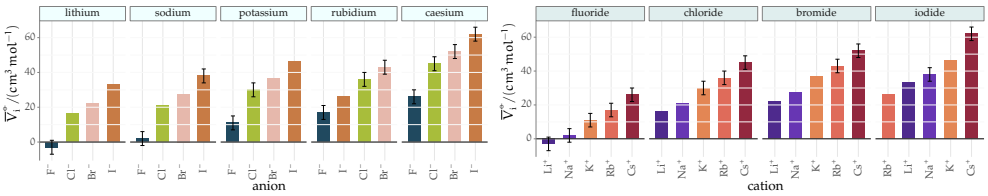

Figure 37: Standard molar volume $\overline{V}_i^{\circ}$ of alkali metal salts in EG grouped by cation (left) and by anion (right).

A.2.2 Aprotic solvents

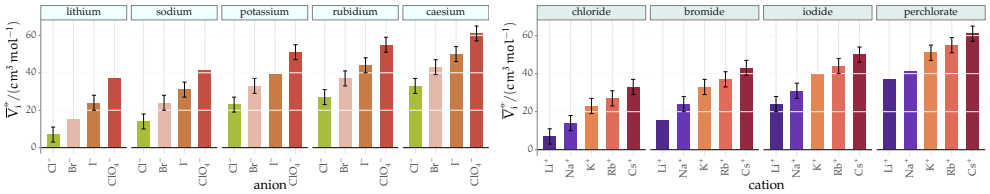

Figure 38: Standard molar volume $\overline{V}_i^{\circ}$ of alkali metal salts in PC grouped by cation (left) and by anion (right).

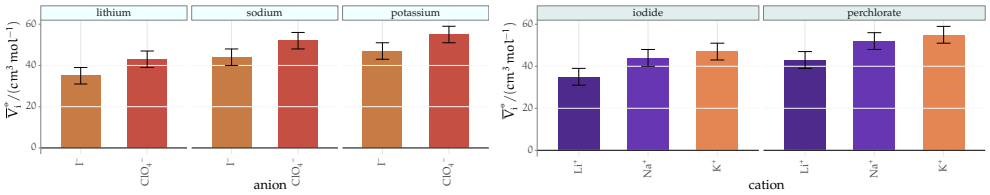

Figure 39: Standard molar volume $\overline{V}_i^{\circ}$ of alkali metal salts in EC grouped by cation (left) and by anion (right).

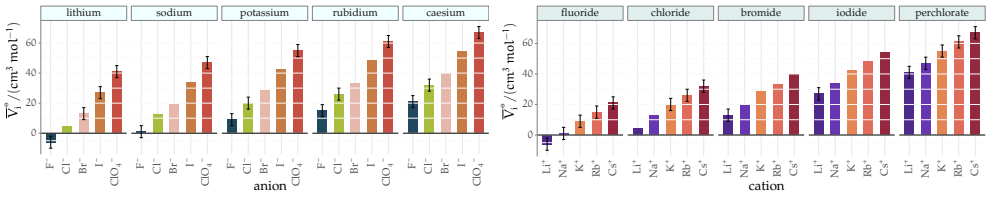

Figure 40: Standard molar volume $\overline{V}_i^{\circ}$ of alkali metal salts in DMSO grouped by cation (left) and by anion (right).

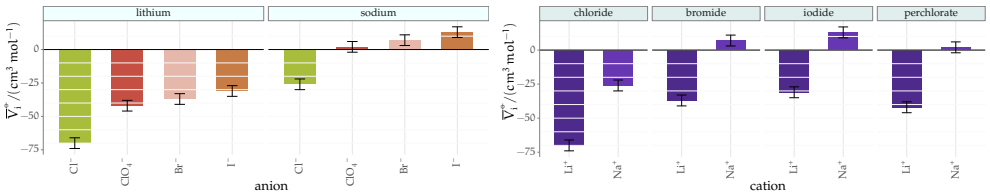

Figure 41: Standard molar volume $\overline{V}_i^{\circ}$ of alkali metal salts in ACE grouped by cation (left) and by anion (right).

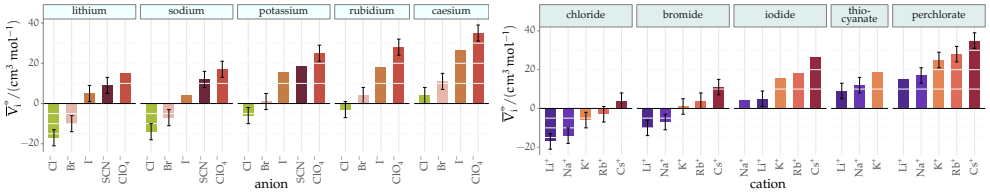

Figure 42: Standard molar volume $\overline{V}_i^{\circ}$ of alkali metal salts in MeCN grouped by cation (left) and by anion (right).

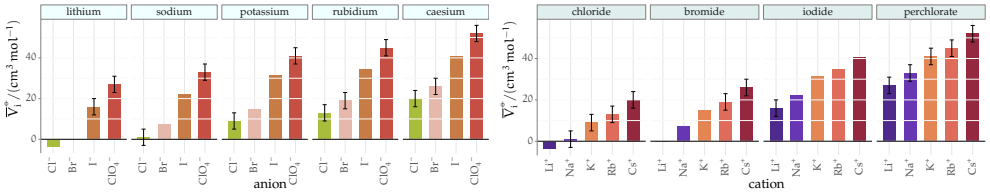

Figure 43: Standard molar volume $\overline{V}_i^{\circ}$ of alkali metal salts in DMF grouped by cation (left) and by anion (right).

A.3 ELECTROSTRICTIVE VOLUME OF ELECTROLYTES

The labels above the bars in each plot indicate the method of estimation of the intrinsic molar volume used in the calculations. M: extrapolation from molten salts, from Pedersen et al. (1984); S: from 'soluble salts' (Marcus, 2010); C: crystal volume, as in Eq. [5].

A.3.1 Protic solvents

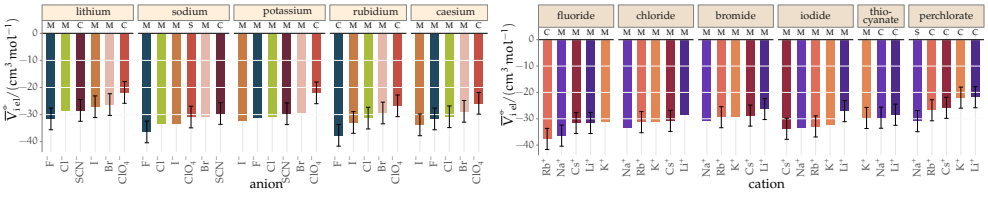

Figure 44: Standard molar electrostrictive volume $\overline{V}^{\ominus}_{i\,el}$ of alkali metal salts in MeOH grouped by cation (left) and by anion (right).

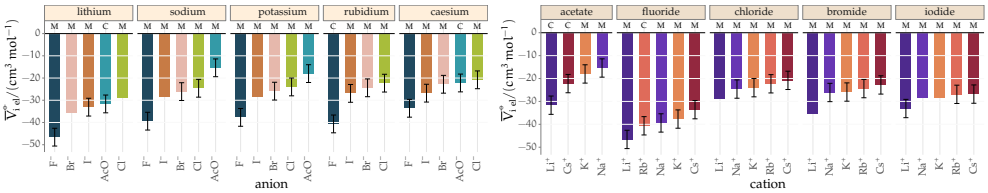

Figure 45: Standard molar electrostrictive volume $\overline{V}^{\ominus}_{i\,el}$ of alkali metal salts in EtOH grouped by cation (left) and by anion (right).

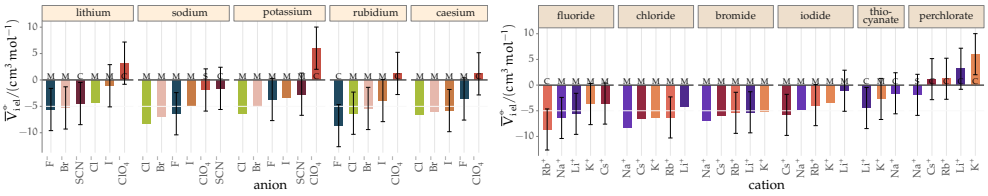

Figure 46: Standard molar electrostrictive volume $\overline{V}^{\ominus}_{i\,el}$ of alkali metal salts in FA grouped by cation (left) and by anion (right).

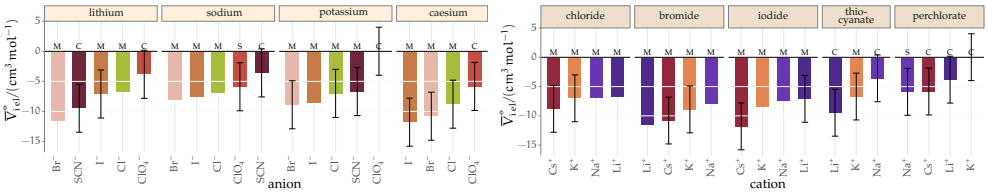

Figure 47: Standard molar electrostrictive volume $\overline{V}^{\ominus}_{i\,el}$ of alkali metal salts in NMF grouped by cation (left) and by anion (right).

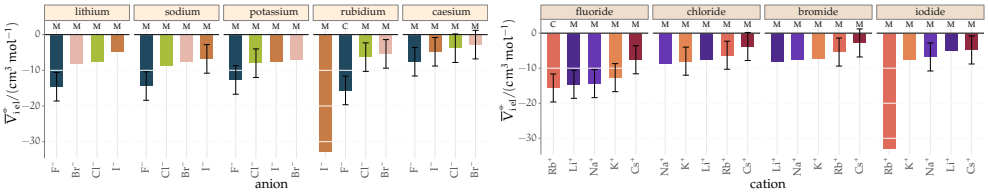

Figure 48: Standard molar electrostrictive volume $\overline{V}^{\ominus}_{i\,el}$ of alkali metal salts in EG grouped by cation (left) and by anion (right).

A.3.2 Aprotic solvents

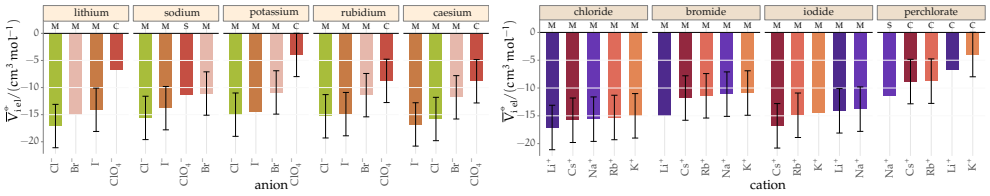

Figure 49: Standard molar electrostrictive volume $\overline{V}^{\ominus}_{i\,el}$ of alkali metal salts in PC grouped by cation (left) and by anion (right).

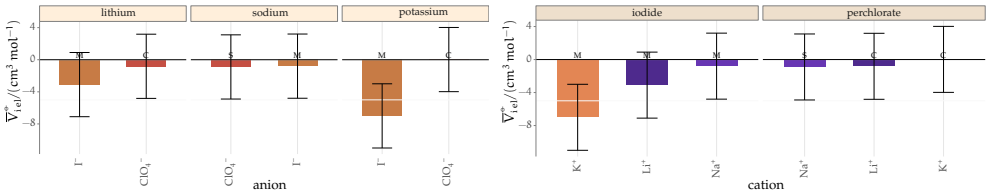

Figure 50: Standard molar electrostrictive volume $\overline{V}^{\ominus}_{i\,el}$ of alkali metal salts in EC grouped by cation (left) and by anion (right).

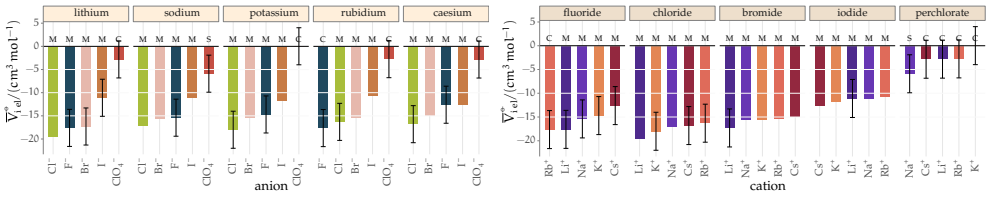

Figure 51: Standard molar electrostrictive volume $\overline{V}^{\ominus}_{i\,el}$ of alkali metal salts in DMSO grouped by cation (left) and by anion (right).

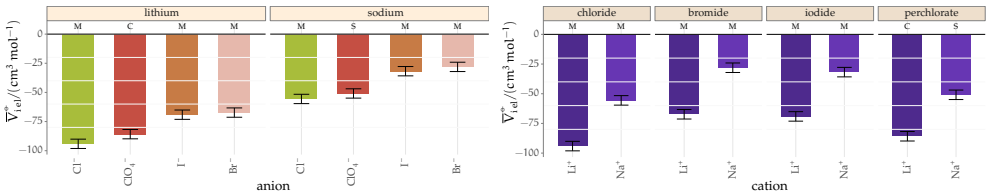

Figure 52: Standard molar electrostrictive volume $\overline{V}^{\ominus}_{i\,el}$ of alkali metal salts in ACE grouped by cation (left) and by anion (right).

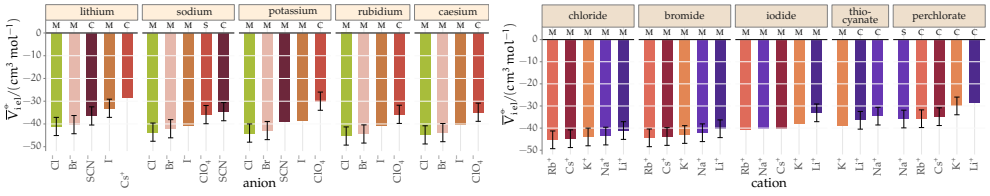

Figure 53: Standard molar electrostrictive volume $\overline{V}^{\ominus}_{i\,el}$ of alkali metal salts in MeCN grouped by cation (left) and by anion (right).

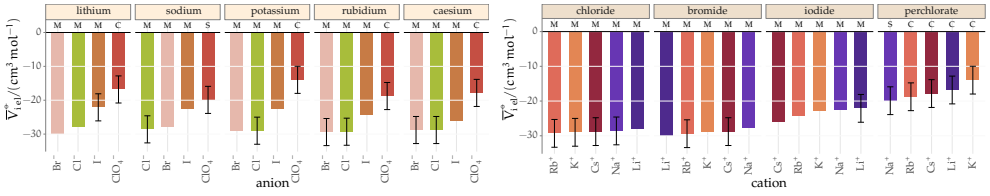

Figure 54: Standard molar electrostrictive volume $\overline{V}^{\ominus}_{i\,el}$ of alkali metal salts in DMF grouped by cation (left) and by anion (right).

A.4 NORMALISED ELECTROSTRICTIVE VOLUMES

The labels above the bars in each plot indicate the method of estimation of the intrinsic molar volume used in the calculations. M: extrapolation from molten salts, from Pedersen et al. (1984); S: from 'soluble salts' (Marcus, 2010); C: crystal volume, as in Eq. [5].

A.4.1 Protic solvents

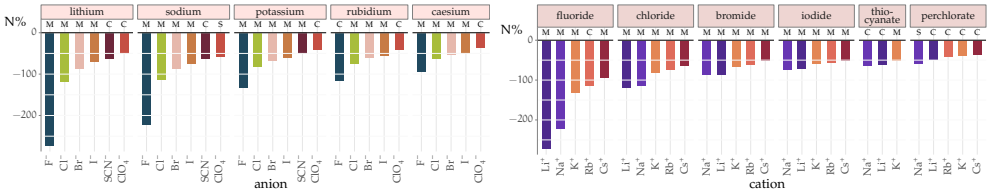

Figure 55: Normalised standard molar electrostrictive volume N% of alkali metal salts in MeOH grouped by cation (left) and by anion (right).

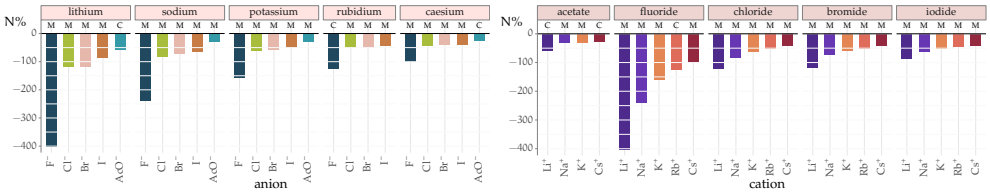

Figure 56: Normalised standard molar electrostrictive volume N% of alkali metal salts in EtOH grouped by cation (left) and by anion (right).

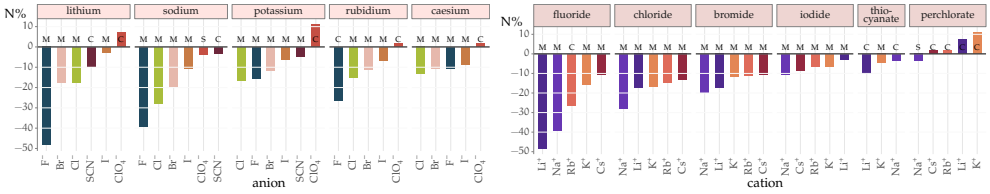

Figure 57: Normalised standard molar electrostrictive volume N% of alkali metal salts in FA grouped by cation (left) and by anion (right).

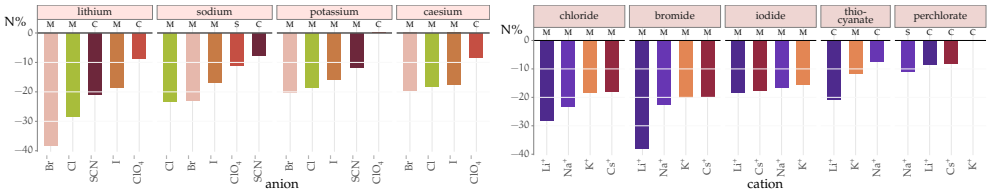

Figure 58: Normalised standard molar electrostrictive volume N% of alkali metal salts in NMF grouped by cation (left) and by anion (right).

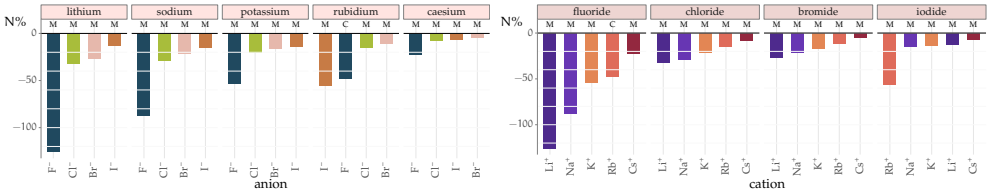

Figure 59: Normalised standard molar electrostrictive volume N% of alkali metal salts in EG grouped by cation (left) and by anion (right).

A.4.2 Aprotic solvents

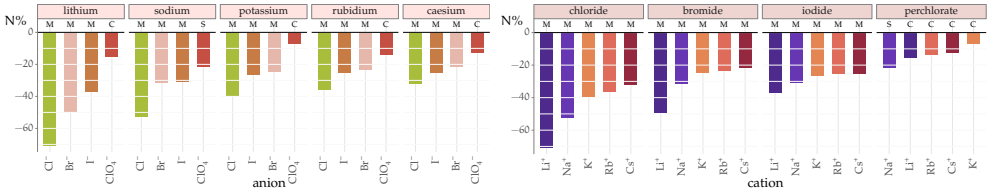

Figure 60: Normalised standard molar electrostrictive volume N% of alkali metal salts in PC grouped by cation (left) and by anion (right).

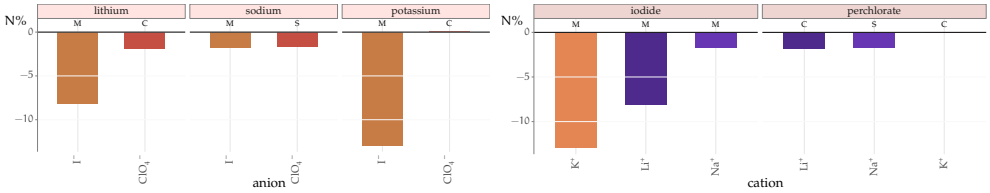

Figure 61: Normalised standard molar electrostrictive volume N% of alkali metal salts in EC grouped by cation (left) and by anion (right).

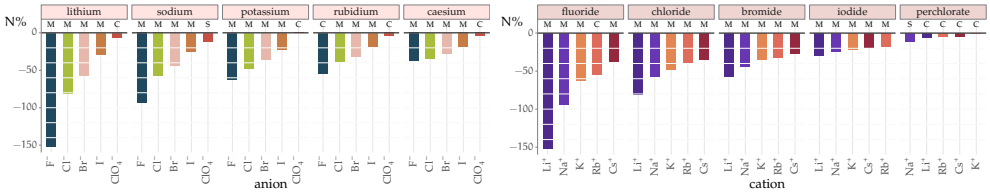

Figure 62: Normalised standard molar electrostrictive volume N% of alkali metal salts in DMSO grouped by cation (left) and by anion (right).

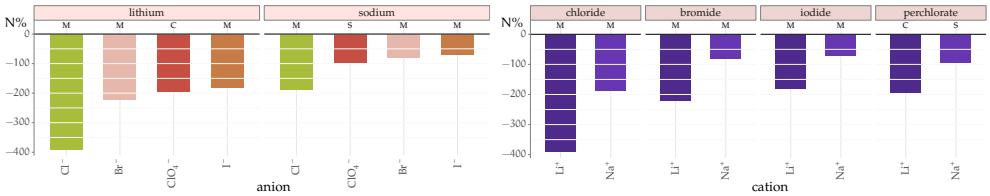

Figure 63: Normalised standard molar electrostrictive volume N% of alkali metal salts in ACE grouped by cation (left) and by anion (right).

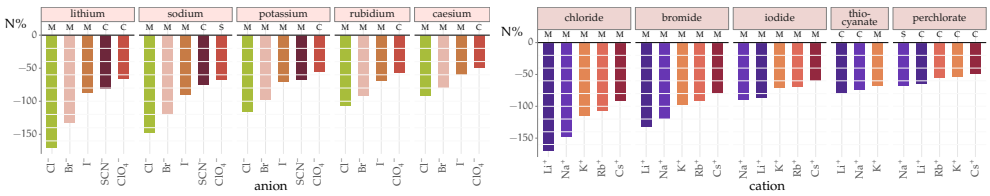

Figure 64: Normalised standard molar electrostrictive volume N% of alkali metal salts in MeCN grouped by cation (left) and by anion (right).

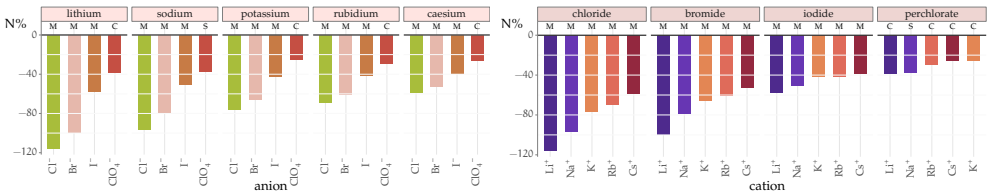

Figure 65: Normalised standard molar electrostrictive volume N% of alkali metal salts in DMF grouped by cation (left) and by anion (right).

B VOLCANO PLOTS

B.1 AQUEOUS IONIC RADII VERSUS AB INITIO RADII

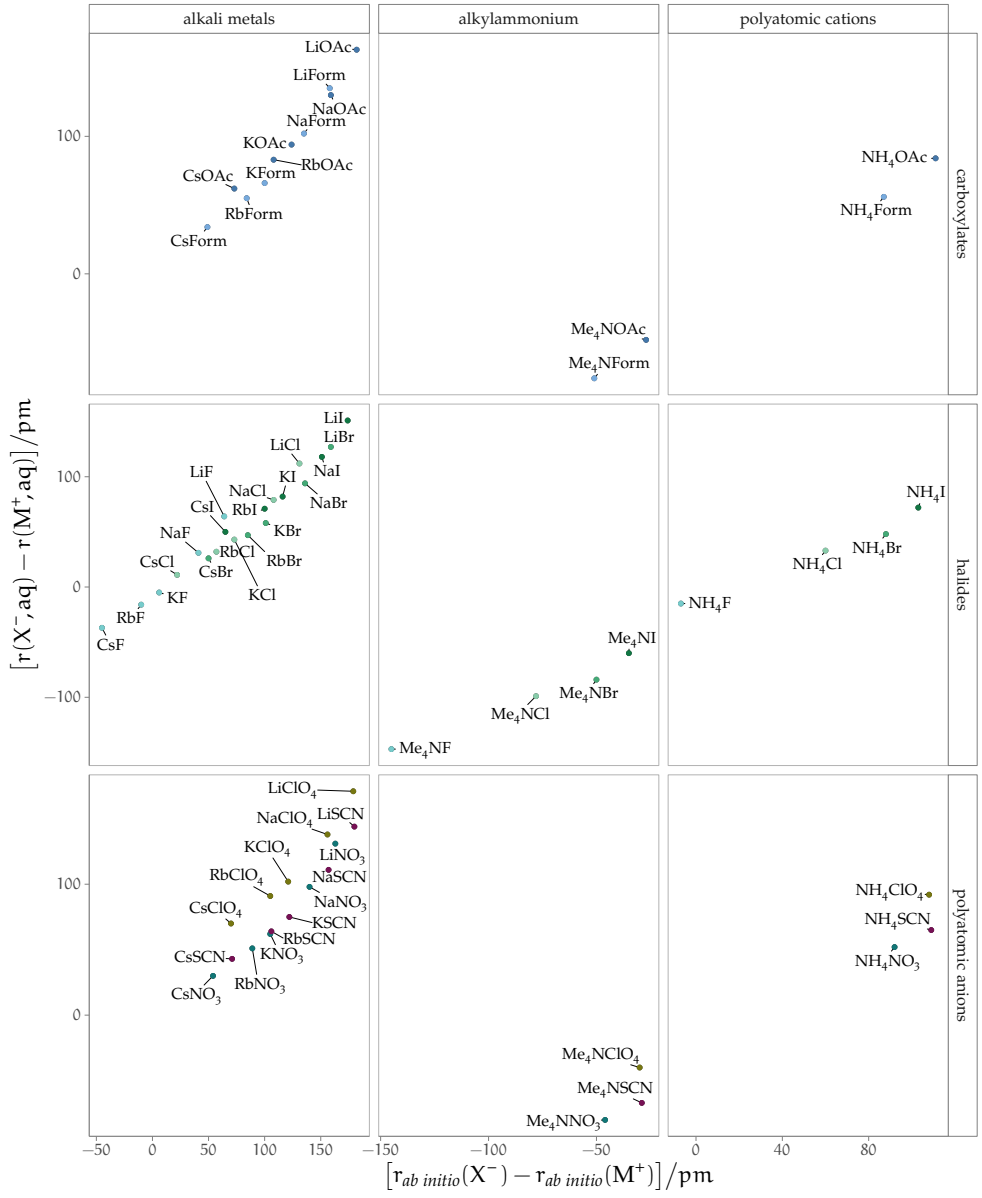

Figure 66: Radii employed (solvated radii in water r) versus the *ab initio* Gaussian radii of ions.

B.2 LINES HIGHLIGHTING CATION TRENDS

B.2.1 Monoatomic ions

Classic volcano plots — enthalpies

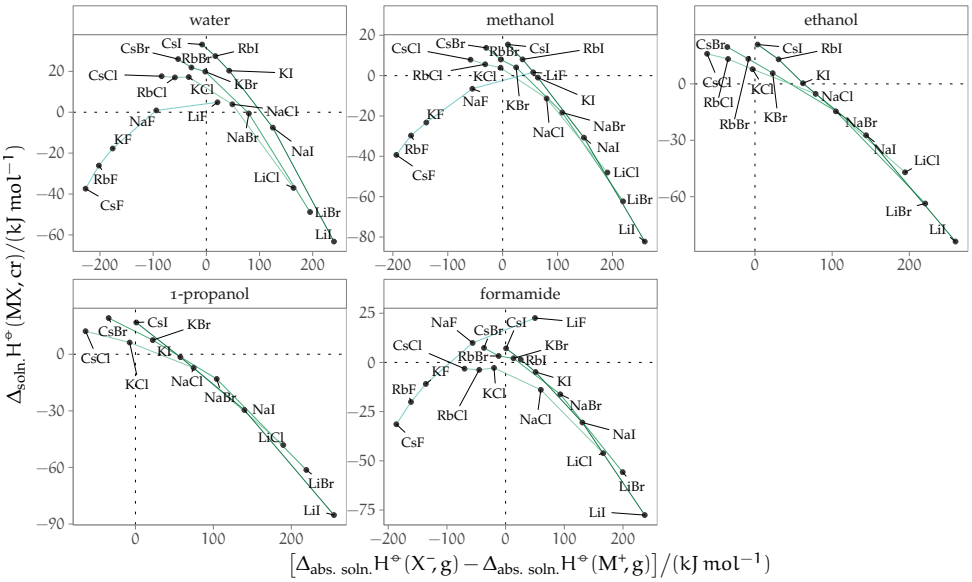

Figure 67: Enthalpy of dissolution of salts $\Delta_{soln.}H^{\ominus}$ versus the difference in the absolute enthalpies of solvation of the constituent ions $\Delta_{abs.\ soln.}H^{\ominus}$ for a range of protic solvents. Coloured lines are drawn to help identify the cation trends.

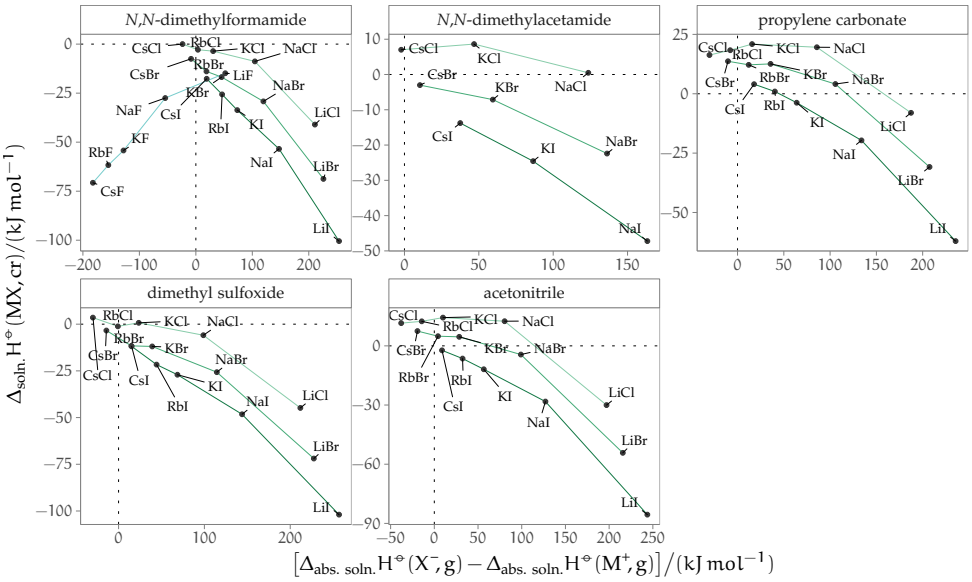

Figure 68: Enthalpy of dissolution of salts $\Delta_{soln.}H^{\ominus}$ versus the difference in the absolute enthalpies of solvation of the constituent ions $\Delta_{abs.\ soln.}H^{\ominus}$ for a range of aprotic solvents. Coloured lines are drawn to help identify the cation trends.

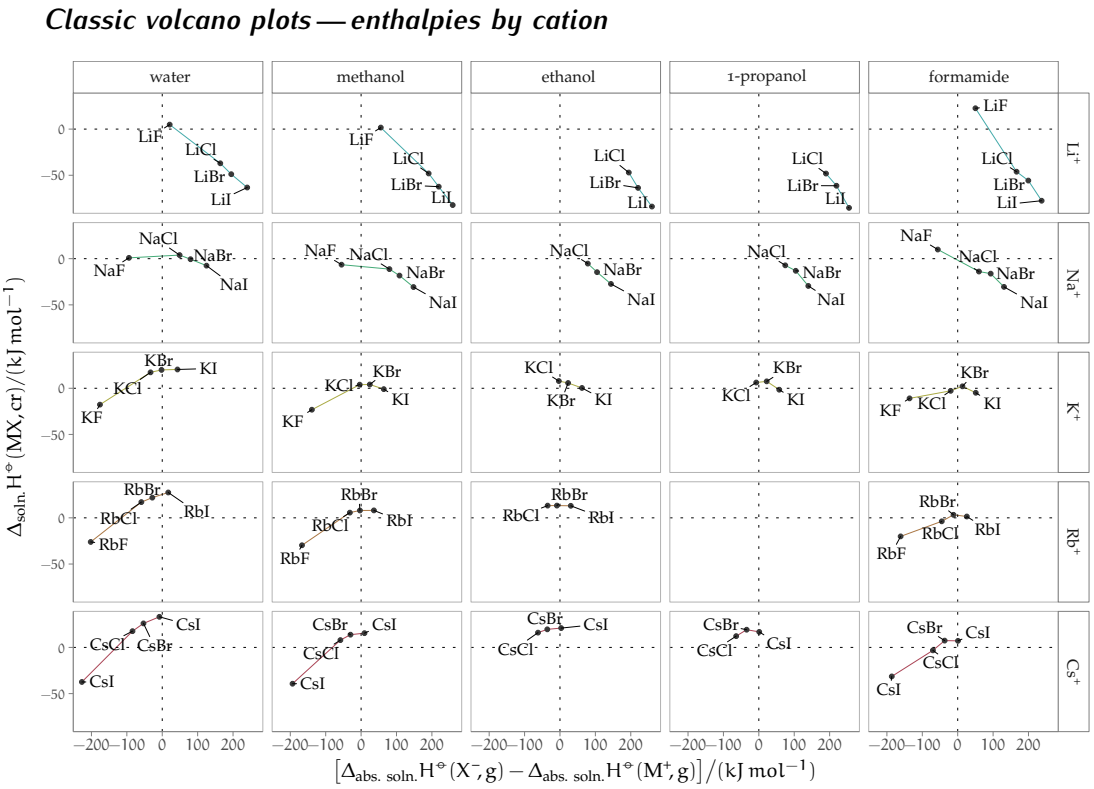

Figure 69: As Fig. 67, but the single cation trends are here shown separately.

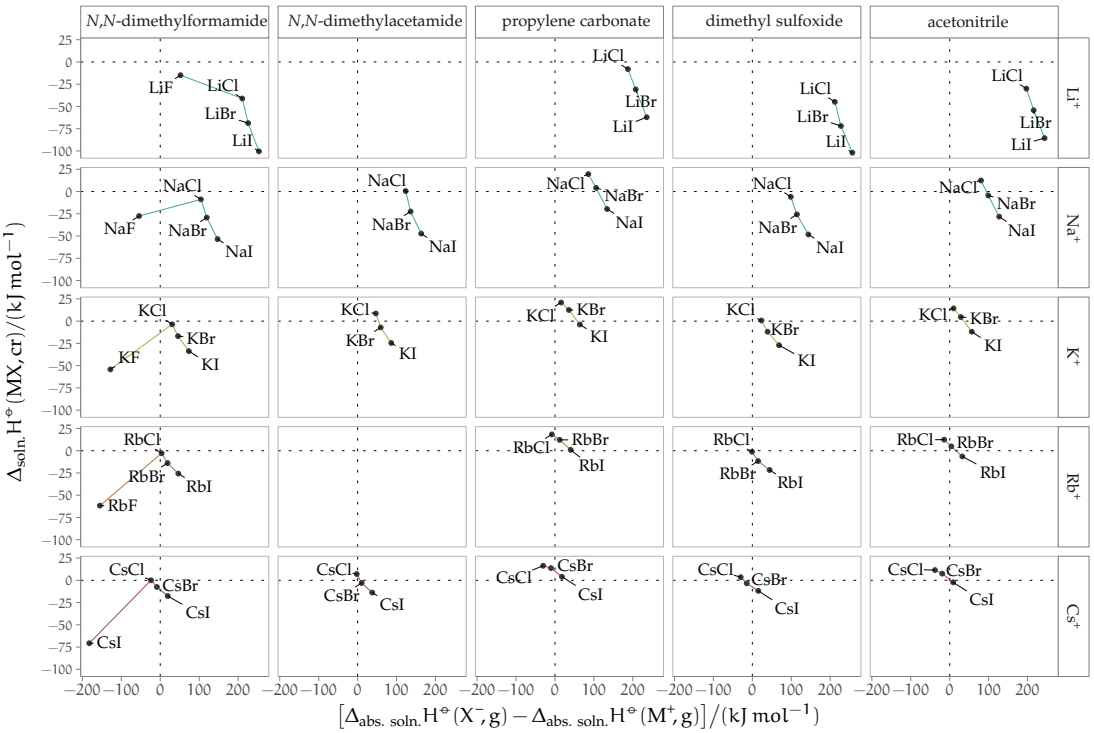

Figure 70: As Fig. 68, but the single cation trends are here shown separately.

Volcano plots versus radii — osmotic coefficients

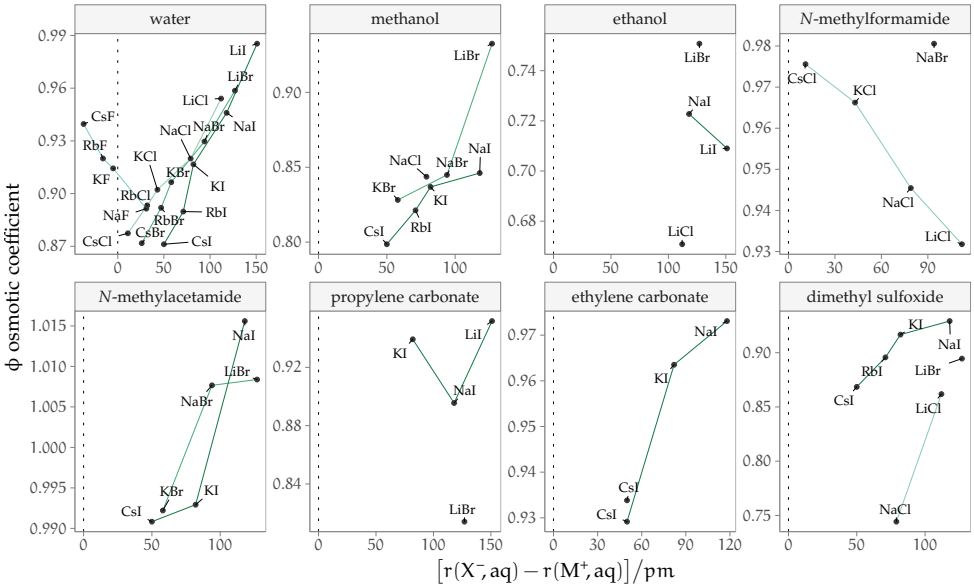

Figure 71: Osmotic coefficients ϕ of salts versus the difference of the radii r of the constituent ions. The electrolyte concentration is $0.4\,\mathrm{mol\,kg^{-1}}$, except for: MeOH ($0.07\,\mathrm{mol\,kg^{-1}}$); PC ($0.18\,\mathrm{mol\,kg^{-1}}$); EC and NMA, ($0.09\,\mathrm{mol\,kg^{-1}}$); DMSO and NMF ($0.05\,\mathrm{mol\,kg^{-1}}$). Coloured lines are drawn to help identify the cation trends.

B.2.2 Polyatomic anions

Volcano plots versus radii — activity and osmotic coefficients

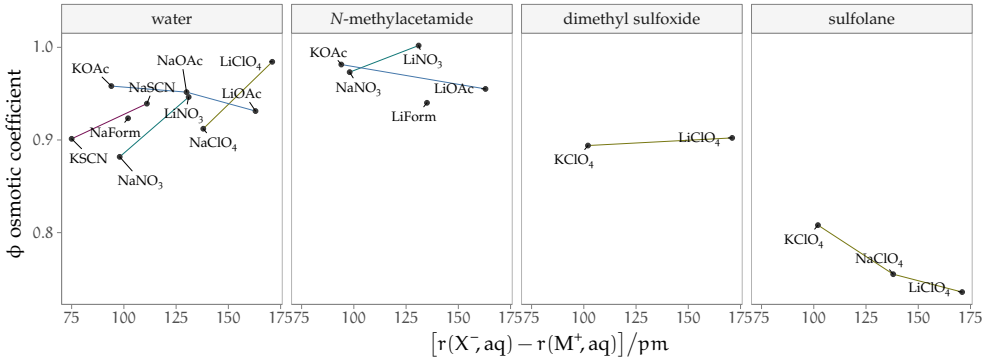

Figure 72: Salts containing polyatomic anions. Electrolyte osmotic coefficients ϕ versus the difference of the radii r of the constituent ions. The electrolyte concentration is 0.4 $mol\,kg^{-1}$ for water; 0.09 $mol\,kg^{-1}$ for NMA; 0.05 $mol\,kg^{-1}$ for SULF and DMSO. Coloured lines are drawn to help identify the cation trends.

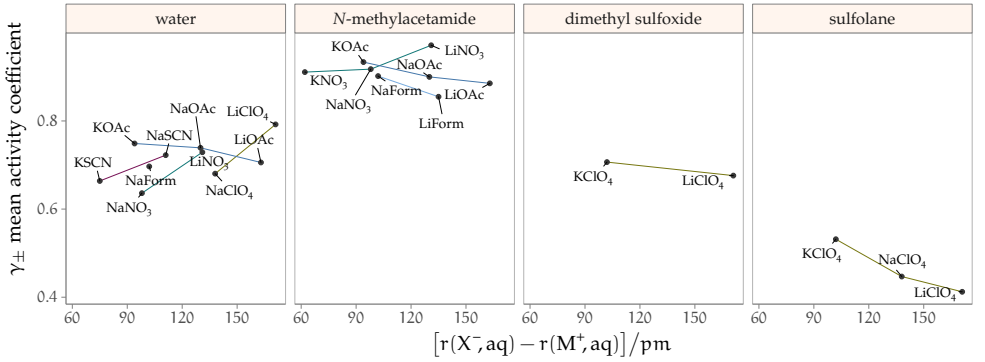

Figure 73: Salts containing polyatomic anions. Electrolyte activity coefficient γ versus the difference of the radii r of the constituent ions. The electrolyte concentration is 0.4 $mol\,kg^{-1}$ for water; 0.09 $mol\,kg^{-1}$ for NMA; 0.05 $mol\,kg^{-1}$ for SULF and DMSO. Coloured lines are drawn to help identify the cation trends.

B.3 LINES HIGHLIGHTING ANION TRENDS

B.3.1 Monoatomic ions

Classic Volcano plots — enthalpies

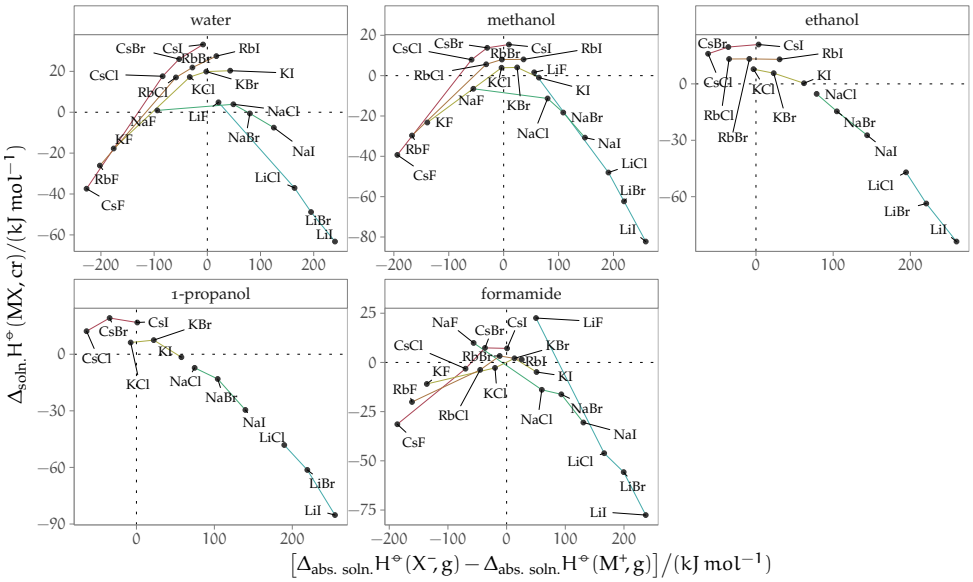

Figure 74: Enthalpy of dissolution of salts $\Delta_{soln.}H^{\ominus}$ versus the difference in the absolute enthalpies of solvation of the constituent ions $\Delta_{abs.\ soln.}H^{\ominus}$ for a range of protic solvents. Coloured lines are drawn to help identify the anion trends.

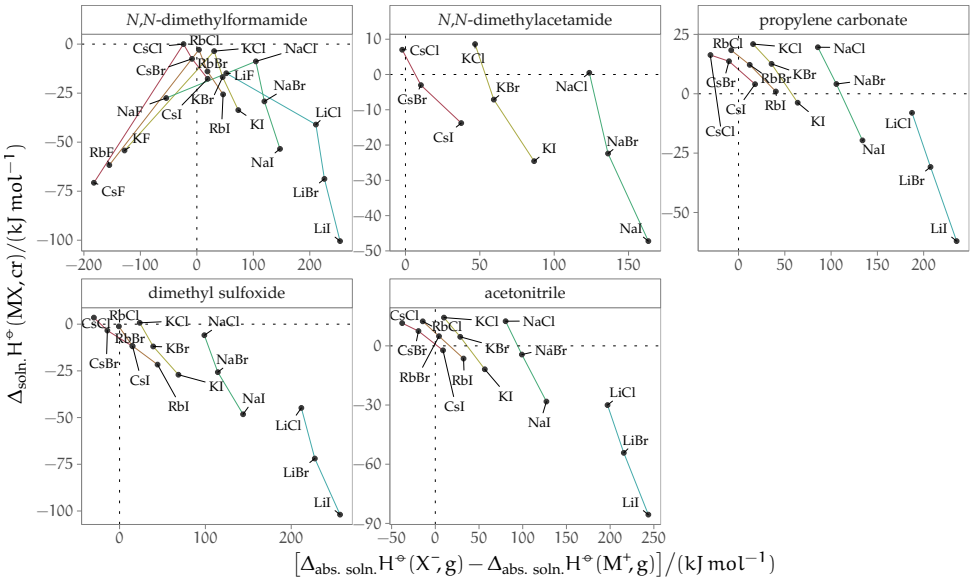

Figure 75: Enthalpy of dissolution of salts $\Delta_{soln.}H^{\ominus}$ versus the difference in the absolute enthalpies of solvation of the constituent ions $\Delta_{abs.\ soln.}H^{\ominus}$ for a range of aprotic solvents. Coloured lines are drawn to help identify the anion trends.

Classic Volcano plots — Gibbs free energies

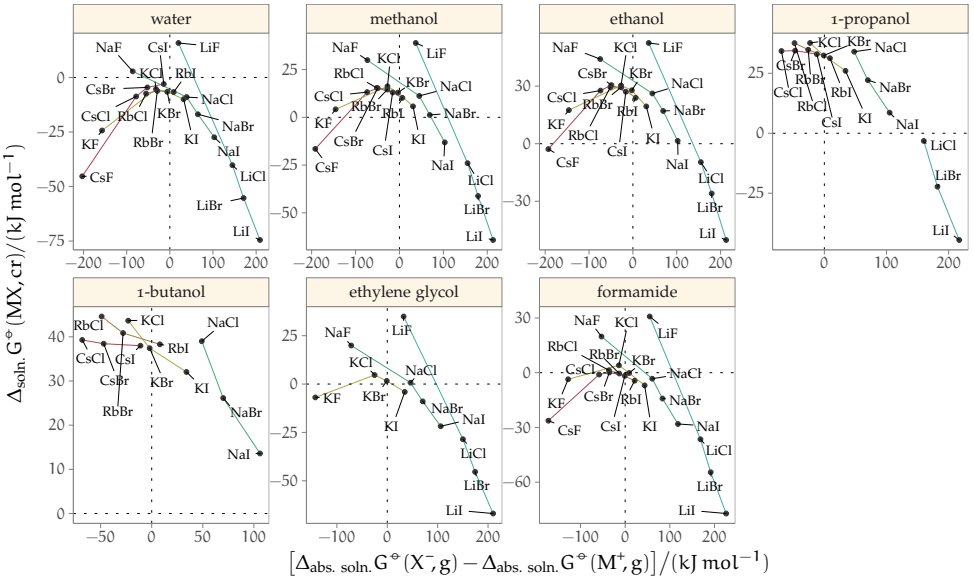

Figure 76: Gibbs free energy of dissolution $\Delta_{soln.}G^{\ominus}$ of salts versus the difference in the absolute free energies of solvation $\Delta_{abs.\ soln.}G^{\ominus}$ of the constituent ions for a range of protic solvents. Coloured lines are drawn to help identify the anion trends.

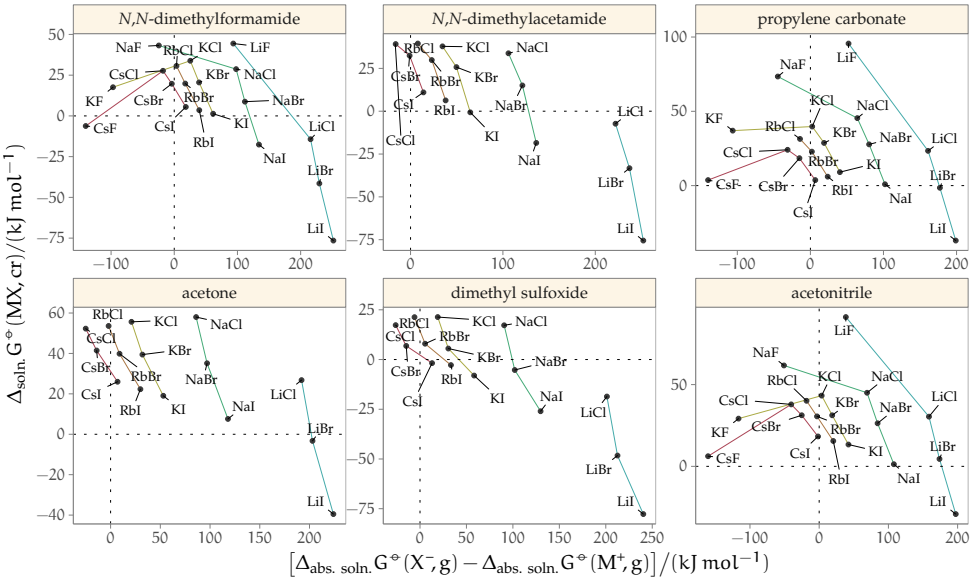

Figure 77: Gibbs free energy of dissolution $\Delta_{soln.}G^{\ominus}$ of salts versus the difference in the absolute free energies of solvation $\Delta_{abs.\ soln.}G^{\ominus}$ of the constituent ions for a range of aprotic solvents. Coloured lines are drawn to help identify the anion trends.

Volcano plots versus radii — enthalpies

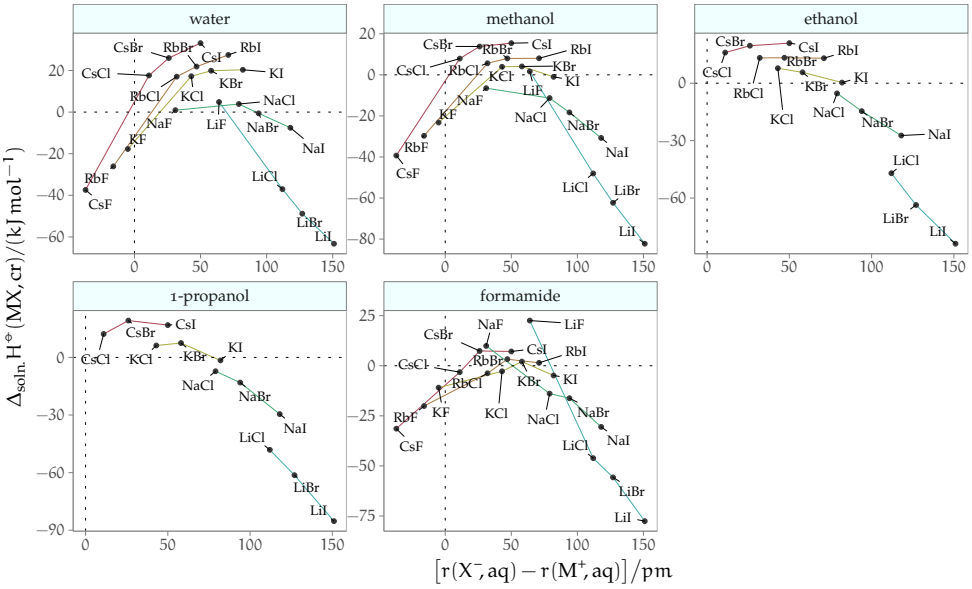

Figure 78: Enthalpy of dissolution of salts $\Delta_{soln.}H^{\circ}$ versus the difference of the radii r of the constituent ions for a range of protic solvents. Coloured lines are drawn to help identify the anion trends.

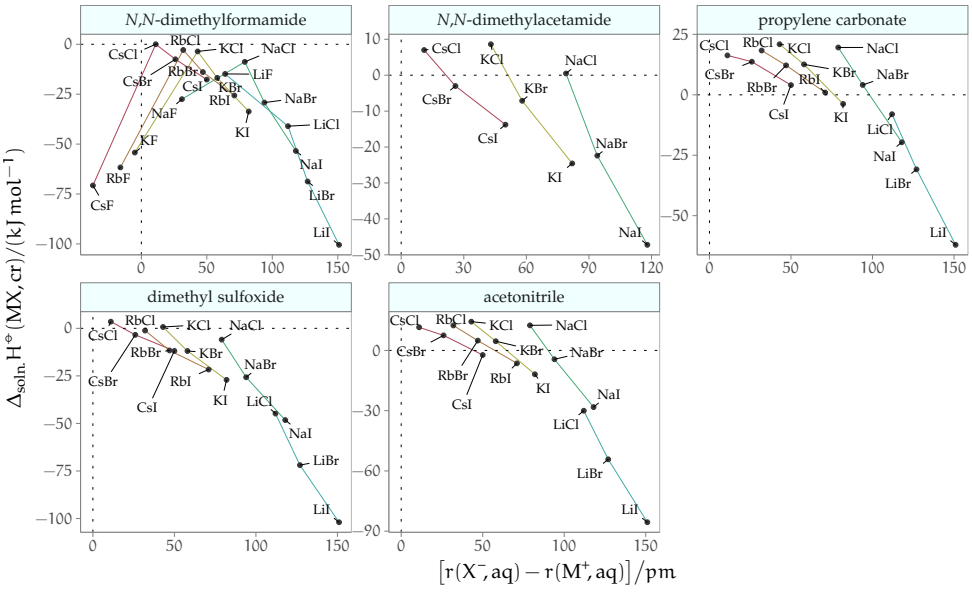

Figure 79: Enthalpy of dissolution of salts $\Delta_{soln.}H^{\circ}$ versus the difference of the radii r of the constituent ions for a range of aprotic solvents. Coloured lines are drawn to help identify the anion trends.

Volcano plots versus radii — Gibbs free energies

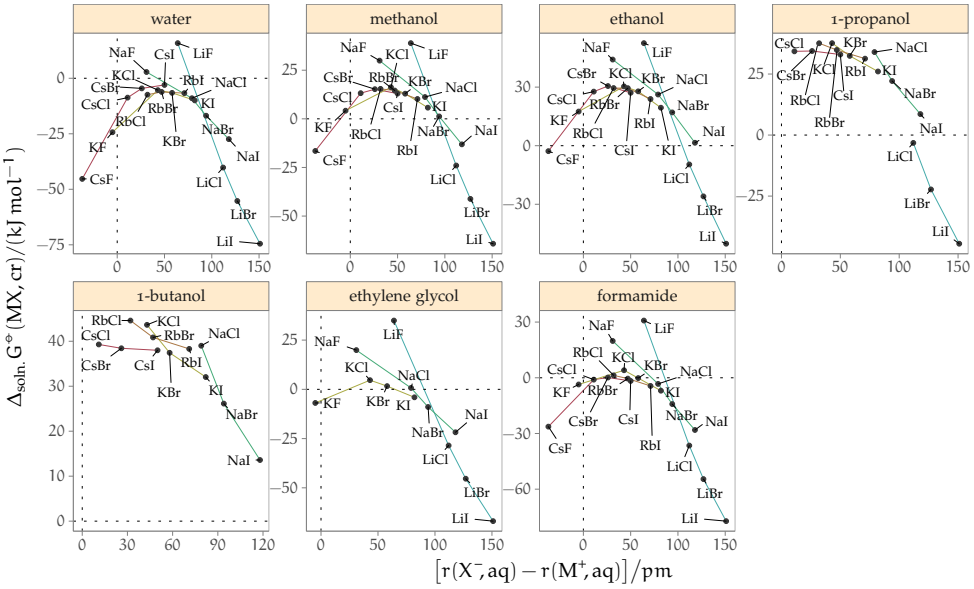

Figure 80: Gibbs free energy of dissolution $\Delta_{soln.}G^{\ominus}$ of salts versus the difference of the radii r of the constituent ions for a range of protic solvents. Coloured lines are drawn to help identify the anion trends.

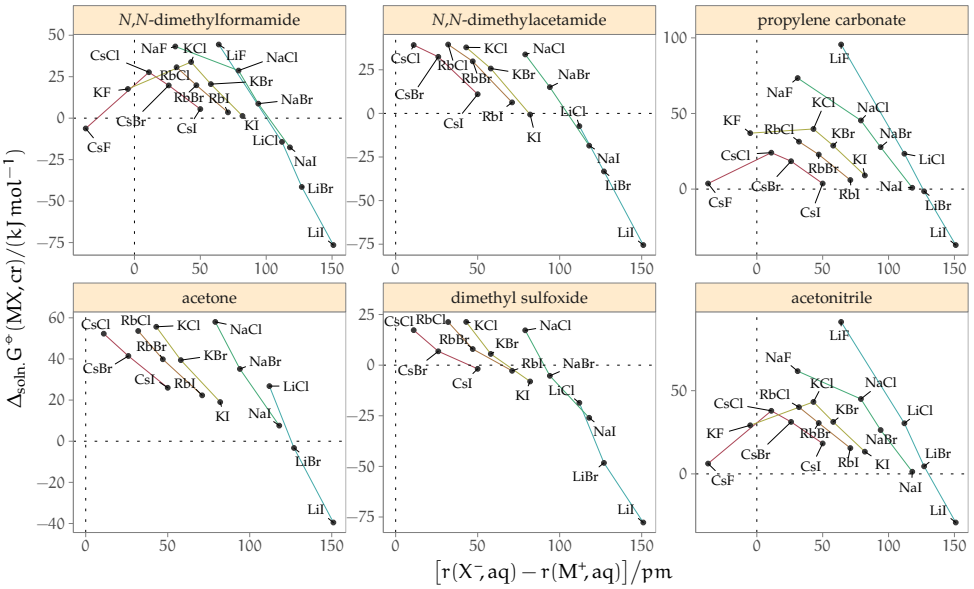

Figure 81: Gibbs free energy of dissolution $\Delta_{soln.}G^{\ominus}$ of salts versus the difference of the radii r of the constituent ions for a range of aprotic solvents. Coloured lines are drawn to help identify the anion trends.

Volcano plots versus radii — osmotic and activity coefficients

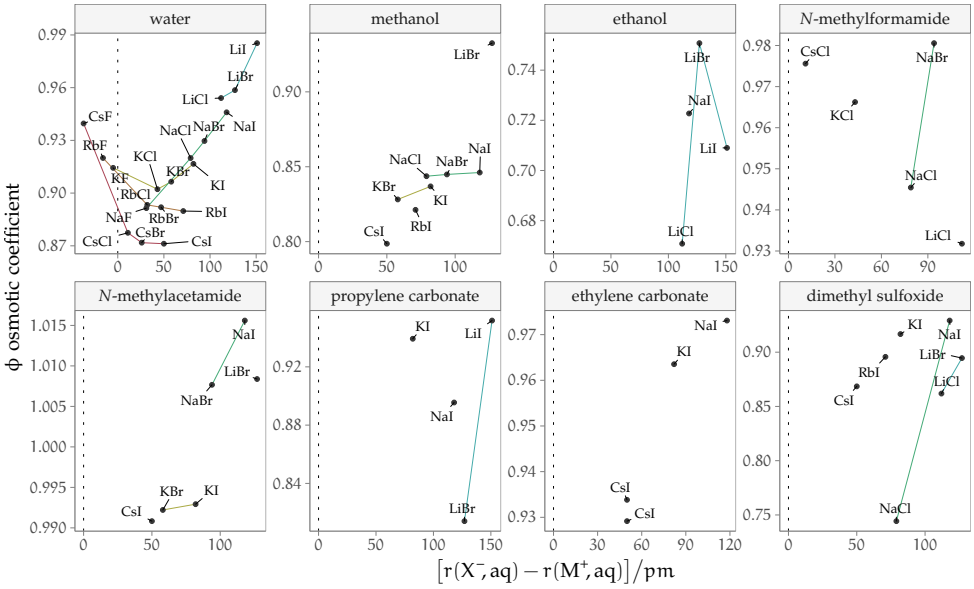

Figure 82: Osmotic coefficients ϕ of salts versus the difference of the radii r of the constituent ions. The electrolyte concentration is $0.4\,\mathrm{mol\,kg^{-1}}$, except for: MeOH ($0.07\,\mathrm{mol\,kg^{-1}}$); PC ($0.18\,\mathrm{mol\,kg^{-1}}$); EC and NMA, ($0.09\,\mathrm{mol\,kg^{-1}}$); DMSO and NMF ($0.05\,\mathrm{mol\,kg^{-1}}$). Coloured lines are drawn to help identify the anion trends.

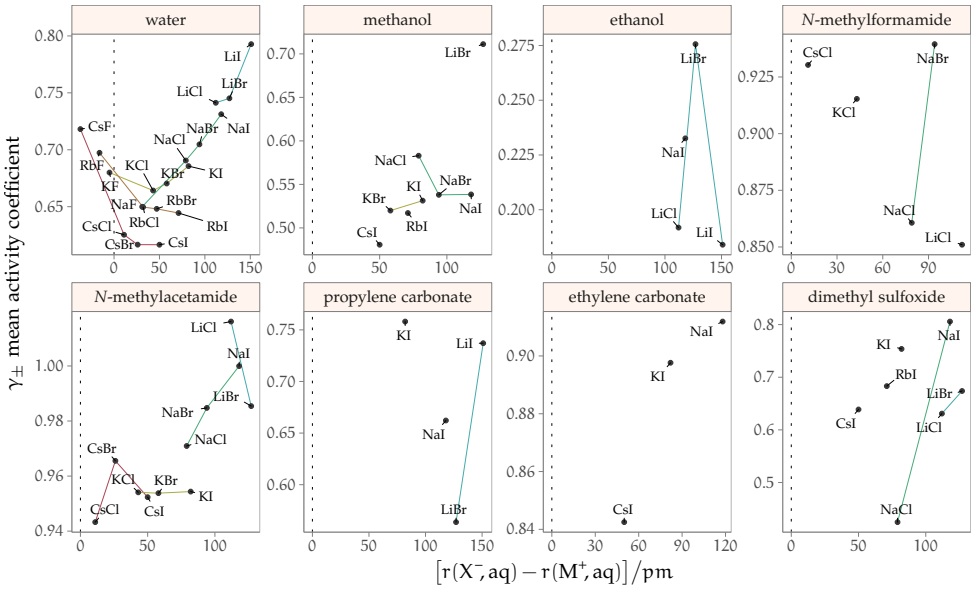

Figure 83: Activity coefficients γ of salts versus the difference of the radii r of the constituent ions. The electrolyte concentration is $0.4\,\mathrm{mol\,kg^{-1}}$, except for: MeOH ($0.07\,\mathrm{mol\,kg^{-1}}$); PC ($0.18\,\mathrm{mol\,kg^{-1}}$); EC and NMA, ($0.09\,\mathrm{mol\,kg^{-1}}$); DMSO and NMF ($0.05\,\mathrm{mol\,kg^{-1}}$). Coloured lines are drawn to help identify the anion trends.

B.4 SOLUBILITIES OF ELECTROLYTES IN SOLVENTS

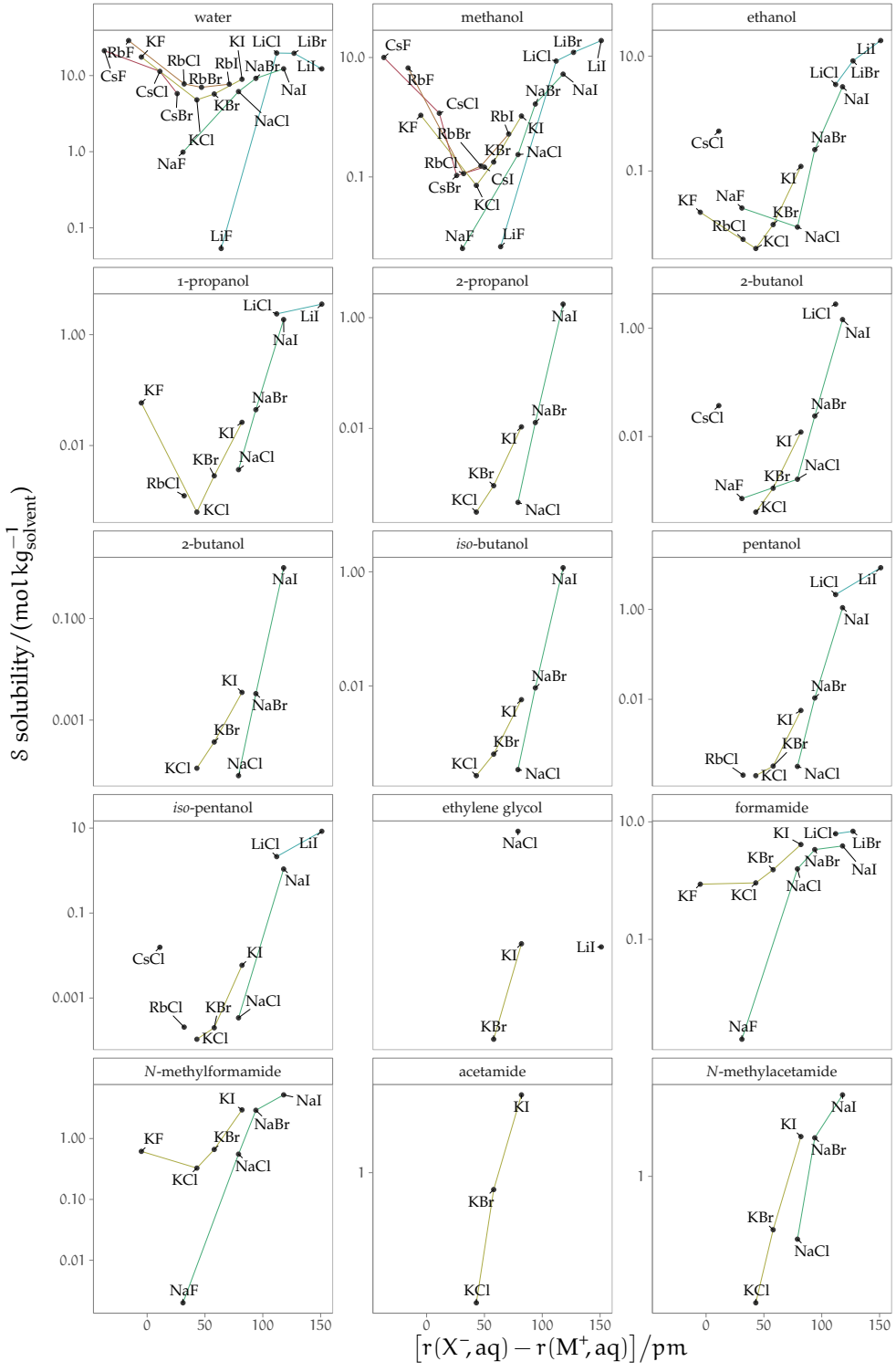

Figure 84: Electrolyte solubility S versus the difference of the radii r of the constituent ions in protic solvents. The y-axis is displayed in logarithmic scale. Coloured lines are drawn to help identify the anion trends.

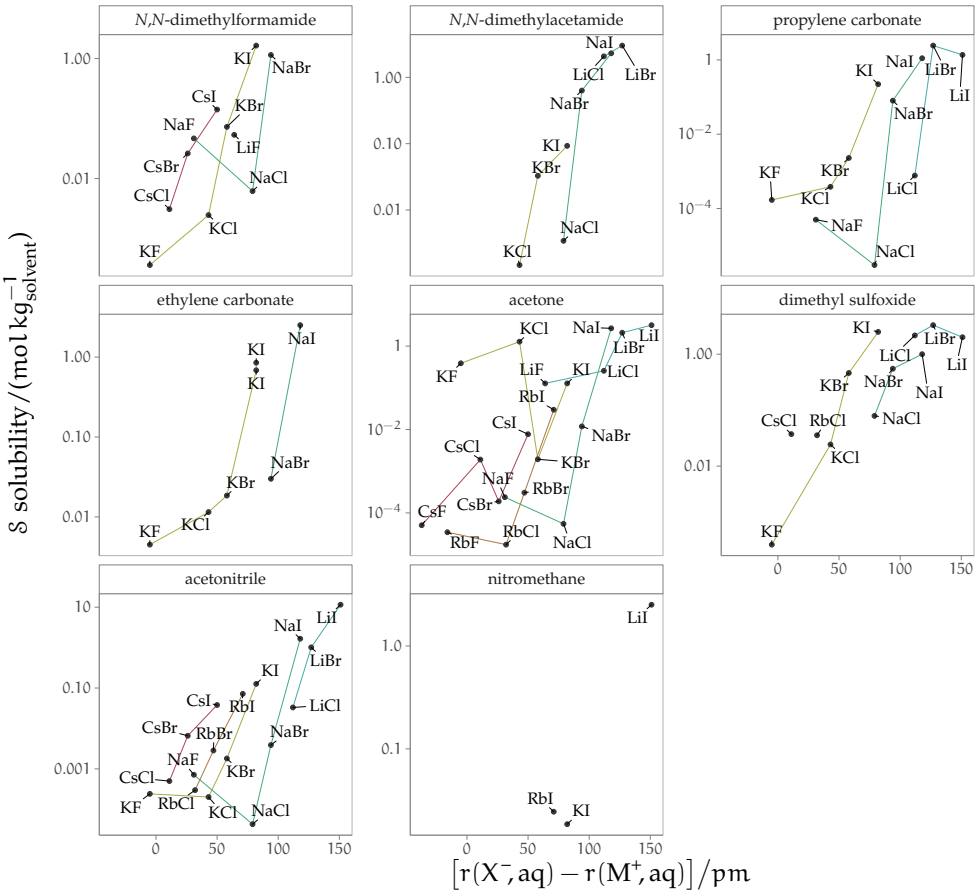

Figure 85: Electrolyte solubility S versus the difference of the radii r of the constituent ions in aprotic solvents. The y-axis is displayed in logarithmic scale. Coloured lines are drawn to help identify the anion trends.

C OSMOTIC AND ACTIVITY COEFFICIENTS

C.1 FITTING MODELS AND COEFFICIENTS

The Pitzer equations (Pitzer, 1973; Pitzer et al., 1973) satisfactorily represent the thermodynamic properties of electrolyte solutions up to concentrations of several molal, thus performing better than other models of comparable complexity and being widely used in chemical engineering. The most important feature introduced in this model is the ionic strength dependence of the second virial coefficient B, implying that the effect of short-range interactions between ion pairs is dependent on the ionic strength I. The Pitzer expressions for the osmotic coefficient ϕ and the activity coefficient γ of a 1 : 1 electrolyte solution are:

$$\phi - 1 = f^{\phi} + mB^{\phi} + m^2 C^{\phi} \quad [11]$$

$$\ln \gamma = f^{\gamma} + mB^{\gamma} + m^2 C^{\gamma} \quad [12]$$

where:

$$f^{\phi} = -A^{\Phi} \frac{\sqrt{I}}{1 + b\sqrt{I}}$$

$$B^{\phi} = \beta^{(0)} + \beta^{(1)} \exp(-\alpha\sqrt{I}) \quad [13]$$

$$f^{\gamma} = -A^{\Phi} \left[\frac{\sqrt{I}}{1 + b\sqrt{I}} + \frac{2}{b} \ln\left(1 + b\sqrt{I}\right) \right]$$

$$B^{\gamma} = 2\beta^{(0)} + \frac{2\beta^{(1)}}{\alpha^2 I} \left[1 - \exp(-\alpha\sqrt{I}) \left(1 + \alpha\sqrt{I} - \frac{1}{2}\alpha^2 I\right) \right] \quad [14]$$

$$C^{\gamma} = \frac{3}{2} C^{\phi} \quad [15]$$

m is the molal concentration in $\mathrm{mol\,kg^{-1}}$;
A^{Φ} is the Debye-Hückel coefficient for the osmotic function:

$$A^{\Phi} = \frac{\sqrt{2\pi N_A \rho_s^*}}{3} \sqrt{\left(\frac{e^2}{4\pi\epsilon_0 \epsilon_R kT} \right)^3}$$

where N_A is the Avogadro constant; ρ_s^* is the density of the pure solvent in $\mathrm{kg\,m^{-3}}$; e is the elementary charge; ϵ_0 is the vacuum permittivity; ϵ_R is the relative permittivity of the solvent; k is the Boltzmann constant and T is the absolute temperature in K.
I is the ionic strength:

$$I = \frac{1}{2} \sum_i m_i {z_i}^2$$

where m_i is the molal concentration in $\mathrm{mol\,kg^{-1}}$, z_i the charge number of the ion i. Thus, Eqs. [11] and [12] contain five parameters that need to be fitted to experimental data: b, α, $\beta^{(0)}$, $\beta^{(1)}$ and C^{ϕ}. Overall, these parameters have *no clear direct physical interpretation*. The parameter b should remain the same for all solutes for the mixed electrolytes expressions to be simple: for aqueous electrolytes, Pitzer (1973) selected the value of $b = 1.2$. In addition, also the same value of $\alpha = 2.0$ was found to be satisfactory for all the values fitted in Pitzer et al. (1973). For each electrolyte,

the second virial coefficient is defined by the parameters $\beta^{(0)}$ and $\beta^{(1)}$; Pitzer et al. (1973) connect $\beta^{(0)}$, which is primarily influenced by the short-range interactions between ions of opposite charge, to the 'structure-making/breaking' properties of the cation and anion. In fact, the $\beta^{(0)}$ coefficients of the electrolytes show a trend where, for a common cation or anion, the $\beta^{(0)}$ is higher the more dissimilar the counterion is in terms of structure making/breaking abilities, and viceversa. This is in concordance with the LMWA discussed in the main text, as a low $\beta^{(0)}$ indicates the presence of attractive interactions between couples of oppositely charged ions of the same 'water affinity'. Comparisons can be made only across values of $\beta^{(0)}$ that have been calculated by employing the same model (in terms of number of parameters) and by adopting the same values for the fixed parameters b and α (or α_1 and α_2 for the models with additional parameters, see below). This is not our case, as the fixed parameters had to be varied in order to fit different experimental data in the same solvent, therefore no further comments are made here regarding this correlation of $\beta^{(0)}$ to the kosmotropic/chaotropic abilities in non-aqueous solvents. C^{ϕ} defines the third virial coefficient and is usually very small according to Pitzer et al. (1973). The coefficients calculated by Pitzer et al. (1973) are listed in Table 35, and the above equations can be used to reproduce the curves for the osmotic and activity coefficients of aqueous electrolytes.

In order to fit 'unusual' behaviour, further α and β terms of the same form can be added to the second virial coefficient expressions B^{ϕ} (Eq. [13]) and B^{γ} (Eq. [14]). This has been widely performed in works where the Pitzer model is fitted to data for non-aqueous electrolytes (Barthel et al., 1986; Barthel, Neueder, Poepke et al., 1998), where the number of parameters is raised to seven: b, α_1, α_2, $\beta^{(0)}$, $\beta^{(1)}$, $\beta^{(2)}$ and C^{ϕ}. For these parameters, Eqs. [13] and [14] are replaced by:

$$B^{\phi} = \beta^{(0)} + \beta^{(1)} \exp\left(-\alpha_1 \sqrt{I}\right) + \beta^{(2)} \exp\left(-\alpha_2 \sqrt{I}\right) \quad [16]$$

$$B^{\gamma} = 2\beta^{(0)} + \xi^{(1)} + \xi^{(2)} \quad [17]$$

where:

$$\xi^{(i)} = \frac{2\beta^{(i)}}{\alpha_i^2 I}\left[1 - \left(1 + \alpha_i\sqrt{I} - \frac{1}{2}\alpha_i^2 I\right)\exp\left(-\alpha_i\sqrt{I}\right)\right]$$

The coefficient values tabulated in Table 32 refer to this model.

The Archer extension of the Pitzer model in seven parameters has also been used (Nasirzadeh, Papaiconomou et al., 2004), and introduces a ionic strength dependence for the third virial coefficient C^{ϕ}, expressing it in terms of the parameters $C^{(0)}$, $C^{(1)}$ and α_3, and consequently also the expression for C^{γ} (Eq. [15]) changes:

$$C^{\phi} = C^{(0)} + C^{(1)} \exp\left(-\alpha_3 \sqrt{I}\right) \quad [18]$$

$$C^{\gamma} = \frac{1}{2}\left(3C^{(0)} + A_3\right) \quad [19]$$

where:

$$A_3 = 4C^{(1)} \frac{6 - (6 + 6\alpha_3\sqrt{I} + 3\alpha_3^2 I + \alpha_3^3\sqrt{I}^3 - \alpha_3^4(I^2/2))\exp -\alpha_3\sqrt{I}}{\alpha_3^4(I^2)}$$

nine parameters need therefore to be adjusted in this model. The coefficients in Table 33 refer to these equations.

Where no model could be fitted, a polynomial function has been used to interpolate the data:

$$y = a_{poly} m^2 + b_{poly} m + c_{poly} \quad [20]$$

where y is either ϕ or γ. The polynomial fitting coefficients are listed in Table 34.

Table 32: The Pitzer model fitting coefficients b, α_1, α_2, $\beta^{(0)}$, $\beta^{(1)}$, $\beta^{(2)}$ and C^{Φ} in non-aqueous solvents. The osmotic and activity coefficients curves can be reproduced in the interval comprised between m^{min} and m^{max} (in $mol\,kg^{-1}$) by employing eq. [11] and eq. [12] with B^{Φ} and B^{γ} defined by eq. [16] and eq. [17].

solvent	electrolyte	ref.	T/K	fit*	m^{min}	m^{max}	A^{Φ}	b	α_1	α_2	$\beta^{(0)}$	$\beta^{(1)}$	$\beta^{(2)}$	C^{Φ}	$\sigma^{\dagger}$
2PrOH	Bu_4NBr	*a*	298.15	Pf	0.030	1.9	2.815	3.2	2	10	0.153 94	−0.442 99	−18.164 84	−0.002 80	0.006
2PrOH	LiCl	*b*	298.15	Pf	0.17	1.5	2.815	3.2	2	10	−0.075 15	0.922 83	−32.810 20	0.138 53	0.004
2PrOH	$LiClO_4$	*c*	298.16	Pf	0.050	1.5	2.815	3.2	2	10	−0.024 70	0.752 12	−14.130 59	0.134 31	0.006
2PrOH	$LiNO_3$	*b*	298.15	Pf	0.20	1.9	2.815	3.2	2	10	0.011 52	0.424 96	−23.198 55	0.042 43	0.004
2PrOH	NaI	*d*	298.15	Pf	0.060	1.5	2.816	3.2	2	12	0.042 97	0.795 35	−29.904 44	0.112 82	0.009
2PrOH	$Pent_4NBr$	*e*	298.15	Pf	0.030	2.6	2.816	3.2	2	12	0.079 67	0.906 01	41.808 78	0.036 75	0.02
2PrOH	Pr_4NBr	*a*	298.15	Pf	0.040	1.3	2.815	3.2	2	15	0.361 67	−1.202 60	−54.480 17	−0.115 43	0.003
ACE	Bu_4NBr	*f*	298.15	Pf	0.010	0.80	2.558	3.2	2	15	0.409 24	−1.502 68	−34.894 56	−0.244 77	0.004
ACE	Bu_4NClO_4	*f*	298.15	Pf	0.020	3.6	2.558	3.2	2	10	0.067 23	0.287 94	2.649 07	−0.007 55	0.007
ACE	LiBr	*f*	298.15	Pf	0.030	0.80	2.558	3.2	2	13	0.345 51	−0.956 79	−50.467 87	−0.192 66	0.004
ACE	$LiClO_4$	*g*	298.16	Pf	0.010	5.9	2.558	3.2	2	20	0.061 84	0.628 48	−63.702 65	0.037 93	0.008
DMA	LiBr	*h*	298.16	Pγ	0.024	0.095	1.313	3.2	2	9	0.186 66	0.102 06	−0.092 09	3.602 14	0.007
DMC	$LiClO_4$	*g*	298.16	Pf	0.030	1.8	51.646	95	2	20	−0.087 34	−1.636 71	4.119 00	0.081 78	0.003
DME	$LiClO_4$	*g*	298.16	Pf	0.010	0.40	13.545	20	2	20	−2.425 56	4.029 13	−1.643 72	2.696 28	0.007
DMF	LiCl	*i*	298.15	Pγ	0.0010	2.0	1.165	3.2	2	9	−0.276 27	−0.221 25	0.360 39	0.131 40	0.07
DMSO	CsI	*j*	298.15	Pγ	0.0032	0.25	0.891	3.2	2	9	−0.326 36	−0.110 35	0.170 95	1.325 66	0.01
DMSO	Et_4NI	*k*	298.15	P	0.0025	0.10	0.891	3.2	2	20	27.642 57	−39.456 06	29.876 61	−69.420 63	0.004
DMSO	KCl	*k*	298.15	P	0.0025	0.025	0.891	3.2	2	20	−56.173 99	57.207 98	−41.369 73	329.918 38	0.001
DMSO	$KClO_4$	*l*	298.15	P	0.011	0.20	0.891	3.2	2	20	1.176 42	−1.628 04	13.526 66	−1.753 51	0.002
DMSO	KI	*k*	298.15	P	0.0025	0.10	0.891	3.2	2	20	14.188 22	−18.688 84	29.254 97	−38.339 45	0.002
DMSO	LiBr	*m*	298.15	Pγ	0.027	0.86	0.891	3.2	2	9	0.247 66	−0.089 72	0.133 31	0.106 30	0.04
DMSO	LiCl	*n*	298.15	Pγ	0.0050	0.40	0.891	3.2	2	9	−0.415 90	−0.134 13	0.203 51	0.671 36	0.03
DMSO	$LiClO_4$	*l*	298.15	P	0.020	0.27	0.891	3.2	2	20	0.252 65	0.208 89	−3.018 40	0.304 69	0.004
DMSO	LiI	*o*	298.15	Pγ	0.10	0.89	0.891	3.2	2	9	0.357 39	−0.084 33	−0.009 10	0.083 10	0.02
DMSO	NaCl	*k*	298.15	P	0.0025	0.070	0.891	3.2	2	20	14.790 14	−25.102 63	−14.659 69	−27.279 91	0.002
DMSO	NaI	*k*	298.15	P	0.0025	0.10	0.891	3.2	2	20	16.576 86	−22.120 22	43.226 16	−40.439 59	0.001
DMSO	NH_4Cl	*k*	298.15	P	0.0025	0.10	0.891	3.2	2	20	28.541 37	−47.352 36	−45.647 17	−56.687 30	0.001
DMSO	NH_4I	*k*	298.15	P	0.0050	0.10	0.891	3.2	2	20	12.009 77	−16.424 90	24.359 17	−30.819 65	0.001

* 'P' Pitzer fit; 'Pf' Pitzer fit, already fitted in literature ref.; 'Pγ' Pitzer fit on γ only; † standard deviation of the residuals.

[a] Barthel, Neueder and Wittmann, 1999; [b] Zafarani-Moattar et al., 2001; [c] Barthel, Neueder, Poepke et al., 1998; [d] Barthel et al., 1986; [e] Kunz, Turq et al., 1992; [f] Barthel, Neueder, Poepke et al., 1999b; [g] Barthel, Neueder, Poepke et al., 1999a; [h] Barthel, Neueder and Schröder, 1997; [i] Butler et al., 1970; [j] Archer et al., 1966; [k] S.-J. Kim et al., 1971; [l] Garnsey et al., 1968; [m] Salomon, 1969a; [n] Dunnett et al., 1965; [o] Salomon, 1970b; [p] Crawford et al., 1967; [q] Bonner, S. J. Kim et al., 1969; [r] Wood et al., 1978; [s] Nasehzadeh et al., 2004; [t] Zafarani-Moattar et al., 1999; [u] Bonner, Paljk et al., 1991; [v] Barthel et al., 1988; [w] Kunz, Barthel et al., 1991; [x] Barthel, Lauermann and Neueder, 1986; [y] Barthel, Neueder and Lauermann, 1985; [z] Nasirzadeh et al., 2004b; [aa] Nasirzadeh et al., 2004; [bb] Nasirzadeh, Papaiconomou et al., 2004; [cc] Zafarani-Moattar et al., 1998; [dd] Nasirzadeh et al., 2004a; [ee] Bonner, 1987; [ff] Nasirzadeh et al., 2003; [gg] Wood et al., 1971; [hh] Wood, Wicker et al., 1971; [ii] Luksha et al., 1966; [jj] Salomon, 1970a; [kk] Salomon, 1969b; [ll] Salomon, 1970c.

solvent	electrolyte	ref.	T/K	fit*	m^{min}	m^{max}	A^{Φ}	b	α_1	α_2	$\beta^{(0)}$	$\beta^{(1)}$	$\beta^{(2)}$	C^{Φ}	$\sigma^{\dagger}$
DMSO	RbI	*p*	298.15	Pγ	0.0050	0.079	0.891	3.2	2	9	0.733 05	−0.148 38	0.222 60	−8.638 04	0.005
EC	CsI	*q*	309.60	P	0.0025	0.10	0.340	3.2	2	20	9.260 04	−13.432 06	25.434 93	−24.002 16	0.003
EC	Et_4NBr	*r*	309.96	P	0.089	0.39	0.339	3.2	2	17	−0.575 55	0.950 01	−10.536 03	0.582 95	0.0004
EC	KI	*r*	309.96	P	0.045	0.62	0.339	3.2	2	17	0.098 58	0.039 64	9.023 85	−0.036 63	0.001
EC	NaI	*r*	309.96	P	0.080	0.73	0.339	3.2	2	17	0.037 18	0.333 62	8.011 05	0.100 93	0.003
EC	NH_4I	*q*	309.60	P	0.0025	0.10	0.340	3.2	2	20	13.219 75	−20.358 84	9.438 14	−36.484 14	0.005
EC	Pr_4NI	*q*	309.60	P	0.0025	0.10	0.340	3.2	2	20	7.350 01	−10.085 16	21.269 58	−20.980 49	0.004
EtOH	Bu_4NBr	*a*	298.15	Pf	0.050	2.5	2.005	3.2	2	10	0.168 12	−0.559 16	−7.583 62	−0.009 90	0.006
EtOH	Et_4NBr	*a*	298.15	Pf	0.040	2.3	2.005	3.2	2	10	0.166 91	−0.729 83	−10.002 47	−0.031 98	0.01
EtOH	$LiClO_4$	*c*	298.16	Pf	0.030	1.5	2.005	3.2	2	10	0.188 78	0.759 94	2.690 17	0.088 82	0.004
EtOH	LiI	*s*	298.15	P	0.010	2	2.006	3.2	2	10	0.256 87	0.225 58	−8.154 23	0.038 77	0.008
EtOH	$LiNO_3$	*t*	298.15	Pf	0.12	2.1	2.006	3.2	2	1.4	1.289 26	10.067 46	−9.163 29	−0.185 75	0.005
EtOH	Me_4GuHCl	*u*	298.15	P	0.20	3	2.006	3.2	2	10	0.184 01	0.130 39	15.808 65	−0.023 39	0.002
EtOH	$Me_4GuHClO_4$	*u*	298.15	P	0.30	7	2.006	3.2	2	10	−0.079 72	−0.883 90	9.147 98	0.006 34	0.004
EtOH	NaI	*d*	298.15	Pf	0.040	1.9	2.007	3.2	2	20	0.159 34	0.596 61	5.984 91	0.071 64	0.01
EtOH	Pr_4NBr	*a*	298.15	Pf	0.040	2.7	2.005	3.2	2	10	0.181 76	−0.701 05	−9.189 50	−0.022 54	0.006
MeCN	Bu_4NBr	*v*	298.15	Pf	0.020	2	1.112	3.2	2	20	−0.008 08	−0.271 86	42.664 58	0.006 15	0.01
MeCN	Bu_4NCl	*v*	298.15	Pf	0.050	2.5	1.112	3.2	2	20	−0.052 01	0.023 15	0.678 78	0.036 66	0.007
MeCN	Bu_4NI	*v*	298.15	Pf	0.050	2.4	1.112	3.2	2	12	−0.024 91	−0.466 04	−11.654 57	0.000 94	0.008
MeCN	Et_4NBr	*v*	298.15	Pf	0.040	0.40	1.112	3.2	2	20	−0.030 12	−0.787 56	35.266 61	−0.049 00	0.007
MeCN	LiBr	*w*	298.15	Pf	0.020	0.84	1.112	3.2	2	7	−0.269 48	−0.737 17	−13.668 48	0.105 31	0.04
MeCN	$LiClO_4$	*g*	298.16	Pf	0.050	1.2	1.112	3.2	2	10	0.091 19	−0.675 65	−4.786 72	−0.023 24	0.004
MeCN	NaI	*d*	298.15	Pf	0.060	1.5	1.112	3.2	2	7	0.061 90	−0.380 15	−0.215 50	−0.021 57	0.005
MeCN	$Pent_4NBr$	*v*	298.15	Pf	0.060	2.2	1.112	3.2	2	20	−0.008 53	−0.197 30	36.697 59	0.005 14	0.003
MeCN	Pr_4NBr	*v*	298.15	Pf	0.040	1.6	1.112	3.2	2	20	0.020 07	−0.648 92	29.685 29	−0.016 11	0.005
MeOH	Bu_4NBr	*x*	298.15	Pf	0.040	1.7	1.295	3.2	2	20	0.110 11	−0.366 31	4.271 36	−0.000 15	0.005
MeOH	Bu_4NClO_4	*x*	298.15	Pf	0.040	2.5	1.295	3.2	2	20	0.010 71	−2.166 27	−34.357 35	−0.022 93	0.007
MeOH	Bu_4NI	*x*	298.15	Pf	0.040	0.90	1.295	3.2	2	20	0.458 17	−2.122 45	−11.656 79	−0.337 12	0.005
MeOH	CsI	*y*	298.15	Pf	0.030	0.10	1.295	3.2	2	7	−11.882 00	20.156 54	−11.418 12	22.466 90	0.004
MeOH	Et_4NBr	*x*	298.15	Pf	0.040	1.9	1.295	3.2	2	20	0.134 15	−0.749 03	41.274 23	−0.029 68	0.007

* 'P' Pitzer fit; 'Pf' Pitzer fit, already fitted in literature ref.; 'Pγ' Pitzer fit on γ only; † standard deviation of the residuals.

[a] Barthel, Neueder and Wittmann, 1999; [b] Zafarani-Moattar et al., 2001; [c] Barthel, Neueder, Poepke et al., 1998; [d] Barthel et al., 1986; [e] Kunz, Turq et al., 1992; [f] Barthel, Neueder, Poepke et al., 1999b; [g] Barthel, Neueder, Poepke et al., 1999a; [h] Barthel, Neueder and Schröder, 1997; [i] Butler et al., 1970; [j] Archer et al., 1966; [k] S.-J. Kim et al., 1971; [l] Garnsey et al., 1968; [m] Salomon, 1969a; [n] Dunnett et al., 1965; [o] Salomon, 1970b; [p] Crawford et al., 1967; [q] Bonner, S. J. Kim et al., 1969; [r] Wood et al., 1978; [s] Nasehzadeh et al., 2004; [t] Zafarani-Moattar et al., 1999; [u] Bonner, Paljk et al., 1991; [v] Barthel et al., 1988; [w] Kunz, Barthel et al., 1991; [x] Barthel, Lauermann and Neueder, 1986; [y] Barthel, Neueder and Lauermann, 1985; [z] Nasirzadeh et al., 2004b; [aa] Nasirzadeh et al., 2004; [bb] Nasirzadeh, Papaiconomou et al., 2004; [cc] Zafarani-Moattar et al., 1998; [dd] Nasirzadeh et al., 2004a; [ee] Bonner, 1987; [ff] Nasirzadeh et al., 2003; [gg] Wood et al., 1971; [hh] Wood, Wicker et al., 1971; [ii] Luksha et al., 1966; [jj] Salomon, 1970a; [kk] Salomon, 1969b; [ll] Salomon, 1970c.

solvent	electrolyte	ref.	T/K	fit*	m^{min}	m^{max}	A^{ϕ}	b	α_1	α_2	$\beta^{(0)}$	$\beta^{(1)}$	$\beta^{(2)}$	C^{ϕ}	$\sigma^{\dagger}$
MeOH	KBr	*y*	298.15	Pf	0.040	0.10	1.295	3.2	2	7	−7.290 22	12.536 50	−5.900 95	14.666 03	0.004
MeOH	KI	*y*	298.15	Pf	0.030	0.80	1.295	3.2	2	7	0.106 16	0.309 28	0.192 86	0.023 24	0.003
MeOH	KOAc	*z*	298.15	Pf	0.17	2.5	1.294	3.2	2	3	0.071 75	0.696 51	−0.693 45	−0.005 25	0.0003
MeOH	KSCN	*aa*	298.15	Pf	0.13	2.7	1.294	3.2	2	1.4	−0.443 78	−5.780 97	5.288 35	0.080 60	0.005
MeOH	LiBr	*bb*	298.15	Pf	0.041	6.9	1.294	3.2	2	7	0.238 14	0.045 91	9.038 92	0.024 46	0.02
MeOH	LiCl	*cc*	298.15	Pf	0.22	4.2	1.294	3.2	2	1.4	−0.180 78	−4.596 38	4.005 88	0.076 21	0.006
MeOH	$LiClO_4$	*dd*	298.15	Pf	0.11	3.8	1.294	3.2	2	1.4	0.878 47	6.354 85	−5.600 88	−0.073 67	0.01
MeOH	$LiNO_3$	*dd*	298.15	Pf	0.12	3.8	1.294	3.2	2	1.4	0.109 89	−1.815 57	1.333 09	0.001 49	0.002
MeOH	LiOAc	*cc*	298.15	Pf	0.24	3.0	1.294	3.2	2	1.4	0.220 18	1.607 45	−1.408 87	−0.015 99	0.005
MeOH	$Me_4GuHClO_4$	*ee*	298.15	P	0.10	8	1.293	3.2	2	10	−0.073 25	−1.143 89	47.817 45	0.004 77	0.03
MeOH	NaBr	*y*	298.15	Pf	0.040	1.2	1.295	3.2	2	7	−0.022 14	0.881 59	−0.483 86	0.185 79	0.002
MeOH	NaCl	*y*	298.15	Pf	0.040	0.20	1.295	3.2	2	7	15.386 89	−29.350 73	24.045 28	−20.744 77	0.003
MeOH	$NaClO_4$	*y*	298.15	Pf	0.060	1.3	1.295	3.2	2	7	0.217 03	−0.072 84	0.800 89	−0.033 46	0.005
MeOH	NaI	*y*	298.15	Pf	0.030	0.80	1.295	3.2	2	7	0.039 87	0.840 33	−0.600 05	0.162 89	0.002
MeOH	NaOAc	*z*	298.15	Pf	0.25	1.8	1.294	3.2	2	1.4	−0.323 89	−3.222 08	3.179 22	0.079 15	0.003
MeOH	NaSCN	*ff*	298.15	Pf	0.16	3.4	1.294	3.2	2	1.4	0.297 89	0.450 82	−0.316 21	−0.025 40	0.003
MeOH	NH_4SCN	*aa*	298.15	Pf	0.23	4.4	1.294	3.2	2	1.4	0.074 17	−0.898 26	0.781 33	−0.008 78	0.009
MeOH	$Pent_4NBr$	*x*	298.15	Pf	0.050	1.6	1.295	3.2	2	20	0.163 23	−0.598 59	−13.345 52	−0.025 87	0.005
MeOH	RbI	*y*	298.15	Pf	0.030	0.40	1.295	3.2	2	7	0.943 24	−1.833 39	1.898 27	−0.921 16	0.003
NMA	Bu_4NBr	*gg*	298.15	P	0.010	1	0.110	3.2	2	10	−0.066 36	−0.161 08	−0.113 84	0.021 27	0.0004
NMA	Bu_4NCl	*gg*	298.15	P	0.010	0.90	0.110	3.2	2	9	0.140 75	0.031 85	−0.177 84	−0.054 23	0.0004
NMA	Bu_4NI	*gg*	298.15	P	0.010	1	0.110	3.2	2	10	−0.343 85	−0.404 58	0.014 86	0.125 85	0.0002
NMA	CsI	*hh*	298.15	P	0.010	0.40	0.110	3.2	2	9	0.087 43	0.013 62	−0.108 64	−0.027 27	0.0003
NMA	Et_4NBr	*gg*	298.15	P	0.010	0.90	0.110	3.2	2	10	−0.119 98	−0.075 94	−0.026 23	−0.023 50	0.0004
NMA	Et_4NCl	*gg*	298.15	P	0.010	0.80	0.110	3.2	2	10	0.058 28	0.011 92	−0.146 35	−0.046 30	0.0003
NMA	KBr	*hh*	298.15	P	0.010	0.40	0.110	3.2	2	11	0.218 92	−0.202 02	−0.026 14	−0.073 25	0.0002
NMA	KI	*hh*	298.15	P	0.010	0.70	0.110	3.2	2	10	0.211 19	−0.189 36	−0.064 82	0.048 57	0.0003
NMA	KOAc	*gg*	298.15	P	0.010	0.80	0.110	3.2	2	10	0.021 11	−0.055 86	−0.140 54	−0.029 58	0.0003
NMA	Kpropion	*gg*	298.15	P	0.010	0.50	0.110	3.2	2	10	0.049 79	0.106 56	−0.283 94	−0.079 68	0.0003
NMA	LiBr	*hh*	298.15	P	0.010	0.60	0.110	3.2	2	4	0.289 62	0.080 52	−0.187 76	0.031 82	0.0002
NMA	LiForm	*gg*	298.15	P	0.010	0.40	0.110	3.2	2	10	−0.255 20	−0.437 23	−0.127 33	0.259 78	0.0001
NMA	$LiNO_3$	*hh*	298.15	P	0.010	0.60	0.110	3.2	2	10	0.296 08	−0.154 23	−0.107 26	0.026 38	0.0002

* 'P' Pitzer fit; 'Pf' Pitzer fit, already fitted in literature ref.; 'Pγ' Pitzer fit on γ only; † standard deviation of the residuals.

[a] Barthel, Neueder and Wittmann, 1999; [b] Zafarani-Moattar et al., 2001; [c] Barthel, Neueder, Poepke et al., 1998; [d] Barthel et al., 1986; [e] Kunz, Turq et al., 1992; [f] Barthel, Neueder, Poepke et al., 1999b; [g] Barthel, Neueder, Poepke et al., 1999a; [h] Barthel, Neueder and Schröder, 1997; [i] Butler et al., 1970; [j] Archer et al., 1966; [k] S.-J. Kim et al., 1971; [l] Garnsey et al., 1968; [m] Salomon, 1969a; [n] Dunnett et al., 1965; [o] Salomon, 1970b; [p] Crawford et al., 1967; [q] Bonner, S. J. Kim et al., 1969; [r] Wood et al., 1978; [s] Nasehzadeh et al., 2004; [t] Zafarani-Moattar et al., 1999; [u] Bonner, Paljk et al., 1991; [v] Barthel et al., 1988; [w] Kunz, Barthel et al., 1991; [x] Barthel, Lauermann and Neueder, 1986; [y] Barthel, Neueder and Lauermann, 1985; [z] Nasirzadeh et al., 2004b; [aa] Nasirzadeh et al., 2004; [bb] Nasirzadeh, Papaiconomou et al., 2004; [cc] Zafarani-Moattar et al., 1998; [dd] Nasirzadeh et al., 2004a; [ee] Bonner, 1987; [ff] Nasirzadeh et al., 2003; [gg] Wood et al., 1971; [hh] Wood, Wicker et al., 1971; [ii] Luksha et al., 1966; [jj] Salomon, 1970a; [kk] Salomon, 1969b; [ll] Salomon, 1970c.

solvent	electrolyte	ref.	T/K	fit*	m^{min}	m^{max}	A^{Φ}	b	α_1	α_2	$\beta^{(0)}$	$\beta^{(1)}$	$\beta^{(2)}$	C^{Φ}	$\sigma^{\dagger}$
NMA	LiOAc	*gg*	298.15	P	0.010	0.40	0.110	3.2	2	4	−0.187 94	−0.207 61	−0.022 12	−0.035 46	0.0001
NMA	LiPropion	*gg*	298.15	P	0.010	0.40	0.110	3.2	2	10	−0.236 05	0.113 79	−0.325 88	0.042 35	0.0002
NMA	Me_4NCl	*gg*	298.15	P	0.010	0.50	0.110	3.2	2	4	−0.140 14	0.238 17	−0.240 24	−0.056 10	0.0003
NMA	NaBr	*hh*	298.15	P	0.010	0.70	0.110	3.2	2	10	0.310 70	−0.054 10	−0.075 37	−0.055 77	0.0001
NMA	NaI	*hh*	298.15	P	0.010	0.80	0.110	3.2	2	10	0.393 65	−0.043 68	−0.125 97	−0.033 90	0.0003
NMA	$NaNO_3$	*hh*	298.15	P	0.010	0.80	0.110	3.2	2	10	−0.030 57	−0.131 99	−0.135 41	−0.010 15	0.0003
NMA	NH_4I	*q*	298.15	P	0.0050	0.10	0.110	3.2	2	10	10.228 54	−14.970 82	−14.411 21	−26.659 89	0.003
NMA	Pr_4NBr	*gg*	298.15	P	0.010	1	0.110	3.2	2	10	−0.100 10	−0.178 07	−0.040 00	0.019 48	0.0002
NMA	Pr_4NCl	*gg*	298.15	P	0.010	0.90	0.110	3.2	2	10	0.109 94	−0.033 72	−0.149 52	−0.042 38	0.0003
NMA	Pr_4NI	*gg*	298.15	P	0.010	0.50	0.110	3.2	2	10	−0.352 73	−0.367 44	0.038 51	0.095 76	0.0003
NMF	CsCl	*ii*	298.15	Pγ	0.010	0.070	0.112	3.2	2	9	−0.206 61	−0.001 40	0.000 75	0.209 49	0.0004
NMF	KCl	*ii*	298.15	Pγ	0.010	0.070	0.112	3.2	2	9	−0.293 28	−0.012 05	0.016 19	−1.698 70	0.002
NMF	LiCl	*ii*	298.15	Pγ	0.010	0.090	0.112	3.2	2	9	−1.144 13	0.005 81	−0.009 96	1.371 66	0.0006
NMF	NaBr	*ii*	298.15	Pγ	0.010	0.080	0.112	3.2	2	9	−0.113 52	−0.001 20	0.000 66	0.340 03	0.0007
NMF	NaCl	*ii*	298.15	Pγ	0.010	0.10	0.112	3.2	2	9	−1.520 11	0.050 51	−0.074 37	13.957 36	0.004
PC	KI	*jj*	298.15	Pγ	0.028	0.20	0.571	3.2	2	9	0.820 03	−0.218 55	0.462 40	−2.796 39	0.02
PC	LiBr	*kk*	298.15	Pγ	0.13	0.65	0.571	3.2	2	9	−0.476 67	−0.123 61	0.563 07	0.306 02	0.004
PC	LiCl	*kk*	298.15	Pγ	0.016	0.032	0.571	3.2	2	9	−121.595 24	6.964 90	−10.439 26	1791.694 05	0.01
PC	LiI	*jj*	298.15	Pγ	0.027	0.87	0.571	3.2	2	9	0.258 92	0.017 39	−0.127 04	0.217 49	0.01
PC	NaI	*ll*	298.15	Pγ	0.15	1.0	0.571	3.2	2	9	0.004 20	−0.074 17	0.179 06	0.077 42	0.010
SULF	$KClO_4$	*l*	298.15	P	0.0034	0.097	1.049	3.2	2	20	3.565 49	−6.566 17	−1.700 23	−9.027 53	0.002
SULF	$LiClO_4$	*l*	298.15	P	0.0071	0.083	1.049	3.2	2	20	−3.651 68	0.832 12	−29.710 71	18.207 97	0.0007
SULF	$NaClO_4$	*l*	298.15	P	0.0060	0.10	1.049	3.2	2	20	4.217 87	−9.144 30	−14.298 67	−7.406 67	0.002

* 'P' Pitzer fit; 'Pf' Pitzer fit, already fitted in literature ref.; 'Pγ' Pitzer fit on γ only; † standard deviation of the residuals.

[a] Barthel, Neueder and Wittmann, 1999; [b] Zafarani-Moattar et al., 2001; [c] Barthel, Neueder, Poepke et al., 1998; [d] Barthel et al., 1986; [e] Kunz, Turq et al., 1992; [f] Barthel, Neueder, Poepke et al., 1999b; [g] Barthel, Neueder, Poepke et al., 1999a; [h] Barthel, Neueder and Schröder, 1997; [i] Butler et al., 1970; [j] Archer et al., 1966; [k] S.-J. Kim et al., 1971; [l] Garnsey et al., 1968; [m] Salomon, 1969a; [n] Dunnett et al., 1965; [o] Salomon, 1970b; [p] Crawford et al., 1967; [q] Bonner, S. J. Kim et al., 1969; [r] Wood et al., 1978; [s] Nasehzadeh et al., 2004; [t] Zafarani-Moattar et al., 1999; [u] Bonner, Paljk et al., 1991; [v] Barthel et al., 1988; [w] Kunz, Barthel et al., 1991; [x] Barthel, Lauermann and Neueder, 1986; [y] Barthel, Neueder and Lauermann, 1985; [z] Nasirzadeh et al., 2004b; [aa] Nasirzadeh et al., 2004; [bb] Nasirzadeh, Papaiconomou et al., 2004; [cc] Zafarani-Moattar et al., 1998; [dd] Nasirzadeh et al., 2004a; [ee] Bonner, 1987; [ff] Nasirzadeh et al., 2003; [gg] Wood et al., 1971; [hh] Wood, Wicker et al., 1971; [ii] Luksha et al., 1966; [jj] Salomon, 1970a; [kk] Salomon, 1969b; [ll] Salomon, 1970c.

Table 33: The Pitzer-Archer model fitting coefficients b, α_1, α_2, α_3, $\beta^{(0)}$, $\beta^{(1)}$, $\beta^{(2)}$, $C^{(0)}$ and $C^{(1)}$ in non-aqueous solvents. The osmotic and activity coefficients curves can be reproduced in the interval comprised between m^{min} and m^{max} (in $mol\,kg^{-1}$) by employing eq. [11] and eq. [12] with B^{Φ} and B^{γ} expressed by eq. [16] and eq. [17] and C^{Φ} and C^{γ} by eq. [18] and eq. [19] respectively. The column 'ref.' lists the publication containing the experimental data. σ is the standard deviation of the residuals.

solvent	electrolyte	ref.	T/K	m^{min}	m^{max}	A^{Φ}	b	α_1	α_2	α_3	$\beta^{(0)}$	$\beta^{(1)}$	$\beta^{(2)}$	$C^{(0)}$	$C^{(1)}$	σ
2PrOH	LiBr	*a*	298.15	0.074	1.5	2.816	3.2	2	7	1	1.321 29	−1.730 97	−3.535 60	0.483 49	−3.662 11	0.003
EtOH	LiBr	*b*	298.15	0.071	3.4	2.003	3.2	2	7	1	0.092 10	0.815 80	3.947 57	0.109 69	0.051 69	0.01
EtOH	LiCl	*c*	298.15	0.18	3.3	2.005	3.2	2	7	1	0.427 55	−0.441 20	−0.217 41	0.100 17	−0.540 95	0.004

[a] Nasirzadeh, Neueder and Kunz, 2005; [b] Nasirzadeh, Neueder and Kunz, 2004; [c] Safarov, 2006;

Table 34: The polynomial fitting coefficients a_{poly}, b_{poly} and c_{poly} for data that could not be fitted by the Pitzer or Pitzer-Archer models. The osmotic and activity coefficients curves can be reproduced in the interval comprised between m^{min} and m^{max} (in $mol\,kg^{-1}$) by employing eq. [20].

solvent	electrolyte	ref.	T/K	m^{min}	m^{max}	a_{poly}	b_{poly}	c_{poly}
DMSO	CsCl	*a*	298.15	0.0025	0.010	1720	−52.340	0.927 75
EC	CsI	*b*	309.96	0.068	0.32	0.306 62	−0.336 68	0.961 65
MeOH	$NaNO_3$	*c*	298.15	0.050	0.75	1.0419	−1.0056	0.764 16
NMA	CsBr	*d*	298.15	0.010	0.20	0.539 04	−0.186 51	0.977 95
NMA	CsCl	*d*	298.15	0.010	0.10	3.8333	−0.755 00	0.980 17
NMA	KCl	*d*	298.15	0.010	0.10	3.7778	−0.626 67	0.979 89
NMA	KNO_3	*d*	298.15	0.010	0.20	1.5171	−0.863 03	0.976 22
NMA	LiCl	*d*	298.15	0.010	0.30	0.114 02	0.455 68	0.974 20
NMA	NaCl	*d*	298.15	0.010	0.30	0.774 43	−0.013 011	0.965 83
NMA	NaForm	*e*	298.15	0.010	0.20	0.974 35	−0.924 22	0.977 12
NMA	NaOAc	*e*	298.15	0.010	0.40	0.682 81	−0.826 02	0.968 83
NMA	NaPropion	*e*	298.15	0.010	0.30	0.680 60	−0.616 59	0.973 18
SULF	$RbClO_4$	*f*	298.15	0.0031	0.029	104.05	−7.4179	0.962 74

[a] S.-J. Kim et al., 1971; [b] Wood et al., 1978; [c] Bonner, 1987; [d] Wood, Wicker et al., 1971; [e] Wood et al., 1971; [f] Garnsey et al., 1968;

Table 35: The Pitzer coefficients b,α,$\beta^{(0)}$,$\beta^{(1)}$ and C^{Φ} in water as tabulated by Pitzer et al. (1973). The osmotic and activity coefficients curves can be reproduced in the interval comprised between m^{min} and m^{max} (in $mol\,kg^{-1}$) by employing eq. [11] and eq. [12]. σ is the standard deviation of the residuals.

solvent	electrolyte	T/K	m^{min}	m^{max}	A^{Φ}	b	α	$\beta^{(0)}$	$\beta^{(1)}$	C^{Φ}	σ
water	Bu_4NBr	298.15	0.000 01	4.5	0.392	1.2	2	−0.0558	−0.5790	−0.001 00	0.007
water	Bu_4NCl	298.15	0.000 01	2.5	0.392	1.2	2	0.2058	−0.4640	−0.058 80	0.001
water	CsBr	298.15	0.000 01	5	0.392	1.2	2	0.0279	0.0139	0.000 04	0.002
water	CsCl	298.15	0.000 01	5	0.392	1.2	2	0.0300	0.0558	0.000 38	0.002
water	CsF	298.15	0.000 01	3.2	0.392	1.2	2	0.1306	0.2570	−0.004 30	0.002
water	CsI	298.15	0.000 01	3	0.392	1.2	2	0.0244	0.0262	−0.003 65	0.001
water	Et_4NBr	298.15	0.000 01	4	0.392	1.2	2	−0.4570	−0.4480	0.013 50	0.001
water	Et_4NCl	298.15	0.000 01	3	0.392	1.2	2	0.0336	−0.1530	0.008 40	0.002
water	Et_4NI	298.15	0.000 01	2	0.392	1.2	2	−0.1930	−0.5990	0.040 10	0.007
water	KBr	298.15	0.000 01	5.5	0.392	1.2	2	0.0569	0.2212	−0.001 80	0.001
water	KCl	298.15	0.000 01	4.8	0.392	1.2	2	0.0484	0.2122	−0.000 84	0.0005
water	KF	298.15	0.000 01	2	0.392	1.2	2	0.0809	0.2021	0.000 93	0.001
water	KI	298.15	0.000 01	4.5	0.392	1.2	2	0.0746	0.2517	−0.004 14	0.001
water	KOAc	298.15	0.000 01	3.5	0.392	1.2	2	0.1587	0.3251	−0.006 60	0.001
water	KSCN	298.15	0.000 01	5	0.392	1.2	2	0.0416	0.2302	−0.002 52	0.001
water	LiBr	298.15	0.000 01	2.5	0.392	1.2	2	0.1748	0.2547	0.005 30	0.002
water	LiCl	298.15	0.000 01	6	0.392	1.2	2	0.1494	0.3074	0.003 59	0.001
water	$LiClO_4$	298.15	0.000 01	3.5	0.392	1.2	2	0.1973	0.3996	0.008 00	0.002
water	LiI	298.15	0.000 01	1.4	0.392	1.2	2	0.2104	0.3730	0	0.006
water	$LiNO_3$	298.15	0.000 01	6	0.392	1.2	2	0.1420	0.2780	−0.005 51	0.001
water	LiOAc	298.15	0.000 01	4	0.392	1.2	2	0.1124	0.2483	−0.005 25	
water	Me_4NCl	298.15	0.000 01	3.4	0.392	1.2	2	0.0149	−0.0830	0.005 70	0.005
water	NaBr	298.15	0.000 01	4	0.392	1.2	2	0.0973	0.2791	0.001 16	0.004
water	NaCl	298.15	0.000 01	6	0.392	1.2	2	0.0765	0.2664	0.001 27	0.001
water	$NaClO_4$	298.15	0.000 01	6	0.392	1.2	2	0.0554	0.2755	−0.001 18	0.001
water	NaF	298.15	0.000 01	1	0.392	1.2	2	0.0215	0.2107	0	0.001
water	NaForm	298.15	0.000 01	3.5	0.392	1.2	2	0.0820	0.2872	−0.005 23	0.001
water	NaI	298.15	0.000 01	3.5	0.392	1.2	2	0.1195	0.3439	0.001 80	0.001
water	$NaNO_3$	298.15	0.000 01	6	0.392	1.2	2	0.0068	0.1783	−0.000 72	0.001
water	NaOAc	298.15	0.000 01	3.5	0.392	1.2	2	0.1426	0.3237	−0.006 29	0.001
water	NaPropion	298.15	0.000 01	3	0.392	1.2	2	0.1875	0.2789	−0.012 77	0.001
water	NaSCN	298.15	0.000 01	4	0.392	1.2	2	0.1005	0.3582	−0.003 03	0.001
water	NH_4Cl	298.15	0.000 01	6	0.392	1.2	2	0.0522	0.1918	−0.003 01	0.001

solvent	electrolyte	T/K	m^{min}	m^{max}	A^{ϕ}	b	α	$\beta^{(0)}$	$\beta^{(1)}$	C^{ϕ}	σ
water	NH_4I	298.15	0.000 01	7.5	0.392	1.2	2	0.0570	0.3157	−0.003 08	
water	Pr_4NBr	298.15	0.000 01	3.5	0.392	1.2	2	0.0108	−0.8260	0.007 80	0.003
water	Pr_4NCl	298.15	0.000 01	2.5	0.392	1.2	2	0.1065	−0.3540	0.009 80	0.002
water	Pr_4NI	298.15	0.000 01	0.50	0.392	1.2	2	−0.2839	−0.8630	0	0.005
water	RbBr	298.15	0.000 01	5	0.392	1.2	2	0.0396	0.1530	−0.001 44	0.001
water	RbCl	298.15	0.000 01	5	0.392	1.2	2	0.0441	0.1483	−0.001 01	0.001
water	RbF	298.15	0.000 01	3.5	0.392	1.2	2	0.1141	0.2842	−0.105 00	0.002
water	RbI	298.15	0.000 01	5	0.392	1.2	2	0.0397	0.1330	−0.001 08	0.001

C.2 PLOTS

C.2.1 Alkali metal halides

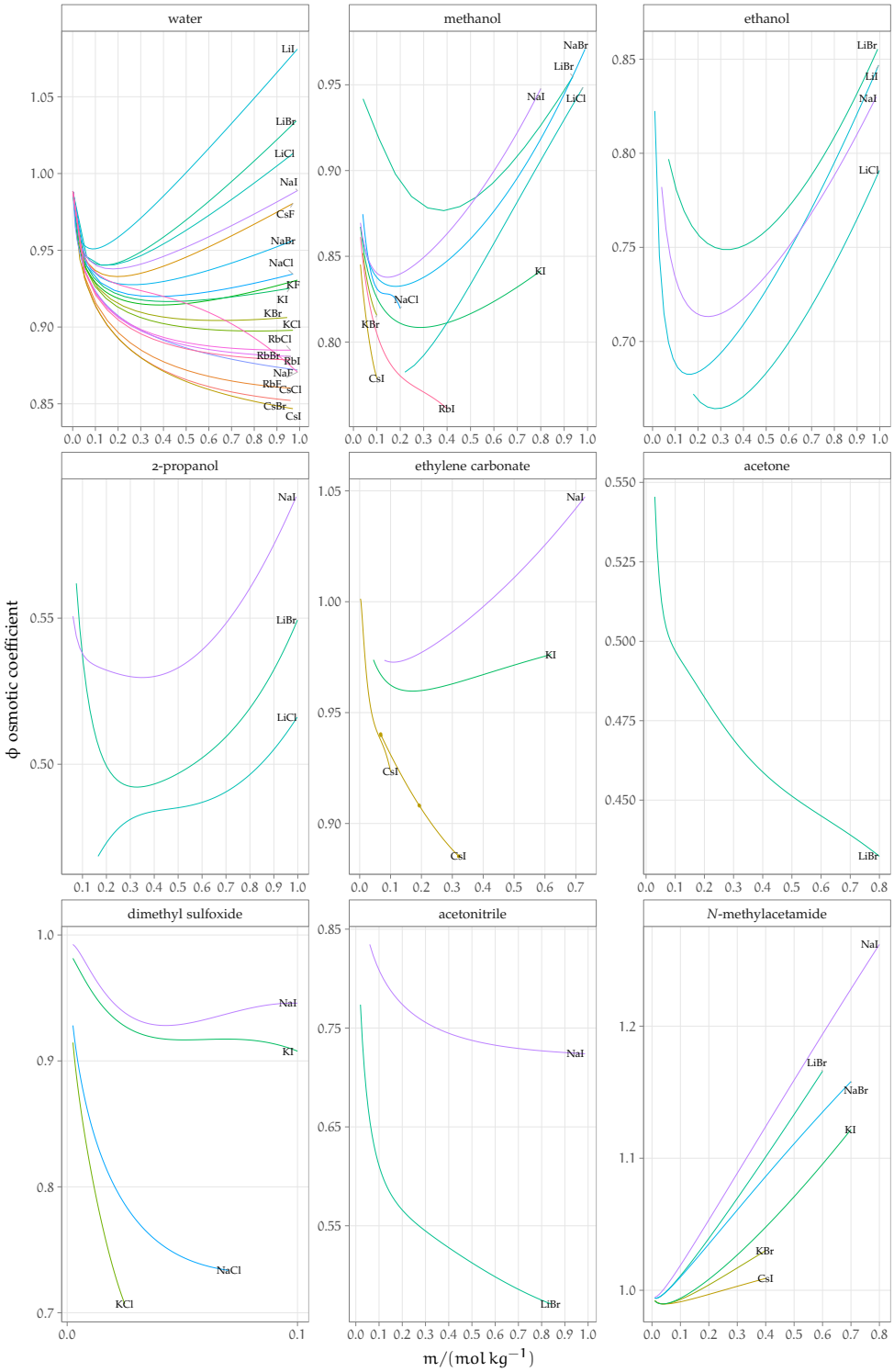

Figure 86: Plots of the osmotic coefficients ϕ of alkali metal halides in non-aqueous solvents at concentration $m < 1\,\mathrm{mol\,kg^{-1}}$.

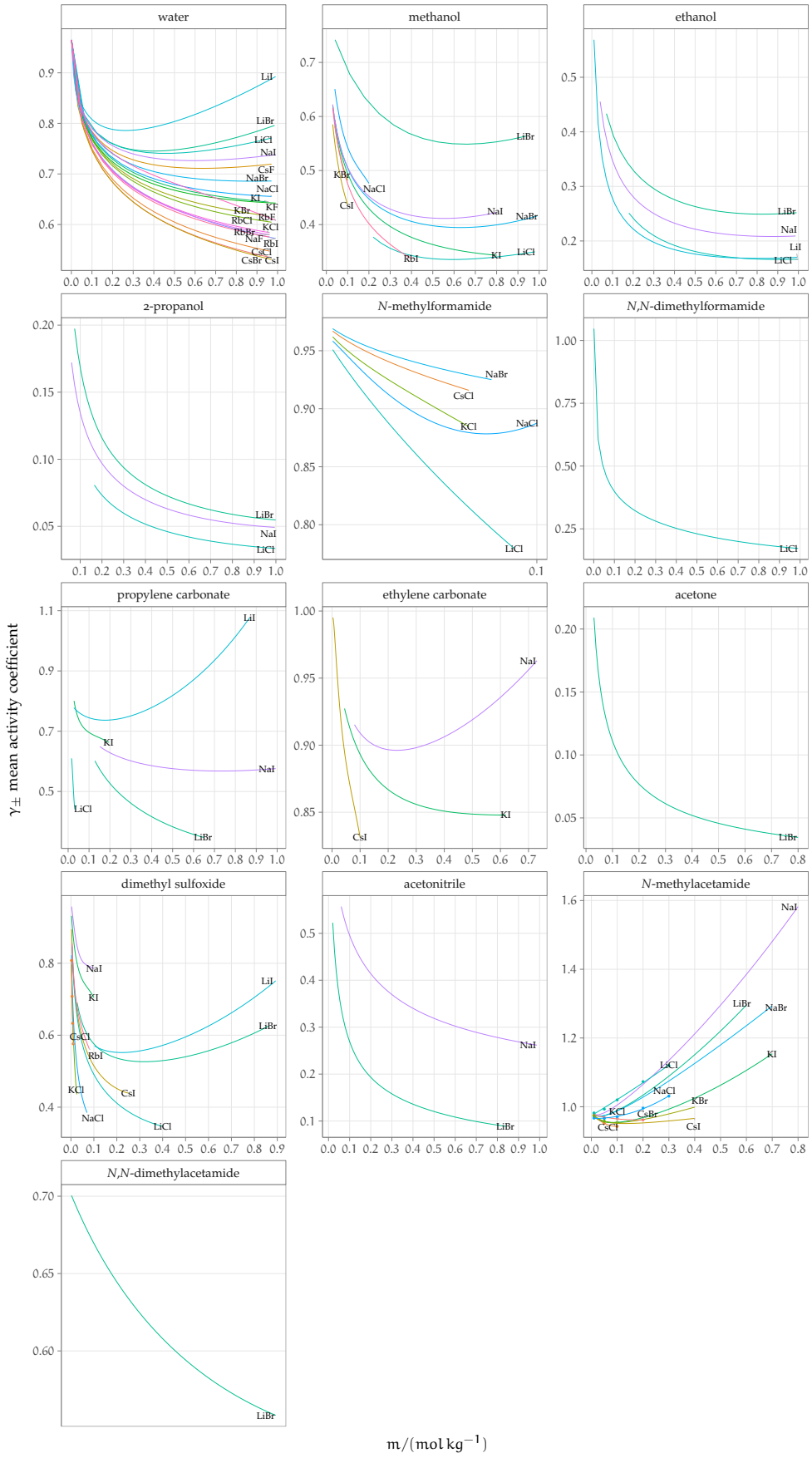

Figure 87: Plots of the activity coefficients γ of alkaly metal halides in non-aqueous solvents at concentration $m < 1\,\mathrm{mol\,kg^{-1}}$.

C.2.2 Polyatomic anions

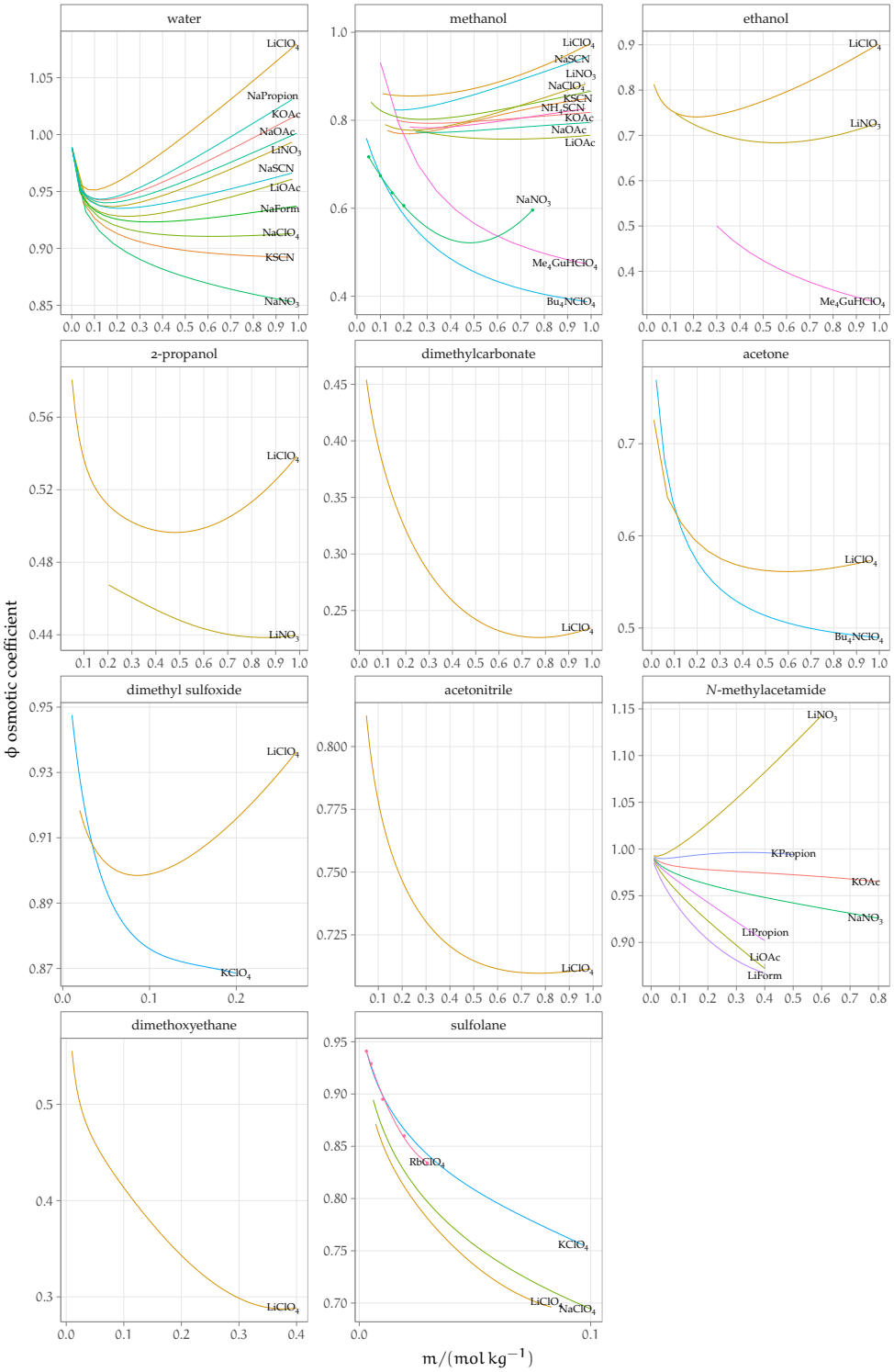

Figure 88: Plots of osmotic coefficients ϕ of salts of polyatomic anions in non-aqueous solvents at concentration $m < 1\,mol\,kg^{-1}$.

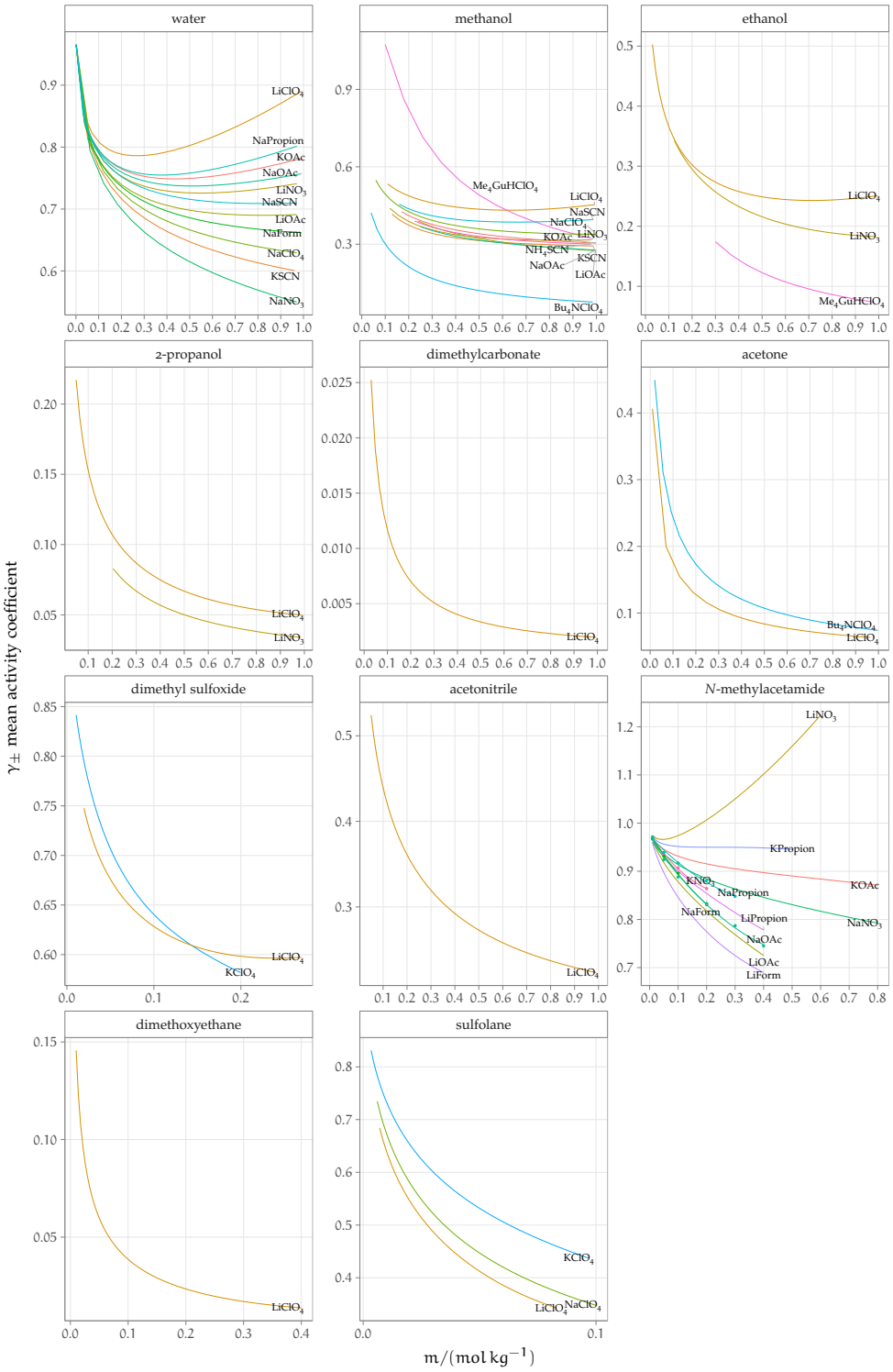

Figure 89: Plots of activity coefficients γ of salts of polyatomic anions in non-aqueous solvents at concentration $m < 1\,\mathrm{mol\,kg^{-1}}$.

c.2.3 Polyatomic cations

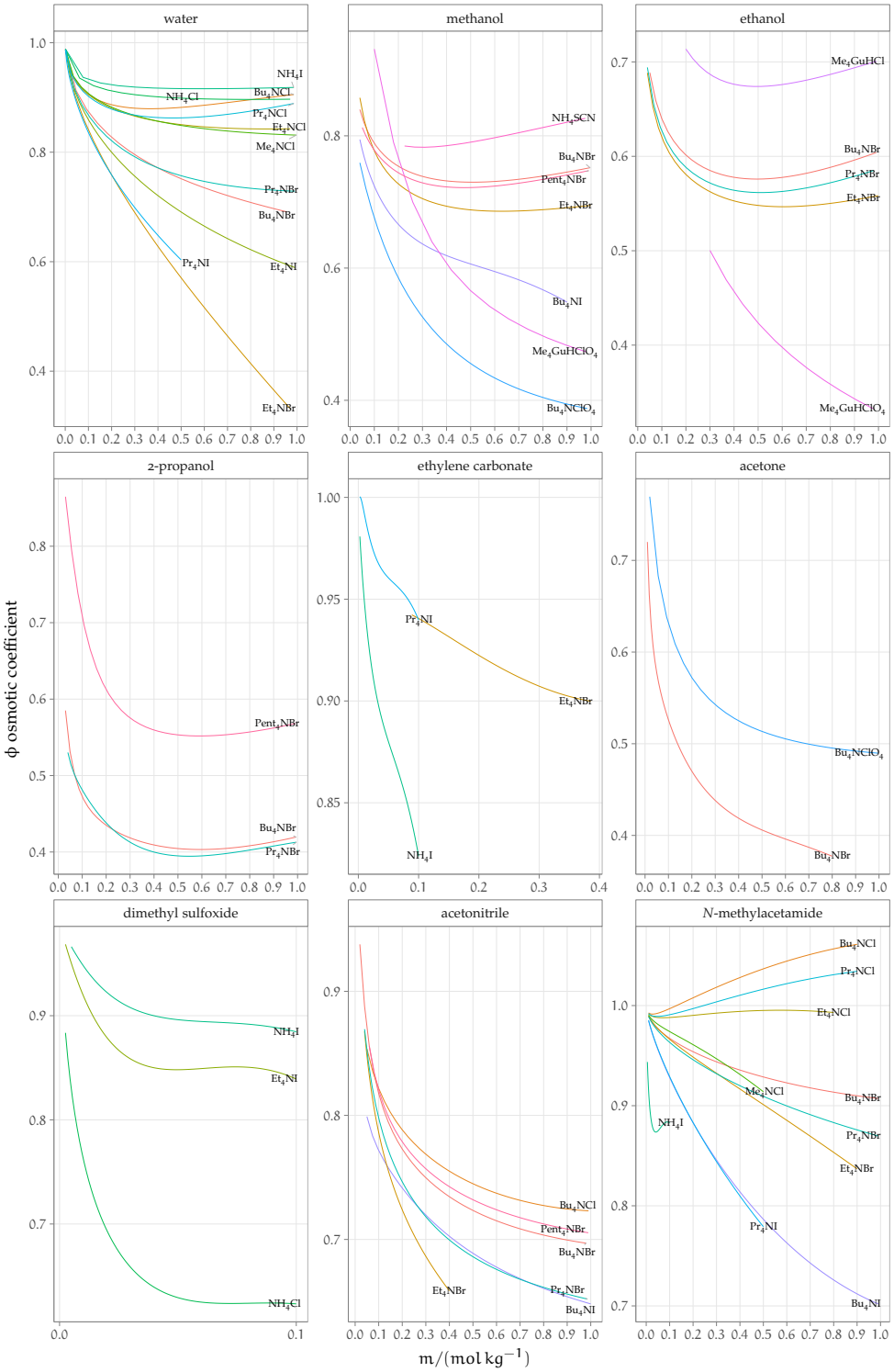

Figure 90: Plots of osmotic coefficients ϕ of salts of polyatomic cations in non-aqueous solvents at concentration $m < 1\,mol\,kg^{-1}$.

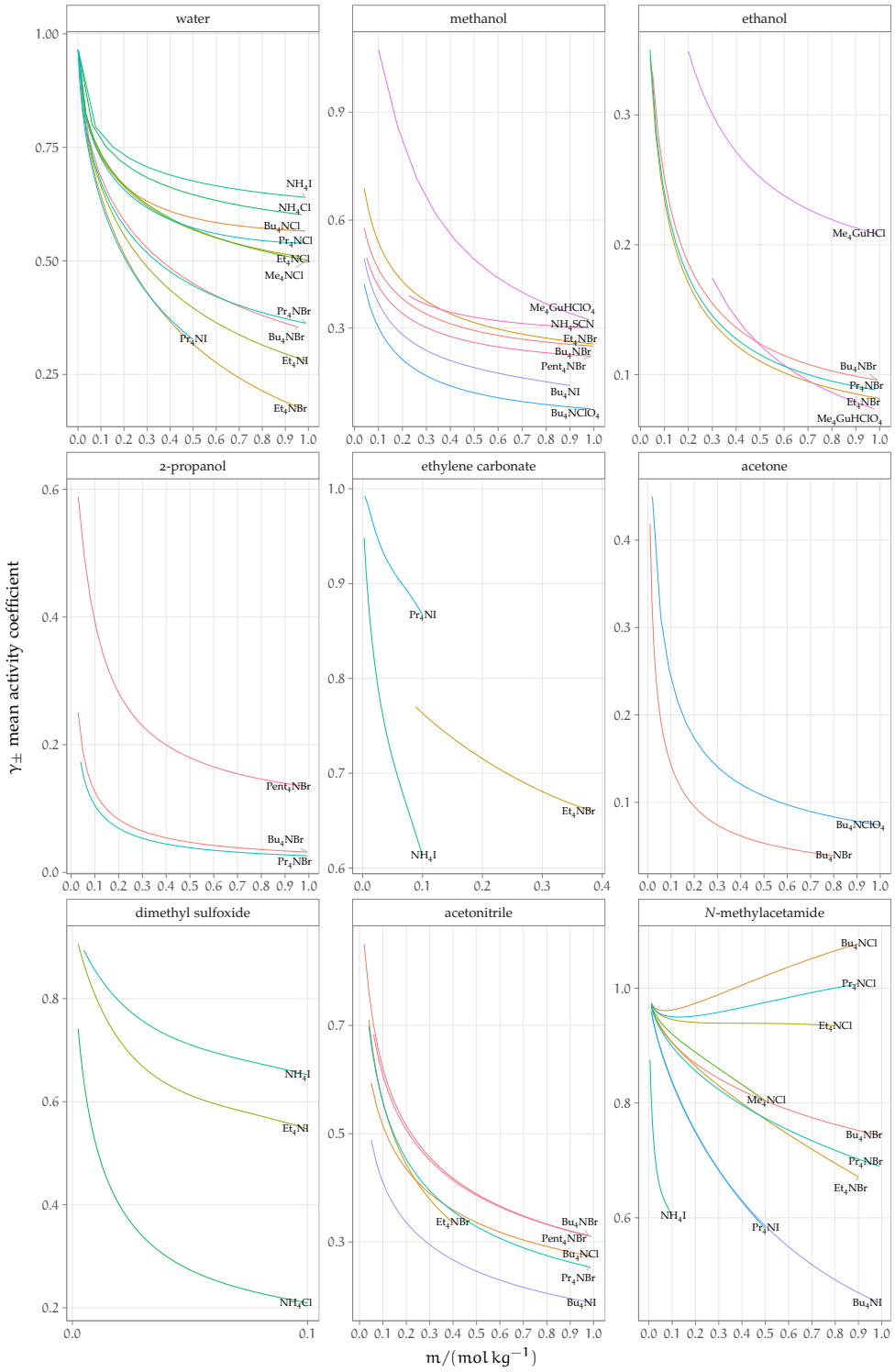

Figure 91: Plots of activity coefficients γ of salts of polyatomic cations in non-aqueous solvents at concentration $m < 1\,\mathrm{mol\,kg^{-1}}$.

BIBLIOGRAPHY FOR THE CURRENT APPENDIX

Archer, M. D. and R. P. H. Gasser

1966 'Electrolyte Solutions in Dimethyl Sulphoxide. Part 2. — Caesium Iodide', *Trans. Faraday Soc.* 62 (o 1966), pp. 3451–3458, DOI: 10.1039/TF9666203451.

Barthel, J. and W. Kunz

1988 'Vapor Pressure Data for Non-aqueous Electrolyte Solutions. Part 5. Tetraalkylammonium Salts in Acetonitrile', *J. Solution Chem.* 17, 5, pp. 399–415, DOI: 10.1007/BF00647308.

Barthel, J. and G. Lauermann

1986 'Vapor Pressure Measurements on Non-aqueous Electrolyte Solutions. Part 3: Solutions of Sodium Iodide in Ethanol, 2-propanol, and Acetonitrile', *J. Solution Chem.* 15, 10, pp. 869–877, DOI: 10.1007/BF00646093.

Barthel, J., G. Lauermann and R. Neueder

1986 'Vapor Pressure Measurements on Non-aqueous Electrolyte Solutions. Part 2. Tetraalkylammonium Salts in Methanol. Activity Coefficients of Various 1 – 1 Electrolytes at High Concentrations', *J. Solution Chem.* 15, 10, pp. 851–867, DOI: 10.1007/BF00646092.

Barthel, J., R. Neueder and G. Lauermann

1985 'Vapor Pressures of Non-aqueous Electrolyte Solutions. Part 1. Alkali Metal Salts in Methanol', *J. Solution Chem.* 14, 9, pp. 621–633, DOI: 10.1007/BF00646055.

Barthel, J., R. Neueder and A. Schröder

1997 'Temperature Dependence of Activity Coefficients and Gibbs Energies of Transfer of LiBr in Acetonitrile, Dimethyl Sulfoxide, and *N*,*N*-dimethylacetamide from EMF Measurements', *Can. J. Chem.* 75, 11, pp. 1500–1507, DOI: 10.1139/v97-180.

Barthel, J., R. Neueder, H. Poepke and H. Wittmann

1998 'Osmotic and Activity Coefficients of Nonaqueous Electrolyte Solutions. 1. Lithium Perchlorate in the Protic Solvents Methanol, Ethanol, and 2-propanol', *J. Solution Chem.* 27, 12, pp. 1055–1066, DOI: 10.1023/A:1022637316064.

1999a 'Osmotic Coefficients and Activity Coefficients of Nonaqueous Electrolyte Solutions. Part 2. Lithium Perchlorate in the Aprotic Solvents Acetone, Acetonitrile, Dimethoxyethane, and Dimethylcarbonate', *J. Solution Chem.* 28, 5, pp. 489–503, DOI: 10.1023/A:1022674613995.

1999b 'Osmotic Coefficients and Activity Coefficients of Nonaqueous Electrolyte Solutions. Part 4. Lithium Bromide, Tetrabutylammonium Bromide, and Tetrabutylammonium Perchlorate in Acetone', *J. Solution Chem.* 28, 12, pp. 1277–1287, DOI: 10.1023/A:1021791823158.

Barthel, J., R. Neueder and H. Wittmann

1999 'Osmotic Coefficients and Activity Coefficients of Nonaqueous Electrolyte Solutions. Part 3. Tetraalkylammonium Bromides in Ethanol and 2-propanol', *J. Solution Chem.* 28, 12, pp. 1263–1276, DOI: 10.1023/A:1021741006320.

Bonner, O. D.

1987 'The Colligative Properties of Certain Electrolytes and Non-electrolytes in Methanol', *J. Solution Chem.* 16, 4, pp. 307–314, DOI: 10.1007/BF00646122.

Bonner, O. D., Š. Paljk and C. Klofutar

1991 'Association Studies of Tetramethylguanidinium Perchlorate and Tetramethylguanidinium Chloride in Ethanol Solutions at 25 °C', *J. Solution Chem.* 20, 5, pp. 539–550, DOI: 10.1007/BF00650808.

Bonner, O. D., S. J. Kim and A. L. Torres

1969 'Comparison of the Osmotic and Activity Coefficients of Some Solutes in Structured Solvents', *J. Phys. Chem.* 73, 6, pp. 1968–1974, DOI: 10.1021/j100726a054.

Butler, J. N. and J. C. Synnott

1970 'Thermodynamics of Lithium Chloride in Dimethylformamide', *J. Am. Chem. Soc.* 92, 9, pp. 2602–2607, DOI: 10.1021/ja00712a002.

Crawford, J. M. and R. P. H. Gasser

1967 'Electrolyte Solutions in Dimethyl Sulphoxide. Part 3.— Rubidium Iodide', *Trans. Faraday Soc.* 63 (0 1967), pp. 2758–2764, DOI: 10.1039/TF9676302758.

Dunnett, J. S. and R. P. H. Gasser

1965 'Electrolyte Solutions in Dimethyl Sulphoxide. Part 1.— Lithium Chloride', *Trans. Faraday Soc.* 61 (0 1965), pp. 922–927, DOI: 10.1039/TF9656100922.

Garnsey, R. and J. E. Prue

1968 'Precise Cryoscopic Determination of Osmotic Coefficients for Solutions of Some Alkali Metal Salts in Dimethyl Sulphoxide and in Sulpholane', *Trans. Faraday Soc.* 64 (0 1968), pp. 1206–1218, DOI: 10.1039/TF9686401206.

Kim, S.-J., O. D. Bonner and D.-S. Shin

1971 'Solvent-solute Interactions in Dimethylsulfoxide', *J. Chem. Thermodyn.* 3, 4, pp. 411–417, DOI: 10.1016/S0021-9614(71)80024-1.

Kunz, W., J. Barthel, L. Klein, T. Cartailler, P. Turq and B. Reindl

1991 'Lithium Bromide in Acetonitrile: Thermodynamics, Theory, and Simulation', *J. Solution Chem.* 20, 9, pp. 875–891, DOI: 10.1007/BF01074950.

Kunz, W., P. Turq, P. Calmettes, J. Barthel and L. Klein

1992 '*n*-tetrapentylammonium Bromide in 2-propanol: Vapor Pressure and Small-angle Neutron Scattering Measurements', *J. Phys. Chem.* 96, 6, pp. 2743–2749, DOI: 10.1021/j100185a063.

Luksha, E. and C. M. Criss

1966 'Thermodynamic Properties of Nonaqueous Solutions. II. Free Energies, Entropies, and Activity Coefficients of Selected Alkali Metal Halides in Anhydrous N-Methylformamide', *J. Phys. Chem.* 70, 5, pp. 1496–1502, DOI: 10.1021/j100877a026.

Nasehzadeh, A., E. Noroozian and H. Omrani

2004 'Experimental and Theoretical Studies of Thermodynamics of Lithium Halide Solutions — Ethanol Mixtures', *J. Chem. Thermodyn.* 36, 3, pp. 245–252, DOI: 10.1016/j.jct.2003.12.002.

Nasirzadeh, K. and R. Neueder

2004a 'Measurement and Correlation of Osmotic Coefficients and Evaluation of Vapor Pressure for Electrolyte Solutions of $LiClO_4$ and $LiNO_3$ in Methanol at 25 °C', *J. Mol. Liq.* 113, 1, pp. 13–20, DOI: 10.1016/j.molliq.2004.02.028.

2004b 'Measurements and Correlation of Osmotic Coefficients and Evaluation of Vapor Pressure for Solutions of KCH_3COO and $NaCH_3COO$ in Methanol at 25 °C', *Acta Chim. Slov.* 51, 1, pp. 117–126, http://acta-arhiv.chem-soc.si/51/51-1-117.pdf.

Nasirzadeh, K., R. Neueder and W. Kunz

2004 'Vapor Pressures, Osmotic and Activity Coefficients of Electrolytes in Protic Solvents at Different Temperatures. 2. Lithium Bromide in Ethanol', *J. Solution Chem.* 33, 11, pp. 1429–1446, ISSN: 1572-8927, DOI: 10.1007/s10953-004-1057-9.

2005 'Vapor Pressures, Osmotic and Activity Coefficients of Electrolytes in Protic Solvents at Different Temperatures. 3. Lithium Bromide in 2-propanol', *J. Solution Chem.* 34, 1, pp. 9–24, ISSN: 1572-8927, DOI: 10.1007/s10953-005-2024-9.

Nasirzadeh, K., N. Papaiconomou, R. Neueder and W. Kunz

2004 'Vapor Pressures, Osmotic and Activity Coefficients of Electrolytes in Protic Solvents at Different Temperatures. 1. Lithium Bromide in Methanol', *J. Solution Chem.* 33, 3, pp. 227–245, DOI: 10.1023/B:JOSL.0000035357.18045.0d.

Nasirzadeh, K. and A. Salabat

2003 'Isopiestic Determination of Osmotic Coefficients and Evaluation of Vapor Pressures for Solutions of Sodium Bromide and Sodium Thiocyanate in Methanol at 25 °C', *J. Mol. Liq.* 106, 1, pp. 1–14, DOI: 10.1016/S0167-7322(03)00016-3.

Nasirzadeh, K. and M. T. Zafarani-Moattar

2004 'Isopiestic Determination of Osmotic Coefficients and Evaluation of Vapor Pressures for Solutions of KI, NH_4SCN and KSCN in Methanol at 25 °C', *J. Mol. Liq.* 111, 1, pp. 7–13, DOI: 10.1016/j.molliq.2003.08.021.

Pitzer, K. S.

1973 'Thermodynamics of Electrolytes. I. Theoretical Basis and General Equations', *J. Phys. Chem.* 77, 2, pp. 268–277, DOI: 10.1021/j100621a026.

Pitzer, K. S. and G. Mayorga

1973 'Thermodynamics of Electrolytes. II. Activity and Osmotic Coefficients for Strong Electrolytes with One or Both Ions Univalent', *J. Phys. Chem.* 77, 19, pp. 2300–2308, DOI: 10.1021/j100638a009.

Safarov, J. T.

2006 'Vapor Pressures of Lithium Bromide or Lithium Chloride and Ethanol Solutions', *Fluid Phase Equilib.* 243, 1-2, pp. 38–44, DOI: 10.1016/j.fluid.2006.02.012.

Salomon, M.

1969a 'Thermodynamics of LiBr in Anhydrous Dimethyl Sulfoxide', *J. Electrochem. Soc.* 116, 10, pp. 1392–1394, DOI: 10.1149/1.2411530.

1969b 'Thermodynamics of Lithium Chloride and Lithium Bromide in Propylene Carbonate', *J. Phys. Chem.* 73, 10, pp. 3299–3306, DOI: 10.1021/j100844a026.

1970a 'Thermodynamics of Lithium and Potassium Iodide in Anhydrous Propylene Carbonate', *J. Electroanal. Chem. Interfacial Electrochem.* 26, 2, pp. 319–329, DOI: 10.1016/S0022-0728(70)80315-1.

1970b 'Thermodynamics of Lithium Iodide in Anhydrous Dimethyl Sulfoxide', *J. Electrochem. Soc.* 117, 3, pp. 325–328, DOI: 10.1149/1.2407502.

1970c 'Thermodynamics of Sodium Iodide in Propylene Carbonate', *J. Electroanal. Chem. Interfacial Electrochem.* 25, 1, pp. 1–8, DOI: 10.1016/S0022-0728(70)80033-X.

Wood, R. H. and R. W. Kreis

1971 'Freezing Points, Osmotic Coefficients, and Activity Coefficients of Salts in *N*-Methylacetamide. II. Tetraalkylammonium Halides and Some Alkali Metal Formates, Acetates, and Propionates', *J. Phys. Chem.* 75, 15, pp. 2319–2325, DOI: 10.1021/j100684a015.

Wood, R. H., R. K. Wicker and R. W. Kreis

1971 'Freezing Points, Osmotic Coefficients, and Activity Coefficients of Salts in *N*-Methylacetamide. I. Alkali Halides and Nitrates', *J. Phys. Chem.* 75, 15, pp. 2313–2318, DOI: 10.1021/j100684a014.

Wood, R. H. and Q. D. Craft

1978 'Freezing Points, Osmotic Coefficients, and Activity Coefficients of Some Salts in Ethylene Carbonate: A High Dielectric Constant Solvent without Hydrogen Bonding', *J. Solution Chem.* 7, 11, pp. 799–812, DOI: 10.1007/BF00650809.

Zafarani-Moattar, M. T. and M. Aria

2001 'Isopiestic Determination of Osmotic and Activity Coefficients for Solutions Of ce LiCl, LiBr, and $LiNO_3$ in 2-propanol at 25 °C', *J. Solution Chem.* 30, 4, pp. 351–363, DOI: 10.1023/A:1010327206913.

Zafarani-Moattar, M. T. and J. Jahanbin-Sardroodi

1999 'Isopiestic Determination of Osmotic Coefficients and Evaluation of Vapor Pressures for Electrolyte Solutions of Some Lithium Salts in Ethanol', *Fluid Phase Equilib.* 166, 2, pp. 207–223, DOI: 10.1016/S0378-3812(99)00293-9.

Zafarani-Moattar, M. T. and K. Nasirzade

1998 'Osmotic Coefficient of Methanol + LiCl, + LiBr, and + $LiCH_3COO$ at 25 °C', *J. Chem. Eng. Data*, 43, 2, pp. 215–219, DOI: 10.1021/je970193e.

D SOLUBILITY DATA COLLECTION

Table 36: Solubility $\mathcal{S}$ of salts in water and non-aqueous solvents. The solubility is expressed in miscellaneous units: w_{salt} stands for the mass fraction of salt; $mol\,kg^{-1}$, g/100g and $g\,kg^{-1}$ refer to the mass of the solvent, whereas $mol\,dm^{-3}$ and $g\,l^{-1}$ refer to the total volume of the solution. Where the units are by volume, the density of the solution is included.

solvent	electrolyte	$\mathcal{S}$	type/units	ρ / g cm^{-3}	t/°C	reference
ACE	CsBr	0.000 040 3	w_{salt}		18	H. Stephen et al., 1963a
ACE	CsCl	0.000 32	w_{salt}		25	H. Stephen et al., 1963a
ACE	$CsClO_4$	0.0015	w_{salt}		25	H. Stephen et al., 1963a
ACE	$CsClO_4$	0.011 83	w_{salt}		25	H. Stephen et al., 1963a
ACE	CsF	0.000 007 7	w_{salt}		18	H. Stephen et al., 1963a
ACE	CsI	0.002	w_{salt}		25	H. Stephen et al., 1963a
ACE	Et_4NBr	0.001 93	w_{salt}		20	H. Stephen et al., 1963a
ACE	Et_4NCl	0.003 37	w_{salt}		20	H. Stephen et al., 1963a
ACE	Et_4NI	0.001 98	w_{salt}		20	H. Stephen et al., 1963a
ACE	KBr	0.000 23	w_{salt}		25	H. Stephen et al., 1963a
ACE	KCl	0.087	w_{salt}		18	H. Stephen et al., 1963a
ACE	$KClO_4$	0.001 55	w_{salt}		25	H. Stephen et al., 1963a
ACE	KF	0.022	w_{salt}		18	H. Stephen et al., 1963a
ACE	KI	0.013 02	w_{salt}		25	H. Stephen et al., 1963a
ACE	KI	0.0284	w_{salt}		25	H. Stephen et al., 1963a
ACE	KSCN	0.172	w_{salt}		22	H. Stephen et al., 1963a
ACE	LiBr	0.154	w_{salt}		20	H. Stephen et al., 1963a
ACE	LiCl	0.2556	$mol\,kg^{-1}$		25	Li et al., 2010
ACE	LiCl	0.0117	w_{salt}		20	H. Stephen et al., 1963a
ACE	$LiClO_4$	12.83	$mol\,kg^{-1}$		25	Chan et al., 1996
ACE	$LiClO_4$	0.5772	w_{salt}		25	H. Stephen et al., 1963a
ACE	LiF	0.0033	w_{salt}		18	H. Stephen et al., 1963a
ACE	LiI	0.2985	w_{salt}		18	H. Stephen et al., 1963a
ACE	$LiNO_3$	0.2367	w_{salt}		20	H. Stephen et al., 1963a
ACE	NaBr	0.001 22	w_{salt}		25	H. Stephen et al., 1963a
ACE	NaCl	0.000 003 2	w_{salt}		18	H. Stephen et al., 1963a
ACE	$NaClO_4$	4.228	$mol\,kg^{-1}$		25	Chan et al., 1996
ACE	$NaClO_4$	4.422	$mol\,kg^{-1}$		25	Chan et al., 1996
ACE	$NaClO_4$	0.341	w_{salt}		25	H. Stephen et al., 1963a
ACE	NaF	0.000 01	w_{salt}		18	H. Stephen et al., 1963a
ACE	NaI	0.286	w_{salt}		25	H. Stephen et al., 1963a
ACE	NaOAc	0.0005	w_{salt}		15	H. Stephen et al., 1963a
ACE	NaSCN	0.985	$mol\,kg^{-1}$		25	Hála, 2004
ACE	NaSCN	0.0641	w_{salt}		18.8	H. Stephen et al., 1963a
ACE	NH_4ClO_4	0.0221	w_{salt}		25	H. Stephen et al., 1963a
ACE	Pr_4NI	39.44	$g\,l^{-1}$	0.8049	25	H. Stephen et al., 1963a
ACE	RbBr	0.000 050 5	w_{salt}		18	H. Stephen et al., 1963a
ACE	RbCl	0.000 002 1	w_{salt}		18	H. Stephen et al., 1963a
ACE	$RbClO_4$	0.000 95	w_{salt}		25	H. Stephen et al., 1963a
ACE	RbF	0.000 003 6	w_{salt}		18	H. Stephen et al., 1963a
ACE	RbI	0.004 92	w_{salt}		25	H. Stephen et al., 1963a
ACE	RbI	0.006 74	w_{salt}		25	H. Stephen et al., 1963a
ACE	RbI	0.0072	w_{salt}		25	H. Stephen et al., 1963a
BuOH	Bu_4NI	0.3838	w_{salt}		25	H. Stephen et al., 1963b
BuOH	CsCl	0.006 21	w_{salt}		25	H. Stephen et al., 1963a
BuOH	$CsClO_4$	0.000 06	w_{salt}		25	H. Stephen et al., 1963a
BuOH	$CsClO_4$	0.000 46	w_{salt}		25	H. Stephen et al., 1963a
BuOH	Et_4NBr	0.2052	w_{salt}		25	H. Stephen et al., 1963b
BuOH	Et_4NI	0.0019	w_{salt}		25	H. Stephen et al., 1963b
BuOH	KBr	0.000 112	w_{salt}		20	H. Stephen et al., 1963a
BuOH	KBr	0.000 132	w_{salt}		25	H. Stephen et al., 1963a
BuOH	KCl	0.000 03	w_{salt}		25	H. Stephen et al., 1963a
BuOH	KCl	0.000 082 2	w_{salt}		20	H. Stephen et al., 1963a
BuOH	$KClO_4$	0.000 045	w_{salt}		25	H. Stephen et al., 1963a

solvent	electrolyte	S	type/units	ρ / g cm^{-3}	t/°C	reference
BuOH	KI	0.002	w_{salt}		25	H. Stephen et al., 1963a
BuOH	KSCN	0.09	mol kg^{-1}		25	Hála, 2004
BuOH	LiCl	0.0956	w_{salt}		25	H. Stephen et al., 1963a
BuOH	LiCl	0.1149	w_{salt}		25	H. Stephen et al., 1963a
BuOH	$LiClO_4$	79.31	g/100g		25	Chan et al., 1996
BuOH	$LiClO_4$	0.4423	w_{salt}		25	H. Stephen et al., 1963a
BuOH	Me_4NBr	0.000 62	w_{salt}		25	H. Stephen et al., 1963b
BuOH	Me_4NCl	0.042	w_{salt}		25	H. Stephen et al., 1963b
BuOH	NaBr	0.002 45	w_{salt}		25	H. Stephen et al., 1963a
BuOH	NaCl	0.000 05	w_{salt}		25	H. Stephen et al., 1963a
BuOH	NaCl	0.000 14	w_{salt}		25	H. Stephen et al., 1963a
BuOH	$NaClO_4$	0.0183	w_{salt}		25	H. Stephen et al., 1963a
BuOH	NaF	0.000 03	w_{salt}		20	H. Stephen et al., 1963a
BuOH	NaI	0.1776	w_{salt}		25	H. Stephen et al., 1963a
BuOH	NH_4ClO_4	0.000 17	w_{salt}		25	H. Stephen et al., 1963a
BuOH	Pr_4NBr	0.4575	w_{salt}		25	H. Stephen et al., 1963b
BuOH	Pr_4NI	0.061	w_{salt}		25	H. Stephen et al., 1963b
BuOH	$RbClO_4$	0.000 02	w_{salt}		25	H. Stephen et al., 1963a
2BuOH	KBr	0.000 044	w_{salt}		25	H. Stephen et al., 1963a
2BuOH	KCl	0.000 008 4	w_{salt}		25	H. Stephen et al., 1963a
2BuOH	KI	0.000 582	w_{salt}		25	H. Stephen et al., 1963a
2BuOH	$LiClO_4$	77.1	g/100g		25	Chan et al., 1996
2BuOH	NaBr	0.000 341	w_{salt}		25	H. Stephen et al., 1963a
2BuOH	NaCl	0.000 004 7	w_{salt}		25	H. Stephen et al., 1963a
2BuOH	NaI	0.1305	w_{salt}		25	H. Stephen et al., 1963a
i-BuOH	KBr	0.000 076	w_{salt}		25	H. Stephen et al., 1963a
i-BuOH	KCl	0.000 02	w_{salt}		25	H. Stephen et al., 1963a
i-BuOH	KCl	0.000 032 6	w_{salt}		20	H. Stephen et al., 1963a
i-BuOH	$KClO_4$	0.000 05	w_{salt}		25	H. Stephen et al., 1963a
i-BuOH	KI	0.000 954	w_{salt}		25	H. Stephen et al., 1963a
i-BuOH	$LiClO_4$	58.05	g/100g		25	Chan et al., 1996
i-BuOH	$LiClO_4$	0.3673	w_{salt}		25	H. Stephen et al., 1963a
i-BuOH	NaBr	0.000 95	w_{salt}		25	H. Stephen et al., 1963a
i-BuOH	NaCl	0.000 02	w_{salt}		25	H. Stephen et al., 1963a
i-BuOH	$NaClO_4$	0.0078	w_{salt}		25	H. Stephen et al., 1963a
i-BuOH	NaI	0.1502	w_{salt}		25	H. Stephen et al., 1963a
i-BuOH	NH_4ClO_4	0.001 27	w_{salt}		25	H. Stephen et al., 1963a
i-BuOH	$RbClO_4$	0.000 04	w_{salt}		25	H. Stephen et al., 1963a
t-BuOH	$LiClO_4$	0.6	g/100g		25	Chan et al., 1996
t-BuOH	$LiClO_4$	0.06	mol kg^{-1}		25	Chan et al., 1996
DMA	KBr	3.9	g kg^{-1}		25	Scrosati et al., 1980
DMA	KCl	0.11	g kg^{-1}		25	Scrosati et al., 1980
DMA	KI	15.4	g kg^{-1}		25	Scrosati et al., 1980
DMA	KSCN	107	g l^{-1}		25	Scrosati et al., 1980
DMA	LiBr	262	g kg^{-1}		25	Scrosati et al., 1980
DMA	LiCl	88	g kg^{-1}		25	Scrosati et al., 1980
DMA	LiI	43	g l^{-1}		25	Scrosati et al., 1980
DMA	LiSCN	4.55	mol kg^{-1}		25	Hála, 2004
DMA	NaBr	65.1	g kg^{-1}		25	Scrosati et al., 1980
DMA	NaCl	0.2	g kg^{-1}		25	Scrosati et al., 1980
DMA	NaI	346	g kg^{-1}		25	Scrosati et al., 1980
DMA	NaSCN	144	g l^{-1}		25	Scrosati et al., 1980
DMF	CsBr	5.58	g kg^{-1}		25	Scrosati et al., 1980
DMF	CsCl	0.52	g kg^{-1}		25	Scrosati et al., 1980
DMF	CsI	36.7	g kg^{-1}		25	Scrosati et al., 1980
DMF	KBr	8.2	g kg^{-1}		25	Scrosati et al., 1980
DMF	KBr	9.1	g kg^{-1}		25	Labban et al., 1991
DMF	KCl	0.182	g kg^{-1}		25	Labban et al., 1991
DMF	KCl	0.185	g kg^{-1}		25	Scrosati et al., 1980
DMF	KF	0.021	g kg^{-1}		25	Labban et al., 1991
DMF	KI	273	g kg^{-1}		25	Scrosati et al., 1980
DMF	$LiClO_4$	7.05	mol kg^{-1}		25	Chan et al., 1996
DMF	LiF	1.39	g kg^{-1}		25	Scrosati et al., 1980
DMF	NaBr	118	g kg^{-1}		25	Scrosati et al., 1980
DMF	NaCl	0.36	g kg^{-1}		25	Scrosati et al., 1980
DMF	NaF	1.96	g kg^{-1}		25	Scrosati et al., 1980

solvent	electrolyte	S	type/units	ρ/g cm^{-3}	t/°C	reference
DMF	NaSCN	295	g kg^{-1}		25	Scrosati et al., 1980
DMF	NH_4Br	147	g kg^{-1}		25	Scrosati et al., 1980
DMF	NH_4I	459	g kg^{-1}		25	Scrosati et al., 1980
DMF	NH_4SCN	154	g kg^{-1}		25	Scrosati et al., 1980
DMSO	CsCl	0.0373	mol kg^{-1}		25	Butler, 1967
DMSO	KBr	50.3	g kg^{-1}		25	Labban et al., 1991
DMSO	KBr	0.5	mol kg^{-1}		25	Butler, 1967
DMSO	KCl	1.96	g kg^{-1}		25	Labban et al., 1991
DMSO	KCl	0.0225	mol kg^{-1}		25	Butler, 1967
DMSO	$KClO_4$	2.5	mol kg^{-1}		25	Butler, 1967
DMSO	KF	0.023	g kg^{-1}		25	Labban et al., 1991
DMSO	KI	2.5	mol kg^{-1}		25	Butler, 1967
DMSO	LiBr	3.3	mol kg^{-1}		25	Butler, 1967
DMSO	LiCl	2.13	mol kg^{-1}		25	Butler, 1967
DMSO	LiCl	2.2	mol kg^{-1}		25	Butler, 1967
DMSO	$LiClO_4$	21.1	g/100g		25	Chan et al., 1996
DMSO	$LiClO_4$	2.65	mol kg^{-1}		25	Butler, 1967
DMSO	$LiClO_4$	2.7	mol kg^{-1}		25	Butler, 1967
DMSO	$LiClO_4$	2.7	mol kg^{-1}		25	Chan et al., 1996
DMSO	LiI	1.22	mol kg^{-1}		25	Butler, 1967
DMSO	LiI	2.8	mol kg^{-1}		25	Butler, 1967
DMSO	NaBr	0.55	mol kg^{-1}		25	Butler, 1967
DMSO	NaCl	0.078	mol kg^{-1}		25	Butler, 1967
DMSO	NaCl	0.08	mol kg^{-1}		25	Butler, 1967
DMSO	$NaClO_4$	1.8	mol kg^{-1}		25	Butler, 1967
DMSO	$NaClO_4$	1.8	mol kg^{-1}		25	Chan et al., 1996
DMSO	NaI	1	mol kg^{-1}		25	Butler, 1967
DMSO	RbCl	0.0356	mol kg^{-1}		25	Butler, 1967
EC	KBr	0.0185	mol kg^{-1}		40	Peruzzi, Ninham et al., 2012
EC	KCl	0.0115	mol kg^{-1}		40	Peruzzi, Ninham et al., 2012
EC	$KClO_4$	0.2779	mol kg^{-1}		40	Peruzzi, Ninham et al., 2012
EC	KF	0.0045	mol kg^{-1}		40	Peruzzi, Ninham et al., 2012
EC	KI	0.671	mol kg^{-1}		40	Harris, 1958
EC	KI	0.6969	mol kg^{-1}		40	Peruzzi, Ninham et al., 2012
EC	KI	0.8512	mol kg^{-1}		25	Peruzzi, Ninham et al., 2012
EC	KNO_3	0.0248	mol kg^{-1}		40	Peruzzi, Ninham et al., 2012
EC	KSCN	0.0034	mol kg^{-1}		25	Peruzzi, Ninham et al., 2012
EC	$LiClO_4$	96.7	g/100g		25	Chan et al., 1996
EC	Me_4NI	2.4	g l^{-1}	1.0678	25	H. Stephen et al., 1963a
EC	NaBr	0.03	mol kg^{-1}		40	Harris, 1958
EC	NaI	2.51	mol kg^{-1}		40	Harris, 1958
EG	KBr	0.1342	w_{salt}		25	H. Stephen et al., 1963b
EG	KI	0.3301	w_{salt}		25	H. Stephen et al., 1963a
EG	KI	0.3329	w_{salt}		25	H. Stephen et al., 1963b
EG	LiI	0.28	w_{salt}		15.3	H. Stephen et al., 1963a
EG	NaCl	0.317	w_{salt}		14.8	H. Stephen et al., 1963a
EG	$NaClO_4$	6.166	mol kg^{-1}		25	Chan et al., 1996
EtOH	CsCl	0.076 97	w_{salt}		25	H. Stephen et al., 1963a
EtOH	$CsClO_4$	0.000 11	w_{salt}		25	H. Stephen et al., 1963a
EtOH	$CsClO_4$	0.000 93	w_{salt}		25	H. Stephen et al., 1963a
EtOH	Et_4NBr	0.346	w_{salt}		20	H. Stephen et al., 1963a
EtOH	Et_4NCl	0.576	w_{salt}		20	H. Stephen et al., 1963a
EtOH	Et_4NI	0.009 14	w_{salt}		20	H. Stephen et al., 1963a
EtOH	KBr	0.001 35	w_{salt}		25	H. Stephen et al., 1963a
EtOH	KBr	0.001 42	w_{salt}		25	H. Stephen et al., 1963a
EtOH	KBr	0.004 53	w_{salt}		20	H. Stephen et al., 1963a
EtOH	KCl	0.0064	mol kg^{-1}		25	Li et al., 2010
EtOH	KCl	0.000 22	w_{salt}		25	H. Stephen et al., 1963a
EtOH	KCl	0.000 294	w_{salt}		25	H. Stephen et al., 1963a
EtOH	KCl	0.000 34	w_{salt}		25	Pinho et al., 2005
EtOH	$KClO_4$	0.000 12	w_{salt}		25	H. Stephen et al., 1963a
EtOH	KF	0.0191	mol kg^{-1}		25	Labban et al., 1997
EtOH	KF	0.001 06	w_{salt}		20	H. Stephen et al., 1963a
EtOH	KI	0.0172	w_{salt}		20.5	H. Stephen et al., 1963a
EtOH	KI	0.0184	w_{salt}		25	H. Stephen et al., 1963a
EtOH	KI	0.019 22	w_{salt}		25	H. Stephen et al., 1963a

solvent	electrolyte	S	type/units	ρ / g cm^{-3}	t/°C	reference
EtOH	KI	0.0211	w_{salt}		25	H. Stephen et al., 1963a
EtOH	KSCN	0.53	mol kg^{-1}		25	Hála, 2004
EtOH	LiBr	0.4189	w_{salt}		25	H. Stephen et al., 1963a
EtOH	LiCl	5.84	mol kg^{-1}		25	Li et al., 2010
EtOH	LiCl	0.0248	w_{salt}		25	H. Stephen et al., 1963a
EtOH	LiCl	0.1957	w_{salt}		20	H. Stephen et al., 1963a
EtOH	$LiClO_4$	151.76	g/100g		25	Chan et al., 1996
EtOH	$LiClO_4$	0.6028	w_{salt}		25	H. Stephen et al., 1963a
EtOH	LiI	0.715	w_{salt}		25	H. Stephen et al., 1963a
EtOH	Me_4NI	0.9	g l^{-1}	0.7894	25	H. Stephen et al., 1963a
EtOH	NaBr	0.022 61	w_{salt}		25	H. Stephen et al., 1963a
EtOH	NaBr	0.023 49	w_{salt}		25	H. Stephen et al., 1963a
EtOH	NaBr	0.024 96	w_{salt}		25	Pinho et al., 2005
EtOH	NaCl	0.000 55	w_{salt}		25	Pinho et al., 2005
EtOH	NaCl	0.000 648	w_{salt}		25	H. Stephen et al., 1963a
EtOH	NaCl	0.000 65	w_{salt}		25	H. Stephen et al., 1963a
EtOH	NaCl	0.001 146	w_{salt}		20	H. Stephen et al., 1963a
EtOH	NaCl	0.001 76	w_{salt}		20	H. Stephen et al., 1963a
EtOH	$NaClO_4$	0.1282	w_{salt}		25	H. Stephen et al., 1963a
EtOH	NaF	0.000 95	w_{salt}		20	H. Stephen et al., 1963a
EtOH	NaI	0.2986	w_{salt}		25	H. Stephen et al., 1963a
EtOH	NaI	0.3023	w_{salt}		25	H. Stephen et al., 1963a
EtOH	NaI	0.3151	w_{salt}		25	H. Stephen et al., 1963a
EtOH	$NaNO_3$	0.000 36	w_{salt}		25	H. Stephen et al., 1963a
EtOH	NaSCN	0.1552	w_{salt}		18.8	H. Stephen et al., 1963a
EtOH	NaSCN	0.1712	w_{salt}		25	Hála, 2004
EtOH	NH_4Br	0.0312	w_{salt}		19	H. Stephen et al., 1963a
EtOH	NH_4ClO_4	0.018 72	w_{salt}		25	H. Stephen et al., 1963a
EtOH	NH_4SCN	0.1907	w_{salt}		18.45	H. Stephen et al., 1963a
EtOH	Pr_4NI	202.9	g l^{-1}	0.8716	25	H. Stephen et al., 1963a
EtOH	RbCl	0.000 78	w_{salt}		25	H. Stephen et al., 1963a
EtOH	$RbClO_4$	0.000 09	w_{salt}		25	H. Stephen et al., 1963a
EtOH	RbSCN	0.197	mol kg^{-1}		25	Hála, 2004
FA	CsBr	152.4	g l^{-1}		25	Scrosati et al., 1980
FA	CsCl	91.5	g l^{-1}		25	Scrosati et al., 1980
FA	KBr	215.3	g kg^{-1}		25	Scrosati et al., 1980
FA	KBr	1.26	mol kg^{-1}		25	Labban et al., 1997
FA	KCl	62.3	g kg^{-1}		25	Scrosati et al., 1980
FA	KCl	0.995	mol kg^{-1}		25	Labban et al., 1997
FA	KF	0.869	mol kg^{-1}		25	Labban et al., 1997
FA	KI	683	g kg^{-1}		25	Scrosati et al., 1980
FA	KSCN	1420	g kg^{-1}		25	Scrosati et al., 1980
FA	LiBr	600	g kg^{-1}		25	Scrosati et al., 1980
FA	LiCl	266	g kg^{-1}		25	Scrosati et al., 1980
FA	$LiClO_4$	13.36	mol kg^{-1}		25	Chan et al., 1996
FA	NaBr	353.4	g kg^{-1}		25	Scrosati et al., 1980
FA	NaBr	3.3134	mol kg^{-1}		25	Hernández-Luis et al., 2016
FA	NaCl	93.8	g kg^{-1}		25	Scrosati et al., 1980
FA	NaCl	1.555	mol kg^{-1}		25	Hernández-Luis et al., 2016
FA	NaF	1.1	g l^{-1}		25	Scrosati et al., 1980
FA	NaF	0.002	mol kg^{-1}		25	Hernández-Luis et al., 2016
FA	NaI	600	g kg^{-1}		25	Scrosati et al., 1980
FA	NaI	3.7767	mol kg^{-1}		25	Hernández-Luis et al., 2016
FA	NaSCN	1435	g kg^{-1}		25	Scrosati et al., 1980
FA	NH_4Br	361	g kg^{-1}		25	Scrosati et al., 1980
FA	NH_4Cl	109.5	g kg^{-1}		25	Scrosati et al., 1980
FA	NH_4I	1043.5	g kg^{-1}		25	Scrosati et al., 1980
FA	NH_4SCN	1015.5	g kg^{-1}		25	Scrosati et al., 1980
FA	RbBr	274.5	g l^{-1}		25	Scrosati et al., 1980
MeCN	CsBr	0.0014	w_{salt}		25	H. Stephen et al., 1963a
MeCN	CsCl	0.000 084	w_{salt}		25	H. Stephen et al., 1963a
MeCN	CsI	0.0098	w_{salt}		25	H. Stephen et al., 1963a
MeCN	Et_4NBr	0.0959	w_{salt}		25	H. Stephen et al., 1963a
MeCN	KBr	0.19	g kg^{-1}		25	Labban et al., 1991
MeCN	KBr	0.000 24	w_{salt}		25	H. Stephen et al., 1963a
MeCN	KCl	0.006	g kg^{-1}		25	Labban et al., 1991
MeCN	KCl	0.000 024	w_{salt}		25	H. Stephen et al., 1963a

solvent	electrolyte	S	type/units	ρ/g cm^{-3}	t/°C	reference
MeCN	KF	0.004	g kg^{-1}		25	Labban et al., 1991
MeCN	KF	0.000 024	w_{salt}		25	H. Stephen et al., 1963a
MeCN	KI	0.020 03	w_{salt}		24	H. Stephen et al., 1963a
MeCN	KI	0.0206	w_{salt}		25	H. Stephen et al., 1963a
MeCN	KSCN	0.1023	w_{salt}		18	H. Stephen et al., 1963a
MeCN	LiBr	0.081	w_{salt}		25	H. Stephen et al., 1963a
MeCN	LiCl	0.0014	w_{salt}		25	H. Stephen et al., 1963a
MeCN	$LiClO_4$	12.99	g/100 g		25	Chan et al., 1996
MeCN	$LiClO_4$	13.6	g/100 g		25	Chan et al., 1996
MeCN	$LiClO_4$	14.46	g/100 g		25	Chan et al., 1996
MeCN	$LiClO_4$	1.4	mol kg^{-1}		25	Chan et al., 1996
MeCN	$LiClO_4$	1.53	mol kg^{-1}		25	Chan et al., 1996
MeCN	$LiClO_4$	1.5419	mol kg^{-1}		24.2	Chan et al., 1996
MeCN	LiI	0.6063	w_{salt}		25	H. Stephen et al., 1963a
MeCN	$LiNO_3$	0.029	w_{salt}		25	H. Stephen et al., 1963a
MeCN	NaBr	0.0004	w_{salt}		25	H. Stephen et al., 1963a
MeCN	NaCl	0.000 002 5	w_{salt}		25	H. Stephen et al., 1963a
MeCN	NaF	0.000 03	w_{salt}		25	H. Stephen et al., 1963a
MeCN	NaI	0.1993	w_{salt}		25	H. Stephen et al., 1963a
MeCN	NaOAc	0.0014	mol dm^{-3}	0.7675	25	Soleymani et al., 2013
MeCN	NH_4SCN	0.988	mol kg^{-1}		18	Hála, 2004
MeCN	Pr_4NI	186.9	g l^{-1}	0.8584	25	H. Stephen et al., 1963a
MeCN	RbBr	0.000 47	w_{salt}		25	H. Stephen et al., 1963a
MeCN	RbCl	0.000 036	w_{salt}		25	H. Stephen et al., 1963a
MeCN	RbI	0.0135	w_{salt}		25	H. Stephen et al., 1963a
MeCN	RbI	0.0165	w_{salt}		25	H. Stephen et al., 1963a
$MeNO_2$	KI	0.003 07	w_{salt}		25	H. Stephen et al., 1963a
$MeNO_2$	LiI	0.252	w_{salt}		25	H. Stephen et al., 1963a
$MeNO_2$	Me_4NI	3.8	g l^{-1}	1.1285	25	H. Stephen et al., 1963a
$MeNO_2$	Pr_4NI	222.4	g l^{-1}	1.158	25	H. Stephen et al., 1963a
$MeNO_2$	RbI	0.005 18	w_{salt}		25	H. Stephen et al., 1963a
MeOH	Bu_4NI	0.7195	w_{salt}		25	H. Stephen et al., 1963b
MeOH	CsBr	2.12	g/100 g		23.3	Stenger, 1996
MeOH	CsBr	0.022	w_{salt}		25	H. Stephen et al., 1963a
MeOH	CsCl	3.26	g/100 g		23.4	Stenger, 1996
MeOH	CsCl	0.0292	w_{salt}		25	H. Stephen et al., 1963a
MeOH	CsCl	0.2659	w_{salt}		25	H. Stephen et al., 1963a
MeOH	$CsClO_4$	0.086	g/100 g		23.3	Stenger, 1996
MeOH	$CsClO_4$	0.000 93	w_{salt}		25	H. Stephen et al., 1963a
MeOH	$CsClO_4$	0.007 42	w_{salt}		25	H. Stephen et al., 1963a
MeOH	CsF	152	g/100 g		22.2	Stenger, 1996
MeOH	CsI	3.45	g/100 g		22	Stenger, 1996
MeOH	CsI	0.0365	w_{salt}		25	H. Stephen et al., 1963a
MeOH	$CsNO_3$	0.309	g/100 g		23.5	Stenger, 1996
MeOH	Et_4NBr	0.583	w_{salt}		20	H. Stephen et al., 1963a
MeOH	Et_4NBr	0.583	w_{salt}		20	H. Stephen et al., 1963a
MeOH	Et_4NBr	0.5985	w_{salt}		25	H. Stephen et al., 1963b
MeOH	Et_4NCl	0.699	w_{salt}		20	H. Stephen et al., 1963a
MeOH	Et_4NCl	0.699	w_{salt}		20	H. Stephen et al., 1963a
MeOH	Et_4NI	0.0905	w_{salt}		20	H. Stephen et al., 1963a
MeOH	Et_4NI	0.0905	w_{salt}		20	H. Stephen et al., 1963a
MeOH	Et_4NI	0.1103	w_{salt}		25	H. Stephen et al., 1963b
MeOH	KBr	2.08	g/100 g		25	Harner et al., 1963
MeOH	KBr	0.0205	w_{salt}		25	H. Stephen et al., 1963a
MeOH	KBr	0.0207	w_{salt}		25	H. Stephen et al., 1963a
MeOH	KBr	0.0212	w_{salt}		25	H. Stephen et al., 1963a
MeOH	KCl	0.5335	g/100 g		25	Harner et al., 1963
MeOH	KCl	0.0736	mol kg^{-1}		25	Li et al., 2010
MeOH	KCl	0.0052	w_{salt}		25	H. Stephen et al., 1963a
MeOH	KCl	0.0053	w_{salt}		25	H. Stephen et al., 1963a
MeOH	KCl	0.005 363	w_{salt}		25	H. Stephen et al., 1963a
MeOH	KCl	0.005 39	w_{salt}		25	Pinho et al., 2005
MeOH	KCl	0.008 26	w_{salt}		20	H. Stephen et al., 1963a
MeOH	$KClO_4$	0.001 05	w_{salt}		25	H. Stephen et al., 1963a
MeOH	KF	2.286	g/100 g		25	Harner et al., 1963
MeOH	KF	10.3	g/100 g		23.4	Stenger, 1996
MeOH	KF	0.001 92	w_{salt}		20	H. Stephen et al., 1963a
MeOH	KF	0.0926	w_{salt}		25	H. Stephen et al., 1963a

solvent	electrolyte	S	type/units	ρ / g cm^{-3}	t/°C	reference
MeOH	KI	17.07	g/100g		25	Harner et al., 1963
MeOH	KI	0.1453	w_{salt}		25	H. Stephen et al., 1963a
MeOH	KI	0.1456	w_{salt}		25	H. Stephen et al., 1963a
MeOH	KI	0.1497	w_{salt}		25	H. Stephen et al., 1963a
MeOH	KI	0.1528	w_{salt}		25	H. Stephen et al., 1963a
MeOH	KNO_3	0.357	g/100g		23.4	Stenger, 1996
MeOH	KNO_3	0.3795	g/100g		25	Harner et al., 1963
MeOH	KOAc	0.1951	w_{salt}		15	H. Stephen et al., 1963a
MeOH	KSCN	2.97	mol kg^{-1}		25	Hála, 2004
MeOH	LiBr	34.29	g/100g		25	Harner et al., 1963
MeOH	LiBr	120	g/100g		22.9	Stenger, 1996
MeOH	LiBr	16.44	mol kg^{-1}		25	Li et al., 2010
MeOH	LiBr	0.5833	w_{salt}		25	H. Stephen et al., 1963a
MeOH	LiCl	20.98	g/100g		25	Harner et al., 1963
MeOH	LiCl	41.8	g/100g		23.2	Stenger, 1996
MeOH	LiCl	10.28	mol kg^{-1}		25	Li et al., 2010
MeOH	LiCl	0.2908	w_{salt}		25	H. Stephen et al., 1963a
MeOH	LiCl	0.2975	w_{salt}		25	H. Stephen et al., 1963a
MeOH	$LiClO_4$	175.6	g/100g		23.4	Stenger, 1996
MeOH	$LiClO_4$	182.25	g/100g		25	Chan et al., 1996
MeOH	$LiClO_4$	0.6457	w_{salt}		25	H. Stephen et al., 1963a
MeOH	LiF	0.0024	g/100g		23.2	Stenger, 1996
MeOH	LiF	0.0176	g/100g		25	Harner et al., 1963
MeOH	LiI	298	g/100g		23.2	Stenger, 1996
MeOH	LiI	0.631	w_{salt}		25	H. Stephen et al., 1963a
MeOH	LiI	0.7744	w_{salt}		25	H. Stephen et al., 1963a
MeOH	$LiNO_3$	42.95	g/100g		25	Harner et al., 1963
MeOH	$LiNO_3$	61.2	g/100g		23.2	Stenger, 1996
MeOH	LiOAc	0.233	w_{salt}		15	H. Stephen et al., 1963a
MeOH	Me_4NBr	0.0414	w_{salt}		25	H. Stephen et al., 1963b
MeOH	Me_4NCl	0.4062	w_{salt}		25	H. Stephen et al., 1963b
MeOH	Me_4NI	4.2	g l^{-1}	0.792	25	H. Stephen et al., 1963a
MeOH	Me_4NI	0.0039	w_{salt}		25	H. Stephen et al., 1963b
MeOH	Me_4NI	0.042	w_{salt}		25	H. Stephen et al., 1963a
MeOH	NaBr	16.09	g/100g		25	Harner et al., 1963
MeOH	NaBr	16.8	g/100g		23	Stenger, 1996
MeOH	NaBr	0.1479	w_{salt}		25	H. Stephen et al., 1963a
MeOH	NaBr	0.1482	w_{salt}		25	H. Stephen et al., 1963a
MeOH	NaBr	0.149 38	w_{salt}		25	Pinho et al., 2005
MeOH	NaCl	1.38	g/100g		25	Stenger, 1996
MeOH	NaCl	1.401	g/100g		25	Harner et al., 1963
MeOH	NaCl	0.238	mol kg^{-1}		25	Li et al., 2010
MeOH	NaCl	0.0129	w_{salt}		25	H. Stephen et al., 1963a
MeOH	NaCl	0.013 75	w_{salt}		25	Pinho et al., 2005
MeOH	NaCl	0.0138	w_{salt}		25	H. Stephen et al., 1963a
MeOH	NaCl	0.013 81	w_{salt}		25	H. Stephen et al., 1963a
MeOH	$NaClO_4$	51.4	g/100g		23.4	Stenger, 1996
MeOH	$NaClO_4$	0.3393	w_{salt}		25	H. Stephen et al., 1963a
MeOH	NaF	0.02	g/100g		22.7	Stenger, 1996
MeOH	NaF	0.0231	g/100g		25	Harner et al., 1963
MeOH	NaF	0.0003	w_{salt}		25	H. Stephen et al., 1963a
MeOH	NaF	0.004 13	w_{salt}		20	H. Stephen et al., 1963a
MeOH	NaForm	0.034	w_{salt}		15	H. Stephen et al., 1963a
MeOH	NaI	62.51	g/100g		25	Harner et al., 1963
MeOH	NaI	79.4	g/100g		23	Stenger, 1996
MeOH	NaI	0.4382	w_{salt}		25	H. Stephen et al., 1963a
MeOH	NaI	0.4461	w_{salt}		25	H. Stephen et al., 1963a
MeOH	NaI	0.4535	w_{salt}		25	H. Stephen et al., 1963a
MeOH	NaI	0.4746	w_{salt}		25	H. Stephen et al., 1963a
MeOH	$NaNO_3$	2.84	g/100g		23.1	Stenger, 1996
MeOH	$NaNO_3$	2.936	g/100g		25	Harner et al., 1963
MeOH	$NaNO_3$	0.0041	w_{salt}		25	H. Stephen et al., 1963a
MeOH	NaOAc	1.58	mol dm^{-3}	0.873	25	Soleymani et al., 2013
MeOH	NaOAc	0.1379	w_{salt}		15	H. Stephen et al., 1963a
MeOH	NaSCN	0.2859	w_{salt}		24.7	H. Stephen et al., 1963a
MeOH	NH_4Br	12.85	g/100g		23.5	Stenger, 1996
MeOH	NH_4Br	0.111	w_{salt}		19	H. Stephen et al., 1963a
MeOH	NH_4Cl	3.52	g/100g		23.5	Stenger, 1996
MeOH	NH_4Cl	0.0324	w_{salt}		19	H. Stephen et al., 1963a

solvent	electrolyte	S	type/units	ρ/g cm^{-3}	t/°C	reference
MeOH	NH_4ClO_4	6.67	g/100g		22.7	Stenger, 1996
MeOH	NH_4ClO_4	0.0641	w_{salt}		25	H. Stephen et al., 1963a
MeOH	NH_4F	2.61	g/100g		23.3	Stenger, 1996
MeOH	NH_4I	59.8	g/100g		23.4	Stenger, 1996
MeOH	NH_4NO_3	18.4	g/100g		23.4	Stenger, 1996
MeOH	NH_4OAc	0.0731	w_{salt}		15	H. Stephen et al., 1963a
MeOH	NH_4SCN	0.3711	w_{salt}		24.58	H. Stephen et al., 1963a
MeOH	Pr_4NBr	0.7288	w_{salt}		25	H. Stephen et al., 1963b
MeOH	Pr_4NI	564.2	g l^{-1}	1.0187	25	H. Stephen et al., 1963a
MeOH	Pr_4NI	0.5728	w_{salt}		25	H. Stephen et al., 1963b
MeOH	RbBr	2.48	g/100g		23.2	Stenger, 1996
MeOH	RbBr	0.0246	w_{salt}		25	H. Stephen et al., 1963a
MeOH	RbCl	1.36	g/100g		23.4	Stenger, 1996
MeOH	RbCl	0.0132	w_{salt}		25	H. Stephen et al., 1963a
MeOH	RbCl	0.0139	w_{salt}		25	H. Stephen et al., 1963a
MeOH	$RbClO_4$	0.054	g/100g		22.8	Stenger, 1996
MeOH	$RbClO_4$	0.0006	w_{salt}		25	H. Stephen et al., 1963a
MeOH	RbF	69.7	g/100g		23	Stenger, 1996
MeOH	RbI	10.8	g/100g		23.3	Stenger, 1996
MeOH	RbI	0.1	w_{salt}		25	H. Stephen et al., 1963a
MeOH	$RbNO_3$	0.46	g/100g		23.4	Stenger, 1996
MeOH	RbSCN	1.377	mol kg^{-1}		25	Hála, 2004
NMA	KBr	50.03	g kg^{-1}		40	Scrosati et al., 1980
NMA	KCl	9.58	g kg^{-1}		40	Scrosati et al., 1980
NMA	KI	316.6	g kg^{-1}		40	Scrosati et al., 1980
NMA	KSCN	210.88	g l^{-1}		40	Scrosati et al., 1980
NMA	LiCl	17.51	g l^{-1}		40	Scrosati et al., 1980
NMA	NaBr	192.31	g kg^{-1}		40	Scrosati et al., 1980
NMA	NaCl	21.09	g kg^{-1}		40	Scrosati et al., 1980
NMA	NaI	562.7	g kg^{-1}		40	Scrosati et al., 1980
NMA	NaSCN	295.1	g l^{-1}		40	Scrosati et al., 1980
NMA	NH_4Br	221.1	g kg^{-1}		40	Scrosati et al., 1980
NMA	NH_4Cl	50.93	g kg^{-1}		40	Scrosati et al., 1980
NMA	NH_4I	358	g l^{-1}		40	Scrosati et al., 1980
NMA	NH_4SCN	352.1	g l^{-1}		40	Scrosati et al., 1980
NMF	KBr	101.7	g kg^{-1}		25	Scrosati et al., 1980
NMF	KBr	0.468	mol kg^{-1}		25	Labban et al., 1997
NMF	KCl	22.4	g kg^{-1}		25	Scrosati et al., 1980
NMF	KCl	0.354	mol kg^{-1}		25	Labban et al., 1997
NMF	KF	0.616	mol kg^{-1}		25	Labban et al., 1997
NMF	KI	491	g kg^{-1}		25	Scrosati et al., 1980
NMF	KSCN	809	g kg^{-1}		25	Scrosati et al., 1980
NMF	NaBr	298	g kg^{-1}		25	Scrosati et al., 1980
NMF	NaBr	2.9286	mol kg^{-1}		25	Hernández-Luis et al., 2016
NMF	NaCl	32.6	g kg^{-1}		25	Scrosati et al., 1980
NMF	NaCl	0.55	mol kg^{-1}		25	Hernández-Luis et al., 2016
NMF	NaF	0.002	mol kg^{-1}		25	Hernández-Luis et al., 2016
NMF	NaI	787	g kg^{-1}		25	Scrosati et al., 1980
NMF	NaI	5.1973	mol kg^{-1}		25	Hernández-Luis et al., 2016
NMF	NaSCN	503	g kg^{-1}		25	Scrosati et al., 1980
NMF	NH_4Cl	58	g kg^{-1}		25	Scrosati et al., 1980
NMF	NH_4I	380	g kg^{-1}		25	Scrosati et al., 1980
NMF	NH_4SCN	744	g kg^{-1}		25	Scrosati et al., 1980
PC	CsBr	0.0098	mol dm^{-3}		25	Muhuri et al., 1993
PC	CsCl	0.0076	mol dm^{-3}		25	Muhuri et al., 1993
PC	$CsClO_4$	0.052	mol dm^{-3}		25	Muhuri et al., 1993
PC	KBr	0.003	mol dm^{-3}		25	Muhuri et al., 1993
PC	KBr	0.0006	mol kg^{-1}		25	Harris, 1958
PC	KBr	0.003 98	mol kg^{-1}		25	Peruzzi, Lo Nostro et al., 2015
PC	KCl	0.000 58	mol dm^{-3}		25	Muhuri et al., 1993
PC	KCl	0.000 367	mol kg^{-1}		25	Peruzzi, Lo Nostro et al., 2015
PC	KCl	0.0004	mol kg^{-1}		25	Harris, 1958
PC	$KClO_4$	0.017	mol dm^{-3}		25	Muhuri et al., 1993
PC	$KClO_4$	0.0457	mol kg^{-1}		25	Peruzzi, Lo Nostro et al., 2015
PC	KF	0.000 17	mol kg^{-1}		25	Peruzzi, Lo Nostro et al., 2015
PC	KI	0.221	mol kg^{-1}		25	Peruzzi, Lo Nostro et al., 2015
PC	KI	0.223	mol kg^{-1}		25	Harris, 1958

solvent	electrolyte	S	type/units	ρ / g cm^{-3}	t/°C	reference
PC	KSCN	1.09	mol kg^{-1}		25	Peruzzi, Lo Nostro et al., 2015
PC	LiBr	1.1	mol dm^{-3}		25	Muhuri et al., 1993
PC	LiBr	2.43	mol kg^{-1}		25	Harris, 1958
PC	LiCl	0.019	mol dm^{-3}		25	Muhuri et al., 1993
PC	LiCl	0.000 77	mol kg^{-1}		25	Harris, 1958
PC	$LiClO_4$	1.4	mol dm^{-3}		25	Muhuri et al., 1993
PC	LiI	1.365	mol kg^{-1}		25	Harris, 1958
PC	NaBr	0.0036	mol dm^{-3}		25	Muhuri et al., 1993
PC	NaBr	0.08	mol kg^{-1}		25	Harris, 1958
PC	NaCl	0.000 17	mol dm^{-3}		25	Muhuri et al., 1993
PC	NaCl	0.000 003	mol kg^{-1}		25	Harris, 1958
PC	$NaClO_4$	2.5	mol dm^{-3}		25	Muhuri et al., 1993
PC	NaF	0.000 05	mol kg^{-1}		25	Harris, 1958
PC	NaI	1.11	mol kg^{-1}		25	Harris, 1958
PC	RbBr	0.0099	mol dm^{-3}		25	Muhuri et al., 1993
PC	RbCl	0.0033	mol dm^{-3}		25	Muhuri et al., 1993
PC	$RbClO_4$	0.025	mol dm^{-3}		25	Muhuri et al., 1993
1PentOH	KBr	0.000 03	w_{salt}		25	H. Stephen et al., 1963a
1PentOH	KBr	0.000 048	w_{salt}		25	H. Stephen et al., 1963a
1PentOH	KCl	0.000 008	w_{salt}		25	H. Stephen et al., 1963a
1PentOH	KCl	0.000 022	w_{salt}		25	H. Stephen et al., 1963a
1PentOH	KI	0.000 893	w_{salt}		25	H. Stephen et al., 1963a
1PentOH	KI	0.000 98	w_{salt}		25	H. Stephen et al., 1963a
1PentOH	KSCN	0.0018	w_{salt}		13	H. Stephen et al., 1963a
1PentOH	LiCl	0.0826	w_{salt}		25	H. Stephen et al., 1963a
1PentOH	LiCl	0.0828	w_{salt}		25	H. Stephen et al., 1963a
1PentOH	LiI	0.5294	w_{salt}		25	H. Stephen et al., 1963a
1PentOH	NaBr	0.001 101	w_{salt}		25	H. Stephen et al., 1963a
1PentOH	NaCl	0.000 017 7	w_{salt}		25	H. Stephen et al., 1963a
1PentOH	NaCl	0.000 02	w_{salt}		25	H. Stephen et al., 1963a
1PentOH	NaI	0.1401	w_{salt}		25	H. Stephen et al., 1963a
1PentOH	NaI	0.1402	w_{salt}		25	H. Stephen et al., 1963a
1PentOH	RbCl	0.000 025	w_{salt}		25	H. Stephen et al., 1963a
i-PentOH	CsCl	0.002 63	w_{salt}		25	H. Stephen et al., 1963a
i-PentOH	$CsClO_4$	0.000 46	w_{salt}		25	H. Stephen et al., 1963a
i-PentOH	KBr	0.003	g/100 g		25	Turner et al., 1913
i-PentOH	KBr	0.000 017 5	w_{salt}		25	H. Stephen et al., 1963a
i-PentOH	KCl	0.0008	g/100 g		25	Turner et al., 1913
i-PentOH	KI	0.098	g/100 g		25	Turner et al., 1913
i-PentOH	LiCl	9.03	g/100 g		25	Turner et al., 1913
i-PentOH	LiI	112.5	g/100 g		25	Turner et al., 1913
i-PentOH	$LiNO_3$	0.0868	w_{salt}		25	H. Stephen et al., 1963a
i-PentOH	NaCl	0.002	g/100 g		25	Turner et al., 1913
i-PentOH	NaI	16.3	g/100 g		25	Turner et al., 1913
i-PentOH	RbCl	0.0025	g/100 g		25	Turner et al., 1913
PrOH	$CsClO_4$	0.000 06	w_{salt}		25	H. Stephen et al., 1963a
PrOH	$CsClO_4$	0.000 46	w_{salt}		25	H. Stephen et al., 1963a
PrOH	KBr	0.035	g/100 g		25	Turner et al., 1913
PrOH	KBr	0.000 314	w_{salt}		25	H. Stephen et al., 1963a
PrOH	KBr	0.000 35	w_{salt}		25	H. Stephen et al., 1963a
PrOH	KCl	0.004	g/100 g		25	Turner et al., 1913
PrOH	KCl	0.000 04	w_{salt}		25	H. Stephen et al., 1963a
PrOH	KCl	0.000 061	w_{salt}		25	H. Stephen et al., 1963a
PrOH	KCl	0.000 07	w_{salt}		20	H. Stephen et al., 1963a
PrOH	$KClO_4$	0.0001	w_{salt}		25	H. Stephen et al., 1963a
PrOH	KF	0.0034	w_{salt}		20	H. Stephen et al., 1963a
PrOH	KI	0.43	g/100 g		25	Turner et al., 1913
PrOH	KI	0.0043	w_{salt}		25	H. Stephen et al., 1963a
PrOH	KI	0.004 42	w_{salt}		25	H. Stephen et al., 1963a
PrOH	KI	0.0046	w_{salt}		15	H. Stephen et al., 1963a
PrOH	LiCl	0.0372	w_{salt}		25	H. Stephen et al., 1963a
PrOH	LiCl	0.1395	w_{salt}		25	H. Stephen et al., 1963a
PrOH	$LiClO_4$	105	g/100 g		25	Chan et al., 1996
PrOH	$LiClO_4$	0.5122	w_{salt}		25	H. Stephen et al., 1963a
PrOH	LiI	0.3221	w_{salt}		25	H. Stephen et al., 1963a
PrOH	NaBr	0.002	w_{salt}		20	H. Stephen et al., 1963a
PrOH	NaBr	0.004 54	w_{salt}		25	H. Stephen et al., 1963a

solvent	electrolyte	S	type/units	ρ/g cm^{-3}	t/°C	reference
PrOH	NaCl	0.000 044 6	w_{salt}		20	H. Stephen et al., 1963a
PrOH	NaCl	0.000 12	w_{salt}		25	H. Stephen et al., 1963a
PrOH	NaCl	0.000 124	w_{salt}		25	H. Stephen et al., 1963a
PrOH	NaCl	0.0004	w_{salt}		25	H. Stephen et al., 1963a
PrOH	$NaClO_4$	0.0466	w_{salt}		25	H. Stephen et al., 1963a
PrOH	NaI	28.22	g/100g		25	Turner et al., 1913
PrOH	NaI	0.2166	w_{salt}		25	H. Stephen et al., 1963a
PrOH	NaI	0.2201	w_{salt}		25	H. Stephen et al., 1963a
PrOH	NaOAc	0.0937	mol dm^{-3}	0.8035	25	Soleymani et al., 2013
PrOH	NaOAc	0.0096	w_{salt}		20	H. Stephen et al., 1963a
PrOH	NH_4ClO_4	0.003 85	w_{salt}		25	H. Stephen et al., 1963a
PrOH	RbCl	0.015	g/100g		25	Turner et al., 1913
PrOH	RbCl	0.000 15	w_{salt}		25	H. Stephen et al., 1963a
PrOH	$RbClO_4$	0.000 06	w_{salt}		25	H. Stephen et al., 1963a
2PrOH	KBr	0.000 11	w_{salt}		25	H. Stephen et al., 1963a
2PrOH	KCl	0.000 023	w_{salt}		25	H. Stephen et al., 1963a
2PrOH	KCl	0.001 235	w_{salt}		20	H. Stephen et al., 1963a
2PrOH	KI	0.001 77	w_{salt}		25	H. Stephen et al., 1963a
2PrOH	$LiClO_4$	112.1	g/100g		25	Chan et al., 1996
2PrOH	NaBr	0.001 31	w_{salt}		25	H. Stephen et al., 1963a
2PrOH	NaCl	0.000 027	w_{salt}		25	H. Stephen et al., 1963a
2PrOH	NaCl	0.000 96	w_{salt}		20	H. Stephen et al., 1963a
2PrOH	NaI	0.2084	w_{salt}		25	H. Stephen et al., 1963a
water	CsBr	0.5523	w_{salt}		25	H. Stephen et al., 1963a
water	CsCl	0.6564	w_{salt}		25	Cohen-Adad et al., 1991
water	$CsClO_4$	0.002	w_{salt}		25	H. Stephen et al., 1963a
water	CsF	0.763	w_{salt}		18	H. Stephen et al., 1963a
water	CsForm	0.8325	w_{salt}		26.2	H. Stephen et al., 1963a
water	$CsNO_3$	0.187	w_{salt}		20	H. Stephen et al., 1963a
water	CsOAc	0.9106	w_{salt}		21.5	H. Stephen et al., 1963a
water	Et_4NBr	0.7365	w_{salt}		25	H. Stephen et al., 1963a
water	Et_4NBr	0.755	w_{salt}		20	H. Stephen et al., 1963a
water	Et_4NCl	0.578	w_{salt}		20	H. Stephen et al., 1963a
water	Et_4NCl	0.585	w_{salt}		25	H. Stephen et al., 1963a
water	Et_4NClO_4	0.0356	w_{salt}		15	H. Stephen et al., 1963a
water	Et_4NI	0.275	w_{salt}		20	H. Stephen et al., 1963a
water	Et_4NI	0.3103	w_{salt}		25	H. Stephen et al., 1963a
water	KBr	0.404	w_{salt}		25	H. Stephen et al., 1963a
water	KBr	0.4065	w_{salt}		25	H. Stephen et al., 1963a
water	KCl	0.262	w_{salt}		25	Cohen-Adad et al., 1991
water	KCl	0.264 76	w_{salt}		25	Pinho et al., 2005
water	$KClO_4$	0.0203	w_{salt}		25	H. Stephen et al., 1963a
water	KF	0.5041	w_{salt}		25	H. Stephen et al., 1963a
water	Kform	0.768	w_{salt}		18	H. Stephen et al., 1963a
water	KI	0.597	w_{salt}		25	H. Stephen et al., 1963a
water	KI	0.598	w_{salt}		25	H. Stephen et al., 1963a
water	KNO_3	0.272	w_{salt}		25	H. Stephen et al., 1963a
water	KNO_3	0.275	w_{salt}		25	H. Stephen et al., 1963a
water	KOAc	0.7293	w_{salt}		25	H. Stephen et al., 1963a
water	KSCN	0.705	w_{salt}		25	H. Stephen et al., 1963a
water	LiBr	0.63	w_{salt}		25	H. Stephen et al., 1963a
water	LiCl	0.456	w_{salt}		25	Cohen-Adad et al., 1991
water	$LiClO_4$	0.3744	w_{salt}		25	Chan et al., 1996
water	LiF	0.001 32	w_{salt}		25	H. Stephen et al., 1963a
water	LiF	0.001 33	w_{salt}		25	H. Stephen et al., 1963a
water	LiF	0.001 51	w_{salt}		25	H. Stephen et al., 1963a
water	LiForm	0.2785	w_{salt}		18	H. Stephen et al., 1963a
water	LiI	0.616	w_{salt}		25	H. Stephen et al., 1963a
water	LiI	0.626	w_{salt}		25	H. Stephen et al., 1963a
water	$LiNO_3$	0.429	w_{salt}		22.1	H. Stephen et al., 1963a
water	LiOAc	0.3128	w_{salt}		25.8	H. Stephen et al., 1963a
water	LiSCN	0.545	w_{salt}		25	H. Stephen et al., 1963a
water	Me_4NClO_4	0.0049	w_{salt}		15	H. Stephen et al., 1963a
water	Me_4NI	58.9	g l^{-1}	1.0155	25	H. Stephen et al., 1963a
water	NaBr	0.486	w_{salt}		25	H. Stephen et al., 1963a
water	NaBr	0.4862	w_{salt}		25	Pinho et al., 2005
water	NaCl	0.2645	w_{salt}		25	Cohen-Adad et al., 1991

solvent	electrolyte	S	type/units	ρ/g cm^{-3}	t/°C	reference
water	NaCl	0.264 83	w_{salt}		25	Pinho et al., 2005
water	$NaClO_4$	17.16	mol kg^{-1}		25	Chan et al., 1996
water	$NaClO_4$	0.677	w_{salt}		25	H. Stephen et al., 1963a
water	$NaClO_4$	0.6782	w_{salt}		25	H. Stephen et al., 1963a
water	NaF	0.0398	w_{salt}		25	H. Stephen et al., 1963a
water	NaForm	0.474	w_{salt}		24	H. Stephen et al., 1963a
water	NaForm	0.5053	w_{salt}		25.5	H. Stephen et al., 1963a
water	NaI	0.6476	w_{salt}		25	H. Stephen et al., 1963a
water	NaI	0.648	w_{salt}		25	H. Stephen et al., 1963a
water	$NaNO_3$	0.476	w_{salt}		25	H. Stephen et al., 1963a
water	$NaNO_3$	0.4783	w_{salt}		25	H. Stephen et al., 1963a
water	NaOAc	5.53	mol dm^{-3}	1.1921	25	Soleymani et al., 2013
water	NaOAc	0.317	w_{salt}		20	H. Stephen et al., 1963a
water	NaSCN	0.5878	w_{salt}		25	H. Stephen et al., 1963a
water	NH_4Br	0.439	w_{salt}		25	H. Stephen et al., 1963a
water	NH_4Cl	0.2834	w_{salt}		25	Cohen-Adad et al., 1991
water	NH_4ClO_4	0.1989	w_{salt}		25	H. Stephen et al., 1963a
water	NH_4ClO_4	0.1995	w_{salt}		25	H. Stephen et al., 1963a
water	NH_4ClO_4	0.2002	w_{salt}		25	H. Stephen et al., 1963a
water	NH_4Form	0.589	w_{salt}		20	H. Stephen et al., 1963a
water	NH_4I	0.639	w_{salt}		25	H. Stephen et al., 1963a
water	NH_4NO_3	0.6763	w_{salt}		25	H. Stephen et al., 1963a
water	NH_4NO_3	0.6817	w_{salt}		25	H. Stephen et al., 1963a
water	NH_4NO_3	0.6819	w_{salt}		25	H. Stephen et al., 1963a
water	NH_4SCN	0.655	w_{salt}		25	H. Stephen et al., 1963a
water	$Pent_4NI$	0.0073	w_{salt}		25	H. Stephen et al., 1963a
water	Pr_4NI	0.1571	w_{salt}		25	H. Stephen et al., 1963a
water	RbBr	0.5369	w_{salt}		25	H. Stephen et al., 1963a
water	RbCl	0.4842	w_{salt}		25	Cohen-Adad et al., 1991
water	$RbClO_4$	0.012	w_{salt}		25	H. Stephen et al., 1963a
water	$RbClO_4$	0.0132	w_{salt}		25	H. Stephen et al., 1963a
water	$RbClO_4$	0.0177	w_{salt}		25	H. Stephen et al., 1963a
water	RbF	0.7506	w_{salt}		18	H. Stephen et al., 1963a
water	RbForm	0.8461	w_{salt}		16.3	H. Stephen et al., 1963a
water	RbI	0.6205	w_{salt}		25	H. Stephen et al., 1963a
water	RbOAc	0.8623	w_{salt}		44.7	H. Stephen et al., 1963a
water	RbSCN	15.65	mol kg^{-1}		25	Hála, 2004

BIBLIOGRAPHY FOR THE CURRENT APPENDIX

Butler, J. N.

1967 'Electrochemistry in Dimethyl Sulfoxide', *J. Electroanal. Chem. Interfacial Electrochem.* 14, 1, pp. 89–116, DOI: 10.1016/0022-0728(67)80136-0.

Chan, C.-Y., K. H. Khoo, E. S. Gryzlova and M.-T. Saugier-Cohen Adad

1996 *IUPAC Solubility Data Series*, ed. by J. W. Lorimer, IUPAC Solubility Data Series, Oxford University Press, vol. 61, https://srdata.nist.gov/solubility/IUPAC/SDS-61/SDS-61.pdf.

Lorimer, J. W.

1991 (ed.), *IUPAC Solubility Data Series*, vol. 47, IUPAC Solubility Data Series, Pergamon Press Ltd, https://srdata.nist.gov/solubility/IUPAC/SDS-47/SDS-47.pdf.

Hála, J.

2004 'IUPAC-NIST Solubility Data Series. 79. Alkali and Alkaline Earth Metal Pseudohalides', *J. Phys. Chem. Ref. Data*, 33, 1, pp. 1–176, DOI: 10.1063/1.1563591.

Harner, R. E., J. B. Sydnor and E. S. Gilreath

1963 'Solubilities of Anhydrous Ionic Substances in Absolute Methanol', *J. Chem. Eng. Data*, 8, 3, pp. 411–412, DOI: 10.1021/je60018a035.

Harris, W. S.

1958 *Electrochemical Studies in Cyclic Esters*, PhD thesis, California Univ., Berkeley, CA (US). Radiation Lab., DOI: 10.2172/4305596.

Hernández-Luis, F., R. Rodríguez-Raposo, H. R. Galleguillos and J. W. Morales

2016 'Solubility of Sodium Halides in Aqueous Mixtures with ϵ-increasing Cosolvents: Formamide, *N*-methylformamide, and *N*-methylacetamide at 298.15 K', *Ind. Eng. Chem. Res.* 55, 3, pp. 812–819, DOI: 10.1021/acs.iecr.5b04614.

Labban, A.-K. S. and Y. Marcus

1991 'The Solubility and Solvation of Salts in Mixed Nonaqueous Solvents. 1. Potassium Halides in Mixed Aprotic Solvents', *J. Solution Chem.* 20, 2, pp. 221–232, DOI: 10.1007/BF00649530.

1997 'The Solubility and Solvation of Salts in Mixed Nonaqueous Solvents. 2. Potassium Halides in Mixed Protic Solvents', *J. Solution Chem.* 26, 1, pp. 1–12, DOI: 10.1007/BF02439440.

Li, M., D. Constantinescu, L. Wang, A. Mohs and J. Gmehling

2010 'Solubilities of NaCl, KCl, LiCl, and LiBr in Methanol, Ethanol, Acetone, and Mixed Solvents and Correlation Using the LIQUAC Model', *Ind. Eng. Chem. Res.* 49, 10, pp. 4981–4988, DOI: 10.1021/ie100027c.

Muhuri, P. K., S. K. Ghosh and D. K. Hazra

1993 'Solubilities of Some Alkali-metal Salts, Tetraphenylarsonium Chloride, and Tetraphenylphosphonium Bromide in Propylene Carbonate at 25 °C Using the Ion-selective Electrode Technique', *J. Chem. Eng. Data*, 38, 2, pp. 242–244, DOI: 10.1021/je00010a014.

Peruzzi, N., P. Lo Nostro, B. W. Ninham and P. Baglioni

2015 'The Solvation of Anions in Propylene Carbonate', *J. Solution Chem.* 44 (6 2015), pp. 1224–1239, DOI: 10.1007/s10953-015-0335-z.

Peruzzi, N., B. W. Ninham, P. Lo Nostro and P. Baglioni

2012 'Hofmeister Phenomena in Nonaqueous Media: The Solubility of Electrolytes in Ethylene Carbonate', *J. Phys. Chem. B*, 116, 49, pp. 14398–14405, DOI: 10.1021/jp309157x.

Pinho, S. P. and E. A. Macedo

2005 'Solubility of NaCl, NaBr, and KCl in Water, Methanol, Ethanol, and Their Mixed Solvents', *J. Chem. Eng. Data*, 50, 1, pp. 29–32, DOI: 10.1021/je049922y.

Scrosati, B. and C. A. Vincent

1980 *Alkali Metal, Alkaline Earth Metal and Ammonium Halides, Amide Solvents*, ed. by A. S. Kertes, IUPAC Solubility Data Series, Pergamon Press Ltd, vol. 11, https://srdata.nist.gov/solubility/IUPAC/SDS-11/SDS-11.pdf.

Soleymani, J., M. Zamani-Kalajahi, B. Ghasemi, E. Kenndler and A. Jouyban

2013 'Solubility of Sodium Acetate in Binary Mixtures of Methanol, 1-propanol, Acetonitrile, and Water at 298.2 K', *J. Chem. Eng. Data*, 58, 12, pp. 3399–3404, DOI: 10.1021/je400625f.

Stenger, V. A.

1996 'Solubilities of Various Alkali Metal and Alkaline Earth Metal Compounds in Methanol', *J. Chem. Eng. Data*, 41, 5, pp. 1111–1113, DOI: 10.1021/je960124k.

Stephen, H. and T. Stephen

1963a (eds.), *Solubilities of Inorganic and Organic Compounds. Binary Systems*, vol. 1.1, Pergamon Press, Oxford.

Stephen, H. and T. Stephen

1963b (eds.), *Solubilities of Inorganic and Organic Compounds. Binary Systems*, vol. 1.2, Pergamon Press, Oxford.

Turner, W. E. S. and C. C. Bissett

1913 'CCIV.— The Solubilities of Alkali Haloids in Methyl, Ethyl, Propyl, and *iso*amyl Alcohols', *J. Chem. Soc., Trans.* 103 (0 1913), pp. 1904–1910, DOI: 10.1039/CT9130301904.

E CUSTOM CONDUCTIVITY CELL

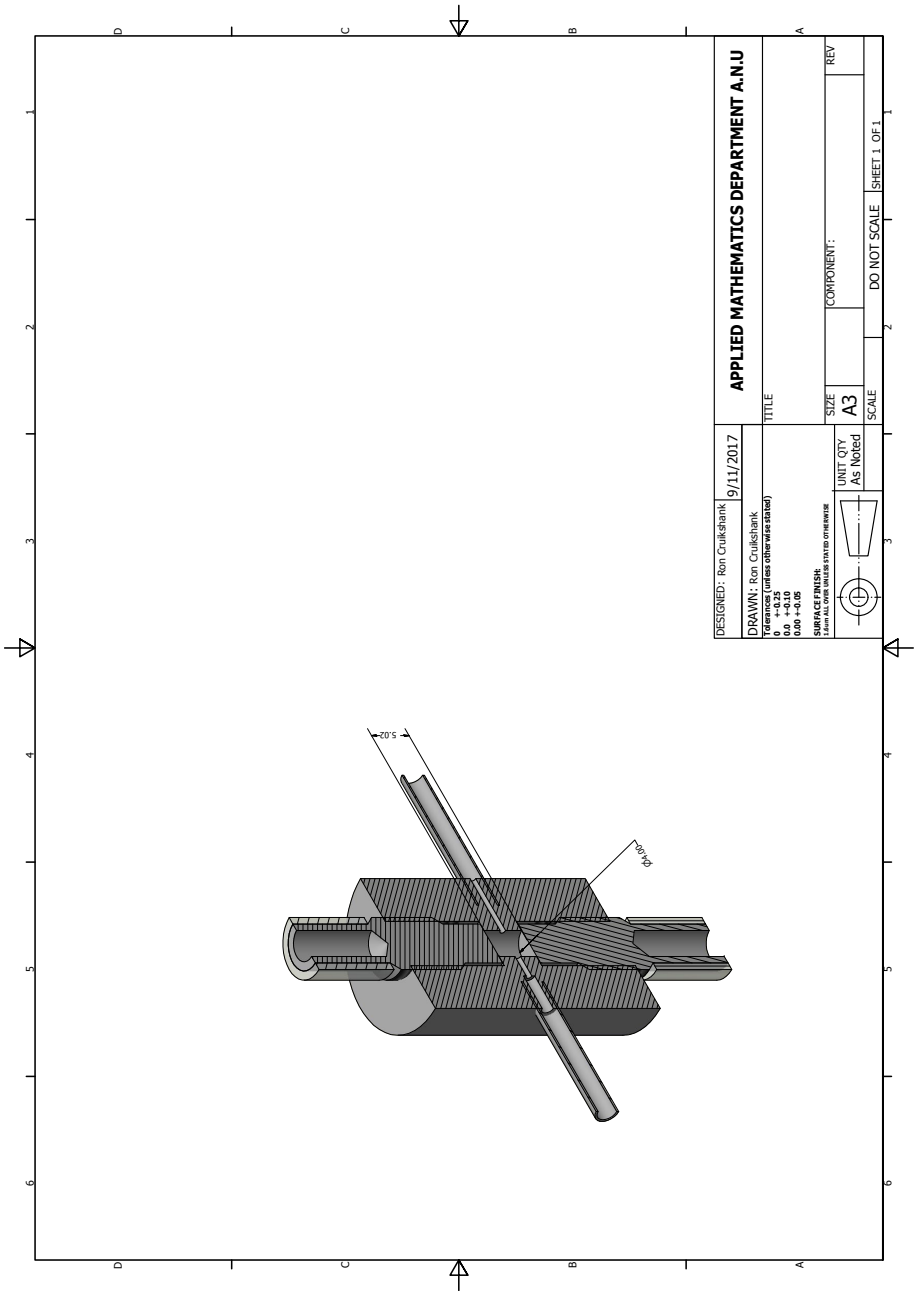

Figure 92: Schematics of the custom-made conductivity cell body, employed as the detector in the SEC experiments. Drawing credits: Mr. Ron Cruikshank, Department of Applied Mathematics, Research School of Physics and Engineering, ANU.

F EFFECT OF WATER IMPURITIES ON SEC AND QCM EXPERIMENTS

In this section, I present and discuss some experiments I performed in order to ascertain the impact of water contamination on the SIE trends for SEC and QCM experiments in non-aqueous solvents.

F.1 Size-exclusion chromatography

In MeOH, the SEC runs of NaF, NaCl and NaBr, when a small amount of water is added to either the sample or the eluent, are compared. Figure 93 shows chromatograms of repeat runs where the water content in the sample or the eluent is approximately doubled. No significant effect is seen on the position of the peak after doubling the water content in the eluent or sample. This suggests that the results we observe are largely unaffected by the presence of small quantities of water.

In contrast, the NaI sample peak in PC has a different shape in the final anhydrous runs with respect to the trial ones (Fig. 94). The trial runs were performed in non-anhydrous eluent, $w_{water}\% \approx 0.04$ for the solvent in the bottle, but the column was not sealed from moisture, so a much higher water content was present in these trial runs. In the anhydrous runs, the water content of the NaI sample is $w_{water}\% = 0.015$. In the non-anhydrous trial case the NaI sample is eluting sharply (also notice that NaBr is behaving as 'sticky'—NaBr has not been tested in the final anhydrous runs due to low solubility), whereas in anhydrous conditions NaI sticks to the stationary phase.

In order to understand the origin of this difference, the anhydrous run of Fig. 24 was repeated for confirmation, and then another run was performed with a NaI sample containing a higher water content. This sample was prepared by adding water to the NaI anhydrous sample ($w_{water}\% = 0.015$), and it had a water content of 1.3% (measured by KF). The three runs at different sample water content are shown in Fig. 95: no difference in the peak shape is observed.

This evidence in PC indicates that the behaviour of ions can indeed change based on the water content in the non-aqueous aprotic solvent, but to induce such a change, the water content needs to be high, as in the trial experiments. This is interesting because it suggests that the amount of water in solution can modulate the behaviour of anions in non-aqueous solvents. This agrees with the rule of thumb proposed in Chapter 4: the ordering of anions in water and non-aqueous aprotic solvents is likely to be different. It is also in accordance with the literature evidence of preferential solvation of anions in aprotic solvents.

However, in DMSO no changes in the peak shape or elution order have been noticed between the non-anhydrous trial runs and the final anhydrous runs (Fig. 96). It is possible that the water content has to be higher in order to affect the behaviour of

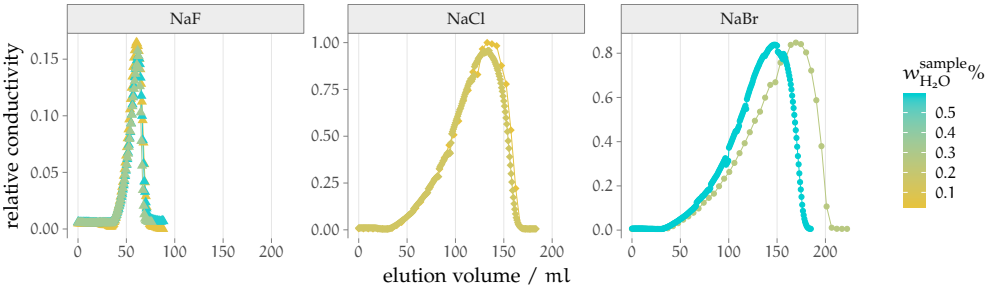

(a) NaF, NaCl and NaBr samples with differing water concentrations.

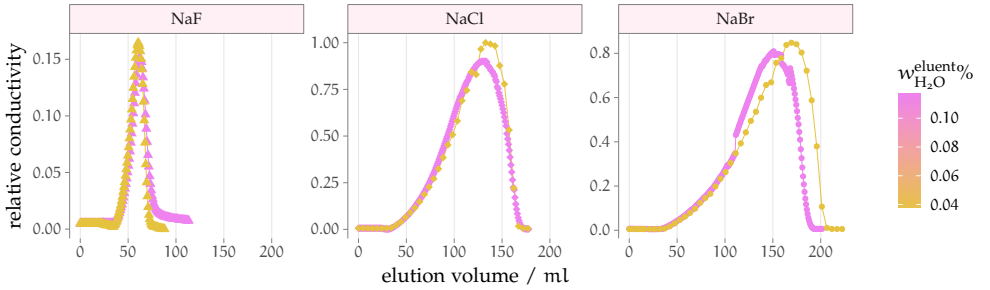

(b) Eluent (MeOH) with varying water concentration.

Figure 93: Effect of the addition of water on the SEC elution peaks of NaF, NaCl and NaBr in MeOH. Water is added to the sample (top) or to the eluent (bottom). The baseline conductivity of the pure solvent has been subtracted and the values of the conductivity rescaled relative to the maximum conductivity being set to 1.

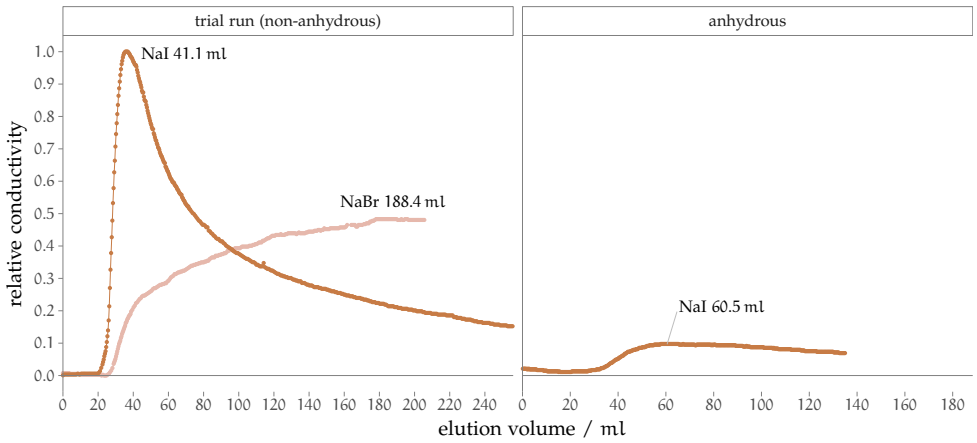

Figure 94: Chromatography runs in PC in different water content conditions. The NaBr sample is constituted of a saturated solution. The NaI data plotted on the anhydrous panel are the same as in Fig. 24 in Chapter 6. The baseline conductivity of the pure solvent has been subtracted and the values of the conductivity rescaled relative to the maximum conductivity being set to 1.

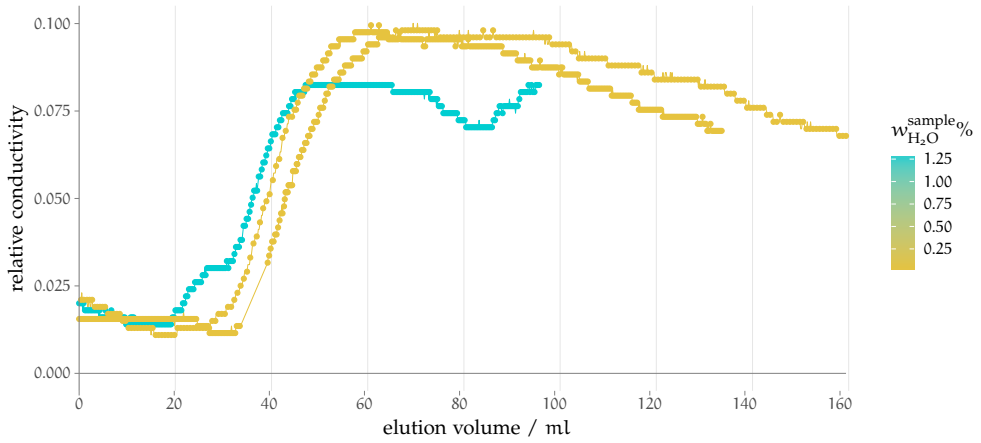

Figure 95: eluent: anhydrous PC. Comparison of NaI samples containing different amounts of water. The baseline conductivity of the pure solvent has been subtracted and the values of the conductivity rescaled relative to the maximum conductivity being set to 1. Please note the y-axis is resized.

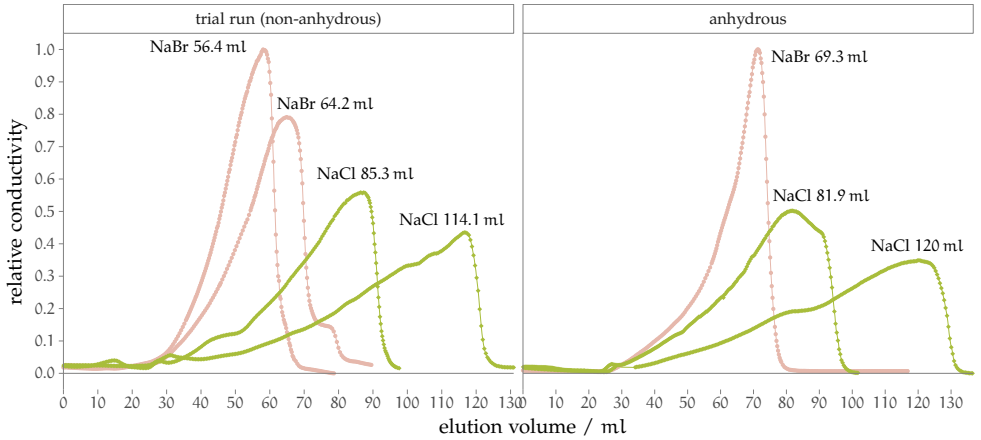

Figure 96: Chromatography runs in DMSO in different water content conditions. Repeat runs of the same sample are plotted. The baseline conductivity of the pure solvent has been subtracted and the values of the conductivity rescaled relative to the maximum conductivity being set to 1. The data plotted on the anhydrous panel are the same as in Fig. 23 in Chapter 6.

anions in DMSO solutions. More experiments are needed in order to ascribe the difference observed for anhydrous and non anhydrous runs in PC with certainty to a water solvation effect rather than experimental variations.

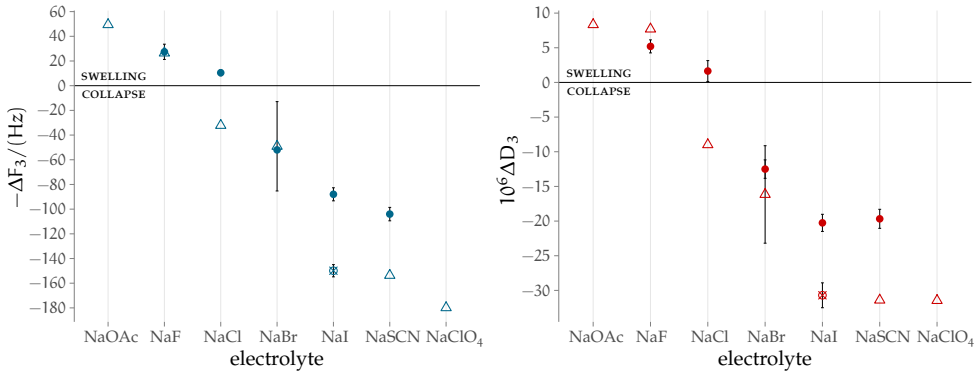

Figure 97: Frequency and dissipation shifts obtained for dry versus non-dry MeOH solutions. The corresponding conformational change of the brush is indicated on the plots. Full circles indicate anhydrous samples, empty triangles non-anhydrous samples, and the crossed circle marks a case where an anhydrous sample was used against a non-dry baseline. The *normalised* frequency shift ΔF_3 is plotted rather than Δf_3, and the frequency shift axis is reversed.

F.2 POLYMER CONFORMATION BY QCM

Regarding the presence of water in the QCM experiments, it must be considered that the brush itself is hygroscopic. In addition, the electrolyte concentrations used is much lower $10^{-3}\,mol\,kg^{-1}$, therefore lower contents of water might be able to affect the system. A study of the shifts in anhydrous and non-anhydrous conditions has been performed for MeOH, and is presented in Fig. 97. The presence of water in the solvent favours the ion-induced collapse of the brush for the chaotropic ions, whereas very little effect is seen for kosmotropic ions. Importantly the presence of water does not appear to influence the observed trend in ion specificity.

F.3 CONCLUSIONS

Studies of the influence of water on the behaviour of non-aqueous systems are a topic that deserves thorough investigation. Hopefully these observations can stimulate studies in the matter, and the results that are be presented in Chapters 6 and 7 need to be considered in light of this information.

G A SUMMARY OF UNSUCCESSFUL APPROACHES

This appendix summarises the experimental projects that did not yield positive results.

G.1 STANDARD MOLAR VOLUME MEASUREMENTS

As the experimental standard molar volumes values of a number of non-aqueous electrolytes are not available in the literature, I attempted to obtain them by measuring the density of their solutions, in order to employ the values so-obtained in the calculations of Chapter 3.
I therefore performed measurements of the density of electrolyte solutions in MeOH with an *Anton-Paar DMA* 5000 density-meter. The reason why this experiment was unsuccessful is that we did not record monotonic trends of density when approaching higher dilution.
Following is a short briefing about the experimental details that could be useful for repeating the measurements successfully.

G.1.1 Measurements of partial molar volumes

Partial molar volumes in solution have been introduced in Section 3.2. In the following discussion, that details the connection between the solution density and the partial molar volume of the electrolyte, only binary solutions are considered, and the solvent is denoted by the subscript '1', whereas the solute by the subscript '2'.
The apparent molal volume ${}^{\phi}\overline{V}_2$ of the solute in solution is defined as:

$$ {}^{\phi}\overline{V}_2 = \frac{V - n_1 \overline{V}_1{}^*}{n_2} \quad (T, P \text{ constant}) \qquad [21] $$

where $\overline{V}_1{}^*$ is the partial molar volume of the pure solvent. The meaning of Eq. [21] is that the apparent molar volume is the molar volume of the solute in the hypothetical situation where the solvent has maintained the volume it had as a pure substance. The apparent molar volumes have little thermodynamic utility, except for their function in the determination of the partial molal quantities. The relationship between apparent and partial molar quantities is the following:

$$ \overline{V}_2 = \left(\frac{\partial V}{\partial n_2}\right)_{T,\,P,\,n_1} = {}^{\phi}\overline{V}_2 + n_2 \left(\frac{\partial\, {}^{\phi}\overline{V}_2}{\partial n_2}\right)_{T,\,P,\,n_1} \qquad [22] $$

From Eq. [22] it is evident that, at infinite dilution:

$$ \lim_{n_2 \to 0} \overline{V}_2 \equiv \overline{V}_2^{\circ} = {}^{\phi}\overline{V}_2 \qquad [23] $$

the apparent molar volume of the solute *coincides* with its standard partial molar volume.
We now need to express ${}^{\phi}\overline{V}_2$ in terms of the *experimental observable*, the density ρ of the solution. The total volume of the solution is related to its density by:

$$ V = \frac{w}{\rho} = \frac{n_1 M_1 + n_2 M_2}{\rho} $$

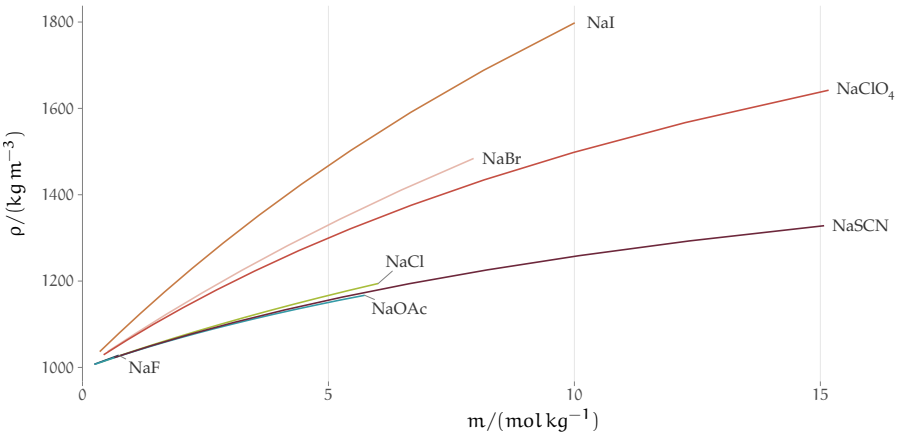

Figure 98: Concentration dependence of the solution density upon molal concentration for the investigated electrolytes. Density data from Söhnel and Novotný (1985).

Where w is the mass of the solution and $w = w_1 + w_2 = n_1 M_1 + n_2 M_2$. Equation Eq. [21] can therefore be rewritten as:

$$\phi\overline{V}_2 = \frac{V - n_1\overline{V}_1^{\circ}}{n_2} = \frac{1}{n_2}\left(\frac{n_1 M_1 + n_2 M_2}{\rho} - n_1\overline{V}_1^{\circ}\right) \qquad [24]$$

If we express the concentration in terms of the molality of solute in solution m_2 ($\mathrm{mol\,kg^{-1}_{(solvent)}}$), then $n_2 \equiv m_2$ and n_1 is the number of moles of solvent in 1000 g of solvent: $n_1 = 1000/M_1$; by substituting in Eq. [24] we have:

$$\boxed{\phi\overline{V}_2 = \frac{1000(\rho^* - \rho)}{m_2\rho\rho^*} + \frac{M_2}{\rho}} \qquad [25]$$

Which expresses the partial molar volume of the solute in terms of the density of the solution, the density of the pure solvent and the molality of solute. In this equation, the densities are expressed in $\mathrm{g\,cm^{-3}}$, the molar masses in $\mathrm{g\,mol^{-1}}$ and the molality of solute in $\mathrm{mol\,kg^{-1}_{(solvent)}}$, therefore the apparent partial molar volume is obtained in $\mathrm{cm^3\,mol^{-1}}$ and a factor of 1000 is present.
By measuring the densities of electrolyte solutions at several finite concentrations, we can therefore calculate the apparent partial molar volume through Eq. [25], and then extrapolate the apparent molar volume to infinite dilution, where it coincides with the *standard partial molar volume* (Eq. [23]). Figure 98 shows the dependence of the density of solutions of the electrolytes of interest upon concentration.

Extrapolation to infinite dilution

In order to obtain the standard partial molar volume $\overline{V}_2^{\circ}$ of an electrolyte, its apparent molar volume, calculated from the measured densities at finite concentration by Eq. [25], needs to be extrapolated to infinite dilution. The RRM equation is the recommended model for the extrapolation (Marcus and Hefter, 2004; Millero, 1972b):

$$\phi\overline{V}_2 = \overline{V}_2^{\circ} + S_V^{DH}\sqrt{c_2} + b_V c_2$$

It satisfactorily fits data up to $\approx 1\,\mathrm{mol\,dm^{-3}}$ for the majority of systems. Therefore, a plot of $\left(\phi\overline{V}_2 - S_V^{DH}\sqrt{c_2}\right)$ versus c_2 is usually linear and yields $\overline{V}_2^{\circ}$ as intercept and b_V as slope.

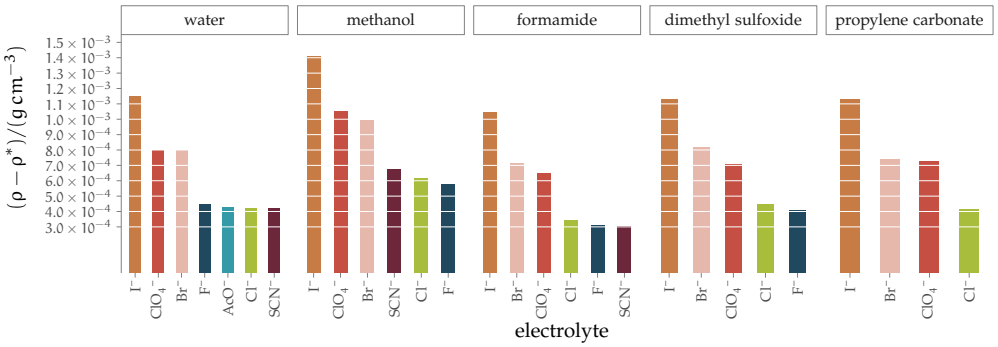

Figure 99: Expected density change of the electrolyte solution with respect to the pure solvent at $c_2 = 0.01\,mol\,dm^{-3}$. Calculated assuming that ${}^{\phi}\overline{V}_2 \approx \overline{V}_2^{\ominus}$ at $c_2 = 0.01\,mol\,dm^{-3}$.

Requirements for good measurements

For the purpose of determining standard partial molar volumes of electrolytes in solutions, the following conditions need to be respected:

ACCURACY: (section 2.4.2 Marcus and Hefter, 2004) For a $0.5\,cm^3\,mol^{-1}$ uncertainty on the partial molar volume, an accuracy at least down to $5 \times 10^{-6}\,g\,cm^{-3}$ in the density determination is needed (see the the calculations in the following subsection).

CONCENTRATION: Measurements down to concentrations of $0.01\,mol\,dm^{-3}$ or less are needed for the extrapolation of the standard partial molar volume, in order to avoid that the data at high concentration ($c_2 > 0.25\,mol\,dm^{-3}$) affect the extrapolation. But, for an electrolyte with an apparent molar volume of $100\,cm^3\,mol^{-1}$ and molar mass $M_i = 100\,g/mol$ in water, the density change at $c_2 = 0.01\,mol\,dm^{-3}$ is about $3 \times 10^{-6}\,g\,cm^{-3}$. Such accuracy is beyond the limits of most techniques, only dilatometry can reach it. The expected density change $(\rho - \rho^*)$ for the electrolytes of interest in water and the non-aqueous solvents investigated experimentally in this thesis is plotted in Fig. 99: an accuracy of at least $1 \times 10^{-5}\,cm^3\,mol^{-1}$ is needed.

TEMPERATURE CONTROL: (section 2.1 Marcus and Hefter, 2004) Although ${}^{\phi}\overline{V}_2$ and $\overline{V}_2^{\ominus}$ of an electrolyte are not particularly sensitive to temperature, the two experimentally measured quantities of the solution, density and volume, are. While in water (isobaric expansivity $\alpha_P \approx 2.5 \times 10^{-4}\,K^{-1}$ a control of at least 0.01 K is required to obtain a precision of about $2 \times 10^{-6}\,g\,cm^{-3}$ (or cm^3 if volume is measured, like in dilatometry), the expansibility of MeOH is about four times the one of water: $\alpha_P \approx 1.2 \times 10^{-3}\,K^{-1}$), then a temperature control of 0.001 K would be necessary to achieve the same precision.

BUBBLES: the presence of microbubbles must be avoided. Solutions are not easy to degas $\Longrightarrow$ sonication; storage of the solutions at or slightly above the measurement temperature.

Errors in the apparent molar volume

Error in ${}^{\phi}\overline{V}_2$:

$$\Delta\,{}^{\phi}\overline{V}_2 = \left|\left(\frac{\partial\,{}^{\phi}\overline{V}_2}{\partial c_2}\right)_{\rho}\right|\Delta c_2 + \left|\left(\frac{\partial\,{}^{\phi}\overline{V}_2}{\partial \rho}\right)_{c_2}\right|\Delta\rho = \left|\frac{M_2}{\rho^*} - {}^{\phi}\overline{V}_2\right|\frac{\Delta c_2}{c_2} + \frac{1000}{c_2}\frac{\Delta\rho}{\rho^*}$$

In dilute solutions the apparent molar volume is not seriously influenced by errors on c_2, but it is largely affected by errors in ρ: in water, if $c_2 = 0.01\,\mathrm{mol\,dm^{-3}}$, a $5 \times 10^{-6}\,\mathrm{g\,cm^{-3}}$ error in ρ causes an error of $c_2 = 0.5\,\mathrm{cm^3\,mol^{-1}}$ in $\Delta^{\phi}\overline{V}_2$.

G.2 TURBIDIMETRY

This work was aimed at investigating the stability of colloids in non-aqueous solvents in the presence of different electrolytes.
We tested Boehmite nanopowders (*Sasol Disperal*). These powders are water or acid dispersible, and I tried dispersing them in non-aqueous solvents. I found that *Disperal D*40 formed stable suspensions in neat MeOH and *Disperal P*2*W* was stable in neat FA and PC . All the suspensions were stable for longer than 20 d.
I then suspended the powders in solutions of the electrolytes in the solvents and monitored the sedimentation kinetics by means of a turbidimeter. Although the preliminary measurements where promising and I thought I was measuring a dependence of the sedimentation kinetics upon the electrolyte present, after repeated runs I realised that the variability in the sedimentation process was very high, rendering the averaged sedimentation curves for different electrolytes undistinguishable.
Therefore, the decrease in turbidity with time does not seem to be due to salt-specific aggregation and sedimentation.

G.3 NMR T_2 RELAXATION TIMES OF SALT SOLUTIONS

NMR can be used to investigate solvation processes. The transversal relaxation time T_2 is sensitive to relaxation phenomena within the sample. It is therefore useful to investigate effects of a solute on the relaxation of the solvent molecules.
We performed measurements on samples made of the seven electrolytes and the four solvents that are the object of the investigating experimental investigations of this thesis, with a benchtop NMR instrument: the *Acorn Area* from *Xigo Nanotools*. We found that the instrument showed variations in the data readings that were not correlated to environmental effects. We later also understood that the magnitude of the effects that we intended to measure are beyond the instrument accuracy, and therefore this project was abandoned.

G.4 SWELLING OF COMMERCIAL HYDROGELS

I have also attempted to monitor the swelling of commercial hydrogels beads in the presence of non-aqueous electrolytes solutions.
On preliminary testing, I found out that the beads would only swell in water and FA, and therefore excluded the other solvents.
I monitored the changes in mass of the bead after being equilibrated in a salt solution with respect to the pure solvent. An overall shrinking trend in the presence of the salt solution was observed, which was promising. But the bead would often break as a consequence of handling. In addition, the weight loss in presence of the electrolytes was very similar across the four salts tested. Also this experiment was abandoned.

BIBLIOGRAPHY

Andrieu-Brunsen, A., S. Micoureau, M. Tagliazucchi, I. Szleifer, O. Azzaroni and G. J. A. A. Soler-Illia

2015 'Mesoporous Hybrid Thin Film Membranes with PMETAC@silica Architectures: Controlling Ionic Gating through the Tuning of Polyelectrolyte Density', *Chem. Mater.* 27, 3, pp. 808–821, DOI: 10.1021/cm5037953.

Ao, Z., G. Liu and G. Zhang

2011 'Ion Specificity at Low Salt Concentrations Investigated with Total Internal Reflection Microscopy', *J. Phys. Chem. C*, 115, 5, pp. 2284–2289, DOI: 10.1021/jp110782g.

Aoki, K., K. Shiraki and T. Hattori

2016 'Salt Effects on the Picosecond Dynamics of Lysozyme Hydration Water Investigated by Terahertz Time-domain Spectroscopy and an Insight into the Hofmeister Series for Protein Stability and Solubility', *Phys. Chem. Chem. Phys.* 18, 22, pp. 15060–15069, DOI: 10.1039/c5cp06324h.

Arakawa, T. and S. N. Timasheff

1984 'Mechanism of Protein Salting in and Salting Out by Divalent Cation Salts: Balance between Hydration and Salt Binding', *Biochemistry*, 23, 25, pp. 5912–5923, DOI: 10.1021/bi00320a004.

Armarego, W. L. F. and C. L. L. Chai

2009 *Purification of Laboratory Chemicals*, 6th ed., Butterworth-Heinemann, Burlington, MA.

Arslanargin, A., A. Powers, T. L. Beck and S. W. Rick

2016 'Models of Ion Solvation Thermodynamics in Ethylene Carbonate and Propylene Carbonate', *J. Phys. Chem. B*, 120, 8, pp. 1497–1508, DOI: 10.1021/acs.jpcb.5b06891.

Asthagiri, D., M. R. Schure and A. M. Lenhoff

2000 'Calculation of Hydration Effects in the Binding of Anionic Ligands to Basic Proteins', *J. Phys. Chem. B*, 104, 36, pp. 8753–8761, DOI: 10.1021/jp001458q.

Aurbach, D., Y. Talyosef, B. Markovsky, E. Markevich, E. Zinigrad, L. Asraf, J. S. Gnanaraj and H.-J. Kim

2004 'Design of Electrolyte Solutions for Li and Li-ion Batteries: A Review', *Electrochim. Acta*, 50, 2-3, pp. 247–254, DOI: 10.1016/j.electacta.2004.01.090.

Ayres, N.

2010 'Polymer Brushes: Applications in Biomaterials and Nanotechnology', *Polym. Chem.* 1 (6 2010), pp. 769–777, DOI: 10.1039/B9PY00246D.

Azzaroni, O., S. Moya, T. Farhan, A. A. Brown and W. T. S. Huck
2005 'Switching the Properties of Polyelectrolyte Brushes Via "Hydrophobic Collapse"', *Macromolecules*, 38, 24, pp. 10192–10199, DOI: 10.1021/ma051549r.

Baldwin, R. L.
1996 'How Hofmeister Ion Interactions Affect Protein Stability', *Biophys. J.* 71, 4, pp. 2056–2063, DOI: 10.1016/S0006-3495(96)79404-3.

Barthel, J., R. Neueder and G. Lauermann
1985 'Vapor Pressures of Non-aqueous Electrolyte Solutions. Part 1. Alkali Metal Salts in Methanol', *J. Solution Chem.* 14, 9, pp. 621–633, DOI: 10.1007/BF00646055.

Barthel, J., R. Neueder and H. Roch
2000 'Density, Relative Permittivity, and Viscosity of Propylene Carbonate + Dimethoxyethane Mixtures from 25 °C to 125 °C', *J. Chem. Eng. Data*, 45, 6, pp. 1007–1011, DOI: 10.1021/je000098x.

Batoulis, H., T. H. Schmidt, P. Weber, J.-G. Schloetel, C. Kandt and T. Lang
2016 'Concentration Dependent Ion-protein Interaction Patterns Underlying Protein Oligomerization Behaviours', *Sci. Rep.* 6, 24131, p. 24131, DOI: 10.1038/srep24131.

Beck, T. L.
2011 'A Local Entropic Signature of Specific Ion Hydration', *J. Phys. Chem. B*, 115, 32, pp. 9776–9781, DOI: 10.1021/jp204883h.

Béguin, F., V. Presser, A. Balducci and E. Frackowiak
2014 'Carbons and Electrolytes for Advanced Supercapacitors', *Adv. Mater.* 26, 14, pp. 2219–2251, DOI: 10.1002/adma.201304137.

Biesalski, M., D. Johannsmann and J. Rühe
2004 'Electrolyte-induced Collapse of a Polyelectrolyte Brush', *J. Chem. Phys.* 120, 18, pp. 8807–8814, DOI: 10.1063/1.1690242.

Bilaničová, D., A. Salis, B. W. Ninham and M. Monduzzi
2008 'Specific Anion Effects on Enzymatic Activity in Nonaqueous Media', *J. Phys. Chem. B*, 112, 38, pp. 12066–12072, DOI: 10.1021/jp805451w.

Bjørnsdottir, I., J. Tjørnelund and S. H. Hansen
1998 'Nonaqueous Capillary Electrophoresis — Its Applicability in the Analysis of Food, Pharmaceuticals and Biological Fluids', *Electrophoresis*, 19, 12, pp. 2179–86, DOI: 10.1002/elps.1150191223.

Böes, E. S., P. R. Livotto and H. Stassen
2006 'Solvation of Monovalent Anions in Acetonitrile and *N*,*N*-dimethylformamide: Parameterization of the IEF-PCM Model', *Chem. Phys.* 331, 1, pp. 142–158, DOI: 10.1016/j.chemphys.2006.08.028.

Bosque, R. and J. Sales
2002 'Polarizabilities of Solvents from the Chemical Composition', *J. Chem. Inf. Comput. Sci.* 42, 5, pp. 1154–1163, DOI: 10.1021/ci025528x.

Boström, M., F. W. Tavares, S. Finet, F. Skouri-Panet, A. Tardieu and B. W. Ninham

2005 'Why Forces between Proteins Follow Different Hofmeister Series for pH above and below pI', *Biophys. Chem.* 117, 3, pp. 217–224, DOI: 10.1016/j.bpc.2005.05.010.

Breslow, R. and T. Guo

1988 'Diels-Alder Reactions in Nonaqueous Polar Solvents. Kinetic Effects of Chaotropic and Antichaotropic Agents and of β-cyclodextrin', *J. Am. Chem. Soc.* 110, 17, pp. 5613–5617, DOI: 10.1021/ja00225a003.

Bromley, L. A.

1973 'Thermodynamic Properties of Strong Electrolytes in Aqueous Solutions', *AIChE J.* 19, 2, pp. 313–320, DOI: 10.1002/aic.690190216.

Bruttel, P. and R. Schlink

2006 *Water Determination by Karl Fischer Titration*, Metrohm Monograph, Metrohm Ltd., Switzerland, http://metrohmsiam.com/foodlab/FL_38/Monograph_WaterDeterminationKF.pdf.

Butler, J. N.

1967 'Electrochemistry in Dimethyl Sulfoxide', *J. Electroanal. Chem. Interfacial Electrochem.* 14, 1, pp. 89–116, DOI: 10.1016/0022-0728(67)80136-0.

Butler, J. N., D. R. Cogley and E. Grunwald

1971 'Selective Solvation of Ions by Water in Propylene Carbonate', *J. Phys. Chem.* 75, 10, pp. 1477–1486, DOI: 10.1021/j100680a018.

Butler, R. N. and M. C. R. Symons

1969 'Solvation Spectra. Part 29. Nuclear Magnetic Resonance Studies of Electrolyte Solutions : Ion-solvent Interactions in Methanol', en, *Trans. Faraday Soc.* 65, pp. 2559–2566, DOI: 10.1039/tf9696502559.

Cacace, M. G., E. M. Landau and J. J. Ramsden

1997 'The Hofmeister Series: Salt and Solvent Effects on Interfacial Phenomena', *Q. Rev. Biophys.* 30, 03, pp. 241–277, DOI: 10.1017/S0033583597003363.

Calligaris, S. and M. C. Nicoli

2006 'Effect of Selected Ions from Lyotropic Series on Lipid Oxidation Rate', *Food Chem.* 94, 1, pp. 130–134, DOI: 10.1016/j.foodchem.2004.11.002.

Carpenter, D. C. and F. E. Lovelace

1935 'The Influence of Neutral Salts on the Optical Rotation of Gelatin. III. Effect of the Halides of Lithium, Sodium, Rubidium and Cesium', *J. Am. Chem. Soc.* 57, 12, pp. 2337–2342, DOI: 10.1021/ja01315a001.

Chan, C.-Y., K. H. Khoo, E. S. Gryzlova and M.-T. Saugier-Cohen Adad

1996 *IUPAC Solubility Data Series*, ed. by J. W. Lorimer, IUPAC Solubility Data Series, Oxford University Press, vol. 61, https://srdata.nist.gov/solubility/IUPAC/SDS-61/SDS-61.pdf.

ChemAxon

2017 *Marvinsketch 17.27.0*, www.chemaxon.com/products/marvin/marvinsketch/.

Chen, R., D. Xu, G. Guo and L. Gui

2003 'Preparation of Ag_2Se and $Ag_2Se_{1-x}Te_x$ Nanowires by Electrodeposition from DMSO Baths', *Electrochem. Commun.* 5, 7, pp. 579–583, DOI: 10.1016/S1388-2481(03)00133-4.

Chernyak, Y.

2006 'Dielectric Constant, Dipole Moment, and Solubility Parameters of Some Cyclic Acid Esters', *J. Chem. Eng. Data*, 51, 2, pp. 416–418, DOI: 10.1021/je050341y.

Chu, X., J. Yang, G. Liu and J. Zhao

2014 'Swelling Enhancement of Polyelectrolyte Brushes Induced by External Ions', *Soft Matter*, 10 (30 2014), pp. 5568–5578, DOI: 10.1039/C4SM00860J.

Collins, K. D.

1997 'Charge Density-dependent Strength of Hydration and Biological Structure', *Biophys. J.* 72, 1, pp. 65–76, DOI: 10.1016/S0006-3495(97)78647-8.

2004 'Ions from the Hofmeister Series and Osmolytes: Effects on Proteins in Solution and in the Crystallization Process', *Methods*, 34, 3, Macromolecular Crystallization, pp. 300–311, DOI: 10.1016/j.ymeth.2004.03.021.

2006 'Ion Hydration: Implications for Cellular Function, Polyelectrolytes, and Protein Crystallization', *Biophys. Chem.* 119, 3, pp. 271–281, DOI: 10.1016/j.bpc.2005.08.010.

2012 'Why Continuum Electrostatics Theories Cannot Explain Biological Structure, Polyelectrolytes or Ionic Strength Effects in Ion-protein Interactions', *Biophys. Chem.* 167, pp. 43–59, DOI: 10.1016/j.bpc.2012.04.002.

Collins, K. D., G. W. Neilson and J. E. Enderby

2007 'Ions in Water: Characterizing the Forces That Control Chemical Processes and Biological Structure', *Biophys. Chem.* 128, 2–3, pp. 95–104, DOI: 10.1016/j.bpc.2007.03.009.

Collins, K. D. and M. W. Washabaugh

1985 'The Hofmeister Effect and the Behaviour of Water at Interfaces', *Q. Rev. Biophys.* 18, 4, pp. 323–422, DOI: 10.1017/S0033583500005369.

Compu Phase

2015 *Termite: A Simple RS232 Terminal*, www.compuphase.com/software_termite.htm.

Conway, B. E.

1977 'Significance of a Volcano Relation of Fajans for Hydration Energies', *J. Solution Chem.* 6, 1, pp. 23–31, DOI: 10.1007/BF00650789.

1987 'Electrochemical Proton Transfer and Cathodic Hydrogen Evolution', *Science Progress (1933-)*, 71, 4 (284), pp. 479–509, http://www.jstor.org/stable/43420696.

Cox, W. M. and J. H. Wolfenden

1934 'The Viscosity of Strong Electrolytes Measured by a Differential Method', *Proc. R. Soc. A*, 145, 855, pp. 475–488, DOI: 10.1098/rspa.1934.0113.

Craig, V. S. J., B. W. Ninham and R. M. Pashley

1993a 'Effect of Electrolytes on Bubble Coalescence', *Nature*, 364, 6435, pp. 317–319, DOI: 10.1038/364317a0.

1993b 'The Effect of Electrolytes on Bubble Coalescence in Water', *J. Phys. Chem.* 97, 39, pp. 10192–10197, DOI: 10.1021/j100141a047.

Craig, V. S. J. and M. Plunkett

2003 'Determination of Coupled Solvent Mass in Quartz Crystal Microbalance Measurements Using Deuterated Solvents', *J. Colloid Interface Sci.* 262, 1, pp. 126–129, DOI: 10.1016/s0021-9797(03)00210-8.

Crawford, M.-J. and T. M. Klapötke

1999 'The Synthesis of Tetraphenylarsonium Azide, $[Ph_4As]^+[N_3]^-$, and the Attempted Preparation of Tetraphenylarsonium Azidodithiocarbonate, $[Ph_4As]^+[SCSN_3]^-$', *Heteroat. Chem.* 10, 4, pp. 325–329, DOI: 10.1002/(SICI)1098-1071(1999)10:4<325::AID-HC11>3.0.CO;2-H.

Criss, C. M. and M. J. Mastroianni

1971 'Some Observations on the Viscosity Coefficients of Ions in Various Solvents', *J. Phys. Chem.* 75, 16, pp. 2532–2534, DOI: 10.1021/j100685a022.

DePhillips, P. and A. M. Lenhoff

2001 'Determinants of Protein Retention Characteristics on Cation-exchange Adsorbents', *J. Chromatogr. A*, 933, 1, pp. 57–72, DOI: 10.1016/S0021-9673(01)01275-4.

Desnoyers, J. E., R. E. Verrall and B. E. Conway

1965 'Electrostriction in Aqueous Solutions of Electrolytes', *J. Chem. Phys.* 43, 1, pp. 243–250, DOI: 10.1063/1.1696464.

dos Santos, A. P., A. Diehl and Y. Levin

2010 'Surface Tensions, Surface Potentials, and the Hofmeister Series of Electrolyte Solutions', *Langmuir*, 26, 13, pp. 10778–10783, DOI: 10.1021/la100604k.

Duignan, T. T., M. D. Baer and C. J. Mundy

2016 'Ions Interacting in Solution: Moving from Intrinsic to Collective Properties', *Curr. Opin. Colloid Interface Sci.* 23, pp. 58–65, DOI: 10.1016/j.cocis.2016.05.009.

Duignan, T. T., M. D. Baer, G. K. Schenter and C. J. Mundy

2017a 'Electrostatic Solvation Free Energies of Charged Hard Spheres Using Molecular Dynamics with Density Functional Theory Interactions', *J. Chem. Phys.* 147, 16, p. 161716, DOI: 10.1063/1.4994912.

Duignan, T. T., M. D. Baer, G. K. Schenter and C. J. Mundy

2017b 'Real Single Ion Solvation Free Energies with Quantum Mechanical Simulation', *Chem. Sci.* 8 (9 2017), pp. 6131–6140, DOI: 10.1039/C7SC02138K.

Duignan, T. T., D. F. Parsons and B. W. Ninham

2013a 'A Continuum Model of Solvation Energies Including Electrostatic, Dispersion, and Cavity Contributions', *J. Phys. Chem. B*, 117, 32, pp. 9421–9429, DOI: 10.1021/jp403596c.

2013b 'A Continuum Solvent Model of the Multipolar Dispersion Solvation Energy', *J. Phys. Chem. B*, 117, 32, pp. 9412–9420, DOI: 10.1021/jp403595x.

2014a 'A Continuum Solvent Model of Ion-ion Interactions in Water', *Phys. Chem. Chem. Phys.* 16 (40 2014), pp. 22014–22027, DOI: 10.1039/C4CP02822H.

2014b 'A Continuum Solvent Model of the Partial Molar Volumes and Entropies of Ionic Solvation', *J. Phys. Chem. B*, 118, 11, pp. 3122–3132, DOI: 10.1021/jp410956m.

2014c 'Collins's Rule, Hofmeister Effects and Ionic Dispersion Interactions', eng, *Chem. Phys. Lett.* 608, Complete, pp. 55–59, DOI: 10.1016/j.cplett.2014.05.056.

Dzubiella, J., M. Fyta, D. Horinek, I. Kalcher, R. R. Netz and N. Schwierz

2009 'Ion-specificity: From Solvation Thermodynamics to Molecular Simulations and Back', in *Specific Ion Effects*, ed. by W. Kunz, pp. 231–265.

Easteal, A. J. and L. A. Woolf

1985 'Self-diffusion and Volumetric Measurements for *N*-Methylformamide and *N,N*-Dimethylformamide at Temperatures from 240 K to 313 K and Pressures up to 300 MPa', *J. Chem. Soc., Faraday Trans. 1*, 81 (11 1985), pp. 2821–2833, DOI: 10.1039/F19858102821.

1988 '(p, V_m, T, x) Measurements for $(1-x)H_2O + xCH_3CN$ in the Range 278 K to 323 K and 0.1 MPa to 280 MPa I. Experimental Results, Isothermal Compressibilities, Isobaric Expansivities, and Partial Molar Volumes', *J. Chem. Thermodyn.* 20, 6, pp. 693–699, DOI: 10.1016/0021-9614(88)90020-1.

Edmondson, S., V. L. Osborne and W. T. S. Huck

2004 'Polymer Brushes *via* Surface-initiated Polymerizations', *Chem. Soc. Rev.* 33 (1 2004), pp. 14–22, DOI: 10.1039/B210143M.

Fajans, K.

1921 'Löslichkeit Und Ionisation Vom Standpunkte Der Atomstruktur', *Naturwissenschaften*, 9, 37, pp. 729–738, DOI: 10.1007/BF01487182.

Fajans, K. and G. Karagunis

1930 'Osmotisches Verhalten Von Starken Elektrolyten in Lösung Und Hydratation Ihrer Ionen', *Angew. Chem.* 43, 48, pp. 1046–1048, DOI: 10.1002/ange.19300434804.

Fajans, K. and O. Johnson

1942 'Ion-solvent Interaction and Individual Properties of Electrolytes', *J. Electrochem. Soc.* 82, 1, pp. 273–287, DOI: 10.1149/1.3071414.

Fennell, C. J., A. Bizjak, V. Vlachy and K. A. Dill
2009 'Ion Pairing in Molecular Simulations of Aqueous Alkali Halide Solutions', *J. Phys. Chem. B*, 113, 19, pp. 6782–6791, DOI: 10.1021/jp809782z.

Fischer, M. H. and G. Moore
1907 'On the Swelling of Fibrin', *Am. J. Physiol. — Leg. Content*, 20, 2, pp. 330–342, http://ajplegacy.physiology.org/content/20/2/330.short.

Fox, J. M., K. Kang, W. Sherman, A. Héroux, G. M. Sastry, M. Baghbanzadeh, M. R. Lockett and G. M. Whitesides
2015 'Interactions between Hofmeister Anions and the Binding Pocket of a Protein', *J. Am. Chem. Soc.* 137, 11, pp. 3859–3866, DOI: 10.1021/jacs.5b00187.

Franks, G. V.
2002 'Zeta Potentials and Yield Stresses of Silica Suspensions in Concentrated Monovalent Electrolytes: Isoelectric Point Shift and Additional Attraction', *J. Colloid Interface Sci.* 249, 1, pp. 44–51, DOI: 10.1006/jcis.2002.8250.

Franks, G. V., S. B. Johnson, P. J. Scales, D. V. Boger and T. W. Healy
1999 'Ion-specific Strength of Attractive Particle Networks', *Langmuir*, 15, 13, pp. 4411–4420, DOI: 10.1021/la9815345.

Fridovich, I.
1963 'Inhibition of Acetoacetic Decarboxylase by Anions. The Hofmeister Lyotropic Series', *J. Biol. Chem.* 238, 2, pp. 592–598, www.jbc.org/content/238/2/592.full.pdf.

Friedman, R.
2013 'Electrolyte Solutions and Specific Ion Effects on Interfaces', *J. Chem. Educ.* 90, 8, pp. 1018–1023, DOI: 10.1021/ed4000525.

Fulop, G. F. and R. M. Taylor
1985 'Electrodeposition of Semiconductors', en, *Annu. Rev. Mater. Sci.* 15, 1, pp. 197–210, DOI: 10.1146/annurev.ms.15.080185.001213.

Funkner, S., G. Niehues, D. A. Schmidt, M. Heyden, G. Schwaab, K. M. Callahan, D. J. Tobias and M. Havenith
2012 'Watching the Low-frequency Motions in Aqueous Salt Solutions: The Terahertz Vibrational Signatures of Hydrated Ions', *J. Am. Chem. Soc.* 134, 2, pp. 1030–1035, DOI: 10.1021/ja207929u.

Gao, Y. Q.
2011 'Simple Theoretical Model for Ion Cooperativity in Aqueous Solutions of Simple Inorganic Salts and Its Effect on Water Surface Tension', *J. Phys. Chem. B*, 115, 43, pp. 12466–12472, DOI: 10.1021/jp2076512.

Gardner, C. L., D. T. Fouchard and W. R. Fawcett
1981 'The Kinetics and Mechanism of the Electroreduction of Sulfur Dioxide in Nonaqueous Media II. Effects of Electrolyte and Solvent on the Mechanism of Reduction', en, *J. Electrochem. Soc.* 128, 11, pp. 2345–2350, DOI: 10.1149/1.2127246.

Giesecke, M., F. Hallberg, Y. Fang, P. Stilbs and I. Furó

2016 'Binding of Monovalent and Multivalent Metal Cations to Polyethylene Oxide in Methanol Probed by Electrophoretic and Diffusion NMR', *J. Phys. Chem. B*, 120, 39, pp. 10358–10366, DOI: 10.1021/acs.jpcb.6b08923.

Giesecke, M., G. Mériguet, F. Hallberg, Y. Fang, P. Stilbs and I. Furó

2015 'Ion Association in Aqueous and Non-aqueous Solutions Probed by Diffusion and Electrophoretic NMR.' en, *Phys. Chem. Chem. Phys.* 17, 5, pp. 3402–3408, DOI: 10.1039/c4cp04446k.

Gujt, J., M. Bešter-Rogač and B. Hribar-Lee

2014 'An Investigation of Ion-pairing of Alkali Metal Halides in Aqueous Solutions Using the Electrical Conductivity and the Monte Carlo Computer Simulation Methods', *J. Mol. Liq.* 190, pp. 34–41, DOI: 10.1016/j.molliq.2013.09.025.

Gurau, M. C., S.-M. Lim, E. T. Castellana, F. Albertorio, S. Kataoka and P. S. Cremer

2004 'On the Mechanism of the Hofmeister Effect', *J. Am. Chem. Soc.* 126, 34, pp. 10522–10523, DOI: 10.1021/ja047715c.

Hála, J.

2004 'IUPAC-NIST Solubility Data Series. 79. Alkali and Alkaline Earth Metal Pseudohalides', *J. Phys. Chem. Ref. Data*, 33, 1, pp. 1–176, DOI: 10.1063/1.1563591.

Hamaguchi, K. and E. P. Geiduschek

1962 'The Effect of Electrolytes on the Stability of the Deoxyribonucleate Helix', *J. Am. Chem. Soc.* 84, 8, pp. 1329–1338, DOI: 10.1021/ja00867a001.

Hamann, S. D. and S. C. Lim

1954 'The Volume Change on Ionization of Weak Electrolytes', *Aust. J. Chem.* 7, 4, pp. 329–334, DOI: 10.1071/CH9540329.

Hanstein, W. G.

1979 'Chaotropic Ions and Their Interactions with Proteins', en, *J. Solid-Phase Biochem.* 4, 3, pp. 189–206, DOI: 10.1007/BF02991894.

Hao, L.-S., Y.-T. Deng, L.-S. Zhou, H. Ye, Y.-Q. Nan and P. Hu

2012 'Mixed Micellization and the Dissociated Margules Model for Cationic/anionic Surfactant Systems', *J. Phys. Chem. B*, 116, 17, pp. 5213–5225, DOI: 10.1021/jp300568k.

Hao, L.-S., N. Yang, G.-Y. Xu, Y.-F. Jia, Q. Liu and Y.-Q. Nan

2016 'Specific Ion Effects on the Micellization of Aqueous Mixed Cationic/anionic Surfactant Systems with Various Counterions', *Colloids Surf., A*, 504, pp. 161–173, DOI: 10.1016/j.colsurfa.2016.05.073.

Harris, W. S.

1958 *Electrochemical Studies in Cyclic Esters*, PhD thesis, California Univ., Berkeley, CA (US). Radiation Lab., DOI: 10.2172/4305596.

Henry, C. L. and V. S. J. Craig
2008 'Ion-specific Influence of Electrolytes on Bubble Coalescence in Nonaqueous Solvents', *Langmuir*, 24, 15, pp. 7979–7985, DOI: 10.1021/la8008738.

Hess, B. and N. F. A. van der Vegt
2009 'Cation Specific Binding with Protein Surface Charges', *Proc. Natl. Acad. Sci. U. S. A.* 106, 32, pp. 13296–13300, DOI: 10.1073/pnas.0902904106.

Heyda, J., M. Lund, M. Ončák, P. Slavíček and P. Jungwirth
2010 'Reversal of Hofmeister Ordering for Pairing of NH_4^+ Vs Alkylated Ammonium Cations with Halide Anions in Water', *J. Phys. Chem. B*, 114, 33, pp. 10843–10852, DOI: 10.1021/jp101393k.

Hofmeister, F.
1888a '11. Zur Lehre Von Der Wirkung Der Salze. Ueber Regelmässigkeiten in der eiweissfällenden Wirkung der Salze und ihre Beziehung zum physiologischen Verhalten derselben.' *Arch. Exp. Pathol. Pharmakol.* 24, 4, pp. 247–260, DOI: 10.1007/BF01918191.
1888b '12. Zur Lehre Von Der Wirkung Der Salze. Ueber die wasserentziehende Wirkung der Salze.' German, *Arch. Exp. Pathol. Pharmakol.* 25, 1, pp. 1–30, DOI: 10.1007/BF01838161.

Hribar, B., N. T. Southall, V. Vlachy and K. A. Dill
2002 'How Ions Affect the Structure of Water', *J. Am. Chem. Soc.* 124, 41, pp. 12302–12311, DOI: 10.1021/ja026014h.

Huddleston, J. G., A. E. Visser, W. M. Reichert, H. D. Willauer, G. A. Broker and R. D. Rogers
2001 'Characterization and Comparison of Hydrophilic and Hydrophobic Room Temperature Ionic Liquids Incorporating the Imidazolium Cation', *Green Chem.* 3 (4 2001), pp. 156–164, DOI: 10.1039/B103275P.

Hyde, A. M., S. L. Zultanski, J. H. Waldman, Y.-L. Zhong, M. Shevlin and F. Peng
2017 'General Principles and Strategies for Salting-Out Informed by the Hofmeister Series', *Org. Process Res. Dev.* 21, 9, pp. 1355–1370, DOI: 10.1021/acs.oprd.7b00197.

Izutsu, K.
2009 *Electrochemistry in Nonaqueous Solutions*, 2nd ed., WILEY, Weinheim, Germany.

Jain, S. and J. C. Ahluwalia
1996 'Differential Scanning Calorimetric Studies on the Effect of Ammonium and Tetraalkylammonium Halides on the Stability of Lysozyme', *Biophys. Chem.* 59, 1, pp. 171–177, DOI: https://doi.org/10.1016/0301-4622(95)00135-2.

Jane, I., A. McKinnon and R. J. Flanagan
1985 'High-performance Liquid Chromatographic Analysis of Basic Drugs on Silica Columns Using Non-aqueous Ionic Eluents', *J. Chromatogr. A*, 323, 2, pp. 191–225, DOI: 10.1016/S0021-9673(01)90384-X.

Jenkins, H. D. B. and Y. Marcus

1995 'Viscosity B-coefficients of Ions in Solution', *Chem. Rev.* 95, 8, pp. 2695–2724, DOI: 10.1021/cr00040a004.

Jenkins, H. D. B. and M. S. F. Pritchett

1984 'A New Approach to the Analysis of Absolute Free Energies, Enthalpies and Entropies of Hydration of Individual Gaseous Ions and Absolute Single-ion Viscosity B-coefficients', *J. Chem. Soc., Faraday Trans. 1*, 80 (3 1984), pp. 721–737, DOI: 10.1039/F19848000721.

Johannsmann, D.

2015 *The Quartz Crystal Microbalance in Soft Matter Research: Fundamentals and Modeling*, Soft and Biological Matter, Springer International Publishing, Cham, Switzerland, DOI: 10.1007/978-3-319-07836-6.

Jones, G. and M. Dole

1929 'The Viscosity of Aqueous Solutions of Strong Electrolytes with Special Reference to Barium Chloride', *J. Am. Chem. Soc.* 51, 10, pp. 2950–2964, DOI: 10.1021/ja01385a012.

Jorné, J. and C. W. Tobias

1975 'Electrodeposition of the Alkali Metals from Propylene Carbonate', *J. Appl. Electrochem.* 5, 4, pp. 279–290, DOI: 10.1007/BF00608791.

Jungwirth, P. and P. S. Cremer

2014 'Beyond Hofmeister', *Nat. Chem.* 6, 4, pp. 261–263, DOI: 10.1038/nchem.1899.

Jungwirth, P. and B. Winter

2008 'Ions at Aqueous Interfaces: From Water Surface to Hydrated Proteins', *Annu. Rev. Phys. Chem.* 59, pp. 343–366, DOI: 10.1146/annurev.physchem.59.032607.093749.

Kabalnov, A., U. Olsson and H. Wennerstroem

1995 'Salt Effects on Nonionic Microemulsions Are Driven by Adsorption/depletion at the Surfactant Monolayer', *J. Phys. Chem.* 99, 16, pp. 6220–6230, DOI: 10.1021/j100016a068.

Kasprowicz, B. and S. Kielich

1967 'On Nonlinear Changes in Refractive Index of Liquids Due to Electrostriction and Electrocaloric Effect', *Acta Phys. Polon.* 31, 4, pp. 787–790.

Kherb, J., S. C. Flores and P. S. Cremer

2012 'Role of Carboxylate Side Chains in the Cation Hofmeister Series', *J. Phys. Chem. B*, 116, 25, pp. 7389–7397, DOI: 10.1021/jp212243c.

Klein, R., M. Kellermeier, M. Drechsler, D. Touraud and W. Kunz

2009 'Solubilisation of Stearic Acid by the Organic Base Choline Hydroxide', *Colloids Surf., A*, 338, 1-3, pp. 129–134, DOI: 10.1016/j.colsurfa.2008.04.049.

Ko, J.-M., H.-W. Rhee, S.-M. Park and C.-Y. Kim

1990 'Morphology and Electrochemical Properties of Polypyrrole Films Prepared in Aqueous and Nonaqueous Solvents', en, *J. Electrochem. Soc.* 137, 3, p. 905, DOI: 10.1149/1.2086576.

Kojić, D., R. Tsenkova, K. Tomobe, K. Yasuoka and M. Yasui

2014 'Water Confined in the Local Field of Ions', *ChemPhysChem*, 15, 18, pp. 4077–4086, DOI: 10.1002/cphc.201402381.

Kou, R., J. Zhang, Z. Chen and G. Liu

2017 'Counterion Specificity of Polyelectrolyte Brushes: Role of the Specific Ion-pairing Interactions', *ChemPhysChem*, Submitted for publication.

Kou, R., J. Zhang, T. Wang and G. Liu

2015 'Interactions between Polyelectrolyte Brushes and Hofmeister Ions: Chaotropes Versus Kosmotropes', *Langmuir*, 31, 38, pp. 10461–10468, DOI: 10.1021/acs.langmuir.5b02698.

Kozisek, F.

2005 'Health Risks from Drinking Demineralised Water', in *Nutrients in drinking-water*, *Nutrients in Drinking Water*, World Health Organization WHO, Geneva, pp. 148–163, www.who.int/water_sanitation_health/dwq/nutrientschap12.pdf.

Kumar, S., X. Yin, B. D. Trapp, J. H. Hoh and M. E. Paulaitis

2002 'Relating Interactions between Neurofilaments to the Structure of Axonal Neurofilament Distributions through Polymer Brush Models', *Biophys. J.* 82, 5, pp. 2360–2372, DOI: 10.1016/S0006-3495(02)75581-1.

Kunz, W.

2009 (ed.), *Specific Ion Effects*, World Scientific Publishing Co. Pte. Ltd., Singapore.

2010 'Specific Ion Effects in Colloidal and Biological Systems', *Curr. Opin. Colloid Interface Sci.* 15, 1-2, pp. 34–39, DOI: 10.1016/j.cocis.2009.11.008.

2014 'Specific Ion Effects, Evidences', in *Encyclopedia of Applied Electrochemistry*, ed. by G. Kreysa, K.-i. Ota and R. F. Savinell, Springer, New York, pp. 2045–2050, ISBN: 978-1-4419-6995-8, DOI: 10.1007/978-1-4419-6996-5.

Kunz, W., L. Belloni, O. Bernard and B. W. Ninham

2004 'Osmotic Coefficients and Surface Tensions of Aqueous Electrolyte Solutions: Role of Dispersion Forces', *J. Phys. Chem. B*, 108, 7, pp. 2398–2404, DOI: 10.1021/jp036113x.

Kunz, W., J. Henle and B. W. Ninham

2004 ''zur Lehre Von Der Wirkung Der Salze' (about the Science of the Effect of Salts): Franz Hofmeister's Historical Papers', *Curr. Opin. Colloid Interface Sci.* 9, 1-2, pp. 19–37, DOI: 10.1016/j.cocis.2004.05.005.

Kunz, W., P. Lo Nostro and B. W. Ninham

2004 'The Present State of Affairs with Hofmeister Effects', *Curr. Opin. Colloid Interface Sci.* 9, 1, pp. 1–18, DOI: 10.1016/j.cocis.2004.05.004.

Kunz, W. and R. Neueder

2009 'An Attempt of a General Overview', in *Specific Ion Effects*, ed. by W. Kunz, World Scientific Publishing Co. Pte. Ltd, Singapore, chap. 1, pp. 3–53, www.worldscientific.com/worldscibooks/10.1142/7261.

Lagi, M., P. Lo Nostro, E. Fratini, B. W. Ninham and P. Baglioni

2007 'Insights into Hofmeister Mechanisms: Anion and Degassing Effects on the Cloud Point of Dioctanoylphosphatidylcholine/water Systems', *J. Phys. Chem. B*, 111, 3, pp. 589–97, DOI: 10.1021/jp065769y.

Larsen, J. W. and L. J. Magid

1974 'Calorimetric and Counterion Binding Studies of the Interactions between Micelles and Ions. Observation of Lyotropic Series', *J. Am. Chem. Soc.* 96, 18, pp. 5774–5782, DOI: 10.1021/ja00825a013.

Leontidis, E.

2002 'Hofmeister Anion Effects on Surfactant Self-assembly and the Formation of Mesoporous Solids', *Curr. Opin. Colloid Interface Sci.* 7, 1-2, pp. 81–91, DOI: 10.1016/S1359-0294(02)00010-9.

2016 'Chaotropic Salts Interacting with Soft Matter: Beyond the Lyotropic Series', *Curr. Opin. Colloid Interface Sci.* 23, pp. 100–109, DOI: 10.1016/j.cocis.2016.06.017.

2017 'Investigations of the Hofmeister Series and Other Specific Ion Effects Using Lipid Model Systems', *Adv. Colloid Interface Sci.* 243, pp. 8–22, DOI: 10.1016/j.cis.2017.04.001.

Lewis, G. N. and M. Randall

1961 *Thermodynamics and the Free Energy of Chemical Substances*, ed. by K. S. Pitzer and L. Brewer, 2nd ed., McGraw-Hill series in advanced chemistry, Graphical derivation of the standard molar volume of ions. Chapter 17 pag. 205, McGraw-Hill Book Company, Inc., N.Y., chap. 17, library.anu.edu.au/record=b1051187.

Li, F., T. Zhang and H. Zhou

2013 'Challenges of Non-aqueous Li-O_2 Batteries: Electrolytes, Catalysts, and Anodes', en, *Energy Environ. Sci.* 6, 4, pp. 1125–1141, DOI: 10.1039/c3ee00053b.

Lide, D. R.

2010 (ed.), *CRC Handbook of Chemistry and Physics*, 90th ed., CRC Press/Taylor and Francis, Boca Raton, FL.

Lin, X.-S., Y. Zou, K.-H. Zhao, T.-X. Yang, P. Halling and Z. Yang

2016 'Tetraalkylammonium Ionic Liquids As Dual Solvents-catalysts for Direct Synthesis of Sugar Fatty Acid Esters', *J. Surfactants Deterg.* 19, 3, pp. 511–517, DOI: 10.1007/s11743-016-1798-7.

Lincot, D.

2005 'Electrodeposition of Semiconductors', *Thin Solid Films*, 487, 1-2, pp. 40–48, DOI: 10.1016/j.tsf.2005.01.032.

Liu, C.-W., F. Wang, L. Yang, X.-Z. Li, W.-J. Zheng and Y. Q. Gao

2014 'Stable Salt-water Cluster Structures Reflect the Delicate Competition between Ion-water and Water-water Interactions', *J. Phys. Chem. B*, 118, 3, pp. 743–751, DOI: 10.1021/jp408439j.

Liu, G. and G. Zhang

2013 *QCM-D Studies on Polymer Behavior at Interfaces*, SpringerBriefs in Molecular Science, Springer, Heidelberg, Germany, DOI: 10.1007/978-3-642-39790-5.

Lo Nostro, P., V. Mazzini, B. W. Ninham, M. Ambrosi, L. Dei and P. Baglioni

2016 'Specific Anion Effects on the Kinetics of Iodination of Acetone', *ChemPhysChem*, 17, 16, pp. 2567–2571, DOI: 10.1002/cphc.201600241.

Lo Nostro, P. and B. W. Ninham

2012 'Hofmeister Phenomena: An Update on Ion Specificity in Biology', *Chem. Rev.* 112, 4, pp. 2286–2322, DOI: 10.1021/cr200271j.

2016 'Editorial: Electrolytes and Specific Ion Effects. New and Old Horizons', *Curr. Opin. Colloid Interface Sci.* 23, A1–A5, DOI: 10.1016/j.cocis.2016.06.007.

Lo Nostro, P., B. W. Ninham, M. Ambrosi, L. Fratoni, S. Palma, D. Allemandi and P. Baglioni

2003 'Hofmeister Effect in Coagels of Ascorbic Acid Based Surfactants', *Langmuir*, 19, 23, pp. 9583–9591, DOI: 10.1021/la034441i.

Lo Nostro, P., B. W. Ninham, S. Milani, A. Lo Nostro, G. Pesavento and P. Baglioni

2006 'Hofmeister Effects in Supramolecular and Biological Systems', *Biophys. Chem.* 124, 3 (Ion Hydration Special Issue 2006), pp. 208–213, DOI: 10.1016/j.bpc.2006.04.004.

Lonetti, B., P. Lo Nostro, B. W. Ninham and P. Baglioni

2005 'Anion Effects on Calixarene Monolayers: A Hofmeister Series Study', *Langmuir*, 21, 6, pp. 2242–9, DOI: 10.1021/la048211v.

Long, Y., T. Wang, L. Liu, G. Liu and G. Zhang

2013 'Ion Specificity at a Low Salt Concentration in Water-methanol Mixtures Exemplified by a Growth of Polyelectrolyte Multilayer', *Langmuir*, 29, 11, pp. 3645–3653, DOI: 10.1021/la400035e.

Lukšič, M., M. Bončina, V. Vlachy and M. Druchok

2012 'Isothermal Titration Calorimetry and Molecular Dynamics Study of Ion-selectivity in Mixtures of Hydrophobic Polyelectrolytes with Sodium Halides in Water', *Phys. Chem. Chem. Phys.* 14 (6 2012), pp. 2024–2031, DOI: 10.1039/C2CP23137A.

Lukšič, M., C. J. Fennell and K. A. Dill

2014 'Using Interpolation for Fast and Accurate Calculation of Ion-ion Interactions', *J. Phys. Chem. B*, 118, 28, pp. 8017–8025, DOI: 10.1021/jp501141j.

Lund, M., B. Jagoda-Cwiklik, C. E. Woodward, R. Vácha and P. Jungwirth

2010 'Dielectric Interpretation of Specificity of Ion Pairing in Water', *J. Phys. Chem. Lett.* 1, 1, pp. 300–303, DOI: 10.1021/jz900151f.

Lyklema, J.

2003 'Lyotropic Sequences in Colloid Stability Revisited', *Adv. Colloid Interface Sci.* 100, pp. 1–12, DOI: 10.1016/S0001-8686(02)00075-1.

Lyklema, J.
2009 'Simple Hofmeister Series', *Chem. Phys. Lett.* 467, 4–6, pp. 217–222, DOI: 10.1016/j.cplett.2008.11.013.

Maiti, K., D. Mitra, S. Guha and S. P. Moulik
2009 'Salt Effect on Self-aggregation of Sodium Dodecylsulfate (SDS) and Tetradecyltrimethylammonium Bromide (TTAB): Physicochemical Correlation and Assessment in the Light of Hofmeister (lyotropic) Effect', *J. Mol. Liq.* 146, 1-2, pp. 44–51, DOI: 10.1016/j.molliq.2009.01.014.

Marcus, Y.
1994 'Viscosity *B*-coefficients, Structural Entropies and Heat Capacities, and the Effects of Ions on the Structure of Water', *J. Solution Chem.* 23, 7, pp. 831–848, DOI: 10.1007/BF00972677.

Marcus, Y.
2004 'The Standard Partial Molar Volumes of Ions in Solution. Part 2. The Volumes in Two Binary Solvent Mixtures with No Preferential Solvation', *J. Solution Chem.* 33, 5, pp. 549–559, DOI: 10.1023/b:josl.0000037775.94071.92.
2005 'The Standard Partial Molar Volumes of Ions in Solution. Part 3. Volumes in Solvent Mixtures Where Preferential Solvation Takes Place', *J. Solution Chem.* 34, 3, pp. 317–331, DOI: 10.1007/s10953-005-3052-1.
2010 'On the Intrinsic Volumes of Ions in Aqueous Solutions', English, *J. Solution Chem.* 39, 7, pp. 1031–1038, DOI: 10.1007/s10953-010-9553-6.
2011 'Electrostriction in Electrolyte Solutions', *Chem. Rev.* 111, 4, pp. 2761–2783, DOI: 10.1021/cr100130d.
2013 'Individual Ionic Surface Tension Increments in Aqueous Solutions', *Langmuir*, 29, 9, pp. 2881–2888, DOI: 10.1021/la3041659.
2015 *Ions in Solution and Their Solvation*, 1st ed., John Wiley & Sons, Inc., Hoboken, NJ, p. 312, ISBN: 1118892305.
2016 'Electrostriction of Several Nonaqueous Solvents under Ambient Conditions and Solvation Numbers of Ions in Them', *J. Phys. Chem. B*, 120, 36, pp. 9755–9758, DOI: 10.1021/acs.jpcb.6b07179.

Marcus, Y. and G. T. Hefter
1997 'The Compressibility of Liquids at Ambient Temperature and Pressure', *J. Mol. Liq.* 73–74, Ion-ion, ion-solvent and solvent-solvent interactions in electrolyte solutions, pp. 61–74, DOI: 10.1016/S0167-7322(97)00057-3.
1999 'On the Pressure and Electric Field Dependencies of the Relative Permittivity of Liquids', *J. Solution Chem.* 28, 5, pp. 575–592, DOI: 10.1023/A:1022687016721.
2004 'Standard Partial Molar Volumes of Electrolytes and Ions in Non-aqueous Solvents', *Chem. Rev.* 104, pp. 3405–3452, DOI: 10.1021/cr030047d.

Marcus, Y., G. T. Hefter and T.-S. Pang
1994 'Ionic Partial Molar Volumes in Non-aqueous Solvents', *J. Chem. Soc., Faraday Trans.* 90, 13, pp. 1899–1903, DOI: 10.1039/FT9949001899.

Mason, P. E., G. W. Neilson, C. E. Dempsey, A. C. Barnes and J. M. Cruickshank

2003 'The Hydration Structure of Guanidinium and Thiocyanate Ions: Implications for Protein Stability in Aqueous Solution', *Proc. Natl. Acad. Sci.* 100, 8, pp. 4557–4561, DOI: 10.1073/pnas.0735920100.

Mason, P. E., C. E. Dempsey, L. Vrbka, J. Heyda, J. W. Brady and P. Jungwirth

2009 'Specificity of Ion-Protein Interactions: Complementary and Competitive Effects of Tetrapropylammonium, Guanidinium, Sulfate, and Chloride Ions', *J. Phys. Chem. B*, 113, 10, pp. 3227–3234, DOI: 10.1021/jp8112232.

McNaught, A. D. and A. Wilkinson

1997 (eds.), *IUPAC. Compendium of Chemical Terminology (the 'Gold Book')*, 2nd ed., XML on-line corrected version: http://goldbook.iupac.org (2006-) created by M. Nic, J. Jirat, B. Kosata; updates compiled by A. Jenkins. Last update: 2014-02-24; version: 2.3.3., Blackwell Scientific Publications, Oxford, DOI: 10.1351/goldbook.

Medda, L., C. Carucci, D. F. Parsons, B. W. Ninham, M. Monduzzi and A. Salis

2013 'Specific Cation Effects on Hemoglobin Aggregation below and at Physiological Salt Concentration', *Langmuir*, 29, 49, pp. 15350–15358, DOI: 10.1021/la404249n.

Medda, L., A. Salis and E. Magner

2012 'Specific Ion Effects on the Electrochemical Properties of Cytochrome *c*', *Phys. Chem. Chem. Phys.* 14, 8, pp. 2875–2883, DOI: 10.1039/c2cp23401g.

Melendres, C. A. and H. G. Hertz

1974 'Magnetic Relaxation of Quadrupolar Nuclei in Nonaqueous Electrolyte Solutions', *J. Chem. Phys.* 61, 10, p. 4156, DOI: 10.1063/1.1681713.

Merchant, S. and D. Asthagiri

2009 'Thermodynamically Dominant Hydration Structures of Aqueous Ions', *J. Chem. Phys.* 130, 19, p. 195102, DOI: 10.1063/1.3132709.

Millero, F. J.

1971 'The Molal Volumes of Electrolytes', *Chem. Rev.* 71, 2, pp. 147–176, DOI: 10.1021/cr60270a001.

1972a 'Compilation of the Partial Molal Volumes of Electrolytes at Infinite Dilution, $\overline{V}^{\circ}$, and the Apparent Molal Volume Concentration Dependence Constants, S_V^* and b_V, at Various Temperatures', in *Water and Aqueous Solutions: Structure, Thermodynamics and Transport Processes*, ed. by R. A. Horne, Wiley-Interscience, New York, chap. Addendum to chapter 13, pp. 565–595.

1972b 'The Partial Molal Volumes of Electrolytes in Aqueous Solutions', in *Water and Aqueous Solutions: Structure, Thermodynamics and Transport Processes*, ed. by R. A. Horne, Wiley-Interscience, New York, chap. 13, pp. 519–564.

Millero, F. J., F. Huang and A. L. Laferiere

2002a 'Solubility of Oxygen in the Major Sea Salts As a Function of Concentration and Temperature', *Mar. Chem.* 78, 4, pp. 217–230, DOI: 10.1016/S0304-4203(02)00034-8.

2002b 'The Solubility of Oxygen in the Major Sea Salts and Their Mixtures at 25 °C', *Geochim. Cosmochim. Acta*, 66, 13, pp. 2349–2359, DOI: 10.1016/S0016-7037(02)00838-4.

Mooi, S. M. and B. Heyne

2012 'Size Does Matter: How to Control Organization of Organic Dyes in Aqueous Environment Using Specific Ion Effects', *Langmuir*, 28, 48, pp. 16524–16530, DOI: 10.1021/la3034885.

Mooi, S. M., S. N. Keller and B. Heyne

2014 'Forcing Aggregation of Cyanine Dyes with Salts: A Fine Line between Dimers and Higher Ordered Aggregates', *Langmuir*, 30, 32, pp. 9654–9662, DOI: 10.1021/la502124b.

Moreira, L. and A. Firoozabadi

2010 'Molecular Thermodynamic Modeling of Specific Ion Effects on Micellization of Ionic Surfactants', *Langmuir*, 26, 19, pp. 15177–15191, DOI: 10.1021/la102536y.

Morris, D. F. C.

1969 'Ionic Radii and Enthalpies of Hydration of Ions. An Appendix to Structure and Bonding 4, 63 (1968)', in *Structure And Bonding*, ed. by P. Hemmerich, C. K. Jørgensen, J. B. Neilands, S. R. S. Nyholm, D. Reinen and R. J. P. Williams, Structure and Bonding, Springer, Berlin, Heidelberg, vol. 6, pp. 157–159, DOI: 10.1007/BFb0118857.

Moya, S. E. and J. Irigoyen

2013 'Recent Advances in the Use of the Quartz Crystal Microbalance with Dissipation for the Study of the Collapse of Polyelectrolyte Brushes', *J. Polym. Sci., Part B: Polym. Phys.* 51, 14, pp. 1068–1072, DOI: 10.1002/polb.23311.

Muhuri, P. K., S. K. Ghosh and D. K. Hazra

1993 'Solubilities of Some Alkali-metal Salts, Tetraphenylarsonium Chloride, and Tetraphenylphosphonium Bromide in Propylene Carbonate at 25 °C Using the Ion-selective Electrode Technique', *J. Chem. Eng. Data*, 38, 2, pp. 242–244, DOI: 10.1021/je00010a014.

Naejus, R., R. Coudert, P. Willmann and D. Lemordant

1998 'Ion Solvation in Carbonate-based Lithium Battery Electrolyte Solutions', *Electrochim. Acta*, 43, 3, pp. 275–284, DOI: 10.1016/S0013-4686(97)00073-X.

Nan, Y.-Q., S.-Q. He, M.-N. Liu, H.-Y. He and L.-S. Hao

2013 'The Influence of Inorganic Salts on the Rheological Properties of 1,3-propanediyl Bis(dodecyl Dimethylammonium Bromide) and Sodium Dodecylsulfonate Aqueous Mixed System', *Colloids Surf., A*, 436, 17, pp. 158–169, DOI: 10.1016/j.colsurfa.2013.06.032.

Nan, Y.-Q., H.-M. Xu, N. Yang, Q. Liu, Y.-F. Jia and L.-S. Hao
2015 'Role of Matching Water Affinities between Oppositely Charged Headgroups in the Rheological Properties of Aqueous Mixed Cationic/anionic Surfactant Systems', *Colloids Surf., A*, 482, pp. 125–137, DOI: 10.1016/j.colsurfa.2015.04.030.

Nicholson, J. P.
2005 'Electrodeposition of Silicon from Nonaqueous Solvents', en, *J. Electrochem. Soc.* 152, 12, pp. C795–C802, DOI: 10.1149/1.2083227.

Ninham, B. W., T. T. Duignan and D. F. Parsons
2011 'Approaches to Hydration, Old and New: Insights through Hofmeister Effects', *Curr. Opin. Colloid Interface Sci.* 16, 6, pp. 612–617, DOI: 10.1016/j.cocis.2011.04.006.

Ninham, B. W. and P. Lo Nostro
2010 *Molecular Forces and Self Assembly. in Colloid, Nano Sciences and Biology*, Cambridge University Press, Cambridge, chap. 7.

Ninham, B. W. and V. Yaminsky
1997 'Ion Binding and Ion Specificity: The Hofmeister Effect and Onsager and Lifshitz Theories', *Langmuir*, 13, 7, pp. 2097–2108, DOI: 10.1021/la960974y.

Obiweluozor, F. O., A. GhavamiNejad, S. Hashmi, M. Vatankhah-Varnoosfaderani and F. J. Stadler
2014 'A NIPAM-zwitterion Copolymer: Rheological Interpretation of the Specific Ion Effect on the LCST', *Macromol. Chem. Phys.* 215, 11, pp. 1077–1091, DOI: 10.1002/macp.201300778.

Okur, H. I., J. Hladílková, K. B. Rembert, Y. Cho, J. Heyda, J. Dzubiella, P. S. Cremer and P. Jungwirth
2017 'Beyond the Hofmeister Series: Ion-specific Effects on Proteins and Their Biological Functions', *J. Phys. Chem. B*, 121, 9, pp. 1997–2014, DOI: 10.1021/acs.jpcb.6b10797.

Oncsik, T., G. Trefalt, M. Borkovec and I. Szilagyi
2015 'Specific Ion Effects on Particle Aggregation Induced by Monovalent Salts within the Hofmeister Series', *Langmuir*, 31, 13, pp. 3799–3807, DOI: 10.1021/acs.langmuir.5b00225.

Padova, J.
1963 'Ion-solvent Interaction. II. Partial Molar Volume and Electrostriction: A Thermodynamic Approach', *J. Chem. Phys.* 39, 6, pp. 1552–1557, DOI: 10.1063/1.1734478.
1964 'Solvation Approach to Ion Solvent Interaction', *J. Chem. Phys.* 40, 3, pp. 691–694, DOI: 10.1063/1.1725191.

Parker, A. J.
1962 'The Effects of Solvation on the Properties of Anions in Dipolar Aprotic Solvents', en, *Q. Rev. Chem. Soc.* 16, 2, pp. 163–187, DOI: 10.1039/qr9621600163.

Parsegian, V. A.
2006 *Van Der Waals Forces*, Cambridge University Press, Cambridge.

Parsons, D. F., M. Boström, P. Lo Nostro and B. W. Ninham

2011 'Hofmeister Effects: Interplay of Hydration, Nonelectrostatic Potentials, and Ion Size', en, *Phys. Chem. Chem. Phys.* 13, 27, pp. 12352–12367, DOI: 10.1039/c1cp20538b.

Parsons, D. F., M. Boström, T. J. Maceina, A. Salis and B. W. Ninham

2010 'Why Direct or Reversed Hofmeister Series? Interplay of Hydration, Non-electrostatic Potentials, and Ion Size', *Langmuir*, 26, 5, pp. 3323–3328, DOI: 10.1021/la903061h.

Parsons, D. F. and B. W. Ninham

2009 'Ab Initio Molar Volumes and Gaussian Radii', *J. Phys. Chem. A*, 113, 6, pp. 1141–1150, DOI: 10.1021/jp802984b.

2011 'Surface Charge Reversal and Hydration Forces Explained by Ionic Dispersion Forces and Surface Hydration', *Colloids Surf., A*, 383, 1, pp. 2–9, DOI: 10.1016/j.colsurfa.2010.12.025.

Parsons, D. F. and A. Salis

2016 'Hofmeister Effects at Low Salt Concentration Due to Surface Charge Transfer', *Curr. Opin. Colloid Interface Sci.* 23, pp. 41–49, DOI: 10.1016/j.cocis.2016.05.005.

Paschek, D. and R. Ludwig

2011 'Specific Ion Effects on Water Structure and Dynamics beyond the First Hydration Shell', *Angew. Chem. Int. Ed.* 50, 2, pp. 352–353, DOI: 10.1002/anie.201004501.

Pearson, R. G.

1963 'Hard and Soft Acids and Bases', *J. Am. Chem. Soc.* 85, 22, pp. 3533–3539, DOI: 10.1021/ja00905a001.

Pedersen, T. G., C. Dethlefsen and A. Hvidt

1984 'Volumetric Properties of Aqueous Solutions of Alkali Halides', English, *Carlsberg Res. Commun.* 49, 3, pp. 445–455, DOI: 10.1007/BF02907785.

Pegram, L. M. and M. T. Record Jr.

2008 'Thermodynamic Origin of Hofmeister Ion Effects', *J. Phys. Chem. B*, 112, 31, pp. 9428–9436, DOI: 10.1021/jp800816a.

Peruzzi, N., P. Lo Nostro, B. W. Ninham and P. Baglioni

2015 'The Solvation of Anions in Propylene Carbonate', *J. Solution Chem.* 44 (6 2015), pp. 1224–1239, DOI: 10.1007/s10953-015-0335-z.

Peruzzi, N., B. W. Ninham, P. Lo Nostro and P. Baglioni

2012 'Hofmeister Phenomena in Nonaqueous Media: The Solubility of Electrolytes in Ethylene Carbonate', *J. Phys. Chem. B*, 116, 49, pp. 14398–14405, DOI: 10.1021/jp309157x.

Petrella, G. and A. Sacco

1978 'Viscosity and Conductance Studies in Ethylene Carbonate at 40 °C', *J. Chem. Soc., Faraday Trans. 1*, 74, pp. 2070–2076, DOI: 10.1039/F19787402070.

Piculell, L. and S. Nilsson
1989 'Anion-specific Salt Effects in Aqueous Agarose Systems. 1. Effects on the Coil-helix Transition and Gelation of Agarose', *J. Phys. Chem.* 93, 14, pp. 5596–5601, DOI: 10.1021/j100351a053.

Pinho, S. P. and E. A. Macedo
2005 'Solubility of NaCl, NaBr, and KCl in Water, Methanol, Ethanol, and Their Mixed Solvents', *J. Chem. Eng. Data*, 50, 1, pp. 29–32, DOI: 10.1021/je049922y.

Pinna, M. C., A. Salis, M. Monduzzi and B. W. Ninham
2005 'Hofmeister Series: The Hydrolytic Activity of *Aspergillus niger* Lipase Depends on Specific Anion Effects', *J. Phys. Chem. B*, 109, 12, pp. 5406–8, DOI: 10.1021/jp050574w.

Pollard, T. P. and T. L. Beck
2016 'Toward a Quantitative Theory of Hofmeister Phenomena: From Quantum Effects to Thermodynamics', *Curr. Opin. Colloid Interface Sci.* 23, pp. 110–118, DOI: 10.1016/j.cocis.2016.06.015.
2017 'Structure and Polarization near the Li^+ Ion in Ethylene and Propylene Carbonates', *J. Chem. Phys.* 147, 16, pp. 161710-1–161710-8, DOI: 10.1063/1.4992788.

Quaino, P., F. Juarez, E. Santos and W. Schmickler
2014 'Volcano Plots in Hydrogen Electrocatalysis — Uses and Abuses', *Beilstein J. Nanotechnol.* 5, Behm, R. J. guest editor, pp. 864–854, DOI: 10.3762/bjnano.5.96.

R Core Team
2017 *R: A Language and Environment for Statistical Computing*, version 3.4.1, R Foundation for Statistical Computing, Vienna, Austria, www.R-project.org/.

Reeve, J. F., Y. M. Allinson and A. Stevens
2005 'High-risk Medication Alert: Intravenous Potassium Chloride', *Australian Prescriber*, 28, 1, pp. 14–16, DOI: 10.18773/austprescr.2005.010.

Riekkola, M.-L.
2002 'Recent Advances in Nonaqueous Capillary Electrophoresis', *Electrophoresis*, 23, 22-23, pp. 3865–83, DOI: 10.1002/elps.200290007.

Roberts, J. M., A. R. Diaz, D. T. Fortin, J. M. Friedle and S. D. Piper
2002 'Influence of the Hofmeister Series on the Retention of Amines in Reversed-phase Liquid Chromatography', *Anal. Chem.* 74, 19, pp. 4927–4932, DOI: 10.1021/ac0256944.

Robertson, T. B.
1911 'Contributions to the Theory of the Mode of Action of Inorganic Salts upon Proteins in Solution', *J. Biol. Chem.* 9, 3, pp. 303–326, www.jbc.org/content/9/3/303.short.

Ru, M. T., S. Y. Hirokane, A. S. Lo, J. S. Dordick, J. A. Reimer and D. S. Clark
2000 'On the Salt-induced Activation of Lyophilized Enzymes in Organic Solvents: Effect of Salt Kosmotropicity on Enzyme Activity', *J. Am. Chem. Soc.* 122, 8, pp. 1565–1571, DOI: 10.1021/ja9935198.

Salis, A. and B. W. Ninham

2014 'Models and Mechanisms of Hofmeister Effects in Electrolyte Solutions, and Colloid and Protein Systems Revisited', en, *Chem. Soc. Rev.* 43, 21 (21 2014), pp. 7358–7377, DOI: 10.1039/C4CS00144C.

Salis, A., M. C. Pinna, D. Bilaničová, M. Monduzzi, P. Lo Nostro and B. W. Ninham

2006 'Specific Anion Effects on Glass Electrode pH Measurements of Buffer Solutions: Bulk and Surface Phenomena', *J. Phys. Chem. B*, 110, 6, pp. 2949–2956, DOI: 10.1021/jp0546296.

Salomäki, M., P. Tervasmäki, S. Areva and J. Kankare

2004 'The Hofmeister Anion Effect and the Growth of Polyelectrolyte Multilayers', *Langmuir*, 20, 9, pp. 3679–3683, DOI: 10.1021/la036328y.

Sanganyado, E., Z. Lu and J. Gan

2014 'Mechanistic Insights on Chaotropic Interactions of Liophilic Ions with Basic Pharmaceuticals in Polar Ionic Mode Liquid Chromatography', *J. Chromatogr. A*, 1368, 3, pp. 82–88, DOI: 10.1016/j.chroma.2014.09.054.

Sassi, P., F. Palombo, R. S. Cataliotti, M. Paolantoni and A. Morresi

2007 'Distributions of H-bonding Aggregates in *tert*-butyl Alcohol: The Pure Liquid and Its Alkane Mixtures', *J. Phys. Chem. A*, 111, 27, pp. 6020–6027, DOI: 10.1021/jp071609q.

Sauerbrey, G.

1959 'Verwendung Von Schwingquarzen Zur Wägung Dünner Schichten Und Zur Mikrowägung', *Z. Phys.* 155, 2, pp. 206–222.

Schmidtchen, F. P.

2010 'Hosting Anions. The Energetic Perspective', *Chem. Soc. Rev.* 39 (10 2010), pp. 3916–3935, DOI: 10.1039/C0CS00038H.

Schott, H.

1984 'Lyotropic Numbers of Anions from Cloud Point Changes of Nonionic Surfactants', *Colloids Surf.* 11, 1, pp. 51–54, DOI: 10.1016/0166-6622(84)80234-6.

1995 'Effect of Inorganic Additives on Solutions of Nonionic Surfactants', *J. Colloid Interface Sci.* 173, 2, pp. 265–277, DOI: 10.1006/jcis.1995.1326.

Schwierz, N., D. Horinek and R. R. Netz

2010 'Reversed Anionic Hofmeister Series: The Interplay of Surface Charge and Surface Polarity', *Langmuir*, 26, 10, pp. 7370–7379, DOI: 10.1021/la904397v.

Schwierz, N., D. Horinek, U. Sivan and R. R. Netz

2016 'Reversed Hofmeister Series —the Rule Rather Than the Exception', *Curr. Opin. Colloid Interface Sci.* 23, pp. 10–18, DOI: 10.1016/j.cocis.2016.04.003.

Scrosati, B. and C. A. Vincent
1980 *Alkali Metal, Alkaline Earth Metal and Ammonium Halides, Amide Solvents*, ed. by A. S. Kertes, IUPAC Solubility Data Series, Pergamon Press Ltd, vol. 11, https://srdata.nist.gov/solubility/IUPAC/SDS-11/SDS-11.pdf.

Seddon, K. R., A. Stark and M.-J. Torres
2000 'Influence of Chloride, Water, and Organic Solvents on the Physical Properties of Ionic Liquids', *Pure Appl. Chem.* 72 (12 2000), pp. 2275–2287, DOI: 10.1351/pac200072122275.

Senske, M., D. Constantinescu-Aruxandei, M. Havenith, C. Herrmann, H. Weingartner and S. Ebbinghaus
2016 'The Temperature Dependence of the Hofmeister Series: Thermodynamic Fingerprints of Cosolute-protein Interactions', *Phys. Chem. Chem. Phys.* 18 (43 2016), pp. 29698–29708, DOI: 10.1039/C6CP05080H.

Shi, Y. and T. Beck
2017 'Deconstructing Free Energies in the Law of Matching Water Affinities', *J. Phys. Chem. B*, 121, 9, pp. 2189–2201, DOI: 10.1021/acs.jpcb.7b00104.

Simka, W., D. Puszczyk and G. Nawrat
2009 'Electrodeposition of Metals from Non-aqueous Solutions', *Electrochim. Acta*, 54, 23, pp. 5307–5319, DOI: 10.1016/j.electacta.2009.04.028.

Smith, D. M., W. M. D. Bryant and J. Mitchell
1939 'Analytical Procedures Employing Karl Fischer Reagent. I. Nature of the Reagent', *J. Am. Chem. Soc.* 61, 9, pp. 2407–2412, DOI: 10.1021/ja01878a041.

Smuts, J. P., X.-Q. Hao, Z. Han, C. Parpia, M. J. Krische and D. W. Armstrong
2014 'Enantiomeric Separations of Chiral Sulfonic and Phosphoric Acids with Barium-doped Cyclofructan Selectors Via an Ion Interaction Mechanism', *Anal. Chem.* 86, 2, pp. 1282–1290, DOI: 10.1021/ac403686a.

Söhnel, O. and P. Novotný
1985 *Densities of Aqueous Solutions of Inorganic Substances*, Elsevier, Amsterdam.

Soniat, M., G. Pool, L. Franklin and S. W. Rick
2016 'Ion Association in Aqueous Solution', *Fluid Phase Equilib.* 407, SI, pp. 31–38, DOI: 10.1016/j.fluid.2015.05.001.

Srivastava, A. and K. Ismail
2014 'Binding of Phenol Red to Cetylpyridinium Chloride at Air-solution and Micelle-solution Interfaces in Aqueous Ethylene Glycol Media', *Colloids Surf., A*, 462, pp. 115–123, DOI: 10.1016/j.colsurfa.2014.08.021.

Stephen, H. and T. Stephen
1963 (eds.), *Solubilities of Inorganic and Organic Compounds. Binary Systems*, vol. 1.1, Pergamon Press, Oxford.

Striegel, A., W. W. Yau, J. J. Kirkland and D. D. Bly
2009 *Modern Size-exclusion Liquid Chromatography: Practice of Gel Permeation and Gel Filtration Chromatography*, 2nd ed., John Wiley & Sons, Inc., Hoboken, NJ.

Sun, Z., W. Zhang, M. Ji, R. Hartsock and K. J. Gaffney
2013 'Contact Ion Pair Formation between Hard Acids and Soft Bases in Aqueous Solutions Observed with 2DIR Spectroscopy', *J. Phys. Chem. B*, 117, 49, SI, pp. 15306–15312, DOI: 10.1021/jp4033854.

Tan, K. Y., J. E. Gautrot and W. T. S. Huck
2011 'Formation of Pickering Emulsions Using Ion-specific Responsive Colloids', *Langmuir*, 27, 4, pp. 1251–1259, DOI: 10.1021/la102904r.

Tarafdar, P. K., S. T. Reddy and M. J. Swamy
2013 'Effect of Hofmeister Series Anions on the Thermotropic Phase Behavior of Bioactive *O*-acylcholines', *J. Phys. Chem. B*, 117, 34, pp. 9900–9909, DOI: 10.1021/jp403964k.

Tayyab, S., S. Qamar and M. Islam
1991 'Size Exclusion Chromatography and Size Exclusion HPLC of Proteins', *Biochem. Educ.* 19, 3, pp. 149–152, DOI: 10.1016/0307-4412(91)90060-L.

Thomas, A. S. and A. H. Elcock
2007 'Molecular Dynamics Simulations of Hydrophobic Associations in Aqueous Salt Solutions Indicate a Connection between Water Hydrogen Bonding and the Hofmeister Effect', *J. Am. Chem. Soc.* 129, 48, pp. 14887–14898, DOI: 10.1021/ja073097z.

Tóth, K., E. Sedlák, M. Sprinzl and G. Zoldák
2008 'Flexibility and Enzyme Activity of NADH Oxidase from *Thermus thermophilus* in the Presence of Monovalent Cations of Hofmeister Series', *Biochim. Biophys. Acta*, 1784, 5, pp. 789–95, DOI: 10.1016/j.bbapap.2008.01.022.

Trompette, J. L.
2015 'The Comparative Breakdown of Passivity of Tin by Fluorides and Chlorides Interpreted through the "law of matching affinities" Concept', *Corros. Sci.* 94, pp. 288–293, DOI: 10.1016/j.corsci.2015.02.012.

Uejio, J. S., C. P. Schwartz, A. M. Duffin, W. S. Drisdell, R. C. Cohen and R. J. Saykally
2008 'Characterization of Selective Binding of Alkali Cations with Carboxylate by x-ray Absorption Spectroscopy of Liquid Microjets', *Proc. Natl. Acad. Sci. U. S. A.* 105, 19, pp. 6809–6812, DOI: 10.1073/pnas.0800181105.

Varhač, R., N. Tomášková, M. Fabián and E. Sedlák
2009 'Kinetics of Cyanide Binding As a Probe of Local Stability/flexibility of Cytochrome *c*', *Biophys. Chem.* 144, 1-2, pp. 21–26, DOI: 10.1016/j.bpc.2009.06.001.

Verhoef, J. C. and E. Barendrecht

1976 'Mechanism and Reaction Rate of the Karl-Fischer Titration Reaction. Part I. Potentiometric Measurements', *J. Electroanal. Chem. Interfacial Electrochem.* 71, 3, pp. 305–315, DOI: 10.1016/S0022-0728(76)80017-4.

Vishnu and V. S. Mishra

1981 'Conductance Studies on the Interaction of Lactose with Alkali-metal Halides in Water and in Formamide', *Carbohydr. Res.* 89, 1, pp. 55–63, DOI: 10.1016/S0008-6215(00)85228-3.

Vlachy, N., M. Drechsler, D. Touraud and W. Kunz

2009 'Anion Specificity Influencing Morphology in Catanionic Surfactant Mixtures with an Excess of Cationic Surfactant', *C. R. Chim.* 12, 1-2, pp. 30–37, DOI: 10.1016/j.crci.2008.10.010.

Vlachy, N., B. Jagoda-Cwiklik, R. Vácha, D. Touraud, P. Jungwirth and W. Kunz

2009 'Hofmeister Series and Specific Interactions of Charged Headgroups with Aqueous Ions', *Adv. Colloid Interface Sci.* 146, 1-2, pp. 42–7, DOI: 10.1016/j.cis.2008.09.010.

Voet, A.

1937 'Quantitative Lyotropy', *Chem. Rev.* 20, 2, pp. 169–179, DOI: 10.1021/cr60066a001.

von Hippel, P. H. and T. Schleich

1969 'Ion Effects on the Solution Structure of Biological Macromolecules', *Acc. Chem. Res.* 2, 9, pp. 257–265, DOI: 10.1021/ar50021a001.

von Hippel, P. H. and K.-Y. Wong

1964 'Neutral Salts: The Generality of Their Effects on the Stability of Macromolecular Conformations', en, *Science*, 145, 3632, pp. 577–580, DOI: 10.1126/science.145.3632.577.

Vrbka, L., M. Mucha, B. Minofar, P. Jungwirth, E. C. Brown and D. J. Tobias

2004 'Propensity of Soft Ions for the Air/water Interface', *Curr. Opin. Colloid Interface Sci.* 9, 1-2, pp. 67–73, DOI: 10.1016/j.cocis.2004.05.028.

Wagman, D. D., W. H. Evans, V. B. Parker, R. H. Schumm, I. Halow, S. M. Bailey, K. L. Churney and R. L. Nuttall

1982 'The NBS Tables of Chemical Thermodynamic Properties. Selected Values for Inorganic and C1 C2 Organic Substance in SI Units', *J. Phys. Chem. Ref. Data*, 11, Supplement 2, https://srd.nist.gov/JPCRD/jpcrdS2Vol11.pdf.

Washabaugh, M. W. and K. D. Collins

1986 'The Systematic Characterization by Aqueous Column Chromatography of Solutes Which Affect Protein Stability', *J. Biol. Chem.* 261, 27, pp. 12477–12485, www.jbc.org/content/261/27/12477.abstract?sid=d9d45068-abf0-4bd4-97c4-ea22f2c2a51e.

Wei, X. and T. Ngai

2012 'Ion-induced Hydrophobic Collapse of Surface-confined Polyelectrolyte Brushes Measured by Total Internal Reflection Microscopy', *Polym. Chem.* 3 (8 2012), pp. 2121–2128, DOI: 10.1039/C2PY20085F.

Weidmann, S.

1956 'Shortening of the Cardiac Action Potential Due to a Brief Injection of KCl Following the Onset of Activity', *J. Physiol.* 132, 1, pp. 157–163, DOI: 10.1113/jphysiol.1956.sp005510.

Weiss, L., A. Tazibt, A. Tidu and M. Aillerie

2012 'Water Density and Polarizability Deduced from the Refractive Index Determined by Interferometric Measurements up to 250 MPa', *J. Chem. Phys.* 136, 12, p. 124201, DOI: 10.1063/1.3698481.

Wiggins, P. M.

1997 'Hydrophobic Hydration, Hydrophobic Forces and Protein Folding', *Physica A*, 238, 1–4, pp. 113–128, DOI: 10.1016/S0378-4371(96)00431-1.

Willott, J. D., B. A. Humphreys, T. J. Murdoch, S. Edmondson, G. B. Webber and E. J. Wanless

2015 'Hydrophobic Effects within the Dynamic pH-response of Polybasic Tertiary Amine Methacrylate Brushes', *Phys. Chem. Chem. Phys.* 17, 5 (5 2015), pp. 3880–3890, DOI: 10.1039/C4CP05292G.

Winter, M. and R. J. Brodd

2004 'What Are Batteries, Fuel Cells, and Supercapacitors?', *Chem. Rev.* 104, 10, pp. 4245–4270, ISSN: 0009-2665, DOI: 10.1021/cr020730k.

Xie, W. J., Z. Zhang and Y. Q. Gao

2016 'Ion Pairing in Alkali Nitrate Electrolyte Solutions', *J. Phys. Chem. B*, 120, 9, pp. 2343–2351, DOI: 10.1021/acs.jpcb.5b10755.

Yang, J.-H., M.-K. Kim, J.-H. Son, H.-J. Cho and Y.-U. Kwon

2007 'Novel Phosphotungstate-titania Nanocomposites from Aqueous Media', *Bull. Korean Chem. Soc.* 28, 7, pp. 1097–1103, DOI: 10.5012/bkcs.2007.28.7.1097.

Yang, Z.

2009 'Hofmeister Effects: An Explanation for the Impact of Ionic Liquids on Biocatalysis', *J. Biotechnol.* 144, 1, pp. 12–22, DOI: 10.1016/j.jbiotec.2009.04.011.

Yu, C.-M., S. Mun and N.-H. L. Wang

2006 'Theoretical Analysis of the Effects of Reversible Dimerization in Size Exclusion Chromatography', *J. Chromatogr. A*, 1132, 1, pp. 99–108, DOI: 10.1016/j.chroma.2006.07.017.

Zhang, Q., R. Zhang, Y. Zhao, H. Li, Y. Q. Gao and W. Zhuang

2014 'Pairing Preferences of the Model Mono-valence Mono-atomic Ions Investigated by Molecular Simulation', *J. Chem. Phys.* 140, 18, pp. 184504-1–184504-9, DOI: 10.1063/1.4874255.

Zhang, T., M. G. Cathcart, A. S. Vidalis and H. C. Allen

2016 'Cation Effects on Phosphatidic Acid Monolayers at Various pH Conditions', *Chem. Phys. Lipids*, 200, pp. 24–31, DOI: 10.1016/j.chemphyslip.2016.06.001.

Zhang, Y. and P. S. Cremer

2006 'Interactions between Macromolecules and Ions: The Hofmeister Series', *Curr. Opin. Chem. Biol.* 10, 6, pp. 658–63, ISSN: 1367-5931, DOI: 10.1016/j.cbpa.2006.09.020.

2010 'Chemistry of Hofmeister Anions and Osmolytes', en, *Annu. Rev. Phys. Chem.* 61, pp. 63–83, DOI: 10.1146/annurev.physchem.59.032607.093635.

Zhang, Y., S. Furyk, D. E. Bergbreiter and P. S. Cremer

2005 'Specific Ion Effects on the Water Solubility of Macromolecules: PNIPAM and the Hofmeister Series', *J. Am. Chem. Soc.* 127, 41, pp. 14505–10, DOI: 10.1021/ja0546424.

Zhao, H.

2016 'Protein Stabilization and Enzyme Activation in Ionic Liquids: Specific Ion Effects.' *J. Chem. Technol. Biotechnol.* 91, 1, pp. 25–50, DOI: 10.1002/jctb.4837.

Žoldák, G., M. Sprinzl and E. Sedlák

2004 'Modulation of Activity of NADH Oxidase from *Thermus thermophilus* through Change in Flexibility in the Enzyme Active Site Induced by Hofmeister Series Anions', *Eur. J. Biochem.* 271, 1, pp. 48–57, DOI: 10.1046/j.1432-1033.2003.03900.x.

Zuman, P. and S. Wawzonek

1978 'Nonaqueous Solvents in Organic Electroanalytical Chemistry', in *The Chemistry of Nonaqueous Solvents. Principles and Basic Solvents*, ed. by J. J. Lagowski, Academic Press, New York, vol. VA, pp. 121–143.